3-28-2019 3:00 PM

Mass Spectrometry-Based Proteomics Analysis Of Bioactive Proteins In EMD That Modulate Adhesion Of Gingival Fibroblast To Improve Bio-Integration Of Dental Implants

David Zuanazzi Machado Jr, *The University of Western Ontario*

Supervisor: Siqueira, Walter L., *The University of Western Ontario*

A thesis submitted in partial fulfillment of the requirements for the Doctor of Philosophy degree in Biochemistry

ABSTRACT

Titanium (Ti) implants are used in dental practice to replace damaged or lost teeth. For effective treatment, the dental implant needs to integrate with the surrounding hard and soft tissues on the implant site. Despite improvements in bone-implant integration that have been achieved through surface modifications, the integration with the soft tissues is still deficient. The oral mucosa that embraces the transmucosal component of the implant only contacts the surface without making a strong attachment with the connective tissue. The lack of attachment offers no protection against bacterial invasion that can lead to local infection and implant loss. Among different modification applied to Ti surfaces, coating the surface with specific proteins is a new area in biomedical research aiming to improve implant biointegration. To this end, proteins that comprise the enamel matrix derivative (EMD) would be good candidates to be used as surface coatings. EMD is a rich protein mixture used as a biomaterial to promotes tissue regeneration by modulating many cells, including gingival fibroblasts, the most abundant cell type of oral connective tissue. However, many proteins containing in EMD are yet to be identified. Considering that surface features are important to modulate protein adsorption, we worked with the hypothesis that we could use the characteristics of different Ti surfaces in a surface-affinity approach to creating unique coatings with EMD. Therefore, it would allow us to identify bioactive proteins within EMD that could be further used as a coating on the implant to promote adhesion of gingival fibroblast to the surface, improving the implant biointegration. Since it is not well-established whether the surface attracts or binds specific proteins from complex mixtures, saliva was used as a

model in combination with mass spectrometry to investigate surface specificity for protein binding of three different Ti surfaces (PT, SLA, and SLActive). By applying this approach, we showed that the Ti surfaces had a low specificity for protein binding due to high similarity on the pellicle composition despite differences in characteristics between surfaces. The lack of binding specificity led us to explore the EMD composition utilizing another strategy. Through the MudPIT methodology, we fractionated EMD in 32 fractions to characterize its proteome. We identified 2000 proteins through tandem mass spectrometry (MS/MS) including novel proteins that are associated with EMD biological activity, i.e. biomineralization, wound healing and biological adhesion. The obtained EMD fractions were then applied to human gingival fibroblast (HGF) to evaluate their capability to promote cell adhesion on a coated surface. The adhesion assay indicated that two EMD fraction (F23 and F24), which contained the adhesion proteins fibrillin-1 and tenascin C, showed a significantly higher response than native EMD and other EMD fractions. Overall, the work presented herein indicated the need for more studies on surface-proteins interaction given the low surface specificity presented by each Ti surface. Also, this thesis provided an in-depth insight on the complexity of EMD protein composition, including the identification of novel proteins that are related to EMD biological activity such as the adhesion of gingival fibroblasts.

Key Words: Dental implants, titanium, size exclusion chromatography, mass spectrometry, proteomics, peptides, gene ontology, fibroblasts, cell adhesion.

DEDICATION

First and foremost, I would like to dedicate this thesis to God and to my beautiful family that always provided me with endless encouragement and support during my academic endeavors. To my lovely wife Maura whose everyday-presence and unconditional love have inspired me to be a better husband and father. Without you, I would never be the person I am today. To my amazing children, Giovanna and Enzo, who have shaped my heart with their hugs, kisses, and words. Holding you in my arms is always breathtaking.

Secondly, I would like to thank my parents who raised me with love, values, and discipline. Words are not enough to demonstrate my gratitude for supporting my decision throughout my life, particularly the hardest ones. To my sister Rebeca, thank you for our never-ending friendship and your presence in my life.

Thank you all for your companionship during this chapter of my life. Surely, without you, none of this would be possible.

ACKNOWLEDGEMENT

First, I would like to express my sincere gratitude to my supervisor Dr. Walter Siqueira for his continuous support during my Ph.D. study. Thank you for your guidance during my development as a scientist and for providing inspiration and encouragement to continue working on dental research. Also, I want to say a big thanks to the past and present members of the Siqueira lab for the time spent together whether working in the lab or drinking coffee. Every one of you has contributed in many different ways during these five years we shared. Cindy, thank you for always being available to assist me with the mass spectrometer and for providing useful insights during our conversations. You have been a real helper.

Thank you to all member of the Junop lab. I genuinely appreciate the support I have received, especially Dr. Murray Junop for generously opening his lab to process my samples and Chris Brown for his patience while showing me how to operate the FPLC system properly. Likewise, I want to extend my gratitude to Dr. Douglas Hamilton and members of the Hamilton Lab for the warm welcome and incredible support while I was using the cell culture room. Thank you, Georgia, Adam, JT, Sarah, and Karrie, for providing the fibroblasts and space and time to culture the cells. At last but not least, I want to thank Dr. Andrew Leask and members of Leask Lab for useful insights and for make yourselves available when needed and for providing the PrestoBlue reagent that was critical to finish my work.

TABLE OF CONTENTS

LIST OF TABLES

LIST OF FIGURES

LIST OF APPENDICES

LIST OF ABBREVIATIONS

Å – angstrom

ACN – acetonitrile

AHSG – alpha-2-HS-glycoprotein

ANOVA – analysis of variation

AnxA1 – annexin A1

AnxA2 – annexin A2

ATP – Adenosine triphosphate

BCA – bicinchoninic acid

BE – binding energy

BMP – bone morphogenetic protein

BSA – bovine serum albumin

BSP – bone sialoprotein

C – carbon

Ca^{2+} - calcium

CID – collisional induced dissociation

CO_2 – carbon dioxide

Cu – copper

Da – Dalton

DMEM – Dulbecco's modified Eagle minimal essential medium

DNA – deoxyribonucleic acid

DPBS – Dulbecco's phosphate-buffered saline

DSSP – dentin sialophosphoprotein

DTT – dithiothreitol

ECD – electron capture dissociation

ECM - Extracellular matrix

EDTA – ethylenediaminetetraacetic acid

EMD – Enamel Matrix Derivative

EMSP1 – enamel matrix serine proteinase 1

ESI – electrospray ionization

ETD - electron transfer dissociation

eV – electronvolt

FA – formic acid

FBS – fetal bovine serum

FGF – fibroblast growth factor

GF – gingival fibroblast

GO – gene ontology

H_2O – water

H_2SO_4 – Sulfuric acid

HCl – Hydrochloric acid

HGF – human gingival fibroblast

HPLC – high-pressure liquid chromatography

Ig – immunoglobulin

kV – kilovolt

LC – liquid chromatography

LC MS/MS – liquid chromatography tandem mass spectrometry

LIT – linear ion trap

LRAP – Leucine-rich amelogenin protein

m/z – mass to charge ratio

mA – milliampere

MC3T3-E1 – osteoblast precursor cell line derived from Mus musculus (mouse) calvaria

MMP-20 – matrix metalloproteinase-20

mRNA – messenger RNA

MS –mass spectrometry

MS/MS – tandem mass spectrometry

MUC – Mucin

MudPIT – multidimensional protein identification technology

MW – molecular weight

NaCl – sodium chloride

NH_4HCO_3 – Ammonium Bicarbonate

nLC-ESI – nano liquid chromatography electrospray ionization

nm – nanometer

O – oxygen

OC – osteocalcin

ODAM – odontogenic ameloblast-associated protein

OH – hydroxyl group

OPG – osteoprotegerin

PANTHER – Protein Analysis Through Evolutionary Relationships

PDL – periodontal ligament

PDLF – periodontal ligament fibroblast

pI – Isoelectric point

prAMEL – recombinant amelogenin

PRP – proline-rich proteins

PT – polished titanium

PTM – post-translational modification

R_a – roughness parameter

RANKL – Receptor activator of nuclear factor kappa-B ligand

RGD – Arg-Gly-Asp

RNA – ribonucleic acid

RP – reverse-phase

RP-LC – reverse-phase liquid chromatography

SCX – strong cation exchanger

SD – standard deviation

SDS – sodium dodecyl sulfate

SDS PAGE –sodium dodecyl sulfate polyacrylamide gel electrophoresis

SEC – size-exclusion chromatography

SEF – surface free energy

SLA – sandblasted/large-grit/acid-etched

SLActive – modified SLA

TFA – Trifluoroacetic acid

TGF – transforming growth factor

Ti – Titanium

TiO_2 – Titanium dioxide

TRAP – Tyrosine-rich amelogenin peptide

UniProt – Universal Protein Resource

VEGF – vascular endothelial growth factor

WB – western blot

WSS – whole saliva supernatant

XPS – X-ray Photoelectron Spectroscopy

µL – microliter

µm – Micrometer

Ala (A) – alanine

Arg (R) – arginine

Asn (N) asparagine

Asp (D) – aspartic acid

Cys (C) – cysteine

Gln (Q) – glutamine

Glu (E) – glutamic acid

Gly (G) – glycine

His (H) – histidine

Ile (I) – isoleucine

Leu (L) – leucine

Lys (K) – lysine

Met (M) – methionine

Phe (F) – phenylalanine

Pro (P) – proline

Ser (S) – serine

Thr (T) – threonine

Trp (W) – tryptophan

Tyr (Y) – tyrosine

Val (V) – valine

CHAPTER 1

Introduction

1.1 – Titanium Dental implant

Titanium (Ti) dental implants have become a widely used biomaterial in dentistry practice to replace damaged or lost teeth due to its reliability and biocompatibility with the surrounding tissues, providing a long-term clinical success rate [1]. Dental implants are commonly placed in the dental arches in a two-steps process, presenting a complex integration within the dental arches, since the device has to interact with three distinct tissue types within the oral cavity: bone, gingival connective tissue and gingival epithelium (Figure 1.1) [2]. Initially, the bone-contacting component is inserted into the bone for periods of up to 6 to 8 weeks, which allows the healing and ingrowth of the bone on the surface, providing a mechanical and biological anchor for the dental implant [3]. The second step involves the attachment of a transmucosal element (also known as abutment) on top of the implant through an incision made in the overlying mucosal tissue [4, 5]. Of interest, the abutment is extremely important to the biointegration of implants since it interacts directly with connective tissue and gingival epithelium after its placement (Figure 1.1). These two steps consist of the biointegration with hard (bone) and soft (mucosa) tissues that surround the implant in the oral cavity.

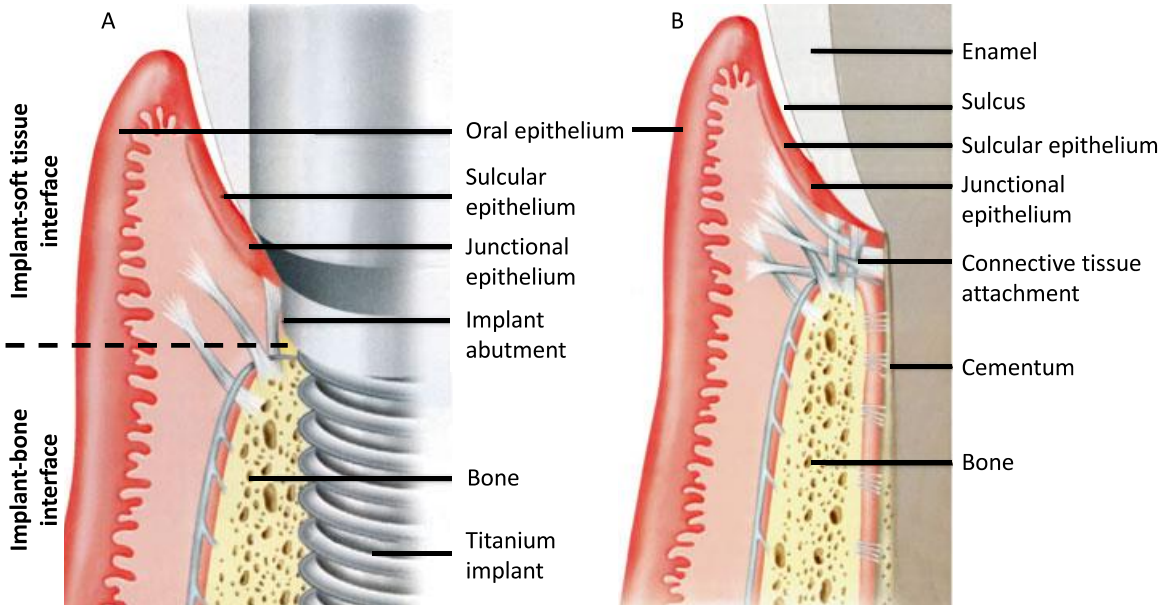

Figure 1.1 - Differences between the integration of dental implants (A) and natural tooth (B) with surrounding soft and hard tissues. Note the lack of connective tissue attachment to the surface of implant abutment due to parallel orientation of gingival fibers on implant surfaces (Modified and used with permission from [6]).

1.2 – Osseointegration

The stability of dental implant is a determinant factor for a successful treatment. It is a two-steps process that is comprised of the primary stability (mechanical fixation) – immediately achieved during implant placement – that is further replaced by the long-term secondary stability (biological) also known as osseointegration [7]. By definition, osseointegration is a dynamic and complex biological process characterized by the formation of new bone around the implant without intervening fibrous or soft tissue, resulting in a functional-biocompatible intimate contact between the implant surface and the novel bone [2]. Once complete, this initial stage is followed by *de novo* bone formation mediated by osteogenic cells and finalized with bone remodeling (i.e. bone resorption followed by bone apposition), which is a lifelong process [8]. The localized injury resulting from the implant placement initiates a series of wound-healing and tissue regeneration events that are modulated by extracellular matrix (ECM) molecules. Different cell types present at the implant-tissue interfaces also play an essential role in this process through the synthesis and release of growth factors and cytokines that will result in the recruitment of osteogenic cells to the implant surface to start bone formation [9].

Particularly, immediately after implant insertion, a series of reactions occur on the implant surface, starting with the adsorption of water molecules that facilitates adsorption of proteins and other molecules derived from the surrounding tissues and blood [10, 11]. These initial reactions between implant and tissue components dictate the further events and determine the biological

activity of the surface beginning with cell attachment. The cell-implant interaction is regulated primarily by a layer of ECM proteins such as fibronectin that adsorbs onto the surface and initiates cell adhesion via integrins, which subsequently leads to cell migration and differentiation, resulting in implant integration to both hard (bone) and soft tissues (gingiva) [12]. Thus, the nature of the surface and its chemical properties directly influences the compositions of the proteins layer formed onto the surface, which will modulate subsequent tissues response [11, 13, 14].

1.3 – Titanium Surfaces

Knowing the importance of the implant surface to osseointegration, several modifications to Ti surface have been applied, mainly focused on altering the structure, topography, and surface chemistry of the commercially pure Ti implant that directly contacts the bone after placement [15-17]. The most used Ti surfaces in implant dentistry are the classical machined or polished titanium (PT), along with SLA (sandblasted/large-grit/acid-etched), and more recently, the modified SLA (modified sandblasted/large-grit/acid-etched) also known as SLActive [3].

Considered the gold standard surface in dentistry for a number of years, PT is characterized by a smooth surface having a low roughness. Later, in an attempt to improve implant treatment, several studies have demonstrated that rough surface significantly increased bone-to-implant contact area and provided a greater resistance to removal, which has been demonstrated to be an

important factor in improving implant osseointegration [3, 18-20]. SLA surface was then introduced showing superior results by reducing healing time in addition to delivering a higher success rates than smooth surface [18, 21]. SLA surface is produced by blasting the smooth Ti with large-grit corundum particles, creating a macro-roughness on the surface that was then etched with a strong acid (mixture of HCl/H_2SO_4), resulting in a microrough surface with micropits ranging from 0.5 to 2 μm in diameter [19], which became a standard for Ti dental implants. Despite improving bone-to-implant interaction, rough surfaces were shown to be effective modulators of cell function by enhancing bone apposition [15-17]. Likewise, at the cellular level, other studies have shown an association between micro-roughness and osteoblast activation, particularly stimulating proliferation, differentiation, and synthesis of osteocalcin, a protein produced by osteoblast during late stage of differentiation [22, 23].

Despite having opposite topographies, PT (smooth) and SLA (rough) surfaces share a common characteristic: both surfaces are hydrophobic, which was determined by numerous investigations that measured the contact angle that water makes with the surface [3, 24-26]. Titanium is known to be biocompatible and resistant to corrosion due to the formation of a titanium oxide (TiO_2) layer on the surface that is formed within nanoseconds after exposure to the air [27]. As the oxide layer is very reactive, it is hydroxylated in water forming –OH groups that interact with other molecules. However, this layer is readily contaminated with hydrocarbons and carbonates from the ambient atmosphere, which makes it hydrophobic [25]. Hydrophobicity of a surface is a limiting factor

for cell responsiveness as it reduces the surface free energy (SFE) that is especially important for initial protein adsorption and cell adhesion [28]. Therefore, studies started to investigate how to rescue surface hydrophilicity aiming to improve implants treatment. In this context, the modified SLA or SLActive was introduced.

SLActive is a chemical modification of the SLA surface. SLActive is produced in the same way as the SLA by sandblasting and acid etching the surface, but with an additional step to avoid carbon contamination. The surface is protected in a nitrogen atmosphere and stored in an isotonic solution of NaCl to retain surface reactiveness and high free energy that is provided by the higher content of oxygen and titanium atoms available on the surface to interact with the tissues [3]. The increase in surface hydrophilicity and SFE results in a surface that is more biologically active, which promotes a faster bone apposition and earlier implant stability during the initial healing phase, in comparison to the hydrophobic SLA [3, 29, 30]. Therefore, the combination of higher surface roughness with surface hydrophilicity – which directly associates with higher SEF – have made a greater impact on osteogenesis, showing these to be a crucial factors for improved osseointegration.

Although dental implant treatment presents a 90% rate of success and a long-term survival rate of 10 years on average [1], it is not perfect, because the bio-integration is incomplete. Despite the fact that, for unknown reasons, the percentage of bone-to-implant contact area averages between 70%–80% [31], the attachment of the surrounding soft tissues, i.e., gingival connective tissue

and epithelium, is still required since there are no collagen fibers attachments to the implants' surface as it occurs on the tooth's surface in a healthy periodontium (Fig. 1). Osseointegration process is essential for the stability of the implant, but the interplay between the titanium surface and soft tissues is a crucial factor to maintain a continual healthy condition of the peri-implant mucosa at the coronal portion of the implant. Failure in achieving a proper implant-soft tissue integration can ultimately lead to epithelial downgrowth, pocket formation, infection, and inflammation also known as peri-implantitis, that can escalate to possible implant loss [32].

1.4 - Biomimetic Technology

Recently, searching for superior results, investigators have turned attention towards the creation of biomimetic surfaces through biochemical modifications, to influence the integration of biomaterials into the periodontium. Advanced technology, yet to be used in clinical dental applications, involves adding specific proteins or peptides to the implant surface to enhance the integration between the Ti and the surrounding bone tissue [33-36]. Many studies have shown that the addition of bioactive coatings, such as hydroxyapatite, polymers, and composites, have directly enhanced bone formation surrounding an implant, both *in vitro* and *in vivo,* when compared to control Ti surfaces [34, 37-40]. For example, specific peptide sequences known to influence cell attachment, such as the RGD motif found in fibronectin, have been reported to directly control osteoblast attachment, spreading and proliferation on Ti surfaces *in vitro* [13, 41, 42]. This rapidly progressing field is

developing the next generation of biomaterials, which shows promising application in dentistry. However, biochemical alterations in implant surfaces have not been fully utilized in any clinical setting due to their large production costs, molecular complexity, and questionable *in vivo* stability. If the proteins or peptides incorporated onto the implant surface could be derived from the same tissue (e.g., bone or teeth) into which the implant is being placed, it is plausible that integration of the Ti implant would be faster, since it is possible that the native bone cells surrounding the implant site would recognize and respond to the protein cues attached to the Ti implant surface. It is for this reason that we have focused on identifying novel enamel matrix proteins as a potential bioactive coating to Ti implants.

1.5 - Enamel Matrix Derivative

Enamel Matrix Derivative (EMD) is purified acid extract of enamel matrix proteins isolated from developing porcine teeth introduced more than twenty years ago that is commercialized by the name of Emdogain® [43]. During teeth development, these constituent proteins are produced by ameloblasts, and upon secretion from the cells, assemble to form a matrix, which then facilitates the nucleation and growth of calcium crystals. The major component of EMD are the amelogenins, a family of hydrophobic proteins derived from different splice variants and enzymatic processing that comprise > 90% of the organic constituent of the enamel matrix [44, 45]. Since then, investigators have determined other components that are less abundant in EMD, including enamelin [46], ameloblastin (also known as sheathlin) [47], along with the enzymes matrix

metalloproteinase-20 (MMP-20) [48], kallikrein-4 (also called enamel matrix serine proteinase 1 or EMSP1) [49], and more recently, odontogenic ameloblast-associated protein (ODAM), also known as apin [50]. In addition, immunoassay studies identified the presence of growth factors that produced TGF-β1, BMP-2 and BMP-4-like activity [51-53]. However, even after more than twenty years of investigation, many EMD components remain uncharacterized to date.

1.5.1 - Influence of EMD in hard and soft tissues

Besides the well-known role of enamel proteins in enamel development, EMD has been significantly studied and applied in regenerative dentistry, particularly in regeneration of periodontal tissues (bone, cementum, and gingiva) [54-56]. Abundant evidence revealed in both *in vitro* and *in vivo* studies indicated that EMD modulate the behavior of a variety of cell types such as osteoblasts, fibroblasts, epithelial, and endothelial cells [56-66]. Particularly, EMD is involved in bone formation and growth through activation of osteoblasts and their precursors in many ways, from stimulating cell adhesion and cell differentiation [67, 68], to promoting osteoblast maturation and proliferation [58, 59]. The effects on osteoblasts also extend to gene expression related to osteogenesis and bone remodeling. EMD significantly increases the expression of mRNA levels of osteocalcin (OC), bone sialoprotein (BSP), and collagen α1 on MC3T3-E1 pre-osteoblasts cell, which are extracellular matrix proteins necessary to osteoblast undergone differentiation that contribute to bone matrix formation and mineralization [58, 61, 69, 70]. In bone remodeling, EMD

enhances osteoprotegerin (OPG) expression in osteoblasts that regulate RANKL levels resulting in reduced osteoclast formation and activity [58, 71].

Recent literature has been suggested that EMD has a significant participation in soft tissue would healing and regeneration [72]. Studies *in vitro* have shown that EMD induce proliferation and migration of endothelial promoting angiogenesis, which were recently attributed to the low-molecular weight amelogenin-derived peptide TRAP [66, 73, 74]. Conversely, EMD seems to have a negative regulatory effect on epithelial cells [65, 75]. Although cell apoptosis is not observed, EMD induces a decrease in epithelial cell proliferation and DNA synthesis that could be mediated by TGF-β-like activity considered part of EMD [76]. On the other hand, several investigators have demonstrated that EMD proteins influence different types of fibroblasts, including (PDLF) and gingival fibroblasts (HGF) [77, 78]. The majority of studies have shown that EMD positively influences cell adhesion, migration, and proliferation of PDLF. However, the effect on HGF are limited to proliferation and migration [78-80]. Few studies that evaluated whether EMD promote adhesion of HGF presented conflicting information [77, 81, 82]. For instance, Van der Pauw et al. demonstrated that HGF had a neutral response for both initial cell attachment or spreading when cells were exposed to EMD proteins [77]. In contrast, when EMD was used to coat zirconium surface, an increase of HGF adhesion was achieved after 4 hours [82]. Gingival fibroblasts are very important for the maintenance and production of gingival and mucosa connective tissue that surround teeth and implant abutment [83], preventing the invasion of bacteria

that leads to local inflammatory state, and further bone resorption resulting in teeth and implant loss [84].

The variety of biological effects exhibited on diverse cell types are believed to be due to different protein that make up EMD. For that reason, many studies have implemented methods to separate EMD proteins in different fractions to study the biological effects on various cell types. Using size-exclusion chromatography (SEC) to separate EMD proteins into different pools, Stout et al. found that low-molecular weight components produced a significantly higher osteogenic response than EMD proteins present in the high-molecular weight range [85]. In another study that evaluated the effect of different EMD fractions obtained by SEC on PDLF, the authors noted that lower molecular weight fractions induced a 2- to 5-fold increase in cell proliferation and the secretion of interleukin-8 and monocyte chemoattractant protein-1, while the release of vascular endothelial growth factor (VEGF) and interleukin-6 by PDLF was achieved when cells were treated with EMD components above 20-kDa [86]. Similar results were obtained by a study that applied EMD and two derived proteins – recombinant 21.3 kDa amelogenin (prAMEL) and 5.3 kDa tyrosine-rich amelogenin peptide (TRAP) – on HGF, that showed an increase in cell proliferation when HGF was exposed to EMD, while a higher migration rate was associated to prAMEL and TRAP [81]. Moreover, Andrukhov et al. observed that fractions containing low-molecular weight proteins also stimulated migration of endothelial cells, suggesting angiogenic activity [73], which was also indicated in

a previous study that found different biological effects delivered by 3 EMD fractions acquired by SEC [87].

Since the amelogenin protein is the main component of EMD (more than 90%), investigators have originally believed that they were the responsible for the biological effects observed in an early study [88]. However, throughout years of research, it has been clear that many results presented by these studies demonstrated that the cellular activities promoted by EMD are not necessarily associated with a single protein but to diverse EMD components that may work in concert to deliver distinct biological response, even expressed in lower quantity. Therefore, it is highly required to investigate EMD composition with advanced techniques suitable to analyze complex samples such as mass spectrometry to unravel the proteins content of EMD aiming to discovery specific constituents that are responsible for the broad effects showed by numerous studies.

1.6 - Mass spectrometry-based proteomics

Proteomics refers to the analysis of entire protein content (proteome) of a cell, tissue, or organism [89], aiming to identify, characterize, and quantify proteins. One of the pillars in modern proteomics studies is the use of mass spectrometry (MS) that it is recognized as a powerful analytical tool to examine diverse molecules such as proteins in biological samples [90, 91]. Mass spectrometry-based proteomics is the chosen methodology to study the proteome of complex proteins mixtures including tissues, cells, and body fluids

such as saliva [92], that also is employed to study post-translation modification (PTM) and protein-protein interactions [93, 94]. Mass spectrometry-based proteomics are currently based on two fundamental methodologies of sample preparation for protein and peptides identification and characterization: the top-down and bottom-up approaches (Figure 1.2).

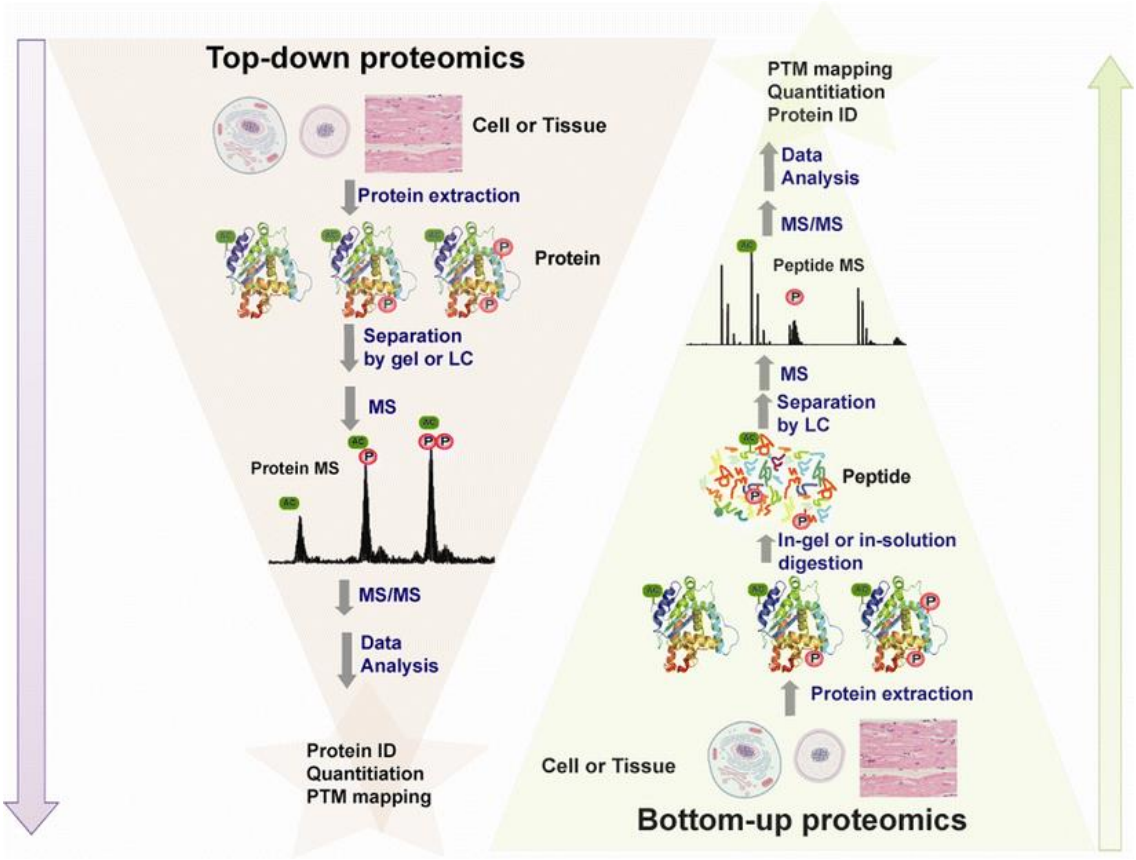

Figure 1.2 - Schematic illustration of the difference between top-down and bottom-up proteomics. In top-down proteomics (left), proteins are extracted from cell or tissue lysates, separated by either gel or LC, and directly analyzed by MS and fragmented by MS/MS to obtain sequence information, which can be used to identify the protein via database searching, and localize PTMs. In bottom-up proteomics (right), proteins extracted from cells or tissue are subjected to proteolytic digestion (often using trypsin)—either in-solution or in-gel—and the resulting peptides are separated using LC and analyzed by MS. Subsequently, the most abundant peptides are fragmented, and the peptide sequence information is used to identify the proteins present in the sample. Numerous strategies are also available for both the relative and absolute quantification of proteins/peptides using bottom-up and top-down proteomics. Used with permission [95].

1.6.1 - Top-down approach

The top-down methods are characterized by the analysis and identification of intact proteins or large protein fragments that are ionized and fragmented in the gas-phase using soft fragmentation methods, such as electron transfer dissociation (ETD), to further be analyzed by the mass spectrometer [96]. The top-down method is traditionally used for characterization of single proteins and simple protein mixture as it provides high sequence coverage of target proteins, allowing the identification of protein isoforms [97, 98]. This approach is also considered superior for analysis of PTM as the soft fragmentation method generates more stable protein fragment with PTM such as phosphorylation [99].

1.6.2 - Bottom-up approach

The bottom-up approach is the preferred method for large-scale analyses of high-complexity samples such as EMD, and therefore, was the method utilized in this thesis. In the bottom-up proteomics, proteins are identified through generated peptides after enzymatic digestion using a sequence-specific protease. Usually, the enzyme of choice in proteomic experiments is trypsin, which is a serine-protease that typically recognizes and cleaves the carboxyl-terminus of the amino acids residues arginine (R) or lysine (K), generating multiple peptides around 14 amino acids long [100]. Proteins can be either digested directly from a biological sample (in-solution), i.e., cell extract or biological fluid such as saliva, or after submitted to a gel-based fractionation

method, such as sodium dodecyl sulfate-polyacrylamide gel electrophoresis (SDS-PAGE), from which protein bands are excised prior to being trypsinized (in-gel digestion) [101].

1.6.2.1 – Protein/peptides Separation Methods

The hundreds of thousands of peptides generated from trypsinization are separated by liquid chromatography and ionized to enter in the gas phase before being introduced into the mass spectrometer, where peptides will be fragmented and detected by the MS analyzer [94]. The liquid chromatography is usually coupled on-line with the mass spectrometer to provide sufficient separation aiming to decrease the complexity of rich biological samples prior to mass analysis [102]. This front-end separation is also important to maximize the identification of low-abundant proteins that would be masked by peptide signals originating from highly abundant proteins. The most common chromatography method is the high-pressure liquid chromatography (HPLC) using a reverse-phase resins (RP) that is directly coupled to an ESI source, which provides continuous separation and ionization. In the reverse phase chromatography, the separation is based on hydrophobic interaction between the column resin (usually alkyl chains with 18 carbons bonded with silica particles known as C18), and peptides that are solubilized in volatile mobile phase that are compatible with ESI [103].

To increase the analytical capacity for complex samples, multidimensional separations before mass analysis are often utilized in proteomics, and it is known

as multidimensional protein identification technology (MudPIT) [104]. In MudPIT, different separation techniques can be combined on-line with the RP-LC such as strong cation exchanger (SCX), which separate molecules by positive charge. The first dimension of MudPIT can be also implemented off-line, i.e., not directly connected with the second dimension RP-LC that is couple with the mass analyzer [105]. This possibility provides not only great flexibility as sample analyses can be repeated, but also it can enhance chromatography and increase loading capacity. In this scenario, size-exclusion chromatography can be a valuable off-line method that separate proteins mixtures by size that can be digested prior to subject to the RP-LC as the on-line second dimension coupled to the ion source and mass spectrometer [106].

1.6.2.2 – Ionization and proteins identification

The ionization method widely used in bottom-up proteomics is the electrospray ionization (ESI) as it is an optimal method of ionization for a wide range of polar biomolecules. ESI consists of applying a high electrical field at the extremity of the separation column generating a charged spray that create droplets containing peptides. Assisted by a heated capillary, these droplets will evaporate by desolvation producing gas-phase peptides ions that enter the inlet of the mass spectrometer to be analyzed [107, 108]. The ESI method was improved with the development of nanoLC technology (nLC-ESI), which used analytical column capable of delivering gradients at nano-scale flow rates (nanoL/min), offering a higher sensitivity for analysis of complex samples by the mass analyzer [102].

The mass analysis in bottom-up proteomics for protein mixtures are commonly carried out by ion-beam and trapping instruments such as linear ion trap (LIT). LITs are versatile instruments that can be connected to a continuous ESI source that permits high-throughput analysis, providing high sensitivity (femtomole level), fast scan rates, and reasonable resolution that is produced by high-quality tandem MS (MS/MS) spectra [109, 110]. Protein identification in most bottom-up applications involves acquisition of MS/MS data through collision-induced dissociation (CID). Differently from ETD, CID is a hard fragmentation method that consists in the fragmentation of peptides (precursor ions), preferentially in the peptide bond, that produce ion fragments that are used to determine the original peptide to properly identify the intact protein through search in a known protein database [111-113].

1.7 - Thesis rationale

Although it is recognized that implant surface is a determinant factor for dental implant integration with the surrounding tissues, it is not well-established whether the surface attracts and binds specific proteins that initiate its biological response to the environment. Many modifications have been applied on Ti implants, but few studies have utilized EMD as a coating. It has been suggested that EMD, when applied *in vivo*, during implant placement does not influence bone formation around the implant [114, 115]. Conversely, recent *in vitro* studies indicate that osteoblasts are activated and up regulated when cultured onto Ti surfaces coated with EMD, as compared to control surfaces [116, 117]. Another *in vitro* study also showed that EMD potentialized the effects of rat calvarial

osteoblasts on cell spreading, proliferation, and differentiation when PT and SLA Ti surfaces were pre-coated with EMD [60].

These studies indicate that most of the work regarding dental implants has focused on the integration of the intraosseous component with bone, with less emphasis on the importance of adhesion of connective tissue to the implant abutment, particularly regarding coating with proteins [118]. Therefore, more work is needed to investigate the influence of EMD proteins on soft tissue growth adjacent to Ti implants. From a clinical perspective, it would be of great significance if the transmucosal component of dental implant biologically attaches the surrounding connective tissue to make a stable connection rather than only a tenuous cellular contact. This would prevent local bacterial infection that can progress to inflammation and eventual implant loss.

1.8 - Scope of thesis

Due to many biological properties associated to EMD and to limited understanding of its composition, our main objective was to identify bioactive proteins within EMD that could be used to develop a biomimetic surface of Ti implants to enhance the implant biointegration with the surrounding soft tissues, particularly proteins that have potential to promote adhesion of gingival fibroblast that could, therefore, be used as a coating onto the surface of the transmucosal component.

Working towards this objective, we first investigated how surface characteristics of three most used Ti surfaces in dental implants – PT, SLA, and

SLActive – influenced proteins binding by using salivary proteins as a model of complex samples to study surface-proteins interaction through mass spectrometry. This approach was used as an attempt to standardize surface-affinity method to separate proteins (Chapter 2). Similar to EMD, saliva is also a complex mixture that contain more than 3,000 proteins identified [119, 120]. By using saliva as a model, we intended to evaluate whether different surface characteristics would adsorb distinctive proteins to form a surface-specific protein layer. Therefore, EMD could be later applied as a coating to Ti surfaces to modulate adhesion of gingival fibroblast to improve integration with the surrounding connective tissue at the peri-implant region.

Considering the complex composition of EMD and the fact that many components remain unknown, we carried out mass spectrometry-based proteomics to investigate the EMD proteome utilizing a multidimensional approach (Chapter 3). To date, large scale MS-based proteomic applications have not been effectively applied to unravel the full proteome of EMD. The objective was to identify proteins within the enamel matrix that can be associated with its diverse biological activity that affect a variety of cell types, in particular proteins that could enhance adhesion of gingival fibroblasts to implant abutment.

After obtaining EMD fractions through size-exclusion chromatography, we investigated in chapter 4 the effect of EMD and its fraction on the adhesion of human gingival fibroblasts *in vitro*. By utilizing the proteome profile of EMD in chapter 3, we have identified proteins in some fractions that are potential

candidates to be used as a coating on dental implants to enhance the tissue-implant interface. Lastly, in chapter 5, we discuss the most relevant results that permeated this thesis considering the impact of the knowledge acquired with these findings and how can be applied in further studies regarding the dental filed.

1.9 – References

1. Simonis, P., T. Dufour, and H. Tenenbaum, *Long-term implant survival and success: a 10-16-year follow-up of non-submerged dental implants.* Clin Oral Implants Res, 2010. **21**(7): p. 772-7.

2. Branemark, P.I., *Introduction to osseointegration.*, in *Tissue integrated prosthesis.* , P.I. Branemark, G.A. Zarb, and T. Albrektsson, Editors. 1985, Quintessence International: Chicago. p. 11–76.

3. Buser, D., et al., *Enhanced bone apposition to a chemically modified SLA titanium surface.* J Dent Res, 2004. **83**(7): p. 529-33.

4. Buser, D., U.C. Belser, and N.P. Lang, *The original one-stage dental implant system and its clinical application.* Periodontol 2000, 1998. **17**: p. 106-18.

5. Berglundh, T., et al., *De novo alveolar bone formation adjacent to endosseous implants.* Clin Oral Implants Res, 2003. **14**(3): p. 251-62.

6. Wadhwani, C.P.K., *Restoring the Dental Implant: The Biological Determinants*, in *Cementation in Dental Implantology: An Evidence-Based Guide*, C.P.K. Wadhwani, Editor. 2015, Springer Berlin Heidelberg: Berlin, Heidelberg. p. 1-14.

7. Albrektsson, T. and G.A. Zarb, *Current interpretations of the osseointegrated response: clinical significance.* Int J Prosthodont, 1993. **6**(2): p. 95-105.

8. Davies, J.E., *Mechanisms of endosseous integration.* Int J Prosthodont, 1998. **11**(5): p. 391-401.

9. Davies, J.E., *Understanding peri-implant endosseous healing.* J Dent Educ, 2003. **67**(8): p. 932-49.

10. Thevenot, P., W. Hu, and L. Tang, *Surface chemistry influences implant biocompatibility.* Curr Top Med Chem, 2008. **8**(4): p. 270-80.

11. Puleo, D.A. and A. Nanci, *Understanding and controlling the bone-implant interface.* Biomaterials, 1999. **20**(23-24): p. 2311-21.

12. Ratner, B.D. and S.J. Bryant, *Biomaterials: where we have been and where we are going.* Annu Rev Biomed Eng, 2004. **6**: p. 41-75.

13. Schuler, M., et al., *Biomimetic modification of titanium dental implant model surfaces using the RGDSP-peptide sequence: a cell morphology study.* Biomaterials, 2006. **27**(21): p. 4003-15.

14. Ellingsen, J.E., *Surface configurations of dental implants.* Periodontol 2000, 1998. **17**: p. 36-46.

15. Cooper, L.F., *A role for surface topography in creating and maintaining bone at titanium endosseous implants.* J Prosthet Dent, 2000. **84**(5): p. 522-34.

16. Cochran, D.L., et al., *Bone response to unloaded and loaded titanium implants with a sandblasted and acid-etched surface: a histometric study in the canine mandible.* J Biomed Mater Res, 1998. **40**(1): p. 1-11.

17. Guo, C.Y., J.P. Matinlinna, and A.T. Tang, *Effects of surface charges on dental implants: past, present, and future.* Int J Biomater, 2012. **2012**: p. 381535.

18. Cochran, D.L., et al., *The use of reduced healing times on ITI (R) implants with a sandblasted and acid-etched (SLA) surface: Early results from clinical trials on ITI (R) SLA implants.* Clinical Oral Implants Research, 2002. **13**(2): p. 144-153.

19. Buser, D., et al., *Influence of surface characteristics on bone integration of titanium implants. A histomorphometric study in miniature pigs.* J Biomed Mater Res, 1991. **25**(7): p. 889-902.

20. Wennerberg, A. and T. Albrektsson, *Suggested guidelines for the topographic evaluation of implant surfaces.* Int J Oral Maxillofac Implants, 2000. **15**(3): p. 331-44.

21. Roccuzzo, M., et al., *Early loading of sandblasted and acid-etched (SLA) implants: a prospective split-mouth comparative study.* Clin Oral Implants Res, 2001. **12**(6): p. 572-8.

22. Costa, D.O., et al., *The differential regulation of osteoblast and osteoclast activity by surface topography of hydroxyapatite coatings.* Biomaterials, 2013. **34**(30): p. 7215-26.

23. Martin, J.Y., et al., *Effect of titanium surface roughness on proliferation, differentiation, and protein synthesis of human osteoblast-like cells (MG63).* J Biomed Mater Res, 1995. **29**(3): p. 389-401.

24. Wennerberg, A., et al., *Nanostructures and hydrophilicity influence osseointegration: a biomechanical study in the rabbit tibia.* Clin Oral Implants Res, 2014. **25**(9): p. 1041-50.

25. Rupp, F., et al., *Enhancing surface free energy and hydrophilicity through chemical modification of microstructured titanium implant surfaces.* J Biomed Mater Res A, 2006. **76**(2): p. 323-34.

26. Zhao, G., et al., *High surface energy enhances cell response to titanium substrate microstructure.* J Biomed Mater Res A, 2005. **74**(1): p. 49-58.

27. Lautenschlager, E.P. and P. Monaghan, *Titanium and titanium alloys as dental materials.* Int Dent J, 1993. **43**(3): p. 245-53.

28. Kieswetter, K., et al., *The role of implant surface characteristics in the healing of bone.* Crit Rev Oral Biol Med, 1996. **7**(4): p. 329-45.

29. Lang, N.P., et al., *Early osseointegration to hydrophilic and hydrophobic implant surfaces in humans.* Clin Oral Implants Res, 2011. **22**(4): p. 349-56.

30. Bosshardt, D.D., et al., *The role of bone debris in early healing adjacent to hydrophilic and hydrophobic implant surfaces in man.* Clin Oral Implants Res, 2011. **22**(4): p. 357-64.

31. Albrektsson, T., et al., *Histologic investigations on 33 retrieved Nobelpharma implants.* Clin Mater, 1993. **12**(1): p. 1-9.

32. Tonetti, M.S., *Risk factors for osseodisintegration.* Periodontol 2000, 1998. **17**: p. 55-62.

33. Roessler, S., et al., *Biomimetic coatings functionalized with adhesion peptides for dental implants.* J Mater Sci Mater Med, 2001. **12**(10-12): p. 871-7.

34. Gotfredsen, K., et al., *Anchorage of TiO2-blasted, HA-coated, and machined implants: an experimental study with rabbits.* J Biomed Mater Res, 1995. **29**(10): p. 1223-31.

35. Costa, D.O., et al., *Control of surface topography in biomimetic calcium phosphate coatings.* Langmuir, 2012. **28**(8): p. 3871-80.

36. Avila, G., et al., *Implant surface treatment using biomimetic agents.* Implant Dent, 2009. **18**(1): p. 17-26.

37. Klinger, M.M., et al., *Proteoglycans at the bone-implant interface.* Crit Rev Oral Biol Med, 1998. **9**(4): p. 449-63.

38. Lacefield, W.R., *Current status of ceramic coatings for dental implants.* Implant Dent, 1998. **7**(4): p. 315-22.

39. Hjorting-Hansen, E., et al., *Osseointegration of subperiosteal implant via guided tissue regeneration. A pilot study.* Clin Oral Implants Res, 1995. **6**(3): p. 149-54.

40. Morra, M., et al., *Effects of molecular weight and surface functionalization on surface composition and cell adhesion to Hyaluronan coated titanium.* Biomed Pharmacother, 2006. **60**(8): p. 365-9.

41. Schuler, M., et al., *Comparison of the response of cultured osteoblasts and osteoblasts outgrown from rat calvarial bone chips to nonfouling KRSR and FHRRIKA-peptide modified rough titanium surfaces.* J Biomed Mater Res B Appl Biomater, 2009. **91**(2): p. 517-27.

42. Bell, B.F., et al., *Osteoblast response to titanium surfaces functionalized with extracellular matrix peptide biomimetics.* Clin Oral Implants Res, 2011. **22**(8): p. 865-72.

43. Hammarstrom, L., L. Heijl, and S. Gestrelius, *Periodontal regeneration in a buccal dehiscence model in monkeys after application of enamel matrix proteins.* J Clin Periodontol, 1997. **24**(9 Pt 2): p. 669-77.

44. Brookes, S.J., et al., *Biochemistry and molecular biology of amelogenin proteins of developing dental enamel.* Arch Oral Biol, 1995. **40**(1): p. 1-14.

45. Lyngstadaas, S.P., et al., *Enamel matrix proteins; old molecules for new applications.* Orthod Craniofac Res, 2009. **12**(3): p. 243-53.

46. Uchida, T., et al., *Immunocytochemical and immunochemical detection of a 32 kDa nonamelogenin and related proteins in porcine tooth germs.* Arch Histol Cytol, 1991. **54**(5): p. 527-38.

47. Hu, C.C., et al., *Sheathlin: cloning, cDNA/polypeptide sequences, and immunolocalization of porcine enamel sheath proteins.* J Dent Res, 1997. **76**(2): p. 648-57.

48. Fukae, M. and T. Tanabe, *Degradation of enamel matrix proteins in porcine secretory enamel.* Connect Tissue Res, 1998. **39**(1-3): p. 123-9; discussion 141-9.

49. Simmer, J.P., et al., *Purification, characterization, and cloning of enamel matrix serine proteinase 1.* J Dent Res, 1998. **77**(2): p. 377-86.

50. Moffatt, P., et al., *Identification of secreted and membrane proteins in the rat incisor enamel organ using a signal-trap screening approach.* Eur J Oral Sci, 2006. **114 Suppl 1**: p. 139-46; discussion 164-5, 380-1.

51. Kawase, T., et al., *Enamel matrix derivative (EMDOGAIN) rapidly stimulates phosphorylation of the MAP kinase family and nuclear accumulation of smad2 in both oral epithelial and fibroblastic human cells.* J Periodontal Res, 2001. **36**(6): p. 367-76.

52. Iwata, T., et al., *Noggin blocks osteoinductive activity of porcine enamel extracts.* J Dent Res, 2002. **81**(6): p. 387-91.

53. Suzuki, S., et al., *Enamel matrix derivative gel stimulates signal transduction of BMP and TGF-{beta}.* J Dent Res, 2005. **84**(6): p. 510-4.

54. Cochran, D.L., et al., *Periodontal regeneration with a combination of enamel matrix proteins and autogenous bone grafting.* J Periodontol, 2003. **74**(9): p. 1269-81.

55. Mellonig, J.T., et al., *Clinical and histologic evaluation of non-surgical periodontal therapy with enamel matrix derivative: a report of four cases.* J Periodontol, 2009. **80**(9): p. 1534-40.

56. Sculean, A., et al., *Healing of human intrabony defects following treatment with enamel matrix proteins or guided tissue regeneration.* J Periodontal Res, 1999. **34**(6): p. 310-22.

57. Lees, J.D., et al., *Cellular uptake and processing of enamel matrix derivative by human periodontal ligament fibroblasts.* Arch Oral Biol, 2013. **58**(4): p. 348-54.

58. He, J., et al., *Emdogain promotes osteoblast proliferation and differentiation and stimulates osteoprotegerin expression.* Oral Surg Oral Med Oral Pathol Oral Radiol Endod, 2004. **97**(2): p. 239-45.

59. Jiang, J., et al., *Emdogain-gel stimulates proliferation of odontoblasts and osteoblasts.* Oral Surg Oral Med Oral Pathol Oral Radiol Endod, 2006. **102**(5): p. 698-702.

60. Miron, R.J., et al., *The effect of enamel matrix proteins on the spreading, proliferation and differentiation of osteoblasts cultured on titanium surfaces.* Biomaterials, 2010. **31**(3): p. 449-60.

61. Miron, R.J., et al., *Influence of enamel matrix derivative on cells at different maturation stages of differentiation.* PLoS One, 2013. **8**(8): p. e71008.

62. Hammarstrom, L., *Enamel matrix, cementum development and regeneration.* J Clin Periodontol, 1997. **24**(9 Pt 2): p. 658-68.

63. Heijl, L., *Periodontal regeneration with enamel matrix derivative in one human experimental defect. A case report.* J Clin Periodontol, 1997. **24**(9 Pt 2): p. 693-6.

64. Yukna, R.A. and J.T. Mellonig, *Histologic evaluation of periodontal healing in humans following regenerative therapy with enamel matrix derivative. A 10-case series.* J Periodontol, 2000. **71**(5): p. 752-9.

65. Groeger, S., A. Windhorst, and J. Meyle, *Influence of Enamel Matrix Derivative on Human Epithelial Cells In Vitro.* J Periodontol, 2016. **87**(10): p. 1217-27.

66. Jonke, E., et al., *Effect of tyrosine-rich amelogenin peptide on behavior and differentiation of endothelial cells.* Clin Oral Investig, 2016. **20**(8): p. 2275-2284.

67. Miron, R.J., et al., *Osteogain improves osteoblast adhesion, proliferation and differentiation on a bovine-derived natural bone mineral.* Clin Oral Implants Res, 2017. **28**(3): p. 327-333.

68. Reseland, J.E., et al., *The effect of enamel matrix derivative on gene expression in osteoblasts.* Eur J Oral Sci, 2006. **114 Suppl 1**: p. 205-11; discussion 254-6, 381-2.

69. Stein, G.S., et al., *Transcriptional control of osteoblast growth and differentiation.* Physiol Rev, 1996. **76**(2): p. 593-629.

70. Rincon, J.C., et al., *Enhanced proliferation, attachment and osteopontin expression by porcine periodontal cells exposed to Emdogain.* Arch Oral Biol, 2005. **50**(12): p. 1047-54.

71. Khosla, S., *Minireview: the OPG/RANKL/RANK system.* Endocrinology, 2001. **142**(12): p. 5050-5.

72. Maymon-Gil, T., et al., *Enamel Matrix Derivative Promotes Healing of a Surgical Wound in the Rat Oral Mucosa.* J Periodontol, 2016. **87**(5): p. 601-9.

73. Andrukhov, O., et al., *Effect of different enamel matrix derivative proteins on behavior and differentiation of endothelial cells.* Dent Mater, 2015. **31**(7): p. 822-32.

74. Bertl, K., et al., *Effects of enamel matrix derivative on proliferation/viability, migration, and expression of angiogenic factor and adhesion molecules in endothelial cells in vitro.* J Periodontol, 2009. **80**(10): p. 1622-30.

75. Kawase, T., et al., *Cytostatic action of enamel matrix derivative (EMDOGAIN) on human oral squamous cell carcinoma-derived SCC25 epithelial cells.* J Periodontal Res, 2000. **35**(5): p. 291-300.

76. Kawase, T., et al., *Anti-TGF-beta antibody blocks enamel matrix derivative-induced upregulation of p21WAF1/cip1 and prevents its inhibition of human oral epithelial cell proliferation.* J Periodontal Res, 2002. **37**(4): p. 255-62.

77. Van der Pauw, M.T., et al., *Enamel matrix-derived protein stimulates attachment of periodontal ligament fibroblasts and enhances alkaline phosphatase activity and transforming growth factor beta1 release of periodontal ligament and gingival fibroblasts.* J Periodontol, 2000. **71**(1): p. 31-43.

78. Rincon, J.C., H.R. Haase, and P.M. Bartold, *Effect of Emdogain on human periodontal fibroblasts in an in vitro wound-healing model.* J Periodontal Res, 2003. **38**(3): p. 290-5.

79. Cattaneo, V., et al., *Effect of enamel matrix derivative on human periodontal fibroblasts: proliferation, morphology and root surface colonization. An in vitro study.* J Periodontal Res, 2003. **38**(6): p. 568-74.

80. Rodrigues, T.L., et al., *Effects of enamel matrix derivative and transforming growth factor-beta1 on human periodontal ligament fibroblasts.* J Clin Periodontol, 2007. **34**(6): p. 514-22.

81. Wyganowska-Swiatkowska, M., et al., *Human gingival fibroblast response to enamel matrix derivative, porcine recombinant 21.3-kDa amelogenin and 5.3-kDa tyrosine-rich amelogenin peptide.* Hum Cell, 2017. **30**(3): p. 181-191.

82. Kwon, Y.D., et al., *Cellular viability and genetic expression of human gingival fibroblasts to zirconia with enamel matrix derivative (Emdogain(R)).* J Adv Prosthodont, 2014. **6**(5): p. 406-14.

83. Palaiologou, A.A., et al., *Gingival, dermal, and periodontal ligament fibroblasts express different extracellular matrix receptors.* J Periodontol, 2001. **72**(6): p. 798-807.

84. Quirynen, M., M. De Soete, and D. van Steenberghe, *Infectious risks for oral implants: a review of the literature.* Clin Oral Implants Res, 2002. **13**(1): p. 1-19.

85. Stout, B.M., et al., *Enamel matrix derivative: protein components and osteoinductive properties.* J Periodontol, 2014. **85**(2): p. e9-e17.

86. Villa, O., et al., *Subfractions of enamel matrix derivative differentially influence cytokine secretion from human oral fibroblasts.* J Tissue Eng, 2015. **6**: p. 2041731415575857.

87. Johnson, D.L., et al., *Cellular effects of enamel matrix derivative are associated with different molecular weight fractions following separation by size-exclusion chromatography.* J Periodontol, 2009. **80**(4): p. 648-56.

88. Hoang, A.M., et al., *Amelogenin is a cell adhesion protein.* J Dent Res, 2002. **81**(7): p. 497-500.

89. Aebersold, R. and M. Mann, *Mass spectrometry-based proteomics.* Nature, 2003. **422**(6928): p. 198-207.

90. Mann, M., R.C. Hendrickson, and A. Pandey, *Analysis of proteins and proteomes by mass spectrometry.* Annu Rev Biochem, 2001. **70**: p. 437-73.

91. Uhlen, M., et al., *Proteomics. Tissue-based map of the human proteome.* Science, 2015. **347**(6220): p. 1260419.

92. Siqueira, W.L., et al., *Proteome of human minor salivary gland secretion.* J Dent Res, 2008. **87**(5): p. 445-50.

93. Yates, J.R., C.I. Ruse, and A. Nakorchevsky, *Proteomics by mass spectrometry: approaches, advances, and applications.* Annu Rev Biomed Eng, 2009. **11**: p. 49-79.

94. Domon, B. and R. Aebersold, *Mass spectrometry and protein analysis.* Science, 2006. **312**(5771): p. 212-7.

95. Gregorich, Z.R., Y.H. Chang, and Y. Ge, *Proteomics in heart failure: top-down or bottom-up?* Pflugers Arch, 2014. **466**(6): p. 1199-209.

96. Mikesh, L.M., et al., *The utility of ETD mass spectrometry in proteomic analysis.* Biochim Biophys Acta, 2006. **1764**(12): p. 1811-22.

97. Hawkridge, A.M., et al., *Quantitative mass spectral evidence for the absence of circulating brain natriuretic peptide (BNP-32) in severe human heart failure.* Proc Natl Acad Sci U S A, 2005. **102**(48): p. 17442-7.

98. Uttenweiler-Joseph, S., et al., *Toward a full characterization of the human 20S proteasome subunits and their isoforms by a combination of proteomic approaches.* Methods Mol Biol, 2008. **484**: p. 111-30.

99. Siuti, N. and N.L. Kelleher, *Decoding protein modifications using top-down mass spectrometry.* Nat Methods, 2007. **4**(10): p. 817-21.

100. Burkhart, J.M., et al., *Systematic and quantitative comparison of digest efficiency and specificity reveals the impact of trypsin quality on MS-based proteomics.* J Proteomics, 2012. **75**(4): p. 1454-62.

101. Shevchenko, A., et al., *In-gel digestion for mass spectrometric characterization of proteins and proteomes.* Nat Protoc, 2006. **1**(6): p. 2856-60.

102. Shen, Y., et al., *High-efficiency nanoscale liquid chromatography coupled on-line with mass spectrometry using nanoelectrospray ionization for proteomics.* Anal Chem, 2002. **74**(16): p. 4235-49.

103. Shen, Y. and R.D. Smith, *Proteomics based on high-efficiency capillary separations.* Electrophoresis, 2002. **23**(18): p. 3106-24.

104. Schirmer, E.C., J.R. Yates, 3rd, and L. Gerace, *MudPIT: A powerful proteomics tool for discovery.* Discov Med, 2003. **3**(18): p. 38-9.

105. Peng, J., et al., *Evaluation of multidimensional chromatography coupled with tandem mass spectrometry (LC/LC-MS/MS) for large-scale protein analysis: the yeast proteome.* J Proteome Res, 2003. **2**(1): p. 43-50.

106. Lecchi, P., et al., *Size-exclusion chromatography in multidimensional separation schemes for proteome analysis.* J Biochem Biophys Methods, 2003. **56**(1-3): p. 141-52.

107. Fenn, J.B., et al., *Electrospray ionization for mass spectrometry of large biomolecules.* Science, 1989. **246**(4926): p. 64-71.

108. Banerjee, S. and S. Mazumdar, *Electrospray ionization mass spectrometry: a technique to access the information beyond the molecular weight of the analyte.* Int J Anal Chem, 2012. **2012**: p. 282574.

109. Yost, R.A. and R.K. Boyd, *Tandem mass spectrometry: quadrupole and hybrid instruments.* Methods Enzymol, 1990. **193**: p. 154-200.

110. Hager, J.W. and J.C. Le Blanc, *High-performance liquid chromatography-tandem mass spectrometry with a new quadrupole/linear ion trap instrument.* J Chromatogr A, 2003. **1020**(1): p. 3-9.

111. Paradela, A. and J.P. Albar, *Advances in the analysis of protein phosphorylation.* J Proteome Res, 2008. **7**(5): p. 1809-18.

112. McLuckey, S.A., D.E. Goeringer, and G.L. Glish, *Collisional activation with random noise in ion trap mass spectrometry.* Anal Chem, 1992. **64**(13): p. 1455-60.

113. Elias, J.E. and S.P. Gygi, *Target-decoy search strategy for increased confidence in large-scale protein identifications by mass spectrometry.* Nat Methods, 2007. **4**(3): p. 207-14.

114. Franke Stenport, V. and C.B. Johansson, *Enamel matrix derivative and titanium implants.* J Clin Periodontol, 2003. **30**(4): p. 359-63.

115. Birang, R., et al., *Effect of enamel matrix derivative on bone formation around intraosseous titanium implant: An experimental study in canine model.* Dent Res J (Isfahan), 2012. **9**(6): p. 790-6.

116. Schwarz, F., et al., *Effect of enamel matrix protein derivative on the attachment, proliferation, and viability of human SaOs(2) osteoblasts on titanium implants.* Clin Oral Investig, 2004. **8**(3): p. 165-71.

117. Qu, Z., et al., *Effect of enamel matrix derivative on proliferation and differentiation of osteoblast cells grown on the titanium implant surface.* Oral Surg Oral Med Oral Pathol Oral Radiol Endod, 2011. **111**(4): p. 517-22.

118. Wang, Y., Y. Zhang, and R.J. Miron, *Health, Maintenance, and Recovery of Soft Tissues around Implants.* Clin Implant Dent Relat Res, 2016. **18**(3): p. 618-34.

119. Grassl, N., et al., *Ultra-deep and quantitative saliva proteome reveals dynamics of the oral microbiome.* Genome Med, 2016. **8**(1): p. 44.

120. Pappa, E., et al., *Saliva Proteomics Analysis Offers Insights on Type 1 Diabetes Pathology in a Pediatric Population.* Front Physiol, 2018. **9**: p. 444.

Chapter 2

Salivary Pellicle Proteome Formed onto Three Different Titanium Surfaces

2.1 Introduction

Titanium (Ti) dental implants have become widely used in dentistry practice to replace damaged or lost teeth due to its reliability, high strength, and biocompatibility [1]. The implant stability is provided through osseointegration which is defined as the formation of new bone around the implant without intervening soft tissue [2]. This involves the recruitment of osteogenic cells to the implant surface, followed by *de novo* bone formation, and finally bone remodeling [3]. This complex process results in a functional-biocompatible, intimate contact between the implant surface and the newly formed bone [2]. During the implant placement in a jaw bone, a series of reactions occur on its surface due to immediate exposure to diverse tissue constituents, including body fluids such as blood, gingival crevicular fluid and saliva, forming a protein-rich pellicle. The initial reactions between the implant surface and the tissue components control and modulate further events that will dictate the biological activity of the surface [4]. The nature of the surface and its chemical properties directly influences the composition of the protein layer adsorbed on the surface, which will further modulate tissues response [5, 6].

Knowing the importance of the implant surface for osseointegration, several modifications to Ti implants have been applied, mainly focusing on

altering the composition, topography, and surface chemistry [7, 8]. The most used surface modifications in clinical settings are the smooth machined titanium (PT), sandblasted/large-grit/acid-etched (SLA), and more recent, the modified SLA (SLActive). These surfaces are effective modulators of cell function by improving bone-to-implant interaction, particularly the rough surfaces [9, 10] that enhance bone-to-implant contact and bone apposition when compared to smooth titanium [10, 11]. At the cellular level, surface roughness has been associated with activation of osteogenic cells by stimulating its proliferation, osteoblasts differentiation as well as protein synthesis [12, 13].

Although it is recognized that the surface is a determinant factor to dental implant integration with the surrounding bone, it is not well-established whether the surface attracts and binds specific proteins that initiate its biological response and promotes osseointegration and tissue healing. Given differences in tissue response obtained by different titanium surfaces (PT, SLA, and SLActive) we hypothesize that titanium surfaces with distinct characteristics such as wettability, topography, and chemistry would differentially bind proteins originating from complex proteins mixtures such as saliva, resulting in the adsorption of specific proteins on each surface, and creating a surface-specific protein pellicle. Herein, we investigate the protein-specificity of the three most used titanium implant surfaces (PT, SLA, and SLActive) by studying the proteome of the adsorbed proteins on each titanium surface and correlating it with surface characteristics upon exposure to saliva.

2.2 Materials and Methods

2.2.1 Samples preparations

2.2.1.1 Saliva collection

Stimulated whole saliva (WS) was collected from three volunteers on three different days between 9:00 and 11:00 a.m. to minimize circadian cycle effects. On each day, a total volume of 5 mL was collected from each volunteer by chewing a piece of Parafilm (25 mm^2) and spitting into a graduated tube immersed in ice. Immediately after collection, saliva samples were centrifuged (14,000 x *g*) at 4°C for 20 min, and the resulting whole saliva supernatant (WSS) was separated from the pellet. A *pool* of WSS was made from the three volunteers, and total protein concentration was measured by the bicinchoninic acid (BCA) assay (Pierce Chemical, Rockford, IL, USA) using bovine serum albumin as the standard. The *pool* of WSS obtained on different days was used in three independent experiments.

2.2.1.2 Titanium surfaces

Discs from three different Ti surface were used in this study; Smooth pickled Ti (PT), and roughened SLA and SLActive Ti topographies. All discs were manufactured and donated by the Institute Straumann A.G. Briefly, 15 mm discs were punched from grade 2 unalloyed Ti sheets. PT surfaces were prepared using diluted nitric acid to clean the surface, and followed by washing the discs in reverse osmosis purified water. SLA surfaces were prepared by

blasting the Ti with corundum particles, followed by etching with HCl/H_2SO_4. SLActive surface was prepared similar to the SLA surfaces but after acid etching, the surface was maintained and stored in an isotonic NaCl solution as previously described [14].

2.2.2 Surface characterization

2.2.2.1 X-ray Photoelectron Spectroscopy (XPS)

The XPS analyses to characterize the surface chemistry composition were carried out for the three Ti surfaces with a Kratos Axis Ultra spectrometer using a monochromatic Al K(alpha) source (15 mA, 14 kV). XPS can detect all elements except hydrogen and helium, probing the sample surface to a depth of 5–10 nm. It has detection limits ranging from 0.1 to 0.5 atomic percent depending on the element. The instrument work function was calibrated to give a binding energy (BE) of 83.96 eV for the Au 4f7/2 line for metallic gold and the spectrometer dispersion was adjusted to give a BE of 932.62 eV for the Cu 2p3/2 line of metallic copper. The Kratos charge neutralizer system was used on all specimens. Survey scan analyses were carried out with an analysis area of 300x700 microns and a pass energy of 160 eV. High resolution Ti 2p analyses were carried out with an analysis area of 300x700 microns and a pass energy of 20 eV. The Ti 2p spectra were curve-fit using the procedure by Biesinger et. al. [15] and analyzed using CasaXPS software (version 2.3.14).

2.2.2.2 Contact angle measurements

The wettability of the Ti surfaces was evaluated from static contact angle measurements using a Ramé-Hart Model 100 goniometer with micro-syringe attachment (manual system) (Ramé-Hart Inc., New York, USA). Drops (8 µL) of distilled water were placed on the Ti surfaces using an end-flat micrometer syringe (Gilmon Instrument Inc., Barrington, IL, USA). Contact angles were measured using a coupled telescope equipped with a protractor eyepiece immediately after water drop was placed on the surface of three different titanium discs. At least three drops on each of the two identically samples were measured and averaged. The experimental error was +/- 2^{o}.

2.2.2.3 Surface roughness measurements

The topographies of PT, SLA and SLActive surfaces were measured using mechanical stylus profilometer to assess coarse, microscale topography (Profilometer Surftest SJ-210, Mitutoyo, Japan). The measurements were done in triplicates. The surface roughness (Ra) was quantified as the arithmetic mean of the absolute values of the height profile deviations from the mean. The coarse surface roughness values were obtained according to accepted standards (ISO 4287:1997).

2.2.3 Coating of titanium surfaces discs with saliva

For each independent test, a set of three discs of each surface was tested, and the adsorbed proteins from each surface was later combined as one

sample for further proteomic analyses. Ti discs with three different surfaces were placed in a 24-well plate and incubated with 100 µg of WSS proteins for 2h at room temperature to allow salivary proteins to bind to the surfaces forming a protein-pellicle. After protein adsorption, the surfaces were rinsed for 10 seconds with deionized water to remove unbound proteins. Proteins that remained adsorbed to the surface were further recovered twice using a solution containing 80% acetonitrile, 0.1% TFA, and 19.9% H_2O followed by sonication for 1 min [16]. Samples were dried in a rotary evaporator and protein concentration was measured through the micro bicinchoninic acid (Micro-BCA) assay (Pierce Chemical, Rockford, IL, USA) prior to tryptic digestion. Three independent experiments were performed on three different days.

2.2.4 Proteomic-based mass spectrometry analysis

2.2.4.1 In–solution Digestion

Eight micrograms of adsorbed proteins from three different surfaces and WSS control were dried by a rotary evaporator, denatured and reduced for 2 h by the addition of 50 µL of 4 M urea, 10 mM dithiothreitol (DTT), and 50 mM NH_4HCO_3, pH 7.8. After four-fold dilution with 50 mM NH_4HCO_3, pH 7.8, tryptic digestion was carried out for 18 h at 37°C, after the addition of 2% (w/w) sequencing-grade trypsin (Promega, Madison, WI, USA). Finally, samples were dried in a rotary evaporator, desalted by C-18 ZipTip® Pipette Tips (Millipore, Billerica, MA, USA), and subjected to mass spectrometry analysis [17].

2.2.4.2 Liquid Chromatography Electrospray Ionization Tandem Mass Spectrometry (LC-ESI-MS/MS)

Mass spectrometric analyses were carried out with a LTQ-Velos (Thermo Scientific, San Jose, CA, USA), which allows for in-line liquid chromatography (Easy nLC II instrument, Thermo Scientific) with the capillary fused silica column (column length 10 cm, column ID 75 µm) packed in-house using C-18 resin of 3 µm spherical beads and 100 Å pores size (Michrom BioResources, Auburn, CA, USA) linked to the mass spectrometer using an electrospray ionization in a survey scan in the range of m/z values 390–2000 tandem MS/MS. All tryptic digested samples were dried by rotary evaporator and re-suspended in 15 µL of 97.5% H_2O/2.4% acetonitrile/0.1% formic acid and then subjected to reversed-phase LC-ESI-MS/MS. The nano-flow reversed-phase HPLC was developed with linear 80-minute gradient ranging from 5% to 55% of solvent B (97.5% acetonitrile, 0.1% formic acid) at a flow rate of 200 nL/min with a maximum pressure of 280 bar. Electrospray voltage and the temperature of the ion transfer capillary were 1.8 kV and 250°C respectively. Each survey scan (MS) was followed by automated sequential selection of seven most abundant ions for CID, with dynamic exclusion of the previously selected ions [18].

2.2.5 Data Analysis

The acquired MS/MS spectra generated were searched against the human protein databases (Swiss PROT and TREMBL, http://ca.expasy.org) using Proteome Discoverer 1.3 software and SEQUEST algorithm (Thermo

Scientific, San Jose, CA, USA). The search parameters using SEQUEST included: (1) trypsin as protease with up to 2 missed cleavages, (2) signal-to-noise ratio of 1.5, (3) mass tolerance of precursor ion of 2 Da, and (4) fragment mass tolerance of 0.8 Da and (5) dynamic modifications of oxidized cysteine and methionine and phosphorylated serine and threonine. Parameter Xcorr was used to validate the existence of a peptide within the sample. Xcorr is a value computed from cross correlation of the experimental MS/MS spectrum vs. the candidate peptides in the database, which reveals how closely the real spectrum relates to candidate peptides. Search results were filtered for a False Discovery Rate of 1%, employing a decoy search strategy utilizing a reverse database. A total of three mass spectrometric runs were carried out for each replicate.

2.2.5 Bioinformatics

For protein identification, at least 2 or more peptides were used as search parameters and filter criteria. The identified proteins for each surface were analyzed using the Venny 2.1 online tool [19]. The proteins were further classified and assigned by biological function, molecular interaction, and subcellular origin that were associated with biointegration of dental implants using the Gene Ontology (GO) terms obtained from the UniProt databases [20].

2.2.6 Statistical analysis

Statistical significance was analyzed using Student's t-test when appropriate. Differences at $p \leq 0.05$ were considered statistically significant.

2.3 Results

2.3.1 Titanium Surfaces Characterization

The XPS analyses of PT, SLA and SLActive titanium surfaces used in this study are shown in XPS spectra in Supplementary Figure A2.1, and the chemical composition of each surface is summarized in Table 2.1. The widescan spectra representing the element composition of all surfaces show the presence of titanium atoms (Ti 2p) peaks at 458.65 eV binding energy, oxygen (O 1s) at 530.05 eV, and carbon (C 1s) at 285.05 eV as the main components of the surfaces. The SLActive presented a higher percentage of Ti (20.8%) and oxygen (53.9%) atoms on the surface, and a much lower carbon content (21.7%) in comparison to the PT and SLA surfaces that show a higher carbon composition (38.9% and 34.4%, respectively). In addition, the thickness of the Ti oxide layer was also measured. The oxide layer of the SLActive surface had 10.4 nanometers (nm) in thickness while the PT had 7.0 nm and SLA 7.4 nm (Table 2.1).

Table 2.1. Surface elemental composition (% atomic concentration) and oxide layer thickness as determined by XPS, and Mean values (± SD) of surface roughness parameter (R_a) and contact angle (°).

Ti Surface	Chemical composition (atom %)								Oxide Thickness	Surface Roughness	Contact Angle
	Al	C	Ca	Cl	F	N	O	Ti	(nm)	(R_a)	(°)
PT	-	38.9	0.3	-	0.3	0.3	41.6	18.6	7.0	0.35 ± 0.04*#	80.04 ± 2.4
SLA	-	34.4	-	-	-	1.6	45.5	18.5	7.4	3.40 ± 0.07*	138.29 ± 2.2
SLActive	1.8	21.7	-	0.4	-	1.4	53.9	20.8	10.5	3.38 ± 0.05#	~ 0

*, # Statistically significant differences ($p < 0.001$) between surfaces using t-test.

The surface topography measurement indicated that the PT (machined) presented a smooth surface (R_a of 0.35 ± 0.04 μm) while both SLA and SLActive surfaces showed higher surface roughness with similar R_a values (3.40 ± 0.07 μm and 3.38 ± 0.05 μm, respectively) (Table 2.1), confirming that the surface roughness of the machined PT discs was significantly lower than the roughness of both SLA and SLActive surfaces.

Lastly, static contact angle measurements were performed to study the wettability and hydrophobicity of all surfaces and are summarized in Table 2.1. The mean contact angles (± SD) for PT, SLA, and SLActive surfaces were 80.04° ± 2.38, 138.29° ± 2.20, and ~ 0°, respectively, which indicates that the SLActive is a superhydrophilic surface, and the SLA is hydrophobic, while the PT surface can be considered slightly hydrophilic [21].

2.3.2 Adsorption specificity of Salivary Protein onto titanium surface discs

To study the specificity of titanium surfaces to protein binding, three Ti surfaces (PT, SLA, and SLActive) were incubated with WSS, and the adsorbed proteins were recovered and analyzed through mass spectrometry (LC-ESI-MS/MS). All keratin type I and II proteins were considered contaminants due to the possibility that they originated from skin desquamation, except the keratin type II cytoskeletal 2 oral that was identified in this study.

The initial analysis that aimed to evaluate the binding capacity of different surfaces regarding number of absorbed proteins revealed considerable variability between each Ti surface. The MS data showed that the SLActive adsorbed a

higher number of proteins (142 ± 16) in comparison to the SLA (111 ± 19) and PT (74 ± 8) surfaces, suggesting that rough surfaces SLA and SLActive significantly adsorbed more proteins than the smooth PT (Figure 2.1). The SLActive surface adsorbed a total of 158, 126, and 143 WSS proteins while the PT titanium 65, 78, and 81 proteins, and the SLA 126, 119, and 89 proteins on experiment #1, #2, and #3, respectively (Figure 2.2). The list of proteins retrieved from all surfaces in each replicate is shown in supplementary Table A2.1.

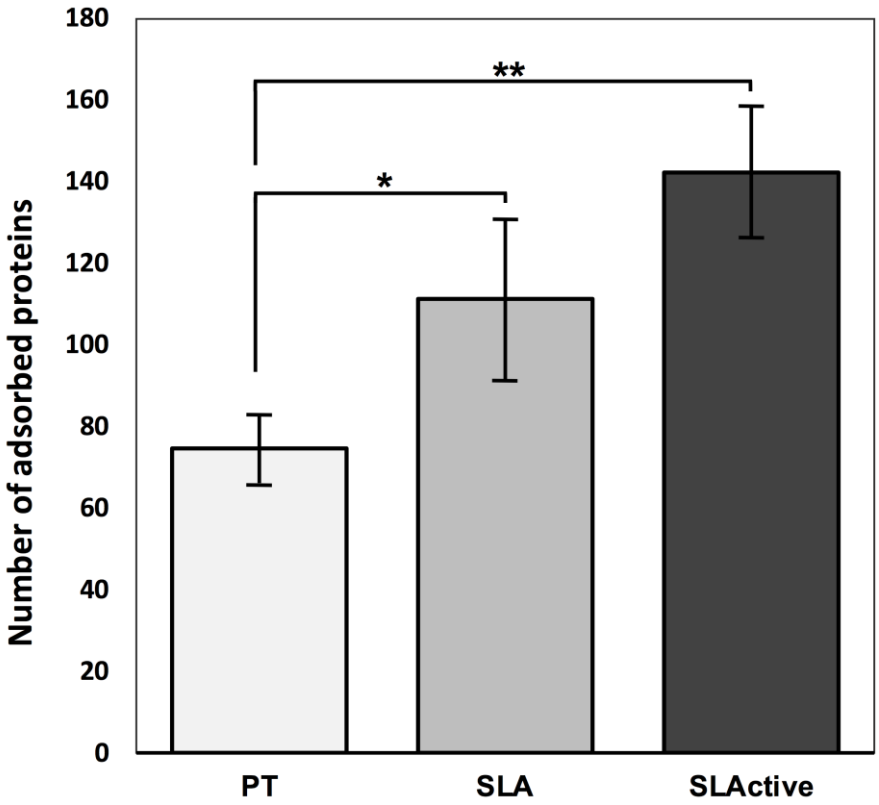

Figure 2.1- Influence of PT, SLA and SLActive titanium surfaces on protein binding showed by the number of adsorbed proteins onto each surface. Bars represent standard deviation of the mean calculated from three independent experiments. The difference between surfaces was calculated using independent t-test; *p=0.041, **p=0.003.

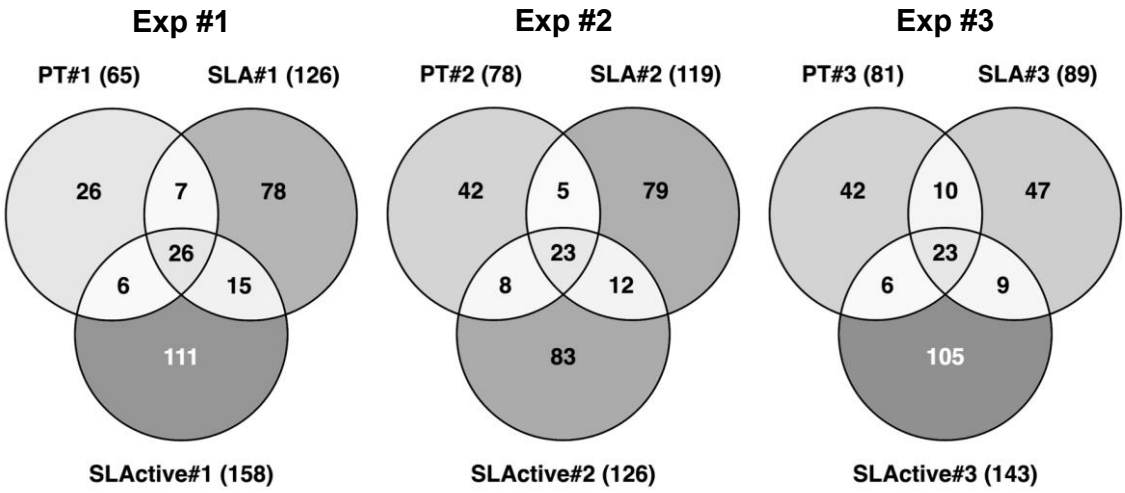

Figure 2.2 - Venn diagrams showing differences in number of proteins identified adsorbed onto the titanium surface PT, SLA, and SLActive in three independent experiments.

Besides differences in number, qualitative variances were also observed in protein binding between the three Ti surfaces. Individual analysis of each replicate suggested that a variability occurs between surfaces in which the majority of proteins adsorbed onto the PT were different from both SLA and SLActive (Figure 2.2 and Supplementary Table A2.1). For example, from 65, 126, and 158 salivary proteins bound to the PT, SLA, and SLActive surfaces on experiment #1, respectively, only 26 proteins were common to all surfaces. Although the variability in proteins adsorption was consistent in all replicates as shown in Figure 2.2, only proteins that were identified in at least two independent experiments were considered having an affinity for a given surface and selected for further analyses. In this scenario, from a total of 603 proteins identified in this study (Supplementary Table A2.1), 83 proteins (13.7%) that matched this criterion were selected. Among these 83 proteins, 37 proteins were adsorbed on the PT surface, 53 on the SLA, and 59 on the SLActive, from a total of 161, 256, and 341 proteins identified on each surface, respectively. The Venn diagram in Figure 2.3 presents the number of proteins that had affinity to each surface and their overlaps between the three groups. Among these proteins, 24 proteins showed specificity for the SLActive surface, 15 exclusively bound on the SLA, and only three proteins preferability adsorbed on the PT (Table 2.2). Contrarily, 25 proteins did not show any specificity for the three surfaces as they were detected on all Ti discs. Therefore, our data indicated that the rough surfaces SLA and SLActive showed a small degree of specificity (29%, and 40%,

respectively) while the smooth PT demonstrated a very low degree (9%), suggesting an overall limited surface specificity for protein-binding.

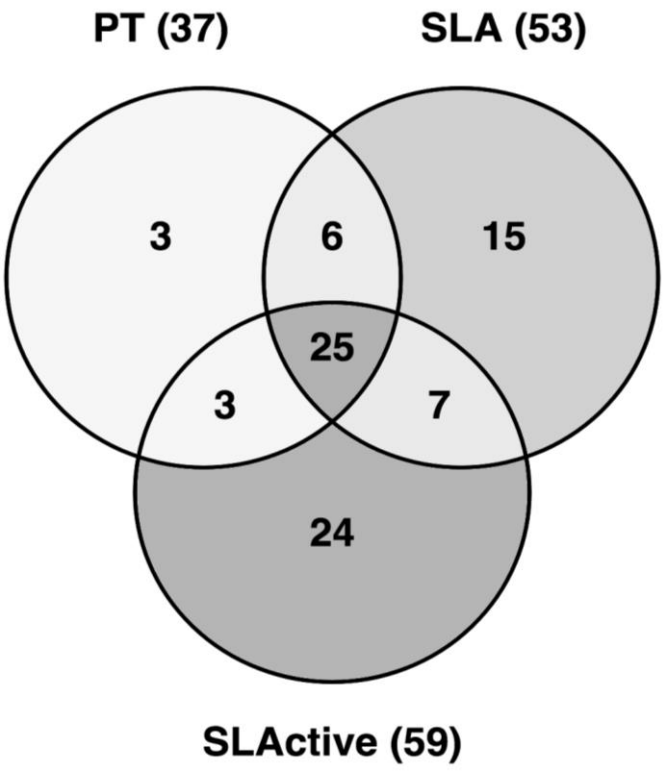

Figure 2.3 - Venn diagrams showing distribution of 83 proteins that adsorbed onto the titanium surface PT (37), SLA (53) and SLActive (59) in at least two independent experiments.

Table 2.2. List of salivary proteins adsorbed at least twice onto all titanium surfaces identified by LC-MS/MS.

Accession Number	Protein name	Molecular Mass (Da)
	PT/SLA/SLActive (25 proteins)	
P04745	Alpha-amylase	57,768
Q12955	Ankyrin-3	480,410
P02647	Apolipoprotein A-I	30,778
Q96DR5	BPI fold-containing family A member 2	27,011
Q8TDL5	BPI fold-containing family B member 1	52,442
P23280	Carbonic anhydrase 6	35,367
P04080	Cystatin-B	11,140
P01036	Cystatin-S	16,214
P04406	Glyceraldehyde-3-phosphate dehydrogenase	36,053
P68871	Hemoglobin subunit beta	15,998
P0DOY2	Ig lambda-2 chain C regions	11,294
P22079	Lactoperoxidase	80,288
P02788	Lactotransferrin	78,182
P61626	Lysozyme C	16,537
Q8WXI7	Mucin-16	1,519,175
Q7Z5P9	Mucin-19	805,253
P98088	Mucin-5AC	585,570
P12273	Prolactin-inducible protein	16,572
P05109	Protein S100-A8	10,835
P06702	Protein S100-A9	13,242
P14618	Pyruvate kinase	57,937
P02814	Submaxillary gland androgen-regulated protein 3B	8,188
Q8WZ42	Titin	3,816,030
P25311	Zinc-alpha-2-glycoprotein	34,259
Q96DA0	Zymogen granule protein 16 homolog B	22,739
	PT (3 proteins)	
P32926	Desmoglein-3	107,533
Q9C0G6	Dynein heavy chain 6, axonemal	475,983
P29401	Transketolase	67,878
	SLA (15 proteins)	
P01009	Alpha-1-antitrypsin	46,737
P02812	Basic salivary proline-rich protein 2	40,799

Q68DE3	Basic helix-loop-helix domain-containing protein KIAA2018	241,681
Q9Y4D8	Probable E3 ubiquitin-protein ligase HECTD4	439,344
A0A024RDF7	Uncharacterized protein	130,254
Q9UDT6	CAP-GLY domain containing linker protein 2	115,837
Q9UBC9	Small proline-rich protein 3	18,154
O15018	PDZ domain-containing protein 2	301,641
Q9ULT8	E3 ubiquitin-protein ligase HECTD1	289,384
Q96K68	cDNA FLJ14473 fis, highly similar to SNC73 protein	53,088
Q15772	Striated muscle preferentially expressed protein kinase	354,289
Q13023	A-kinase anchor protein 6	256,720
Q9Y485	DmX-like protein 1	337,839
Q92954	Proteoglycan 4	151,061
Q8WXG9	G-protein coupled receptor 98	693,069
	SLActive (24 proteins)	
P02808	Statherin	7,304
P15515	Histatin-1	6,963
P23284	Peptidyl-prolyl cis-trans isomerase	23,743
P30740	Leukocyte elastase inhibitor	42,742
Q02505	Mucin-3A	345,127
Q9UKN1	Mucin-12	558,164
Q8N3C7	CAP-Gly domain-containing linker protein 4	76,317
P20930	Filaggrin	435,170
O43166	SIPA1L1 protein	200,029
Q6P0Q8	Microtubule-associated serine/threonine-protein kinase 2	196,436
B4DNY3	Adenylyl cyclase-associated protein	43,706
Q5VUA4	Zinc finger protein 318	251,112
B7ZKN7	BLM protein	117,063
Q9UF83	Uncharacterized protein DKFZp434B061	59,412
Q7Z589	BRCA2-interacting transcriptional repressor EMSY	141,468
Q5TAX3	Terminal uridylyltransferase 4	185,166
Q92824	Proprotein convertase subtilisin/kexin type 5	206,942
Q8IVF2	Protein AHNAK2	616,629
Q7Z6Z7	E3 ubiquitin-protein ligase HUWE1	481,891
Q13707	ACTA2 protein	36,807
O15075	Serine/threonine-protein kinase DCLK1	82,224
Q9UPN3	Microtubule-actin cross-linking factor 1, isoforms 1/2/3/5	838,308
P46013	Proliferation marker protein Ki-67	358,694
Q9Y6V0	Protein piccolo	560,699
	PT/SLA (6 proteins)	
P60709	Actin, cytoplasmic 1	41,737

P01833	Polymeric immunoglobulin receptor	83,284
P05164	Myeloperoxidase	83,869
Q8N4F0	BPI fold-containing family B member 2	49,172
P01034	Cystatin-C	15,799
P07737	Profilin-1	15,054
	PT/SLActive (3 proteins)	
P01876	Ig alpha-1 chain C region	37,655
Q7Z460	CLIP-associating protein 1	169,451
P02768	Serum albumin	69,367
	SLA/SLActive (7 proteins)	
P80303	Nucleobindin-2	50,223
P0DOX7	Immunoglobulin kappa light chain	23,379
Q99102	Mucin-4	231,518
Q5VV67	Peroxisome proliferator-activated receptor gamma coactivator-related protein 1	177,544
Q8TAX7	Mucin-7	39,159
Q5SW79	Centrosomal protein 170kDa	175,293
P23528	Cofilin-1	18,502

** Protein identified in plasma after matching Plasma Protein Database*

2.3.3 Proteome of salivary pellicle formed onto different titanium surfaces

The characterization of the salivary proteome adsorbed onto the PT, SLA, and SLActive Ti discs was carried out to explore the composition of the protein-pellicle formed onto each surface since dental implants are exposed to saliva during placement. The protein annotation of the 83 proteins was based on the UniProt identifiers using the gene ontology (GO) terms to categorize the protein adsorbed to each surface. The analysis was tailored to emphasize functions and interactions associated with biointegration of dental implants with the surrounding tissues of the oral cavity, i.e., bone and soft tissues. The classification of the proteins with affinity to different Ti surfaces showed a high similarity between surfaces regarding biological function, molecular interaction and sub-cellular localization (Figure 2.4). The analysis showed that a similar number of proteins adsorbed onto each surface are involved in immune response, including proteins with antimicrobial activity. Likewise, the number of proteins adsorbed on the PT, SLA and SLActive surfaces that are related to tissue development and regeneration were almost identical (13, 15, and 15, respectively).

It is worth mentioning that many of these proteins are common to other surfaces, and that they carry more than one function. For example, cystatin-C and myeloperoxidase that were detected on the PT and SLA are players in tissue remodeling and immune response. Also, CLIP-associating protein-1 that was identified on both PT and SLActive is known to be involved in biological adhesion and tissue regeneration. The most significant overlap includes 25

proteins that showed affinity to all three surfaces. This group contains proteins such as the zinc-alpha-2-glycoprotein that participate in biological adhesion and tissue regeneration, and apolipoprotein A-I, that has roles in cell adhesion and immune defense (Table 2.2). Interestingly, most of the 25 proteins common to all surfaces are proteins associated with the immune response (13 proteins) such as cystatin B, calgranulin A and B (also known as protein S100-A8 and S100-A9), lysozyme C, lactoperoxidase, mucins 5AC, 16, and 19, and lactotransferrin. Particularly, among these, 4 proteins are also involved in biomineralization (cystatin B, lactotransferrin S100-A8 and S100-A9), in addition to three other proteins exclusively found on the SLActive surface (histatin 1, statherin, and peptidyl-prolyl cis-trans isomerase B), and cystatin C that was detected on both PT and SLA surfaces. Lastly, our results show that among 83 proteins adsorbed onto the surfaces, 56 (~ 67%) were also identified in serum, including albumin, hemoglobin, Immunoglobulins, and apolipoproteins A-I (Supplementary Table A2.2).

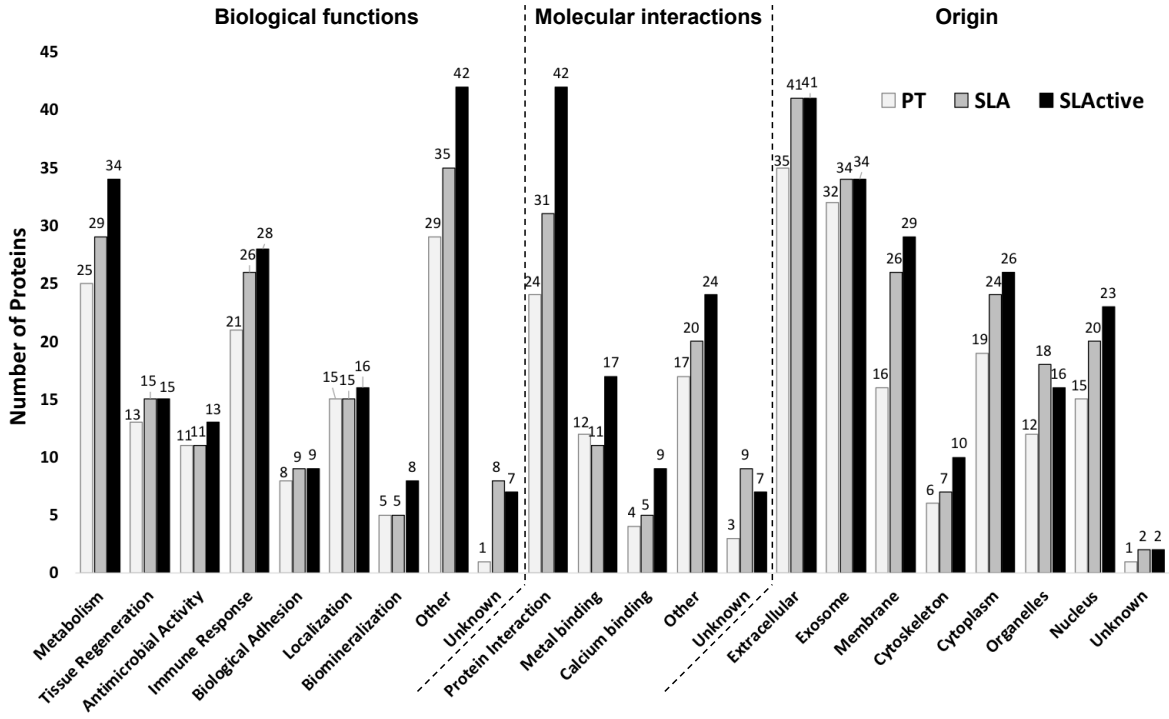

Figure 2.4 - Histogram showing the distribution of proteins adsorbed at least twice onto each titanium surface according to biological functions, molecular interactions and origin acquired from UniProt using GO terms. Proteins having more than one function, interaction, and origin were counted multiple times.

2.4 Discussion

During placement, dental implants are exposed to complex biological fluids in the oral cavity, such as blood, gingival crevicular fluid, and saliva before starting the osseointegration process. It is well-known that the surface physico-chemical properties directly influence the adsorption and formation of a protein layer that modulate the biological response from the surrounding tissues [4]. However, it is unclear whether the pellicle composition is specific to a given surface due to variances in surface energy, topography and chemistry between distinct substrata. Likewise, it is uncertain which proteins from saliva preferably bind to distinct titanium modifications. Therefore, the present study aimed to evaluate the surface-specificity for protein binding of three titanium surfaces utilized in dental practice (PT, SLA, and SLActive) after incubation with WSS, and to further characterize the salivary-pellicle formed onto each surface.

The characterization of each titanium surface showed differences in roughness, chemistry, and surface free energy (wettability) as expected (Table 2.1). The topography measurement indicated that both SLA and SLActive are rougher surfaces than the PT that presented a lower R_a value (< 1) as detailed in other studies [11, 22]. Regarding surface chemistry, which is well-known to play a pivotal role in protein-surface interactions [23], the XPS analysis showed that chemical composition was also distinct between the Ti surfaces, mainly between SLActive and the other two surfaces (SLA and PT) as shown in Table 2.2. The analysis revealed that the SLActive surface presented a higher titanium and oxygen content and lower carbon contamination. These characteristics are

directly related to higher surface energy and hydrophilicity that was showed by the nearly zero contact angle of the SLActive to the water during measurement [14]. Changes in surface chemistry achieved by surface roughness impact both surface charge (free energy) and wettability, which are recognized as being able to modulate protein binding by influencing the interactions between the surface and the surrounding protein-rich-aqueous environment [24]. Another difference observed between the surfaces was that the SLActive presented a titanium oxide layer 30% thicker than both SLA and PT surfaces. The oxide layer is created by the reaction of highly reactive titanium atoms with oxygen forming the outer layer of the titanium surface that generate a higher net charge. This could be another factor in increasing the adsorption of proteins onto the oxide layer coated surfaces [25].

The parameters aforementioned can explain the variances observed on protein binding when looking specifically at each titanium surface considered in this study. The MS data indicated that the SLActive Ti was more capable of adsorbing proteins from saliva as the protein-pellicle composition was more diverse on average (142 proteins) than on the rough-hydrophobic SLA (111 proteins) and the smooth PT (74 proteins) surfaces (Figure 2.1). After isolating the effect of surface topography on protein adsorption, the data also indicates a more diverse pellicle composition formed on the rough surfaces. This observation is likely due to the larger contact area that rough surfaces have, which is known to directly impact protein amount and diversity since a larger area provides more binding sites for proteins to interact with the surface [26, 27].

However, it is not possible to associate the influence of one surface characteristic such as topography on protein binding because the resulted roughness from the surface treatment also transforms the surface chemistry and free energy [24, 26, 28]. As shown in recent studies, it is extremely challenging to isolate the effect that surface topography, chemistry, and surface free energy have on protein adsorption because they work cooperatively to guide protein-surface interactions, particularly involving complex protein mixture [29, 30]. Therefore, these results suggest that an interplay between surface characteristics have a combined influence on protein binding on the surfaces evaluated in this study.

To evaluate protein-binding specificity, only proteins that were detected at least in two independent experiments on the same surface were considered as having affinity to a surface. This criterion was selected as these proteins were more likely to make specific interaction with the surface, and only those that bound solely to the surface were considered surface-specific. Under these conditions, 83 proteins were then selected from a total of 603 proteins identified, in which the PT showed an affinity for 37 proteins, SLA for 53, and SLActive for 59 proteins, resulting in different pellicle compositions. Although the selective adsorption of protein possibly occurred due to variances between surfaces, a high surface specificity was not observed; instead, it was limited. The proteome analysis revealed that each surface modification had different degrees of specificity. The PT surface showed the lowest degree of specificity with only 3 proteins exclusively bound to the surface (9%), while on the SLA, the specificity

increased to 29%. The highest degree of specificity was presented by the SLActive that adsorbed 24 unique proteins, which is equivalent to 40% of the proteins adhered to the surface. Since the majority of adsorbed proteins are also found adsorbed onto another, it is reasonable to suggest that the Ti surfaces in this study presented a low specificity for protein binding. Interestingly, from 83 proteins, 25 were common to all surfaces including the most abundant salivary proteins alpha-amylase, carbonic anhydrase, mucin-5AC, and lysozyme C among others. These findings suggest a lack of surface-specificity but high affinity for titanium substrata despite the surface modifications (Table 2.2). The absences of specificity can be attributed to a combination of factors such as surface characteristics, complexity of the protein mixture, and competition for binding [29, 30]. Given the complexity that involves protein-surface interactions, it is very challenging to determine which factors could have caused the low surface specificity revealed in this study. Therefore, more studies are needed to understand the dynamics involved in protein-surface interactions, especially regarding complex protein mixtures as saliva.

The characterization of the salivary proteome and its composition on the enamel surface has been investigated [31], but few studies have explored the salivary pellicle formed onto titanium surfaces [32, 33]. Given the complexity of protein-surface interaction, the work has been largely done on studying the adsorption of few salivary proteins that are used by bacteria to colonize the titanium surfaces that could lead to peri-implantitis and implant loss [21, 34]. By employing mass spectrometry-based proteomics, we could identify a total of 83

proteins that adsorbed onto three distinctive titanium surfaces, some of which have been reported by other studies, such as alpha-amylase, IgA, cystatins, albumin, IgG, prolactin-inducible protein, and lactotransferrin [32, 33, 35]. Our findings are supported by a recent study that identified salivary proteins on smooth Ti surfaces through 2D-SDS-PAGE and mass spectrometry [32]. The authors detected alpha-amylase, cystatins (D, SA, and S), IgA, and prolactin-inducible protein (PIP) forming the salivary pellicle, which is a small number of proteins in comparison to our study. The limited number of proteins identified was probably due to protein degradation during pellicle formation that occurred overnight, which could have allowed proteases contained in saliva to cleave salivary proteins that would have adsorbed onto the surface. Differently, in our study the Ti surfaces were incubated during 2 hours at room temperature, which reduced the exposure to degradation. As a result, we identified a larger number of proteins (37 proteins) adsorbed on the smooth PT, such as the calgranulins A and B (S100A8 and S100A9), cystatins B and C. Particularly, we detected zinc-alpha2-glycoprotein, which was suggested by the authors that it does not adhere to titanium due to higher abundance of the PIP. Contrarily, the present study showed that zinc-alpha2-glycoprotein not only binds to the smooth PT but also to the rough SLA and SLActive surfaces in the presence of PIP, suggesting that zinc-alpha2-glycoprotein has a high affinity for titanium regardless of surface modification, and that PIP does not interfere in this interaction. The adsorption of zinc-alpha2-glycoprotein on Ti surfaces may have an importance on the biointegration of implants. Studies have shown that it promotes cell adhesion

comparable to fibronectin due to the presence of Arg-Gly-Asp (RGD) motif [36, 37], which mediates cell attachment via integrins on the surface of cells such as gingival fibroblasts [38] and osteoblastic cells [39].

Furthermore, other glycoproteins were also identified such as mucins (Mucin-4, 5AC, 7, 12, 16, and 19), lysozyme C, and lactotransferrin. Although mucins are mainly associated with lubrication of oral tissues, Mucin-5AC and Mucin-7 are recognized to have protective functions against microorganisms as they have the ability to form a gel that binds to microorganisms to facilitate their removal from the oral cavity [40]. Besides lysozyme C and lactotransferrin, other proteins that participate in immune response and antimicrobial activity were also detected on all surfaces, including immunoglobulins, S100A8, S100A9, cystatin B and S, and lactoperoxidase in addition to cystatin C and myeloperoxidase, only identified on both PT and SLA surfaces, and histatin 1 that only absorbed onto the SLActive. Besides being a antimicrobial protein, histatin 1 is also involved in biological adhesion that has been showed to enhance cell adhesion and spreading of oral fibroblasts and epithelial cells onto Ti surface in a canine model suggesting the applicability of histatin-1 to improve implant biointegration [41]. The detection of histatin 1 might be questioned since histatins are prone to degradation once reach the oral cavity [42]. However, histatin 1 is known to make protein-protein interaction in saliva with alpha-amylase [43], which also make complexes with other proteins such as mucins [44]. Protein-protein interaction also occur with lysozyme, which is recognized to interact with mucins [45] and albumin [46]. According to a recent study, lysozyme not only binds to

titanium alone, but it interacts with albumin in a cooperative manner while maintaining its antimicrobial activity, whether adsorbed alone to the surface or complexed [46]. Protein-protein interactions are extremely important in biological systems for protection against degradation and to deliver proper biological function [47].

The presence of antimicrobial proteins on Ti surfaces may provide a protective role against microorganism colonization around the implant under healthy conditions or in periodontitis-susceptible patients with an adequate infection control, since implant loss is highly linked to unsuccessful treatment when patient carries ongoing periodontitis [48]. For example, the adsorption of lactotransferrin on Ti surfaces may contribute to preventing local infection at the implanted site since it is recognized as a potent inhibitor of periodontal pathogens such as *Porphyromonas gingivalis* and *Prevotella intermedia* by inhibiting biofilm formation [49, 50]. Likewise, the adsorption of cystatin-C may be beneficial to prevent peri-implantitis since it shows antimicrobial activity against multiresistant coagulase-negative staphylococci that are known to adhere onto Ti surface causing implant failure [51, 52]. Moreover, a study showed that the adsorption of *Streptococcus mutans* was reduced on titanium surface coated with saliva in comparison to non-coated surface. However, when the surface was coated with serum only, the number of bacteria on the surface increased [33]. It is plausible that the adsorption of antimicrobial proteins onto the implant surface is continuous due to the constant flow of saliva, which could assist in maintaining homeostasis around the dental implant during the healing

phase. Saliva could help preventing local infection and inflammation that can lead to peri-implantitis and possible implant loss. However, in another study that used a flow-cell system, the authors observed no significant difference in colonization and cell viability of *Streptococcus oralis* on titanium coated with diluted saliva (25%) [21], which could have been the reason for lack of protection. Although it is still debatable whether saliva can promote or hinder bacteria colonization onto dental implant surfaces, it is possible that the constant flow of salivary proteins may facilitate protein adsorption onto Ti surfaces to help protect the surfaces against bacteria colonization during the implant biointegration with the surrounding tissues.

It is important to mention that 67% of proteins adsorbed onto all titanium surfaces combined have been detected in serum, such as albumin, immunoglobulins, apolipoprotein A-I, S100A8 and S100A9, and myeloperoxidase to name a few (Supplementary Table A2.2). Serum proteins are extremely important for osseointegration since the titanium implants are covered by blood once placed into the bone [53]. Many studies have tried to identify possible biomarkers in serum that immediately adhere on the implant surface, and could activate osteoblast-precursors cell triggering the subsequent osteogenesis [54, 55]. In a recent proteomic study, Romero-Gavilán et al. identified proteins from human serum on different Ti surface (smooth and blasted acid-etched) that are directly or indirectly involved in bone metabolism, biological adhesion and immune response. Many of these proteins were identified in the current study, such as peptidyl-prolyl cis-trans isomerase B, lysozyme C, and proteoglycan 4

[55]. In another report, the adsorption of both serum and saliva proteins to titanium surface were studied through SDS-PAGE/Western blot [33]. Among the proteins investigated (IgA, IgG, fibronectin, fibrinogen, albumin, amylase, Cystatin S and SN), the authors identified all serum proteins on Ti surface coated with saliva except albumin. Alpha-amylase was the only salivary protein detected while cystatin S and SN were not found. In our work, however, we showed that not only cystatin S adsorbs on Ti surfaces, but also cystatin B and C among many other salivary proteins and proteins derived from serum, which enter the oral cavity through the gingival crevicular fluid. Although serum proteins are found in saliva in smaller amount compared to proteins secreted from salivary glands (major and minors), and originating from oral epithelium [56], our findings suggest that Ti surfaces have high affinity for serum proteins despite not being in direct contact to the gingival sulcus – which occurs with dental implants – from where serum proteins navigate to reach the oral cavity. Therefore, Ti surfaces may play an important role in providing a reactive surface to bind proteins from serum which are known to be important for the biointegration of dental implants.

Of interest, many proteins that participate in host defense are also involved in mineralization and bone metabolism, such as the multi-function lactotransferrin [57]. Besides its significant participation in innate immune response [58], lactotransferrin may be directly involved in bone morphogenesis as it positively regulates osteoblast proliferation, differentiation, and bone growth [59, 60] while also inhibiting osteoblast apoptosis [61], which are essential

functions to promote osteogenesis and osseointegration. Other proteins identified herein involved in bone metabolism are cystatin B and C, S100A8 and S100A9. Cystatin B and C are cysteine proteinase inhibitors that actively participate in modulating bone metabolism by inactivating osteoclast activity via Inhibition of cathepsin K enzyme activity [62-64], a cysteine proteinase essential in bone resorption [65] and calcification, which suggests a contribution in bone formation [66]. Similarly, both S100A8 and S100A9 have been related with inflammation and bone resorption. They belong to a family of calcium-binding proteins that are produced by epithelial tissues, as well as neutrophils and macrophages in inflammatory response [67] that are also expressed in human bone and cartilage cells. Studies have shown that both S100A8 and S100A9 may participate in early stage of inflammatory osteoarthritis [68] by stimulating osteoclast formation and activity through Toll-like receptor 4 during ongoing osteoclastogenesis [69]. S100A8 and S100A9 are also associated with periodontal diseases as studies have found both proteins in high levels in gingival crevicular fluid of gingival tissues with gingivitis and periodontitis [70, 71]. However, there is evidence that S100A8 is associated with osteoblast differentiation, while both proteins have been linked not only to the maturation processes of osteoblast and chondrocyte, but also to cartilage matrix calcification and its substitution with trabecular bone [66], which may positively contribute during the osseointegration process that involves bone apposition and bone remodeling.

In summary, this is the first study that explored the binding specificity of the Ti surfaces PT, SLA, and SLActive to salivary proteins, and the composition of salivary pellicle formed on each surface. Although topography, chemistry, and energy were significant different between the surfaces, our findings suggested that they were not determinant to produce a salivary pellicle with high surface-specificity. Additionally, this study showed that the Ti surfaces adsorbed several salivary proteins involved in biological functions that are important to assist the biointegration of dental implants in the oral cavity. However, more studies are necessary to investigate how Ti surfaces covered with salivary proteins can influence the biological response from surrounding tissues during implant treatment.

2.5 References

1. Plecko, M., et al., *Osseointegration and biocompatibility of different metal implants--a comparative experimental investigation in sheep.* BMC Musculoskelet Disord, 2012. **13**: p. 32.

2. Branemark, P.I., *Introduction to osseointegration.*, in *Tissue integrated prosthesis.* , P.I. Branemark, G.A. Zarb, and T. Albrektsson, Editors. 1985, Quintessence International: Chicago. p. 11–76.

3. Davies, J.E., *Mechanisms of endosseous integration.* Int J Prosthodont, 1998. **11**(5): p. 391-401.

4. Ellingsen, J.E., *Surface configurations of dental implants.* Periodontol 2000, 1998. **17**: p. 36-46.

5. Puleo, D.A. and A. Nanci, *Understanding and controlling the bone-implant interface.* Biomaterials, 1999. **20**(23-24): p. 2311-21.

6. Schuler, M., et al., *Biomimetic modification of titanium dental implant model surfaces using the RGDSP-peptide sequence: a cell morphology study.* Biomaterials, 2006. **27**(21): p. 4003-15.

7. Cooper, L.F., *A role for surface topography in creating and maintaining bone at titanium endosseous implants.* J Prosthet Dent, 2000. **84**(5): p. 522-34.

8. Le Guehennec, L., et al., *Surface treatments of titanium dental implants for rapid osseointegration.* Dent Mater, 2007. **23**(7): p. 844-54.

9. Cochran, D.L., et al., *Bone response to unloaded and loaded titanium implants with a sandblasted and acid-etched surface: a histometric study in the canine mandible.* J Biomed Mater Res, 1998. **40**(1): p. 1-11.

10. Cochran, D.L., et al., *The use of reduced healing times on ITI (R) implants with a sandblasted and acid-etched (SLA) surface: Early results from clinical trials on ITI (R) SLA implants.* Clinical Oral Implants Research, 2002. **13**(2): p. 144-153.

11. Buser, D., et al., *Enhanced bone apposition to a chemically modified SLA titanium surface.* J Dent Res, 2004. **83**(7): p. 529-33.

12. Costa, D.O., et al., *The differential regulation of osteoblast and osteoclast activity by surface topography of hydroxyapatite coatings.* Biomaterials, 2013. **34**(30): p. 7215-26.

13. Martin, J.Y., et al., *Effect of titanium surface roughness on proliferation, differentiation, and protein synthesis of human osteoblast-like cells (MG63).* J Biomed Mater Res, 1995. **29**(3): p. 389-401.

14. Rupp, F., et al., *Enhancing surface free energy and hydrophilicity through chemical modification of microstructured titanium implant surfaces.* J Biomed Mater Res A, 2006. **76**(2): p. 323-34.

15. Biesinger, M.C., et al., *Resolving surface chemical states in XPS analysis of first row transition metals, oxides and hydroxides: Sc, Ti, V, Cu and Zn.* Applied Surface Science, 2010. **257**(3): p. 887-898.

16. Siqueira, W.L., et al., *Quantitative proteomic analysis of the effect of fluoride on the acquired enamel pellicle.* PLoS One, 2012. **7**(8): p. e42204.

17. Zuanazzi, D., et al., *Postnatal Identification of Zika Virus Peptides from Saliva.* J Dent Res, 2017. **96**(10): p. 1078-1084.

18. Crosara, K.T.B., et al., *Merging in-silico and in vitro salivary protein complex partners using the STRING database: A tutorial.* J Proteomics, 2018. **171**: p. 87-94.

19. Oliveros, J.C. *Venny. An interactive tool for comparing lists with Venn's diagrams.* http://bioinfogp.cnb.csic.es/tools/venny/index.html. 2007-2015.

20. UniProt, C., *UniProt: a hub for protein information.* Nucleic Acids Res, 2015. **43**(Database issue): p. D204-12.

21. Dorkhan, M., et al., *Effects of saliva or serum coating on adherence of Streptococcus oralis strains to titanium.* Microbiology, 2012. **158**(Pt 2): p. 390-7.

22. Grassi, S., et al., *Histologic evaluation of early human bone response to different implant surfaces.* J Periodontol, 2006. **77**(10): p. 1736-43.

23. Hallab, N.J., et al., *Evaluation of metallic and polymeric biomaterial surface energy and surface roughness characteristics for directed cell adhesion.* Tissue Eng, 2001. **7**(1): p. 55-71.

24. Kilpadi, D.V. and J.E. Lemons, *Surface energy characterization of unalloyed titanium implants.* J Biomed Mater Res, 1994. **28**(12): p. 1419-25.

25. Sunny, M.C. and C.P. Sharma, *Titanium-protein interaction: changes with oxide layer thickness.* J Biomater Appl, 1991. **6**(1): p. 89-98.

26. Sela, M.N., et al., *Adsorption of human plasma proteins to modified titanium surfaces.* Clin Oral Implants Res, 2007. **18**(5): p. 630-8.

27. Rechendorff, K., et al., *Enhancement of protein adsorption induced by surface roughness.* Langmuir, 2006. **22**(26): p. 10885-8.

28. Lim, Y.J., et al., *Surface characterizations of variously treated titanium materials.* Int J Oral Maxillofac Implants, 2001. **16**(3): p. 333-42.

29. Rabe, M., D. Verdes, and S. Seeger, *Understanding protein adsorption phenomena at solid surfaces.* Adv Colloid Interface Sci, 2011. **162**(1-2): p. 87-106.

30. Wilson, C.J., et al., *Mediation of biomaterial-cell interactions by adsorbed proteins: a review.* Tissue Eng, 2005. **11**(1-2): p. 1-18.

31. Lee, Y.H., et al., *Proteomic evaluation of acquired enamel pellicle during in vivo formation.* PLoS One, 2013. **8**(7): p. e67919.

32. Dorkhan, M., G. Svensater, and J.R. Davies, *Salivary pellicles on titanium and their effect on metabolic activity in Streptococcus oralis.* BMC Oral Health, 2013. **13**: p. 32.

33. Lima, E.M., et al., *Adsorption of salivary and serum proteins, and bacterial adherence on titanium and zirconia ceramic surfaces.* Clin Oral Implants Res, 2008. **19**(8): p. 780-5.

34. Edgerton, M., S.E. Lo, and F.A. Scannapieco, *Experimental salivary pellicles formed on titanium surfaces mediate adhesion of streptococci.* Int J Oral Maxillofac Implants, 1996. **11**(4): p. 443-9.

35. Cavalcanti, I.M., et al., *Salivary pellicle composition and multispecies biofilm developed on titanium nitrided by cold plasma.* Arch Oral Biol, 2014. **59**(7): p. 695-703.

36. Lei, G., et al., *Characterization of zinc-alpha(2)-glycoprotein as a cell adhesion molecule that inhibits the proliferation of an oral tumor cell line.* J Cell Biochem, 1999. **75**(1): p. 160-9.

37. Takagaki, M., et al., *Zn-alpha 2-glycoprotein is a novel adhesive protein.* Biochem Biophys Res Commun, 1994. **201**(3): p. 1339-47.

38. Bax, D.V., et al., *Cell adhesion to fibrillin-1 molecules and microfibrils is mediated by alpha 5 beta 1 and alpha v beta 3 integrins.* J Biol Chem, 2003. **278**(36): p. 34605-16.

39. Ogikubo, O., et al., *Regulation of Zn-alpha2-glycoprotein-mediated cell adhesion by kininogens and their derivatives.* Biochem Biophys Res Commun, 1998. **252**(1): p. 257-62.

40. Tabak, L.A., *Structure and function of human salivary mucins.* Crit Rev Oral Biol Med, 1990. **1**(4): p. 229-34.

41. van Dijk, I.A., et al., *Histatin 1 Enhances Cell Adhesion to Titanium in an Implant Integration Model.* J Dent Res, 2017. **96**(4): p. 430-436.

42. Helmerhorst, E.J., et al., *Oral fluid proteolytic effects on histatin 5 structure and function.* Arch Oral Biol, 2006. **51**(12): p. 1061-70.

43. Siqueira, W.L., et al., *Identification and characterization of histatin 1 salivary complexes by using mass spectrometry.* Proteomics, 2012. **12**(22): p. 3426-35.

44. Crosara, K.T.B., et al., *Revealing the Amylase Interactome in Whole Saliva Using Proteomic Approaches.* BioMed Research International, 2018. **2018**: p. 15.

45. Wickstrom, C., et al., *Macromolecular organization of saliva: identification of 'insoluble' MUC5B assemblies and non-mucin proteins in the gel phase.* Biochem J, 2000. **351 Pt 2**: p. 421-8.

46. Rosch, C., et al., *Albumin-lysozyme interactions: Cooperative adsorption on titanium and enzymatic activity.* Colloids Surf B Biointerfaces, 2017. **149**: p. 115-121.

47. Moffa, E.B., et al., *In Vitro Identification of Histatin 5 Salivary Complexes.* PLoS One, 2015. **10**(11): p. e0142517.

48. Sgolastra, F., et al., *Periodontitis, implant loss and peri-implantitis. A meta-analysis.* Clin Oral Implants Res, 2015. **26**(4): p. e8-16.

49. Dashper, S.G., et al., *Lactoferrin inhibits Porphyromonas gingivalis proteinases and has sustained biofilm inhibitory activity.* Antimicrob Agents Chemother, 2012. **56**(3): p. 1548-56.

50. Wakabayashi, H., et al., *Inhibitory effects of lactoferrin on growth and biofilm formation of Porphyromonas gingivalis and Prevotella intermedia.* Antimicrob Agents Chemother, 2009. **53**(8): p. 3308-16.

51. Hanif, A., et al., *Complications in implant dentistry.* Eur J Dent, 2017. **11**(1): p. 135-140.

52. Nguyen, T.H., M.D. Park, and M. Otto, *Host Response to Staphylococcus epidermidis Colonization and Infections.* Front Cell Infect Microbiol, 2017. **7**: p. 90.

53. MacDonald, D.E., et al., *Adsorption and dissolution behavior of human plasma fibronectin on thermally and chemically modified titanium dioxide particles.* Biomaterials, 2002. **23**(4): p. 1269-79.

54. Dodo, C.G., et al., *Proteome analysis of the plasma protein layer adsorbed to a rough titanium surface.* Biofouling, 2013. **29**(5): p. 549-57.

55. Romero-Gavilan, F., et al., *Proteome analysis of human serum proteins adsorbed onto different titanium surfaces used in dental implants.* Biofouling, 2017. **33**(1): p. 98-111.

56. Barros, S.P., et al., *Gingival crevicular fluid as a source of biomarkers for periodontitis.* Periodontol 2000, 2016. **70**(1): p. 53-64.

57. Cavalcanti, Y.W., et al., *Titanium Surface Roughing Treatments contribute to Higher Interaction with Salivary Proteins MG2 and Lactoferrin.* J Contemp Dent Pract, 2015. **16**(2): p. 141-6.

58. Weinberg, E.D., *Human lactoferrin: a novel therapeutic with broad spectrum potential.* J Pharm Pharmacol, 2001. **53**(10): p. 1303-10.

59. Hou, J.M., et al., *Lactoferrin Induces Osteoblast Growth through IGF-1R.* Int J Endocrinol, 2015. **2015**: p. 282806.

60. Cornish, J., *Lactoferrin promotes bone growth.* Biometals, 2004. **17**(3): p. 331-5.

61. Hou, J.M., et al., *Lactoferrin inhibits apoptosis through insulin-like growth factor I in primary rat osteoblasts.* Acta Pharmacol Sin, 2014. **35**(4): p. 523-30.

62. Manninen, O., et al., *Impaired osteoclast homeostasis in the cystatin B-deficient mouse model of progressive myoclonus epilepsy.* Bone Rep, 2015. **3**: p. 76-82.

63. Laitala-Leinonen, T., et al., *Cystatin B as an intracellular modulator of bone resorption.* Matrix Biol, 2006. **25**(3): p. 149-57.

64. Brage, M., et al., *Different cysteine proteinases involved in bone resorption and osteoclast formation.* Calcif Tissue Int, 2005. **76**(6): p. 439-47.

65. Littlewood-Evans, A., et al., *Localization of cathepsin K in human osteoclasts by in situ hybridization and immunohistochemistry.* Bone, 1997. **20**(2): p. 81-6.

66. Zreiqat, H., et al., *S100A8/S100A9 and their association with cartilage and bone.* J Mol Histol, 2007. **38**(5): p. 381-91.

67. Rammes, A., et al., *Myeloid-related protein (MRP) 8 and MRP14, calcium-binding proteins of the S100 family, are secreted by activated monocytes via a novel, tubulin-dependent pathway.* J Biol Chem, 1997. **272**(14): p. 9496-502.

68. Zreiqat, H., et al., *S100A8 and S100A9 in experimental osteoarthritis.* Arthritis Res Ther, 2010. **12**(1): p. R16.

69. Grevers, L.C., et al., *S100A8 enhances osteoclastic bone resorption in vitro through activation of Toll-like receptor 4: implications for bone destruction in murine antigen-induced arthritis.* Arthritis Rheum, 2011. **63**(5): p. 1365-75.

70. Kojima, T., et al., *Human gingival crevicular fluid contains MRP8 (S100A8) and MRP14 (S100A9), two calcium-binding proteins of the S100 family.* J Dent Res, 2000. **79**(2): p. 740-7.

71. Lundy, F.T., et al., *Quantitative analysis of MRP-8 in gingival crevicular fluid in periodontal health and disease using microbore HPLC.* J Clin Periodontol, 2001. **28**(12): p. 1172-7.

Chapter 3

New insights on the proteome of enamel matrix derivative (EMD)

3.1 Introduction

Enamel matrix derivative (EMD) is a complex mixture of proteins produced by ameloblasts that is extracted from developing porcine teeth [1]. The major constituent of EMD are the amelogenins, a family of hydrophobic low-molecular weight proteins highly conserved across various species including porcine and human that comprise > 90% of the organic constituent of the enamel matrix [2]. The remaining portion consist of other proteins that are secreted by the ameloblasts in smaller quantity, including the enamelin [3], ameloblastin (or sheathlin) [4], matrix metalloproteinase-20 (MMP-20) [5], kallikrein-4 (also known as enamel matrix serine proteinase 1) [6], and tuftelin [7]. In addition, immunoassay studies indicated the possible presence of growth factors-like proteins similar to transforming growth factor-β (TGF-β) and bone morphogenetic proteins (BMP-2, and BMP-4) [8-10]. Besides its physiologic role in enamel development, EMD has been significantly studied and applied as a biomaterial by the name of Emdogain® (Institut Straumann AG) in regenerative dentistry for the past twenty years [11]. The combination of numerous clinical cases, *in vitro*, and *in vivo* studies have demonstrated that EMD promote bone regeneration by modulating osteoblasts behavior [12], stimulate proliferation and migration of endothelial cells in angiogenesis [13, 14] that are essential for wound healing

[15], and stimulates cell proliferation, differentiation, and gene expression on periodontal ligament fibroblasts [16]. Studies have hypothesized that the diverse biological effects on numerous cell types could be due to unknow constituents that comprise EMD [11, 17]. Therefore, the discovery of novel proteins within EMD is strongly recommended to fully understand which protein/peptides could direct or indirectly influence various cells types in distinct biological processes such as osteogenesis and wound healing [15, 18]. Herein, we carried out a proteome analysis using a two-dimensional liquid chromatography approach including off-line size-exclusion chromatography (SEC) followed by and reverse-phase liquid chromatography coupled with mass spectrometer (RP-HPLC-ESI-MS/MS) to identify potential candidates as bioactive proteins that constitute the EMD. Since the EMD is a complex protein mixture, the fractionation by SEC would decrease its complexity by separating it in many fractions. In this way, it would be possible to identify the low-abundant proteins that are masked by the highly abundant amelogenins.

3.2 Materials and Methods

3.2.1 EMD Stock and Fractions preparation

EMD stock was prepared according to standard protocols from Institute Straumann. Briefly, vials containing 30 mg of lyophilized EMD (heat-treated) were prepared by dissolving it in 3 mL of sterile 0.1% acetic acid and kept at 4°C for 1h to make a stock solution of 10 mg/mL prior to fractionation. For column separations, 2 mg of EMD was aliquoted in separate 1.5 mL tubes, dried and

resuspended in 200 µL of sterile 0.025 M sodium acetate buffer (pH 4) at 4°C, giving a final concentration of 10 mg/mL. EMD was kept at 4°C for 2h and subjected to size-exclusion chromatography (SEC) on an ÄKTA FPLC system using a high-resolution 10 x 300 mm column (ENrich™ SEC 650, Bio-Rad). The column was equilibrated until stable base line and eluted with 0.025 M sodium acetate buffer (pH 4 at 4°C) monitored at 280 nm, and 50 fractions of 0.5 mL were collected at a flow rate of 0.1 mL/min. Micro bicinchoninic acid (micro-BCA) assay (Pierce Chemical, Co., Rockford, IL, USA) was performed to measure the total protein concentration from each fraction using bovine serum albumin as protein standard. Based on the chromatogram (Figure 3.1A) and confirmed by the micro-BCA assay, 32 fractions that contained proteins (F19 to F50) were further analyzed by mass spectrometry.

3.2.2 Sodium Dodecyl Sulfate-Polyacrylamide Gel Electrophoresis (SDS-PAGE)

To confirm separation of EMD proteins by molecular weight, EMD and some EMD fractions were resolved on 4%-15% polyacrylamide gels using the sodium dodecyl sulfate polyacrylamide gel electrophoresis (SDS-PAGE) as described by Laemmli [19]. Fraction selection was based on proteins amount observed in the chromatogram and micro-BCA assay. We selected one high molecular-weight fraction (F24), five fractions with higher protein quantity in the middle range located at the two highest peaks in the chromatogram (F29, F30, F31, F38, and F38), and the last three fractions of fractionation (F48, F49, F50). Ten µg of EMD control and factions with higher protein quantity were loaded in

the gel, while the fractions with low protein quantity were used fully. Resolved bands were stained with coomassie brilliant blue R-250 (Bio-Raid) and photographed.

3.2.3 Mass spectrometry-based proteomics analysis of EMD fractions

3.2.3.1 In-solution digestion

Aliquots of 10 µg of EMD stock and EMD fractions were prepared prior to mass spectrometry analysis as described previously [20]. Briefly, all samples were dried by a rotary evaporator (Eppendorf, Parkway, NY, USA), denatured and reduced with 4 M urea, 10 mM DTT (Dithiothreitol) in 50 mM NH_4HCO_3 (pH 7.8), at 37 °C for 1h. After 4-fold dilution with 50 mM NH_4HCO_3 (pH 7.8), samples were subjected to in-solution digestion with 2% (w/w) sequencing-grade trypsin (Promega, Madison, WI, USA) for 18 h at 37°C. Finally, samples were desalted by C-18 ZipTip® pipette tips (Millipore, Billerica, MA, USA) and further analyzed by LC-ESI-MS/MS.

3.2.3.2 Nano flow Liquid Chromatography Electrospray Ionization Tandem Mass Spectrometry (nLC-ESI-MS/MS)

Peptide separation and mass spectrometric analyses were carried out with a LTQ-Velos (Thermo Scientific, San Jose, CA, USA), which allows in-line liquid chromatography with the capillary-fused silica C18 column 10 cm X 75 µm (Pico Tip TM EMITTER, New Objective, Woburn, MA) packed in-house using Magic C18 resin of 3 µm diameter and 100 Å pores size (Michrom

BioResources, Auburn, CA) linked to mass spectrometer using an electrospray ionization in a survey scan in the range of m/z values 390–2000 MS/MS. All EMD fractions samples were dried by rotary evaporator and resuspended in 15 µL of 97.5% H_2O/2.4% acetonitrile/0.1% formic acid and then subjected to reversed-phase LC-ESI-MS/MS. The nano-flow reversed-phase HPLC was developed with linear 85-min gradient ranging from 5 to 55% of solvent B (97.5% acetonitrile/, 0.1% formic acid) at a flow rate of 300 nL/min with a maximum pressure of 280 bar. Electrospray voltage and the temperature of the ion-transfer capillary were 1.8 kV and 250°C, respectively. Each survey scan (MS) was followed by automated sequential selection of seven ions for CID, with dynamic exclusion of the previously selected ions.

3.2.3.3 Protein identification

The acquired MS/MS spectra generated were searched against specific Sus scrofa protein database (Swiss PROT and TREMBL, http://ca.expasy.org) for all samples using SEQUEST algorithm in Proteome Discoverer 1.3 software. Parameter Xcorr were used to validate the existence of a peptide within the sample. Xcorr is a value computed from cross correlation of the experimental MS/MS spectrum vs. the candidate peptides in the database, which shows how closely the real spectrum relates to candidate peptides. Search results were filtered for a False Discovery Rate of 1%, employing a decoy search strategy utilizing a reverse database. A total of three mass spectrometric runs were carried out for each sample. For protein identification, at least 2 or more peptides were used as previously described [20].

3.2.3.4 Bioinformatics analyses

The identified proteins of each EMD fractions were classified and assigned by biological function, molecular interaction, and subcellular origin using Gene Ontology (GO) terms (https://www.ebi.ac.uk/QuickGO/) and PANTHER (Protein Analysis Through Evolutionary Relationships) classification system (http://pantherdb.org/) [21] and analyzed with web-based tool ClustVis [22].

3.3 Results

3.3.1 EMD Fractionation

EMD stock were subject to a high-resolution SEC column and the fractionation is shown in a chromatogram in Figure 3.1A. A total of 32 EMD fractions (F19 – F50) of 0.5 mL were collected. The chromatogram shows that the EMD proteins started to be collected in fraction 19 when a slight peak was observed that continued constant until fraction 26, which presented a sharp signal increase. The highest peaks (4 major peaks that overlapped) corresponding to higher amount of protein were collected as fractions 26 to 34. Another distinct peak was detected and collected as fractions 38 to 41, and the low-abundant EMD constituents were collected as fractions 42 to 50 later confirmed in the SDS-PAGE (Figure 3.1A). Selected EMD fractions were resolved in SDS-PAGE gel to confirm the sequential separation of EMD content by molecular weight (Figure 3.1B). As shown in Figure 3.1B, fraction 24 (F24) presented thin high-molecular-weight bands, fractions 29, 30, 31 displayed

bands below 25 kDa, while bands below 10 kDa with low- molecular weight protein/peptides are more evident in fractions 38 and 39 that faded until the last fractions 48, 48, and 50. The EMD control lane displays diverse molecular-weight bands indicating EMD complexity. The most prominent bands in the gel are noticed below the 25 kDa mark where the amelogenins family members are located, recognized as the most abundant components of the EMD proteins [2].

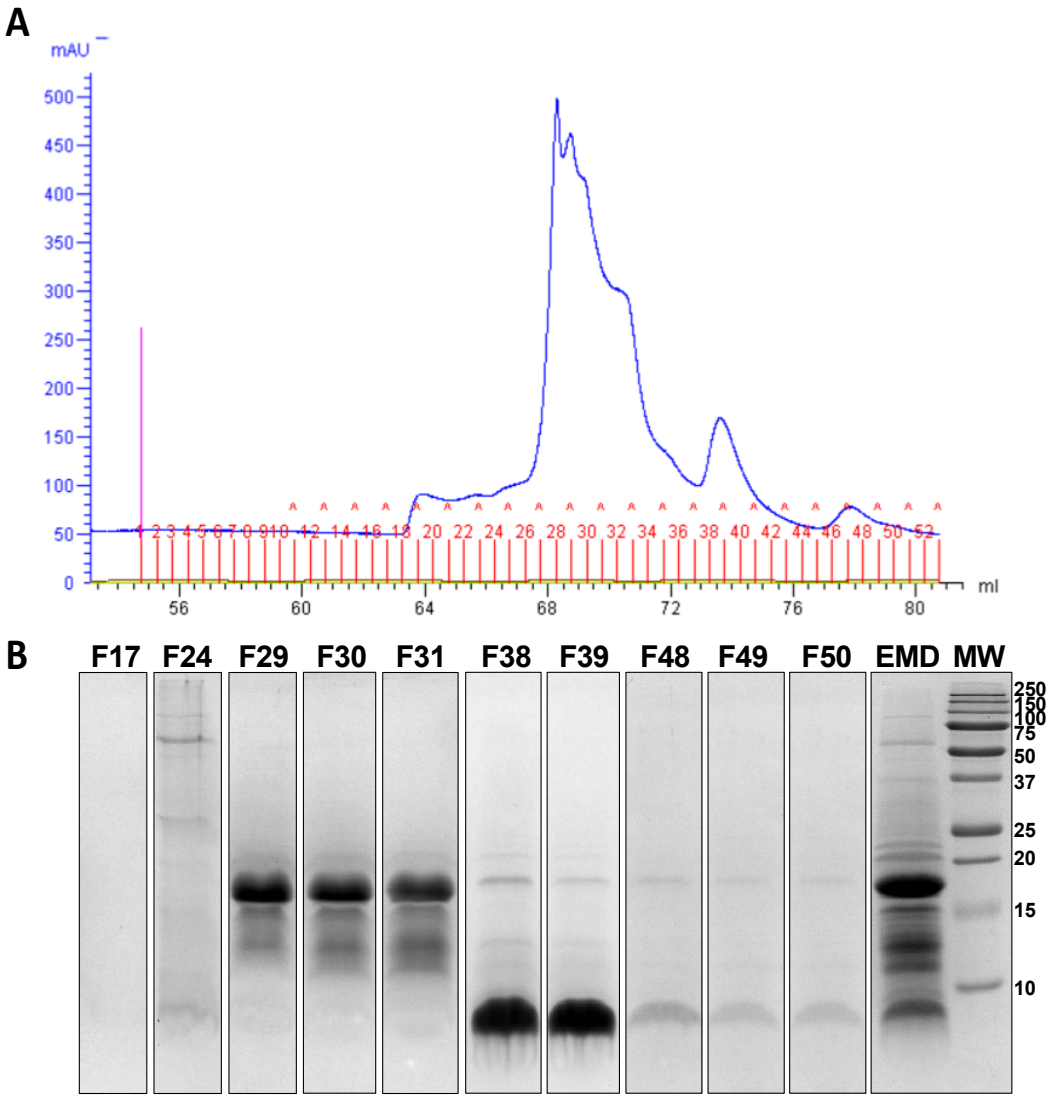

Figure 3.1 – Separation of EMD proteins through Size-exclusion chromatography and SDS-PAGE. **A)** Fractionation of EMD by SEC using a FPLC system. Note that EMD proteins started to elute from the column in fraction F19 that continued until fraction 50. **B)** EMD and EMD fractions F24, F29, F30, F31, F38, F38, F48, F49, F50 that were resolved in 4-15% SDS-PAGE gel to confirm separation by molecular-weight. Lane EMD represents whole EMD as control. Lane MW represents molecular weight marks. Lane F17 represents fraction with no protein as the negative control.

3.3.2 Mass spectrometry analysis of EMD

The nLC-ESI-MS/MS analysis of the unfractionated (whole) EMD identified a total of 190 proteins of which 166 were characterized proteins and 24 were classified as uncharacterized after matching and searching in the *Sus scrofa* (pig) protein database (Figure 3.2). Differently, the investigation of fractionated EMD (all fractions) identified a much larger number of proteins. From a total of 4147 proteins (summing all fractions), we identified 2000 unique proteins, which consisted of 1785 characterized (89.3%) and 215 uncharacterized (10.7%) after removing duplicates (Supplementary Table A3.2). The distribution of all proteins identified in each fraction is represented in the histogram in Figure 3.2A. The EMD fractions F19 to F28 showed a greater protein diversity in comparison with other fractions in the mid-molecular weight range (F29 to F42), while fraction F43 to F50 also showed an increase in protein composition.

Differences in fraction content were also presented in the base-peak chromatograms originated from the RP-HPLC monitored by the mass spectrometer, which revealed distinct elution patterns of tryptic peptides for different EMD fractions ranging between 17 and 46 min (Supplementary Figure A3.1).

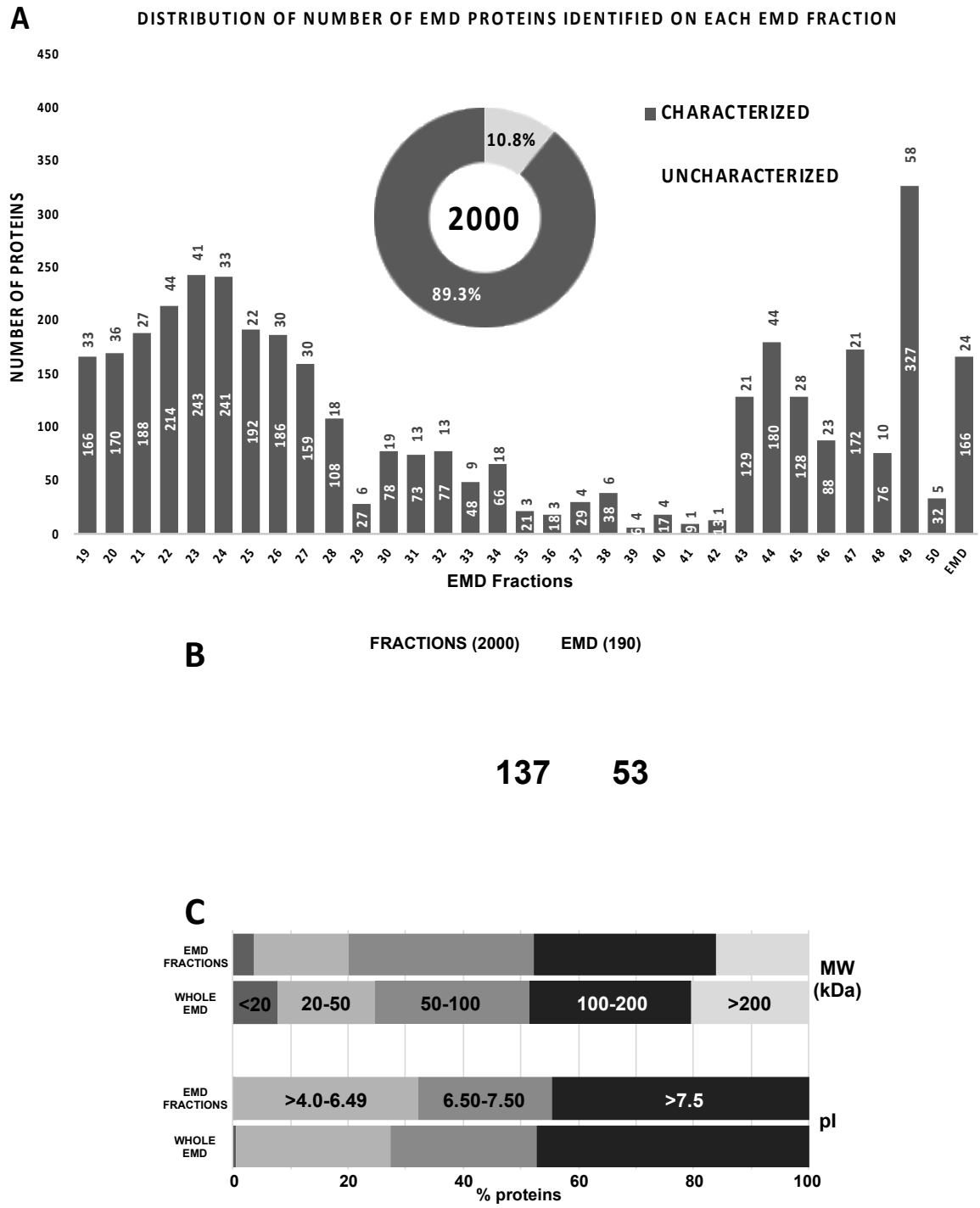

Figure 3.2 - A) Histogram showing the distribution of number of proteins of EMD control e EMD fraction obtained from SEC. B) Venn diagrams showing the number of identified proteins in fractionated EMD (2000) and EMD control (190). C) Distribution of proteins of whole EMD and EMD fractions according to molecular weight (MW) and Isoelectric point (pI).

Despite showing a significant increase in protein identification through fractionation by SEC, the proteome analysis of the EMD control identified 53 proteins (27.9%) that were not found in any other fraction (Figure 3.2B, and Supplementary Table A3.1). However, the proteins identified in both the EMD control and fractions show similar distribution regarding molecular weight (MW) and isoelectric point (pI) (Figure 3.2C). Around 50% of the proteins on both samples have MW lower/higher than 100 kDa, showing also similar distribution on the other MW ranges. Likewise, around 50% of the proteins have an isoelectric point lower/higher than 7.5, while ~ 24% of protein have pI at the range of neutral pH and 28% are at the acidic range. These results indicate that the whole EMD portraits a very close picture of its content regarding these parameters, but not concerning protein composition since the fractionation by SEC presented a 10-fold increase in protein identification.

3.3.3 EMD proteome

For the proteome analysis of EMD (control and fractions), the tryptic generated peptides subjected to three runs in the nLC-ESI-MS/MS were identified by the SEQUEST search following the parameters described in methods. From 2000 unique proteins, the well-recognized constituents of EMD were identified, including the amelogenins (23 and 18 kDa), enamelin, ameloblastin (also called sheathlin or amelin), odontogenic ameloblast-associated protein (also known as apin), annexin A2, along with the two enamel-specific proteases, matrix metalloproteinase (MMP)-20 (enamelysin), and enamel matrix serine protease 1 (kallikrein-4). The list of all 2000 protein is

found in the supplementary data (Supplementary Table A3.1). As expected, the most abundant proteins were the amelogenins, particularly the 23 kDa amelogenin, which was detected in all 32 fractions, and the 18 kDa amelogenin in 8 fractions (F27, F28, F29, F30, F38, F40, F42, F45) (Table 3.1 and Supplementary Table A3.1). The second most abundant protein was the enamelin (31 fractions) followed by ameloblastin (27), MMP-20 (24), and dentin sialophosphoprotein (DSSP) (21), which has never been described as an EMD component. We identified many other proteins that are not constituents of EMD, including alpha-2-HS-glycoprotein (AHSG) also known as fetuin-A (12 fractions), protein S100-A6 (9), annexin A1 (AnxA1) (8), annexin A2 (AnxA2) (8), and alpha-1B-glycoprotein (8) among many others. As an example, Figure 3.3 shows an example of MS/MS scan of precursor ions chosen from the survey scan with the matched b and y ions indicated in the graph. The peptides ions were later identified as a tryptic peptide K.DITSDTSGDYQK.A from annexin A1 (UniProt accession # P19619) and peptide K.HTLNQVDSVKVWPR.R from alpha-2-HS-glycoprotein (UniProt accession # P29700). Additionally, we identified many proteins derived from blood, such as hemoglobin (27 fractions), serotransferrin (13), immunoglobulin G (13), and serum albumin (5), proteins involved in metabolic pathways (glyceraldehyde-3-phosphate dehydrogenase and malate dehydrogenase, mitochondrial), and cell cycle (Histone-lysine N-methyltransferase and adenomatous polyposis coli). We also identified structural proteins such as keratins, for instance, keratins type I and II (14, and

18 fractions, respectively), 8 types of collagen (collagens type I and XVII identified in 7 fractions), and microtubule-associated protein in 11 fractions.

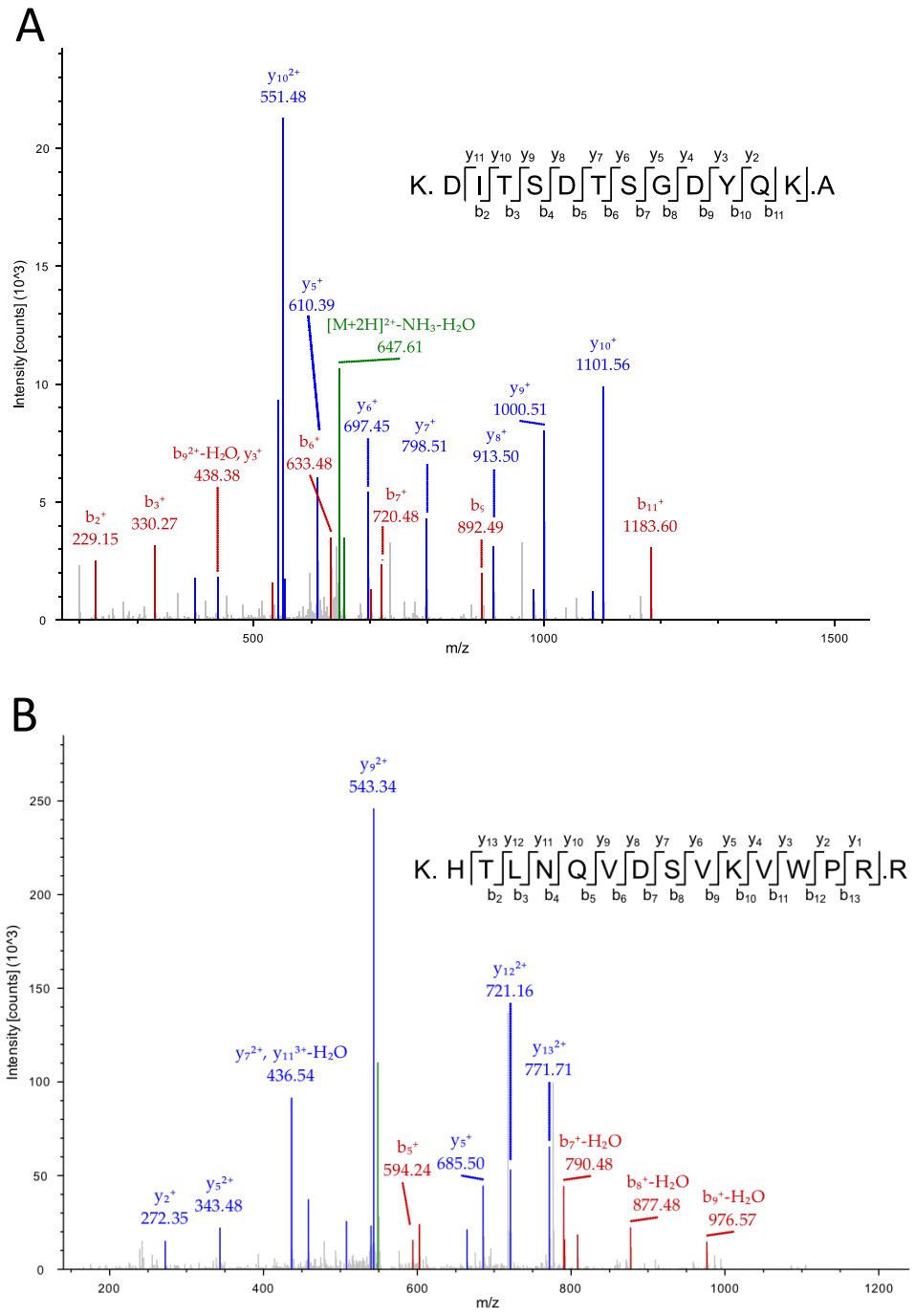

Figure 3.3 - MS/MS spectrum of a tryptic peptide A) K.DITSDTSGDYQK.A from annexin A1 (P19619) and B) K.HTLNQVDSVKVWPR.R from alpha-2-HS-glycoprotein (P29700). Matching b and y ions are shown in the m/z spectra.

3.3.4 Gene ontology analysis of EMD identified proteins

The identified proteins from EMD fractions were further classified according to biological function, molecular interactions, and sub-cellular localization utilizing PANTHER classification system (http://pantherdb.org/) and GO annotation terms (GO) (https://www.ebi.ac.uk/QuickGO/). The comparison between the whole EMD and EMD fractions revealed that the proportional distribution according to the categories was very similar, regardless of the number of proteins in each category as shown in Figure 3.4. Overall, the proteins that comprise the EMD are involved in many biological processes including cellular (46.5%), metabolic (29.7%), and developmental processes (10.4%), localization (9.4%), and biological regulation (16.8%). Interestingly, we identified several proteins that are implicated in biological adhesion (89), immune response (63) and biomineralization (29) (Table 3.1). Moreover, the analysis regarding molecular function showed that a large number of proteins have catalytic activity (483; 24.2%), and that 634 proteins (31.7%) bind to other molecules in which 51% (324) make protein-protein interactions, 29% (186) interact with nucleic acids, while 33 proteins have affinity to calcium ions. Despite originated from various location, the diverse proteins are mostly part of the cell (29.8%), organelles (19.9%), and membranes (12.5%), while 10.4% are associated in macromolecular complexes, and 44 proteins are part of the extracellular matrix (ECM) (Figure 3.4). The distribution in sub-categories is presented in more details in the supplementary data (Supplementary Figure A3.2A, B, and C).

Table 3.1 - List of EMD proteins identified associated with biomineralization, wound healing, extracellular matrix, biological adhesion and immune response and which fractions were detected according to PANTHER and GO terms. Note: BM (Biomineralization), WH (Wound Healing), ECM (Extracellular matrix), BA (Biological Adhesion, IR (Immune response)

Accession Number	Protein name	BM	WH	ECM	BA	IR	Fraction
F1RJ58	Neurofibromin 1	x	x	x	x	x	32
F1S279	Nephroblastoma overexpressed	x	x	x	x		45
E9M2M3	Receptor protein serine/threonine kinase	x	x			x	28
A0A286ZXU9	FAT atypical cadherin 4	x	x		x		26, 34
F1RVB3	Odontogenic ameloblast-associated protein	x	x				19, 21, 23, 24
F1SAQ5	Uncharacterized protein	x	x			x	34
A0A287B086	Fibroblast growth factor (FGF)	x	x				21
F1SI16	Receptor protein serine/threonine kinase	x	x		x		23, 44
I3LVF2	Patched 1	x	x				21
Q9XSN6	Enamel matrix serine proteinase 1 (Kallikren-4)	x		x			19, 20, 21, 22, 23
Q9TQY2	23 kDa amelogenin	x		x			19 – 50
Q9TQY1	18 kDa amelogenin	x		x			27, 28, 29, 30, 38, 40, 42, 45
Q28989	Ameloblastin (Sheathlin)	x		x			19 – 39, 41, 42, 43, 44, 45, 46
P79287	Matrix metalloproteinase-20 (MMP-20)	x		x			19 – 29, 34 – 38, 40, 43 – 48, 50
C9W8E7	Dentin sialophosphoprotein (Fragment)	x		x			20, 23 – 28, 31 – 35, 43, 44, 48, 49
P29700	Alpha-2-HS-glycoprotein (Fetuin-A)	x		x			19 – 28, 30, 37

F1SN67	Fibrillin-1	x		x	x	x	19, 24, 26
O97939	Enamelin	x		x			19 – 48, 50
A0A287AN90	Matrix metalloproteinase (MMP-9)	x		x		x	27
I3LQP2	Pleckstrin homology like domain family B member 2		x	x	x		26, 27, 37, 49
F1SS24	Fibronectin 1		x	x	x		31
F1RW71	Multimerin 1		x	x			43
F1SMW3	Serpin family B member 5		x	x			21
F1RL90	PPARG coactivator 1 beta	x				x	39, 43, 47
F1S518	Additional sex combs like 1, transcriptional regulator	x				x	20, 46
A0A287ARL0	Protein tyrosine kinase 2 beta	x			x	x	28
K7GT68	Integrin subunit alpha 6	x			x	x	19
K7GPY3	Ectodysplasin A	x			x	x	47
F1SEI1	Twist family bHLH transcription factor 1	x					24
F1S703	Pappalysin 2	x					31
P16960	Ryanodine receptor 1 (RYR-1)	x					23
F1SUW7	Uncharacterized protein	x					45
P19619	Annexin A1	x	x			x	19, 20, 21, 22, 23, 24, 25, 26
Q9GLP1	Coagulation factor V		x				19, 22, 33, 43, 44, 48
F1S8J5	Chromodomain-helicase-DNA-binding protein 8		x				22, 24, 35
F1RSU5	Fms related tyrosine kinase 1		x			x	22, 28, 34
P43368	Calpain-3		x				19, 49
F1SQ60	Heart development protein with EGF like domains 1		x		x		22, 47
F1STQ5	Keratinocyte differentiation factor 1		x				21
I3L9Z3	Serine/threonine-protein kinase		x		x	x	21
K7GQL2	Coagulation factor XIII A chain		x				19
F1SMI2	Tripartite motif containing 32		x			x	25

A7UGA9	Coagulation factor II receptor (Fragment)	x			26
F1RIH6	Transmembrane protein 201	x			23
Q0PM28	Pigment epithelium-derived factor		x		19, 20, 21, 22, 23, 24, 25, 26, 27
A0A287BLD2	Collagen type I alpha 1 chain		x		19, 20, 21, 22, 23, 25, 26
A3EX84	Galectin		x	x	21, 23, 26, 27
A5A8W4	Tenascin X		x		25, 26, 47
F1SQ09	Lumican precursor		x		19, 20, 21, 22
Q9TTB4	Fibromodulin		x		20, 21, 22
F1RQI0	Collagen type XII alpha 1 chain		x		22, 25, 26
F1RJ55	Oligodendrocyte myelin glycoprotein		x		44, 47
O19112	Cartilage intermediate layer protein 1 (CILP-1)		x		49
I3LUR7	Collagen type VI alpha 3 chain		x		44
I3LJU9	Tenascin		x		24
I3LDG8	Collagen type XXVII alpha 1 chain		x		32
I3LBV3	Protein Wnt		x		22
F1SV70	Matrix metalloproteinase		x		45
F1SFA7	Uncharacterized protein		x		26
F1SA65	Fibrillin 3		x		49
F1S662	Laminin subunit gamma 2		x		24
F1RG45	Angiotensinogen		x		23
D3JCV7	Protein Wnt		x		27
A0A287AGN9	Spondin 1		x		44
A0A287A0A6	Collagen type VI alpha 6 chain		x		49
F1S663	Uncharacterized protein		x	x	49
F1SX59	Versican		x	x	45
I3LHG2	Tectorin alpha		x	x	49
F1SBB3	Laminin subunit alpha 3			x	19, 20, 22, 23,

			24, 25, 26, 27
F1SGT7	DS cell adhesion molecule	x	19, 20, 22, 23, 24, 31
I3LDQ1	Talin 2	x	31, 41, 49, 50
P37176	Endoglin (CD antigen CD105)	x	27, 44, 46
F1RMV7	LY6/PLAUR domain containing 3	x	19, 34, 44
I3LRQ5	Phosphatase and actin regulator	x	20, 27, 49
A0A287A428	Plakophilin 4	x	26, 44, 49
F1RXE4	Tensin 4	x	24, 47, 49
F1RUG5	WNK lysine deficient protein kinase 3	x	20, 25, 43
A0A287AG36	Laminin subunit alpha 1	x	27, 47
F1SKK7	Cadherin EGF LAG seven-pass G-type receptor 3	x	44, 49
A0A287AEH1	Laminin subunit alpha 5	x	24, 43
A0A287BAD8	LIM domain 7	x	19, 49
I3LG79	Desmocollin 3	x	24, 43
A0A287BLY8	Talin 1	x	21, 48
A0A287B5M2	Mucin-4 precursor	x	33, 49
F1SER9	Uncharacterized protein	x	23, 44
A0A287AG74	Membrane associated guanylate kinase, WW and PDZ domain containing 2	x	19, 21
A0A287BIY4	Cadherin 8	x	44
A0A287AEM7	Cadherin EGF LAG seven-pass G-type receptor 2	x	45
A0A287BL69	Cadherin related family member 1	x	44
F1RSA2	Calcium-transporting ATPase	x	27
C3VPJ4	Claudin	x	44
A0A287ATF2	Desmoglein 2	x	34
A0A287AA14	Desmoplakin	x	49
E7FM66	Disintegrin and metalloprotease domain-containing protein 5 (Fragment)	x	47

I3LEB9	EPH receptor B1	x	44
A0A287BQC4	FAT atypical cadherin 3	x	20
F1SFE3	Fermitin family member 2	x	46
A0A287BGJ4	FRAS1 related extracellular matrix 1	x	40
F1S794	Hepatic and glial cell adhesion molecule	x	26
F1SGE7	Integrin beta	x	44
A0A287BHP4	Integrin beta	x	32
F1RYP4	Integrin subunit alpha 4	x	50
K7GSU6	Integrin subunit alpha E	x	46
A0A287BCR9	Junctional cadherin 5 associated	x	19
F1SGG1	Keratin 18	x	27
Q7YS22	Lymphatic endothelial hyaluronan receptor LYVE-1 (Fragment)	x	26
A0A287A7V5	Myelin-oligodendrocyte glycoprotein	x	34
F1SRM1	Myosin X	x	22
Q2EN76	Nucleoside diphosphate kinase B (NDK B)	x	19
F1RUR8	Par-3 family cell polarity regulator	x	49
I3LGN8	Plakophilin 1	x	49
F1SPK1	Plexin D1	x	24
A0A287ABC9	Protein tyrosine kinase 2	x	22
F1S1M6	Protocadherin 19	x	45
A0A287ARC5	Protocadherin gamma subfamily C, 4	x	21
F1S0W0	Rap guanine nucleotide exchange factor 1	x	38
F1RNT6	Repulsive guidance molecule family member b	x	34
F1SG15	Rho GTPase activating protein 6	x	30
I3L8F6	SH3 domain binding protein 1	x	49
A0A286ZNC2	SRC kinase signaling inhibitor 1	x	25
F1SI04	Sushi, nidogen and EGF like domains 1	x	25
A0A287BF71	Tight junction protein 1	x	49

F1SP25	Transmembrane protein 245	x		23
I3LFP3	Uncharacterized protein	x		33
F1SMF4	Integrin subunit alpha 2	x		45
F1S9C8	Cadherin 24	x		47
A0A286ZTM0	Integrin subunit alpha X	x		49
K9J6K2	Utrophin	x		47
Q29123	Vascular cell adhesion molecule	x		27
A0A2C9F393	Vinculin	x		49
F1RFK7	BAI1 associated protein 2 like 1	x	x	28
K7GT47	Linker for activation of T-cells	x	x	48
K9IVR7	WD repeat domain 1	x	x	23
F1SGG3	Keratin 1		x	20 – 22, 25, 28 – 31, 38, 40, 43, 46
F1RMN7	Hemopexin		x	19, 20, 21, 22, 23, 24, 25, 26, 27
Q07717	Beta-2-microglobulin (Lactollin)		x	19, 22, 23, 24, 25, 26, 30
A0A075B7I5	Uncharacterized protein		x	19, 20, 21, 22, 23, 24, 25
Q29014	Alpha-1 acid glycoprotein (Fragment)		x	22, 23, 24, 25, 26, 27
Q0Z8U2	40S ribosomal protein S3		x	19, 20, 21, 22, 23, 24
I3L728	Uncharacterized protein		x	19, 22, 23
A5A776	Lysosomal trafficking regulator (Fragment)		x	20, 43, 49
A0A075B7J0	Uncharacterized protein		x	20, 26, 27
K7GLC3	CD101 molecule		x	43, 47
A0A287BCA4	Scavenger receptor cysteine rich family member with 5 domains		x	33, 47
A0A287AWP8	Complement C5a anaphylatoxin		x	25, 49
A0A287AUN9	Transient receptor potential cation channel subfamily M member 4		x	19, 23

F1RLM0	Uncharacterized protein	x	45, 49
Q8MHT8	MHC class I antigen	x	24
Q6S7D8	SLA-1 (Fragment)	x	34
Q4A3R3	Deleted in malignant brain tumors 1 protein (Hensin)	x	47
Q0MRZ9	MHC class I antigen	x	37
L7WLW9	MHC class I antigen	x	23
K9J4S2	E3 ubiquitin-protein ligase TRIM11	x	43
K7GKU8	Mannan binding lectin serine peptidase 2	x	34
I3W8V5	Mast/stem cell growth factor receptor	x	20
I3LQQ8	Colony stimulating factor 3 receptor	x	48
I3LQ81	Rho guanine nucleotide exchange factor 5	x	23
I3L8L2	Aminopeptidase	x	22
I3L7L0	Uncharacterized protein	x	28
F1SSC2	Cyclin dependent kinase 13	x	19
F1SNR5	OTU deubiquitinase 7A	x	21
F1SMZ7	60 kDa heat shock protein, mitochondrial	x	44
F1SML7	Inosine-5'-monophosphate dehydrogenase	x	38
F1SMJ1	Complement component C7	x	21
F1SIY2	Pellino E3 ubiquitin protein ligase 1	x	22
F1SFH8	B-cell CLL/lymphoma 6	x	45
F1S8C6	Mitochondrial antiviral signaling protein	x	34
F1S861	Nuclear factor kappa B subunit 2	x	22
F1S4G0	Growth factor independent 1 transcriptional repressor	x	31
F1RUA7	NFKB activating protein	x	24
F1RRV6	N-myc downstream regulated 1	x	20
F1S418	Uncharacterized protein	x	24
F1RGE8	Uncharacterized protein	x	49
F1RFH0	Uncharacterized protein	x	22

A2TF48	Myeloid differentiation primary response protein MyD88	x	33
A0A287AZE3	Scavenger receptor cysteine-rich type 1 protein M130	x	26

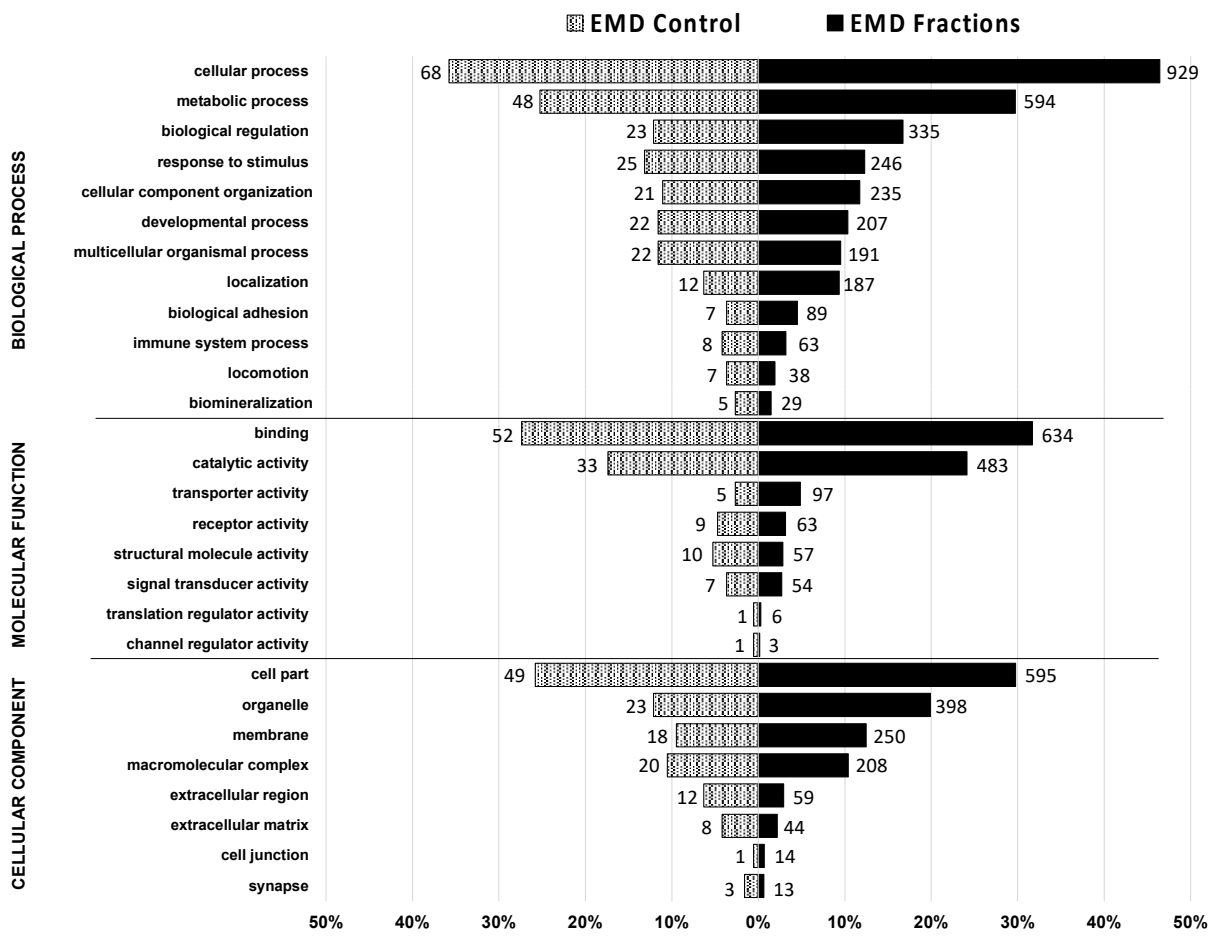

Figure 3.4 - Classification by biological functions of proteins identified in EMD control and EMD fractions. Sorting of the functions of these proteins was based on their annotations in the database. Proteins involved in more than one biological function were counted multiple times.

Lastly, a specific analysis was done to identified proteins in categories according to GO terms that are related to EMD primary biological functions, which include biomineralization, wound healing, and biological adhesion (Table 3.1). Twenty-nine proteins that participate in biomineralization were identified, including the classical EMD constituents amelogenins, ameloblastin, enamelin, kallikren-4, MMP-20, annexin A2, and apin, along with novel EMD proteins, such as the dentin sialophosphoprotein, alpha-2-HS-glycoprotein, PPARG coactivator 1 beta, matrix metalloproteinase-9 precursor, neurofibromin 1, and FAT atypical cadherin 4, which also have a role in wound healing and biological adhesion. Among the proteins linked directly or indirectly to wound healing and biological adhesion, we highlight the annexin A1, tenascin X, lumican precursor, fibrillin-1, laminin subunit alpha-3, and fibromodulin. Fibroblast growth factor and fibronectin-1 were also detected but only in one fraction at low levels. Proteins that participate in immune response were also revealed including keratin-1, immunoglobulin G, and hemopexin among others. The separate analysis of each fraction indicated that the larger number of proteins associated with biomineralization, wound healing, and immune defense are present in the high molecular range, in particular fractions F19, F21, F23 and F24 as shown in the heat map in Figure 3.5 (Supplementary Table A3.2).

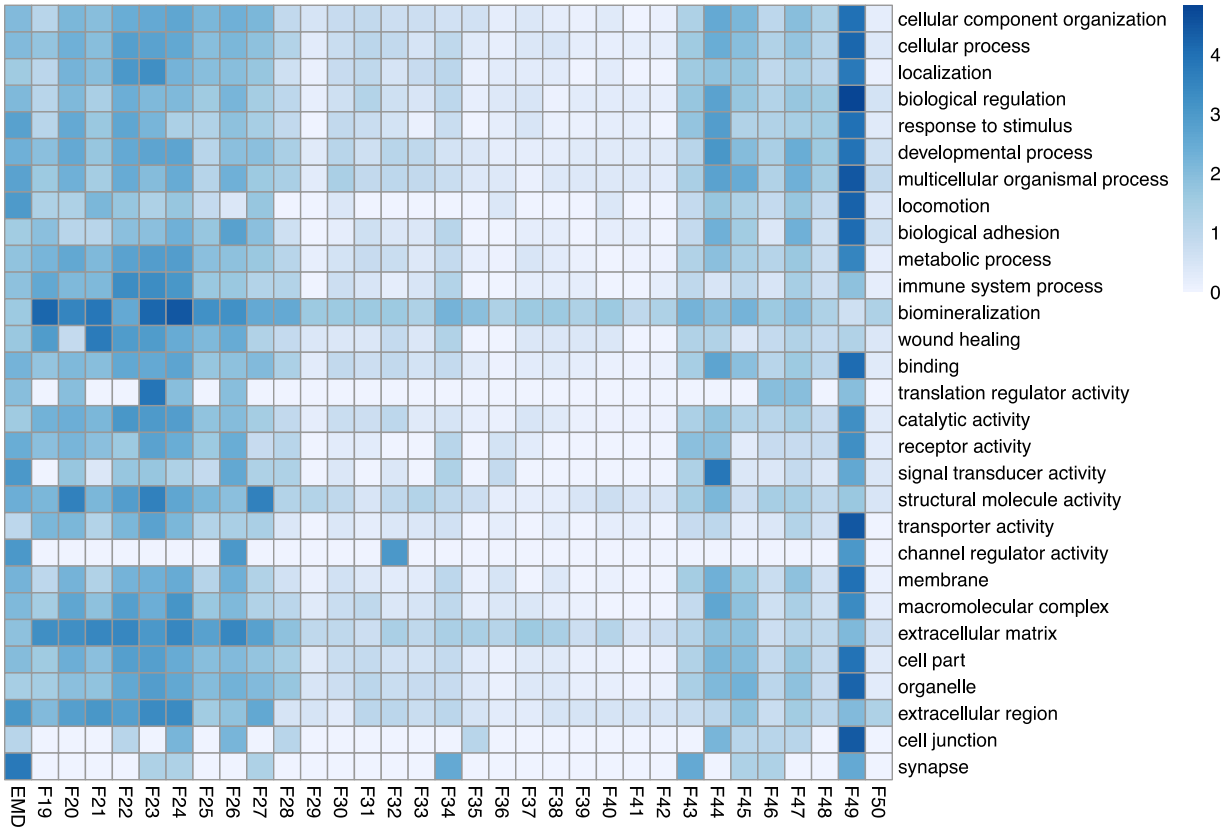

Figure 3.5 - Heat maps showing the classification by biological functions per fractions. Unit variance scale is applied to each row, i.e., intensity is relative to number of proteins identified on each category.

3.4 Discussion

Although EMD was introduced 20 years ago, it is still a subject of great interest due to its capability to promote regeneration of the periodontium (cementum, periodontal ligament and alveolar bone) [23, 24]. Many studies have shown that EMD affects diverse cell types such as osteoblasts [25], fibroblasts [26], epithelial [27], and endothelial cells [28]. EMD not only induce bone formation but also has been implicated in stimulating wound healing [29]. However, the active component/components responsible for its extensive biological effects remain unclear [11]. The use of SEC to fractionate EMD in previous studies provided limited information on EMD composition since the analysis was mostly done on samples retrieved from distinct peaks rather than to the whole EMD content, which allowed the identification of the most abundant proteins such as the amelogenins, ameloblastin [17, 30]. Different from past studies that submitted EMD to SEC at flow rates ranging from 0.2mL/min to 1mL/min [10, 30, 31], in this study we utilized a slower flow rate (0.1mL/min) which allowed a better separation resulting in a larger number of fractions.

To our knowledge, this is the first comprehensive characterization of EMD proteome. In this study, we utilized the well-stablished method to explore protein mixtures known as multi-dimension protein identification technology (MudPIT), which consists of using a 2-dimensional liquid chromatography before identification of sample composition through mass spectrometry [32]. First, off-line size-exclusion chromatography was carried out to separate the EMD proteins by molecular weight as the first dimension resulting in 32 fractions with

proteins/peptides. Next, each fraction was tryptic digested prior to the second-dimension separation, which involved an on-line reversed-phase high-performance liquid chromatography that was followed by the identification of proteins by the mass spectrometer (RP-HPLC-ESI-MS/MS). This approach enhances separation and significantly increases the chance to identify low-abundant proteins in complex mixtures. As a result, a total of 2000 proteins were identified in the fractionated EMD in comparison to 190 proteins in the whole EMD, which represented a 10-fold increase in identification.

The proteome analysis revealed that several proteins were found in consecutive fractions as observed in the SDS-PAGE gel. The most abundant protein was the 23 kDa amelogenin form that was detected in all 32 fractions, which is a cleavage product of the full-length 25 kDa amelogenin. The splice variant 18 kDa amelogenin was also found in many fractions, but the well-known amelogenin-derived peptides, 5.3 kDa tyrosine-rich amelogenin polypeptides (TRAP), and the 6.5 kDa splicing variant leucine rich-amelogenin peptide (LRAP) were not identified, which was expected. The search engine identifies the protein in the database from which the detected peptide is originated and not all post-enzymatic peptides and variants. For example, the peptide K.WYQNMIR.H that was found in all fractions is shared by all amelogenins sequence, including the low-molecular weight peptides TRAP and LRAP. Since this peptide was detected in samples in the low-molecular weight range below 10 kDa is reasonable to assume they originated from the TRAP and LRAP.

The vast majority of EMD constituents identified in this study are cellular components (membrane, cytoskeleton, organelles, nucleus) that are implicated in various biological processes during amelogenesis when proteins are involved in cellular (46.5%), metabolic (29.7%), and developmental processes (10.4%), biological regulation (16.8%), and localization (9.4%), which mostly included protein transport (Figure 3.3). Many subcellular proteins that are involved in cell cycle as well as in transcription were detected, such as ATP binding proteins, 60 different zinc-fingers, and coiled-coil domain proteins. In addition, the data identified many kinases and phosphatases that are key regulatory components in many cellular processes, such as signal transduction pathways and cell cycle control. Notably, we found 483 proteins with catalytic activity within the EMD such as hydrolases, transferases, oxidoreductases, and enzyme regulator (Supplementary Figure 3.2B). The enzymatic activities that occur in the enamel matrix are attributed to the only two proteinases previously proven to be secreted into the enamel matrix during enamel development, kallikrein-4 and MMP-20 [33]. Although we cannot identify the source of the other enzymes identified in EMD here, our data suggest that many proteins are intracellular enzymes involved in cell metabolism and cell cycle, for example, that can be derived from ameloblasts and cells that surround the enamel organ, and that are retrieved during the extraction process of EMD. This large number of enzymes could also explain the proteins found in the low-molecular weight range that were likely identified by their related peptides originated from proteolytic degradation (Figure 3.2A, and Supplementary Table A3.2). More studies are necessary to

investigate the biological role of these enzymes in EMD and whether or not protein degradation in EMD impact its biological activity.

Moreover, as shown by previous studies [34, 35], proteins derived from blood are present in EMD. We detected, for instance, serotransferrin, serum albumin, and mainly hemoglobin that appeared nearly in all fraction. Likewise, circulating proteins that belong to the immune response such as immunoglobulin G, hemopexin and alpha-1 acid glycoprotein were also identified. Since blood vessels are not located within the secreted enamel matrix, the proteins aforementioned were likely derived from surrounding blood vessels from the dental follicle located close to the ameloblasts that can perforate the outer enamel epithelium [36]. Throughout the four phases of amelogenesis, particularly from the secretory phase to the early maturation stage in which the EMD is likely recovered, the specialized ameloblasts present high metabolism involving complex signaling pathways that are actively and specifically orchestrated to produce and export large amount of enamel matrix proteins to the extracellular space to form the enamel [33].

The proteome analysis also presented large variations between EMD fractions regarding biological classification (Figure 3.3B). A specific analysis to identify fractions with proteins involved in EMD biological functions revealed a greater number of proteins in high-molecular weight fractions (F19 to 26) that are involved in biomineralization and wound healing, many of which have not been previously described as EMD constituent, including, annexin A1 (AnxA1), dentin sialophosphoprotein (DSSP), profilin, protein S100-A6, and fibrillin-1 to name a

few (Table 3.1, Figure 3.3B). Beside the amelogenins, which are recognized to comprise approximately >90% of the organic matter of enamel matrix [2], proteins previously established as EMD constituents that are involved with biomineralization were also identified, such as enamelin [4], ameloblastin [37], the enzymes kallikrein-4 [6], and MMP-20 [38], along with the recently identified odontogenic ameloblast-associated protein or apin [39]. However, the low-molecular weight amelotin, which has been considered an enamel matrix protein, was not detected [40]. A possible explanation for its absence lies on when EMD is extracted, which likely occurs during the secretory stage of amelogenesis when the enamel matrix has a soft consistency, and not when amelotin is secreted by the ameloblasts, which takes place during the maturation stage of amelogenesis [41].

Another interesting finding to highlight is the identification of DSPP, which is the most abundant non-collagenous extracellular matrix protein in dentin [42]. Although DSPP is secreted by odontoblasts during dentinogenesis, it was identified in 21 fractions. DSPP is a multidomain protein that undergoes proteolytic cleavage generating 3 proteins that regulate dentin mineralization: dentin sialoprotein (DSP), dentin glycoprotein (DGP), and dentin phosphoprotein (DPP) [43]. It is not possible to determine whether the identified peptides derived from the whole DSPP or its proteolytic products. Nevertheless, our results indicate that EMD also contains dentin-matrix proteins as the DSPP and collagen type I, and not just enamel-derived components. The presence of DSPP in EMD could explain the successful application for dentin-pulp

regeneration obtained by previous studies [44-46]. However, more studies are needed to evaluate whether DPSS within EMD may contribute to bone regeneration in periodontal lesions.

Similar to any biological system, protein-protein interactions also occur within the enamel matrix [47, 48]. The proteome analysis showed that among 634 proteins classified as having binding affinity for diverse molecules (Figure 3.4), 324 proteins make protein-protein interactions, while 33 proteins have calcium (Ca^{2+}) as a ligand (Supplement Figure A3.2B). As an example, we identified alpha-2-HS-glycoprotein (AHSG), and annexin A2 (AnxA2) as proteins that were reported interacting *in vivo* with amelogenin, ameloblastin, and enamelin [47]. Although not considered classical constituents of EMD, AHSG and AnxA2 were detected in 12 and 8 EMD fractions, respectively. AHSG is a circulating serum protein mainly synthesized in the liver by hepatocytes [49]. However, a recent study provided more evidence that AHSG is also produced in bone by osteocytes and in a lower amount by osteoblasts [50]. AHSG has also been identified in the porcine EMD in a recent proteomic study [51], confirming our findings. AHSG is a calcium phosphate-binding proteins that regulates endochondral ossification and calcified matrix metabolism [52]. It inhibits mineralization and precipitation of basic calcium phosphate that prevents pathological calcification by facilitating the formation of calciprotein molecules, which are colloidal stable mineral-protein complexes composed of calcium-phosphate crystals [53, 54]. All these features suggest its importance for biomineralization.

Likewise, AnxA2 is a protein with high affinity to Ca^{2+} ions that is also involved in bone metabolism and matrix mineralization [55, 56]. Expressed in many cells, AnxA2 is a multifunction protein that participating in other biological processes such as membrane trafficking, endocytic pathway, and exocytosis [57]. Studies have found AnxA2 in secretory vesicles of ameloblasts in both early and late maturation stages during tooth development [48, 58]. Moreover, recently, expression of AnxA2 was revealed to be important not only to matrix maturation but pre-osteoblast proliferation and osteogenic gene expression, suggesting that AnxA2 have many roles in osteogenesis [55].

Furthermore, AnxA1, another member of the annexins family was detected in 8 EMD fractions. Similar to AnxA2, AnxA1 has high affinity to calcium allowing the biding of up to eight Ca^{2+} ions [59], which involves regulation of calcium-dependent signal transduction pathways, Ca^{2+} trafficking, and intracellular Ca^{2+} concentration [60]. In a proteome analysis of matrix vesicles, a recent study found AnxA1 inside vesicles secreted to the extracellular matrix from mineralizing osteoblasts suggesting its involvement in osteogenesis [61]. Another study observed that AnxA1 null mice showed a delay in intramembranous ossification of the skull indicating a possible function in bone formation through the regulation of osteoblast differentiation [62]. In addition to potential roles in bone physiology, recent evidence points out that AnxA1 has significant participation in innate immune response, inflammation, and wound repair, being labeled as a pro-resolving mediator [63]. Among diverse functions, AnxA1 regulates differentiation and proliferation of activated T-cells by promoting

rearrangement of the actin cytoskeleton, cell polarization and cell migration [64]. It also modulates neutrophil recruitment facilitating resolution of inflammation and repair by recruiting monocytes to clear apoptotic cells [65, 66].

Finally, another multifunction protein worth mentioning is the calcium-binding protein fibrillin-1. It is a large glycoprotein protein constituent of ECM that is involved in biomineralization and cell adhesion [67]. Fibrillin-1 controls TGF-beta bioavailability and regulates TGF-β and BMP levels, which is important to maturation of osteoblast [68], ECM formation and remodeling that are critical steps for bone formation [69, 70]. Besides, fibrillin-1 participates in cell adhesion mediation through the cell-surface receptors integrins alphavbeta3 and alpha5beta1, which are expressed in gingival and periodontal ligament fibroblasts, having a critical role in cell attachment and spreading [71]. Other proteins that participate directly or indirectly in biological adhesion and wound healing were found in few EMD fraction, such as tenascin X [72], lumican precursor [73], fibromodulin [74], fibronectin 1 [75], and fibroblast growth factor (FGF) [76]. Several investigators have shown that EMD impact considerably inflammatory response and promote wound healing in both *in vitro* and *in vivo* studies by affecting leukocytes, fibroblasts, endothelial cells [15, 29, 77], showing the wide applicability of EMD in clinical practice.

To conclude, this study indicates that EMD is a very complex protein mixture that contains many proteins that have not been previously described. Although amelogenins are the major constituents, the discovery of novel proteins can lead to a better understanding of the biological mechanisms involved in oral tissues

regeneration. Since there is not a consensus on which protein is responsible for EMD biological activity on many different cells, it is possible that different combination of proteins found in specific fractions could deliver an enhanced response for specific tissues. Therefore, this study brings a new perspective on EMD composition to future exploration of the effect of other EMD proteins at the tissue and cellular levels to achieve optimized results for tissue regeneration.

3.5 References

1. Hammarstrom, L., L. Heijl, and S. Gestrelius, *Periodontal regeneration in a buccal dehiscence model in monkeys after application of enamel matrix proteins.* J Clin Periodontol, 1997. **24**(9 Pt 2): p. 669-77.

2. Lyngstadaas, S.P., et al., *Enamel matrix proteins; old molecules for new applications.* Orthod Craniofac Res, 2009. **12**(3): p. 243-53.

3. Uchida, T., et al., *Immunocytochemical and immunochemical detection of a 32 kDa nonamelogenin and related proteins in porcine tooth germs.* Arch Histol Cytol, 1991. **54**(5): p. 527-38.

4. Hu, C.C., et al., *Sheathlin: cloning, cDNA/polypeptide sequences, and immunolocalization of porcine enamel sheath proteins.* J Dent Res, 1997. **76**(2): p. 648-57.

5. Fukae, M. and T. Tanabe, *Degradation of enamel matrix proteins in porcine secretory enamel.* Connect Tissue Res, 1998. **39**(1-3): p. 123-9; discussion 141-9.

6. Simmer, J.P., et al., *Purification, characterization, and cloning of enamel matrix serine proteinase 1.* J Dent Res, 1998. **77**(2): p. 377-86.

7. Bashir, M.M., W.R. Abrams, and J. Rosenbloom, *Molecular cloning and characterization of the bovine tuftelin gene.* Arch Oral Biol, 1997. **42**(7): p. 489-96.

8. Kawase, T., et al., *Enamel matrix derivative (EMDOGAIN) rapidly stimulates phosphorylation of the MAP kinase family and nuclear accumulation of smad2 in both oral epithelial and fibroblastic human cells.* J Periodontal Res, 2001. **36**(6): p. 367-76.

9. Iwata, T., et al., *Noggin blocks osteoinductive activity of porcine enamel extracts.* J Dent Res, 2002. **81**(6): p. 387-91.

10. Suzuki, S., et al., *Enamel matrix derivative gel stimulates signal transduction of BMP and TGF-{beta}.* J Dent Res, 2005. **84**(6): p. 510-4.

11. Miron, R.J., et al., *Twenty years of enamel matrix derivative: the past, the present and the future.* J Clin Periodontol, 2016. **43**(8): p. 668-83.

12. Yoneda, S., et al., *The effects of enamel matrix derivative (EMD) on osteoblastic cells in culture and bone regeneration in a rat skull defect.* J Periodontal Res, 2003. **38**(3): p. 333-42.

13. Schlueter, S.R., D.L. Carnes, and D.L. Cochran, *In vitro effects of enamel matrix derivative on microvascular cells.* J Periodontol, 2007. **78**(1): p. 141-51.

14. Bertl, K., et al., *Effects of enamel matrix derivative on proliferation/viability, migration, and expression of angiogenic factor and adhesion molecules in endothelial cells in vitro.* J Periodontol, 2009. **80**(10): p. 1622-30.

15. Miron, R.J., M. Dard, and M. Weinreb, *Enamel matrix derivative, inflammation and soft tissue wound healing.* J Periodontal Res, 2015. **50**(5): p. 555-69.

16. Lossdorfer, S., et al., *Enamel matrix derivative promotes human periodontal ligament cell differentiation and osteoprotegerin production in vitro.* J Dent Res, 2007. **86**(10): p. 980-5.

17. Johnson, D.L., et al., *Cellular effects of enamel matrix derivative are associated with different molecular weight fractions following separation by size-exclusion chromatography.* J Periodontol, 2009. **80**(4): p. 648-56.

18. Sculean, A., et al., *Healing of human intrabony defects following treatment with enamel matrix proteins or guided tissue regeneration.* J Periodontal Res, 1999. **34**(6): p. 310-22.

19. Laemmli, U.K., *Cleavage of structural proteins during the assembly of the head of bacteriophage T4.* Nature, 1970. **227**(5259): p. 680-5.

20. Siqueira, W.L., et al., *Proteome of human minor salivary gland secretion.* J Dent Res, 2008. **87**(5): p. 445-50.

21. Mi, H., et al., *PANTHER version 11: expanded annotation data from Gene Ontology and Reactome pathways, and data analysis tool enhancements.* Nucleic Acids Res, 2017. **45**(D1): p. D183-D189.

22. Metsalu, T. and J. Vilo, *ClustVis: a web tool for visualizing clustering of multivariate data using Principal Component Analysis and heatmap.* Nucleic Acids Res, 2015. **43**(W1): p. W566-70.

23. Cochran, D.L., et al., *Periodontal regeneration with a combination of enamel matrix proteins and autogenous bone grafting.* J Periodontol, 2003. **74**(9): p. 1269-81.

24. Mellonig, J.T., et al., *Clinical and histologic evaluation of non-surgical periodontal therapy with enamel matrix derivative: a report of four cases.* J Periodontol, 2009. **80**(9): p. 1534-40.

25. Stein, G.S., et al., *Transcriptional control of osteoblast growth and differentiation.* Physiol Rev, 1996. **76**(2): p. 593-629.

26. Cattaneo, V., et al., *Effect of enamel matrix derivative on human periodontal fibroblasts: proliferation, morphology and root surface colonization. An in vitro study.* J Periodontal Res, 2003. **38**(6): p. 568-74.

27. Groeger, S., A. Windhorst, and J. Meyle, *Influence of Enamel Matrix Derivative on Human Epithelial Cells In Vitro.* J Periodontol, 2016. **87**(10): p. 1217-27.

28. Jonke, E., et al., *Effect of tyrosine-rich amelogenin peptide on behavior and differentiation of endothelial cells.* Clin Oral Investig, 2016. **20**(8): p. 2275-2284.

29. Maymon-Gil, T., et al., *Enamel Matrix Derivative Promotes Healing of a Surgical Wound in the Rat Oral Mucosa.* J Periodontol, 2016. **87**(5): p. 601-9.

30. Kuramitsu-Fujimoto, S., et al., *Novel biological activity of ameloblastin in enamel matrix derivative.* J Appl Oral Sci, 2015. **23**(1): p. 49-55.

31. Mumulidu, A., et al., *Purification and analysis of a 5kDa component of enamel matrix derivative.* J Chromatogr B Analyt Technol Biomed Life Sci, 2007. **857**(2): p. 210-8.

32. Schirmer, E.C., J.R. Yates, 3rd, and L. Gerace, *MudPIT: A powerful proteomics tool for discovery.* Discov Med, 2003. **3**(18): p. 38-9.

33. Bartlett, J.D., *Dental enamel development: proteinases and their enamel matrix substrates.* ISRN Dent, 2013. **2013**: p. 684607.

34. Kirkham, J., et al., *Maturation in developing permanent porcine enamel.* J Dent Res, 1988. **67**(9): p. 1156-60.

35. Strawich, E. and M.J. Glimcher, *Tooth 'enamelins' identified mainly as serum proteins. Major 'enamelin' is albumin.* Eur J Biochem, 1990. **191**(1): p. 47-56.

36. Cerri, P.S., et al., *Light microscopy and computer three-dimensional reconstruction of the blood capillaries of the enamel organ of rat molar tooth germs.* J Anat, 2004. **204**(Pt 3): p. 191-5.

37. Krebsbach, P.H., et al., *Full-length sequence, localization, and chromosomal mapping of ameloblastin. A novel tooth-specific gene.* J Biol Chem, 1996. **271**(8): p. 4431-5.

38. Bartlett, J.D., et al., *Enamelysin mRNA displays a developmentally defined pattern of expression and encodes a protein which degrades amelogenin.* Connect Tissue Res, 1998. **39**(1-3): p. 101-9; discussion 141-9.

39. Moffatt, P., et al., *Identification of secreted and membrane proteins in the rat incisor enamel organ using a signal-trap screening approach.* Eur J Oral Sci, 2006. **114 Suppl 1**: p. 139-46; discussion 164-5, 380-1.

40. Iwasaki, K., et al., *Amelotin--a Novel Secreted, Ameloblast-specific Protein.* J Dent Res, 2005. **84**(12): p. 1127-32.

41. Abbarin, N., et al., *The enamel protein amelotin is a promoter of hydroxyapatite mineralization.* J Bone Miner Res, 2015. **30**(5): p. 775-85.

42. Prasad, M., W.T. Butler, and C. Qin, *Dentin sialophosphoprotein in biomineralization.* Connect Tissue Res, 2010. **51**(5): p. 404-17.

43. MacDougall, M., et al., *Dentin phosphoprotein and dentin sialoprotein are cleavage products expressed from a single transcript coded by a gene on human chromosome 4. Dentin phosphoprotein DNA sequence determination.* J Biol Chem, 1997. **272**(2): p. 835-42.

44. Darwish, S.S., et al., *Root maturation and dentin-pulp response to enamel matrix derivative in pulpotomized permanent teeth.* J Tissue Eng, 2014. **5**: p. 2041731414521707.

45. Igarashi, R., et al., *Porcine enamel matrix derivative enhances the formation of reparative dentine and dentine bridges during wound healing of amputated rat molars.* J Electron Microsc (Tokyo), 2003. **52**(2): p. 227-36.

46. Nakamura, Y., et al., *The induction of reparative dentine by enamel proteins.* Int Endod J, 2002. **35**(5): p. 407-17.

47. Wang, H., et al., *Enamel matrix protein interactions.* J Bone Miner Res, 2005. **20**(6): p. 1032-40.

48. Bartlett, J.D., et al., *3. Protein-protein interactions of the developing enamel matrix.* Curr Top Dev Biol, 2006. **74**: p. 57-115.

49. Memoli, B., et al., *Fetuin-A gene expression, synthesis and release in primary human hepatocytes cultured in a galactosylated membrane bioreactor.* Biomaterials, 2007. **28**(32): p. 4836-44.

50. Mattinzoli, D., et al., *FGF23-regulated production of Fetuin-A (AHSG) in osteocytes.* Bone, 2016. **83**: p. 35-47.

51. Zilm, P.S. and P.M. Bartold, *Proteomic identification of proteinase inhibitors in the porcine enamel matrix derivative, EMD((R)).* J Periodontal Res, 2011. **46**(1): p. 111-7.

52. Jahnen-Dechent, W., et al., *Fetuin-A regulation of calcified matrix metabolism.* Circ Res, 2011. **108**(12): p. 1494-509.

53. Brylka, L. and W. Jahnen-Dechent, *The role of fetuin-A in physiological and pathological mineralization.* Calcif Tissue Int, 2013. **93**(4): p. 355-64.

54. Heiss, A., et al., *Structural basis of calcification inhibition by alpha 2-HS glycoprotein/fetuin-A. Formation of colloidal calciprotein particles.* J Biol Chem, 2003. **278**(15): p. 13333-41.

55. Genetos, D.C., et al., *Impaired osteoblast differentiation in annexin A2- and -A5-deficient cells.* PLoS One, 2014. **9**(9): p. e107482.

56. Gillette, J.M. and S.M. Nielsen-Preiss, *The role of annexin 2 in osteoblastic mineralization.* J Cell Sci, 2004. **117**(Pt 3): p. 441-9.

57. Grindheim, A.K., J. Saraste, and A. Vedeler, *Protein phosphorylation and its role in the regulation of Annexin A2 function.* Biochim Biophys Acta, 2017. **1861**(11 Pt A): p. 2515-2529.

58. Goldberg, M., et al., *Annexins I-VI in secretory ameloblasts and odontoblasts of rat incisor.* J Biol Buccale, 1990. **18**(4): p. 289-98.

59. Rosengarth, A. and H. Luecke, *A calcium-driven conformational switch of the N-terminal and core domains of annexin A1.* J Mol Biol, 2003. **326**(5): p. 1317-25.

60. Gerke, V. and S.E. Moss, *Annexins: from structure to function.* Physiol Rev, 2002. **82**(2): p. 331-71.

61. Xiao, Z., et al., *Analysis of the extracellular matrix vesicle proteome in mineralizing osteoblasts.* J Cell Physiol, 2007. **210**(2): p. 325-35.

62. Damazo, A.S., et al., *Role of annexin 1 gene expression in mouse craniofacial bone development.* Birth Defects Res A Clin Mol Teratol, 2007. **79**(7): p. 524-32.

63. Leoni, G. and A. Nusrat, *Annexin A1: shifting the balance towards resolution and repair.* Biol Chem, 2016. **397**(10): p. 971-9.

64. D'Acquisto, F., et al., *Annexin-1 modulates T-cell activation and differentiation.* Blood, 2007. **109**(3): p. 1095-102.

65. McArthur, S., et al., *Definition of a Novel Pathway Centered on Lysophosphatidic Acid To Recruit Monocytes during the Resolution Phase of Tissue Inflammation.* J Immunol, 2015. **195**(3): p. 1139-51.

66. Sugimoto, M.A., et al., *Annexin A1 and the Resolution of Inflammation: Modulation of Neutrophil Recruitment, Apoptosis, and Clearance.* J Immunol Res, 2016. **2016**: p. 8239258.

67. Smaldone, S. and F. Ramirez, *Fibrillin microfibrils in bone physiology.* Matrix Biol, 2016. **52-54**: p. 191-197.

68. Tiedemann, K., et al., *Fibrillin-1 directly regulates osteoclast formation and function by a dual mechanism.* J Cell Sci, 2013. **126**(Pt 18): p. 4187-94.

69. Ramirez, F. and D.B. Rifkin, *Extracellular microfibrils: contextual platforms for TGFbeta and BMP signaling.* Curr Opin Cell Biol, 2009. **21**(5): p. 616-22.

70. Nistala, H., et al., *Fibrillin-1 and -2 differentially modulate endogenous TGF-beta and BMP bioavailability during bone formation.* J Cell Biol, 2010. **190**(6): p. 1107-21.

71. Bax, D.V., et al., *Cell adhesion to fibrillin-1 molecules and microfibrils is mediated by alpha 5 beta 1 and alpha v beta 3 integrins.* J Biol Chem, 2003. **278**(36): p. 34605-16.

72. Egging, D., et al., *Wound healing in tenascin-X deficient mice suggests that tenascin-X is involved in matrix maturation rather than matrix deposition.* Connect Tissue Res, 2007. **48**(2): p. 93-8.

73. Karamanou, K., et al., *Lumican as a multivalent effector in wound healing.* Adv Drug Deliv Rev, 2018. **129**: p. 344-351.

74. Zheng, Z., et al., *Fibromodulin Is Essential for Fetal-Type Scarless Cutaneous Wound Healing.* Am J Pathol, 2016. **186**(11): p. 2824-2832.

75. Lenselink, E.A., *Role of fibronectin in normal wound healing.* Int Wound J, 2015. **12**(3): p. 313-6.

76. Matsumoto, S., et al., *The Effect of Control-released Basic Fibroblast Growth Factor in Wound Healing: Histological Analyses and Clinical Application.* Plast Reconstr Surg Glob Open, 2013. **1**(6): p. e44.

77. Hoang, A.M., T.W. Oates, and D.L. Cochran, *In vitro wound healing responses to enamel matrix derivative.* J Periodontol, 2000. **71**(8): p. 1270-7.

Chapter 4

Influence of EMD and EMD fraction on adhesion of human gingival fibroblasts

4.1 Introduction

For the past twenty years, enamel matrix derivative (EMD) has been widely used in regenerative dentistry to treat and repair periodontal tissues, including alveolar bone, periodontal ligament (PDL), cementum, and gingiva [1, 2]. EMD is a protein mixture extracted from developing porcine teeth that is constituted mostly by amelogenin protein and derived peptides (LRAP and TRAP) that represent ~ 90% of the enamel matrix [3]. The remaining constituents account for other proteins secreted in less quantity by the ameloblasts, including the enamelin [4], ameloblastin (also known as sheathlin) [5], odontogenic ameloblast-associated protein [6], and the enzymes matrix metalloproteinase-20 (MMP-20) [30], and kallikrein-4 (or enamel matrix serine proteinase 1) [7].

Numerous *in vitro* and *in vivo* studies in addition to clinical cases have shown the ability of EMD to assist and promote hard and soft tissue regeneration [8] by affecting a variety of cell, such as osteoblast [9], epithelial cells [10], endothelial cells [11, 12], and fibroblasts [13]. For example, the biological effects of EMD on osteoblast are well reported showing an enhancement in cell

adhesion [14], differentiation [15], maturation [16], and proliferation [17]. However, the influence of EMD proteins on oral fibroblasts vary between studies and different fibroblasts, i.e., human periodontal ligament fibroblasts (PDLF) and gingival fibroblasts (HGF). While the majority of reports agree that EMD significantly enhances proliferation and migration of both PDLF and, at a less extent, HGF [18-22], other studies show different results between PDLF and HGF regarding cell adhesion [23, 24]. It has been demonstrated that EMD induces attachment of HPLD [22, 23, 25, 26], but the influence of EMD on HGF adhesion remains inconclusive given inconsistent finding obtained by few studies [23, 24, 27]. For instance, Van der Pauw et al. showed that EMD increased cell adhesion of PDLF but not HGF on EMD-coated culture dishes [23]. Conversely, in another report, EMD seemed to promote attachment of HGFs on zirconia surface when EMD was used as a coating [24].

Since it has been proposed that EMD effects on diverse cells are due to different EMD components, the fractionation of EMD through chromatography has been utilized by various studies in an attempt to isolate and identify active proteins within the matrix [28-30]. In a recent study, Villa and co-workers showed that EMD proteins comprising the lower-molecular weight fractions increased 2- to 5-fold PDLF proliferation, whereas EMD components above 20 kDa had a different effect on the cell by stimulating the released of cytokines associated with angiogenesis [30]. In another study that investigated the response of HGF to native EMD and two of its components – recombinant 21.3 kDa amelogenin and tyrosine-rich amelogenin peptide (TRAP) – the authors

concluded that none of the EMD treatments induced or improved adhesion of HGF [27].

The attachment of HGF on dental materials such as dental implant is paramount to enhance the integration of gingival connective tissue with the implant surface in order to prevent the down growth of junctional epithelium and bacterial colonization [31]. Given the limited understanding on the effect of EMD may have on the attachment of HGF, we herein propose to use a multi-dimension chromatography approach combining size-exclusion chromatography and reverse-phase liquid-chromatography coupled with a mass spectrometer to identify EMD components associated with cell adhesion that could, therefore, promote attachment of gingival fibroblasts.

4.2 Material and Methods

4.2.1 EMD Stock and EMD Fractions preparation

Vials containing 30mg of lyophilized EMD (heat-treated) was donated by Institute Straumann and prepared according to the company standard protocol as previous described [32]. EMD stock solution of 10 mg/mL was prepared by dissolving the vial content in 3 mL of cold-sterile 0.1% acetic acid and kept in the fridge (4°C) for 1h. Next, 2mg of EMD were aliquoted, dried and resuspended for column separation in 200 µL of 0.025 M sodium acetate buffer (pH 4) at 4°C. EMD aliquots (10 mg/ml) were kept at 4°C for 2h before subjected to size-exclusion chromatography (SEC) on a ÄKTA fast-performance liquid chromatograph (FPLC) system (GE Healthcare) using a 10 x 300 mm column

(ENrich™ SEC 650, Bio-Rad). The column was equilibrated and EMD proteins were eluted with 0.025 M sodium acetate buffer (pH 4 at 4°C) monitored using absorbance at 280 nm. A total of 32 EMD fractions of 0.5 mL were collected at a flow rate of 0.1 $mLmin^{-1}$. Total proteins concentration from each sample was carried out by micro bicinchoninic acid (micro-BCA) assay (Pierce Chemical, Co., Rockford, IL, USA) using bovine serum albumin as protein standard. EMD control and EMD-fraction were further aliquoted for mass spectrometry analysis and for adhesion assay on gingival fibroblasts.

4.2.2 Sodium Dodecyl Sulfate-Polyacrylamide Gel Electrophoresis (SDS-PAGE)

Unfractionated EMD and EMD fractions were separated on 15% SDS-PAGE as described previously [28]. As the purpose was to confirm column separation by molecular weight, we selected only few fractions (F17, F27, F28, F29, F40, F41, F42, F43, and F44) showed by high peak in the chromatogram to load in the gel given low proteins quantity collected in other fractions (Figure 1b). Resolved bands were stained with Coomassie brilliant blue R-250 and photographed to visualize the protein content of loaded fractions in comparison with EMD control.

4.2.3 Mass spectrometry analysis of EMD fractions

4.2.3.1 In-solution digestion

Prior to mass spectrometry analysis, aliquots of 10 µg of EMD stock and fractions were dried by a rotary evaporator (Eppendorf, Parkway, NY, USA), denatured and reduced for 1h by adding 50 µL of solution containing 4 M urea, 10 mM DTT in 50 mM NH_4HCO_3 (pH 7.8), at 37 °C. After 4-fold dilution with 50 mM NH_4HCO_3 (pH 7.8), EMD samples were subjected to in-solution digestion with 2% (w/w) sequencing-grade trypsin (Promega, Madison, WI, USA) for 18 h at 37°C. Following trypsinization, samples were desalted by C-18 ZipTip® pipette tips (Millipore, Billerica, MA, USA) and further analyzed by nano-flow LC-ESI-MS/MS.

4.2.3.2 Nano-Liquid Chromatography Electrospray Ionization Tandem Mass Spectrometry (nLC-ESI-MS/MS analysis)

Following trypsinization, samples were dried by rotary evaporator, resuspended in 20 µL of 0.1% trifluoroacetic acid (TFA) and desalted by C-18 ZipTip® pipette tips (Millipore, Billerica, MA, USA). The eluted peptides derived from EMD samples were dried, resuspended in 15 µL of 97.5% H 2 O/2.4% acetonitrile/0.1% formic acid, and further subjected to RP-HPLC-ESI-MS/MS. Mass spectrometric analyses were carried out with a LTQ-Velos (Thermo Scientific, San Jose, CA, USA) coupled with a nano-flow reverse-phase HPLC capillary-fused silica C18 column (column length 10 mm, column id 75 µm, 3 µm spherical beads, and 100 A pores size) linked to mass spectrometer that uses an ESI in a survey scan in the range of m/z values 390–2000 MS/MS. The nano-flow RP-HPLC was developed with linear 85-min gradient ranging from 5 to 55% of solvent B (97.5% ACN, 0.1% formic acid) at a flow rate of 300 nL/min with a

maximum pressure of 280 bar. Electrospray voltage and the temperature of the ion-transfer capillary were 1.8 kV and 250°C, respectively. Each survey scan (MS) was followed by automated sequential selection of seven peptides for CID, with dynamic exclusion of the previously selected ions.

4.2.3.3 EMD Proteome analysis

The acquired MS/MS spectra generated were searched against pig (*Sus scrofa*) protein database (Uniprot) for all EMD samples using Proteome Discoverer 1.3 software and SEQUEST algorithm. Parameter Xcorr were used to validate the existence of a peptide within the sample. Xcorr is a value computed from cross correlation of the experimental MS/MS spectrum vs. the candidate peptides in the database, which reveals how closely the real spectrum relates to candidate peptides. Sequence-reversed protein databases were used as decoys to evaluate the false discovery rate of 1% during the search. At least 2 or more peptides were used for protein identification. The proteome of each EMD fractions were analyzed using Gene Ontology (GO) terms to search for proteins involved in biological adhesion and that are found in the extracellular matrix.

4.2.4 Human Gingival Fibroblasts isolation and growth

Human gingival fibroblasts (HGF) were obtained from healthy gingival tissue using explant cultures from four individuals [33]. HGF were maintained in T-75 tissue culture plastic flasks (75 cm^2) using high glucose Dulbecco's modification of Eagle's medium (DMEM; Invitrogen, USA) supplemented with

10% fetal bovine serum (FBS; Gibco, USA) and 1x antibiotics and antimycotics (antibiotics; 25 µg/ml amphotericin B, 50 µg/ml gentamicin, 100 µg/ml penicillin G, Invitrogen). Cells were expanded at 37°C in a humidified atmosphere of 95% air 5% CO_2 and medium was changed twice a week. After reaching 80% confluence, HGF were trypsinized to detached from the growth surface (0.25% trypsin, 0.1% glucose, citrate-saline buffer (pH 7.8), Gibco) and seeded in a new T-75 flask. Only cells between passages 2 and 8 were used for experiments.

4.2.5 Adhesion assays

For the adhesion assay [34, 35], 96-well culture plates (Cellstar®, Greiner, USA) were coated with 100 µL of EMD, EMD fractions (25 µg/mL in 0.1 M carbonate buffer), and fibronectin (10 µg/mL) as the positive control, and incubated overnight at 4°C for proteins adsorption. After incubation, coating solutions were removed and wells were blocked with 1% casein for 1h at room temperature followed by rinse with Dulbecco's phosphate-buffered saline (DPBS, pH 7.2, Gibco, USA). Then, cells were seeded in DMEM serum-free medium at a density of 10,000 cells per well and incubated for 40 min at 37°C (95% air, 5% CO_2) to allow cells to adhere. At the time indicated, medium was aspirated, and wells were rinsed twice with DPBS to remove non-adherent cells. Next, to measure adherent HGF, PrestoBue™ (Invitrogen) was used according to the manufacturer's protocol. Briefly, 100 µL of cell culture serum-free medium containing 10 µL of PrestoBlue™ reagent was added into each well and incubated for 2h at 37°C in a humidified atmosphere (95% air, 5% CO_2). Fluorescence was measured in a spectrophotometer (excitation 560nm,

emission 590 nm) [36]. Values acquired from the no-cell control was subtracted from each individual well. Experiments were performed in triplicates in three independent experiments. Cells morphology was observed in a phase contrast microscopy at x40 magnification using a Axio Observer.Z1 microscope (Carl Zeiss, Göttingen, Germany) and images were captured with Axiovision Software Release 4.8.

4.2.6 Statistical Analysis

Statistical analyses were done using one-way ANOVA and Dunnett test between control (Fibronectin) and EMD/EMD fractions, and ANOVA and Tukey's post hoc test between EMD and EMD fractions using IBM SPSS Statistics version 24 (IBM Corp. Armonk, NY: IBM Corp.). *p* values less than 0.05 were taken to be significant.

4.3 Results

4.3.1 EMD Fractionation

The chromatogram in Figure 4.1A shows the resulted fractionation of EMD proteins by size-exclusion chromatography. EMD proteins started to come out form the SEC column as fraction 19 until they eluted completely in fraction 50, resulting in a total of 32 samples. The larger amount of protein was collected around fractions 27 to 33 whereas the remaining fractions had a lower quantity. The fractionation was repeated until enough protein amount was reached for the proteomic analysis and adhesion assay. However, fractions 44 to 50 that

presented the lowest amount were combined in one sample to reach the minimal concentration required for the adhesion assay.

Some EMD fractions indicated on the SEC chromatogram with higher amount (peak height) were chosen to be resolved in a SDS-PAGE gel to confirm EMD separation by molecular weight (Figure 4.1B). High-molecular weight proteins were more evident in fraction F27 but started to fade in later fractions while more bands below between 15 kDa started to appear. Fractions F27, F28, and F29 showed a major protein band between 20 and 15 kDa that almost disappeared in the later fractions that are represented as F40-F44, which were enriched in proteins below 10 kDa, including the amelogenin LRAP and TRAP peptides.

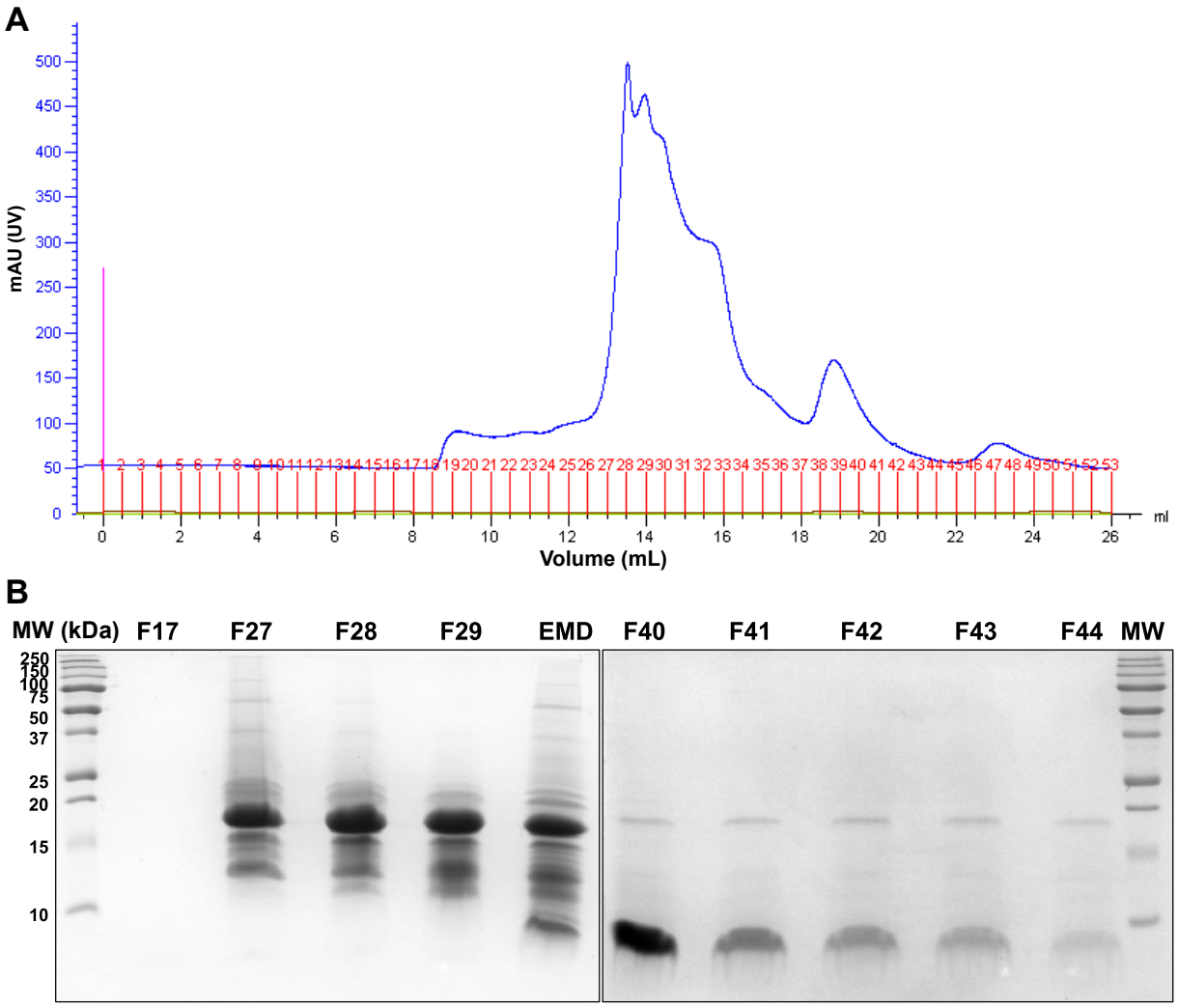

Figure 4.1 - EMD proteins fractionation. **A)** Chromatogram showing the fractionation of EMD proteins through size-exclusion chromatography (SEC) that resulted in 32 samples (F19 to F50). *Note. Numbers above the x-axis represents the fractions' numbers.* **B)** SDS-PAGE of EMD and selected EMD fractions (F17, F27, F28, F29, F40, F41, F42, F43, and F44) demonstrating decrease in molecular weight during protein elution. Lanes MW refer to molecular weight standards with sizes marked on the left and on the right; lane EMD refers to enamel matrix derivative; lane F17 to F44 represents EMD fractions that were loaded in the gel. Note that the lack of bands in lane F17 corresponds to no signal in the chromatogram.

4.3.2 Mass Spectrometry analysis

The characterization of EMD proteins of each fraction by mass spectrometry identified a total of 89 proteins that are involved in biological adhesion and 44 proteins that are found in the extracellular matrix (ECM). The distribution of proteins per fraction is displayed in the histogram in Figure 4.2. The fractions with a larger number of identified proteins involved in adhesion were F26 (13), F24 (12), followed by F19, F22, F23 with 9 proteins each. Fractions F44, F47 (11), and F49 (19) of the low-molecular weight range also presented representative numbers that likely include enzymatic-product peptides derived from high-molecular weight proteins identified in these fractions (Table 4.1). The mid-range fractions (F29 to F42) presented fewer proteins that participate in both ECM and biological adhesion, in particular samples F29, F35, F36, F39, and F42 did not show any proteins in the latter category. Conversely, the high-molecular weight fractions showed more proteins associated with ECM.

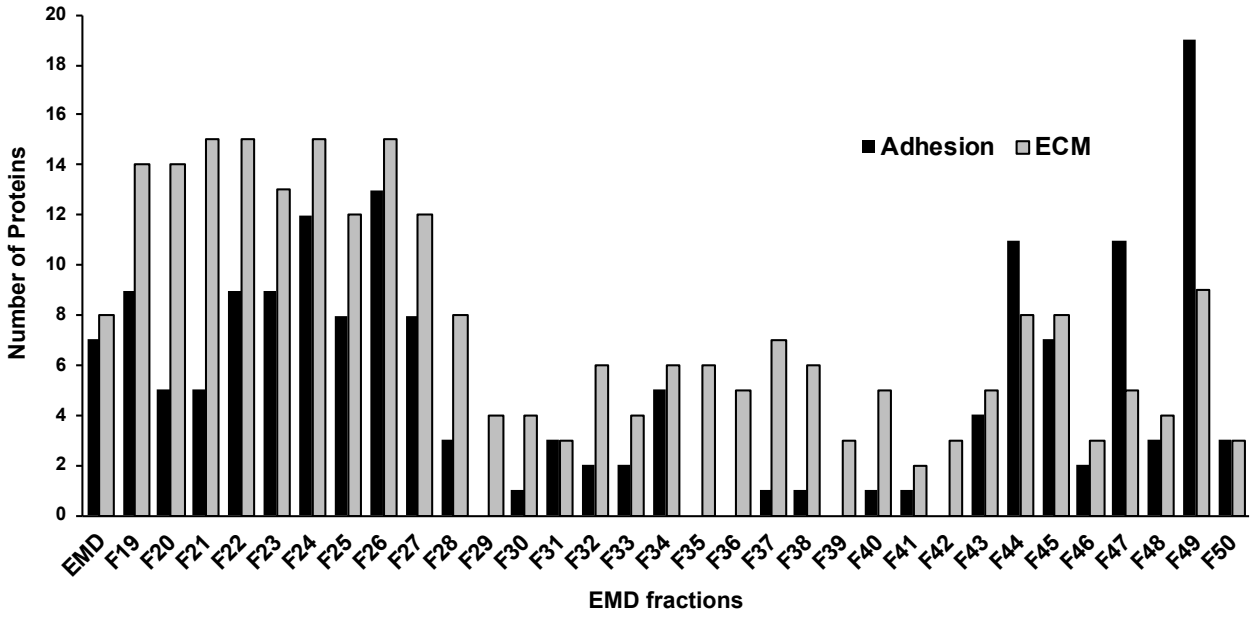

Figure 4.2 - Distribution of proteins/peptides on each EMD fraction (F19 to F50) classified as part of the extracellular matrix and that are involved in biological adhesion.

4.3.3 Proteomic analysis

As expected, the amelogenins were identified, particularly the 23 kDa amelogenins detected in all 32 fractions and the 18 kDa amelogenins variant detected in 8 fractions (F27, 28, 29, 30, 38, 40, 42, and 45) (Table 4.1). The identification of amelogenin in the low-molecular weight fractions indicate the presence of the amelogenin derived-peptides 6.5 kDa leucine-rich amelogenin protein (LRAP) and 5.3 kDa tyrosine-rich amelogenin peptide (TRAP) showed in the SDS-PAGE gel (Figure 4.1B). Since LRAP and TRAP peptides share same amino acid sequence with the amelogenins, it was not possible to differentiate them between all amelogenin-derived products. Other classical EMD constituents were also present in the majority of fractions, including enamelin (detected in 31 fractions, excepted in F49), and ameloblastin (also known as sheathlin) identified in 27 fractions (excepted in F40, and F47 – F50). In addition, the two enamel-specific proteases, matrix metalloproteinase (MMP)-20 (enamelysin), and kallikrein-4 (known as enamel matrix serine protease 1) were detected along with the new recent EMD member odontogenic ameloblast-associated protein (ODAM) (Table 4.1). Interestingly, we also detected in high abundance (21 fractions) the dentin sialophosphoprotein (DSSP), which has never been described as an EMD component.

Other ECM proteins were present in many samples, such as alpha-2-HS-glycoprotein (F19 – F28, F30, F37), annexins A1 and A2 (AnxA1, and AnxA2) (F19, F20, F21, F22, F23, F24, F25, F26), pigment epithelium-derived factor (F19, 20, 21, 22, 23, 24, 25, 26, 27), lumican precursor (F19, F20, F21, F22),

and tenascin XB (F25, F26, F47) as the most abundant (Table 1). Among 88 proteins involved in biological adhesion, the majority were found in few fractions such as galectin-3 (F26, F27), fibronectin 1 (F31), fibromodulin (F20, F21, F22), and fibrillin-1 (F19, F24, F26). Nonetheless, collagen type I alpha 1 chain (F19, F20, F21, F22, F23, F25, F26), Laminin subunit alpha 3 (F19, F20, F22, F23, F24, F25, F26, F27), DS cell adhesion molecule (F19, F20, F22, F23, F24, F31) were found in more fractions within the high-molecular weight range.

4.3.4 Adhesion of human gingival fibroblasts

After identifying EMD proteins related to biological adhesion and extracellular matrix, we compared the ability of HGF to adhere to fibronectin, unfractionated EMD and EMD fractions in a standard adhesion assay. Our results indicated that HGF adhesion to fibronectin was significantly greater than to EMD or EMD fractions (Figure 4.3) (ANOVA and Dunnett test, $p < 0.001$). However, when isolating the effects of EMD and different EMD fractions, fractions F23 and F24 demonstrated a significant higher response than whole EMD and casein (negative control) (ANOVA and Tukey test, $p < 0.001$). These high-molecular weight fractions contain many ECM proteins that are involved in biological adhesion which includes fibrillin-1, collagen type I alpha 1 chain, AnxA1, AnxA2, laminin subunit alpha, and DS cell adhesion molecule (Table 4.1). Finally, the morphology of fibroblasts exposed to fibronectin showed a cell shape consistent with adherence and initial spreading when visualized by the microscope (Figure 4.4). Differently, cell incubated with whole EMD and EMD fractions showed a rounded shape indicating limited initial adhesion. Although

F23 and F24 showed a significant increase in cell adhesion compared to unfractionated EMD, the cell morphology of HGF was not affected. Collectively, these data indicate that despite containing ECM and adhesion proteins, EMD showed a limited capacity to promote attachment of HGF in comparison to fibronectin.

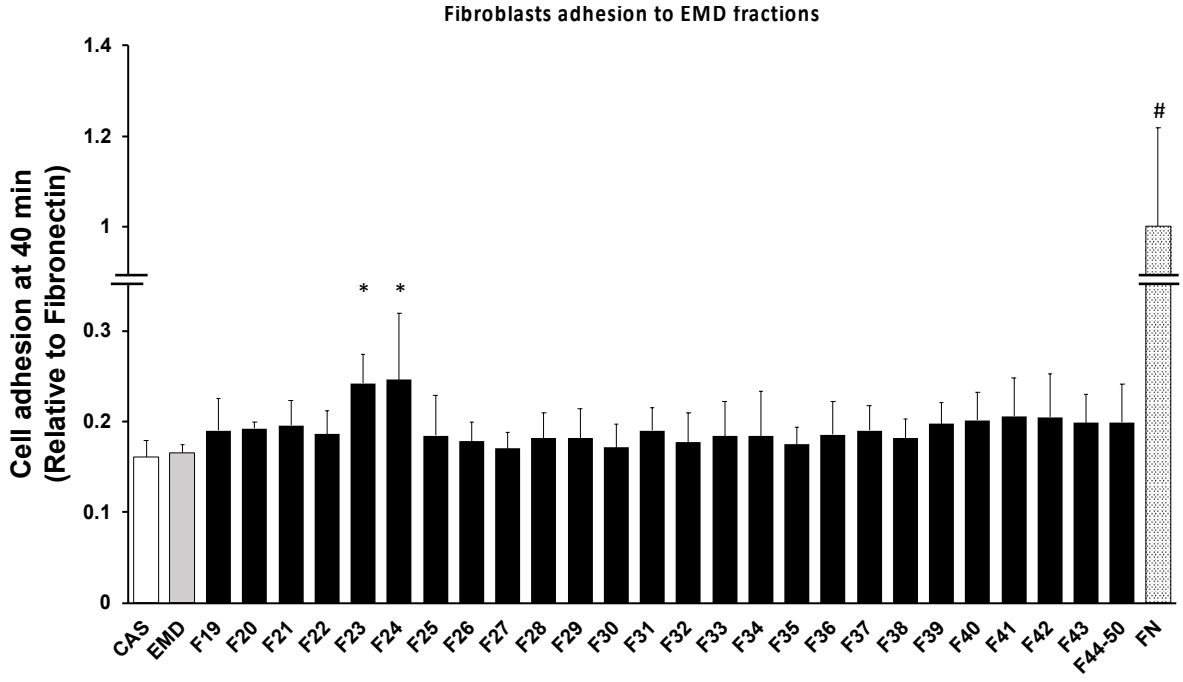

Figure 4.3 - Adhesion assays (40 min) of HGF cells seeded on culture plates coated with casein (1% CAS) as negative control, fibronectin (FN, 10 µg/mL) as positive control, EMD and EMD fractions F19 to F44-50 (25 µg/mL). (Data are expressed as mean ± standard deviation. Number symbol denotes significant difference between control and all other fractions, ANOVA and Dunnett test, $p < 0.001$; asterisk denotes significant difference between EMD and EMD fractions, ANOVA and Tukey test, $p < 0.001$).

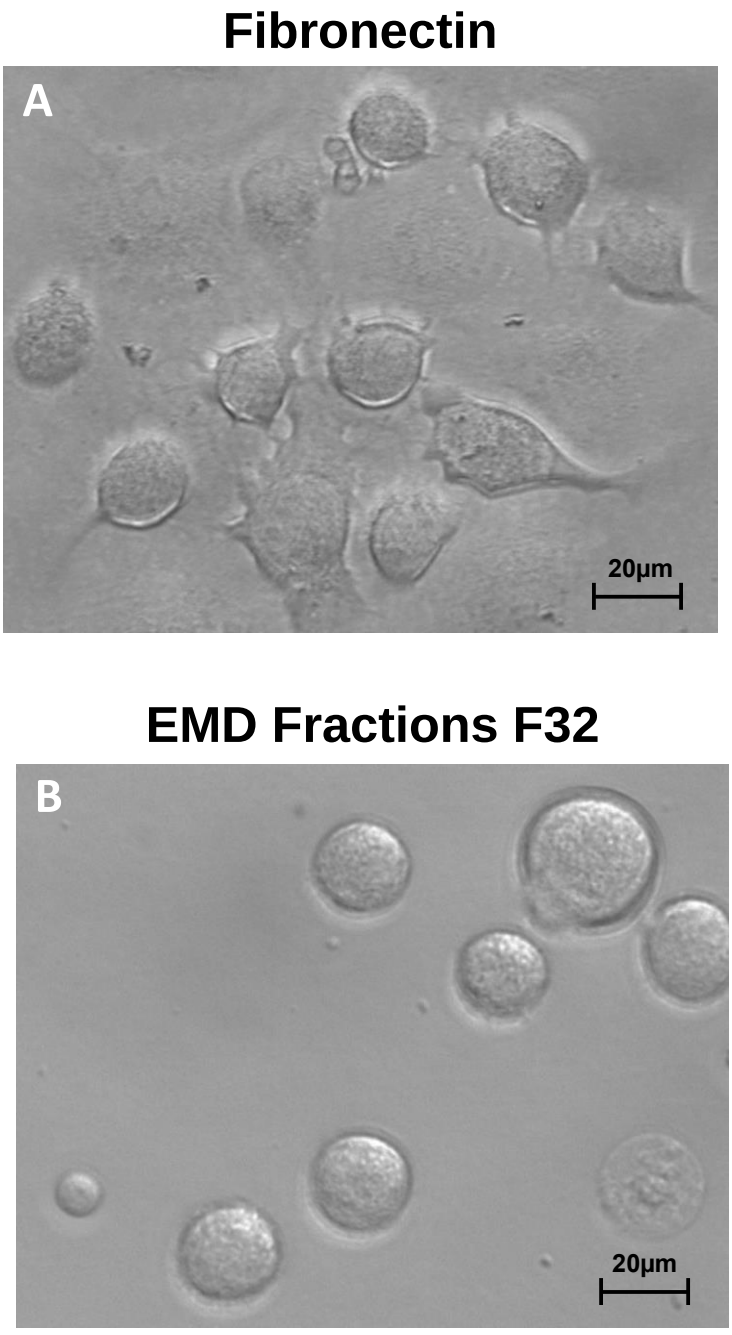

Figure 4.4 - Effects of fibronectin (control) and EMD fraction F32 on cell appearance and adhesion in human gingival fibroblast cell cultures. Cell suspension was seeded (10,000 cells/well) onto 96-well culture plates coated with (A) fibronectin (10 µg/mL) and (B) EMD fractions F32 (25 µg/mL) as an example, and incubated for 40min in serum-free medium at 37°C in a humidified atmosphere of 95% air 5% CO_2.

Table 4.1- List of proteins identified in EMD fractions associated with ECM (44) and biological adhesion (89), the corresponding molecular-weight (MW), and fractions in which the proteins were detected.

Accession Number	Protein name	MW (kDa)	ECM	Adhesion	Fraction
Q9TQY2	23 kDa amelogenin	18.3	x		19 – 50
Q9TQY1	18 kDa amelogenin	15.0	x		27, 28, 29, 30, 38, 40, 42, 45
Q28989	Ameloblastin (Sheathlin)	44.9	x		19 – 39, 41, 42, 43, 44, 45, 46
O97939	Enamelin	128.3	x		19 – 48, 50
P79287	Matrix metalloproteinase-20 (MMP-20) (Enamelysin)	54.0	x		19 – 29, 34 – 38, 40, 43 – 48, 50
C9W8E7	Dentin sialophosphoprotein (Fragment)	57.4	x		20, 23 – 28, 31 – 35, 43, 44, 48, 49
P29700	Alpha-2-HS-glycoprotein (Fetuin-A)	38.4	x		19 – 28, 30, 37
Q0PM28	Pigment epithelium-derived factor	45.6	x		19, 20, 21, 22, 23, 24, 25, 26, 27
P19619	Annexin A1	38.7	x		19, 20, 21, 22, 23, 24, 25, 26
A0A287BI04	Annexin A2	36.3	x		19, 20, 21, 22, 23, 24, 25, 26
Q9XSN6	Enamel matrix serine proteinase 1 (Kallikren-4)	27.2	x		19, 20, 21, 22, 23
F1RVB3	Odontogenic ameloblast-associated protein	30.6	x		19, 21, 23, 24
F1SQ09	Lumican precursor	38.8	x		19, 20, 21, 22
Q9TTB4	Fibromodulin	16.7	x		20, 21, 22
F1RJ55	Oligodendrocyte myelin glycoprotein	49.8	x		44, 47
O19112	Cartilage intermediate layer protein 1 (CILP-1)	67.4	x		49
I3LDG8	Collagen type XXVII alpha 1 chain	183.4	x		32
I3LBV3	Protein Wnt	39.4	x		22
F1SV70	Matrix metalloproteinase	58.9	x		45
F1SFA7	Collagen alpha-2(I) chain precursor	104.4	x		26
F1SA65	Fibrillin 3	297.8	x		49
F1RG45	Angiotensinogen	51.0	x		23

D3JCV7	Protein Wnt	45.3	x		27
A0A287AGN9	Spondin 1	84.6	x		44
F1RW71	Multimerin 1	137.7	x		43
F1SMW3	Serpin family B member 5	42.1	x		21
A0A287AN90	Matrix metalloproteinase-9 precursor (MMP-9)	74.6	x		27
A0A287BLD2	Collagen type I alpha 1 chain	138.0	x	x	19, 20, 21, 22, 23, 25, 26
I3LQP2	Pleckstrin homology like domain family B member 2	140.0	x	x	26, 27, 37, 49
F1RQI0	Collagen type XII alpha 1 chain	332.6	x	x	22, 25, 26
F1SN67	Fibrillin-1	312.2	x	x	19, 24, 26
A5A8W4	Tenascin XB	446.8	x	x	25, 26, 47
A3EX84	Galectin-3	27.2	x	x	26, 27
F1SS24	Fibronectin 1	270.4	x	x	31
F1RJ58	Neurofibromin 1	319.3	x	x	32
F1S279	Nephroblastoma overexpressed	39.2	x	x	45
I3LJU9	Tenascin	205.3	x	x	24
I3LUR7	Collagen type VI alpha 3 chain	317.6	x	x	44
A0A287A0A6	Collagen type VI alpha 6 chain	228.4	x	x	49
F1S663	Laminin subunit gamma-1 precursor	162.7	x	x	49
F1S662	Laminin subunit gamma 2	130.8	x	x	24
F1S0W7	Laminin subunit gamma 3	169.9	x	x	27
F1SX59	Versican	369.2	x	x	45
I3LHG2	Tectorin alpha	230.3	x	x	49
F1SBB3	Laminin subunit alpha 3	367.8		x	19, 20, 22, 23, 24, 25, 26, 27
F1SGT7	DS cell adhesion molecule	208.9		x	19, 20, 22, 23, 24, 31
I3LDQ1	Talin 2	267.3		x	31, 41, 49, 50
P37176	Endoglin (CD antigen CD105)	70.2		x	27, 44, 46
F1RMV7	LY6/PLAUR domain containing 3	36.0		x	19, 34, 44
I3LRQ5	Phosphatase and actin regulator	76.9		x	20, 27, 49
A0A287A428	Plakophilin 4	115.6		x	26, 44, 49
F1RXE4	Tensin 4	76.0		x	24, 47, 49
F1RUG5	WNK lysine deficient protein kinase 3	191.4		x	20, 25, 43
A0A287AG36	Laminin subunit alpha 1	333.6		x	27, 47
F1SKK7	Cadherin EGF LAG seven-pass G-type receptor 3	357.8		x	44, 49
A0A287AEH1	Laminin subunit alpha 5	395.4		x	24, 43

A0A287BAD8	LIM domain 7	147.5	x	19, 49
I3LG79	Desmocollin 3	99.8	x	24, 43
A0A286ZXU9	FAT atypical cadherin 4	529.9	x	26, 34
A0A287BLY8	Talin 1	239.2	x	21, 48
A0A287B5M2	Mucin-4 precursor	131.9	x	33, 49
F1SER9	FAT tumor suppressor homolog 1	505.9	x	23, 44
A0A287AG74	Membrane associated guanylate kinase, WW and PDZ domain containing 2	139.5	x	19, 21
F1SQ60	Heart development protein with EGF like domains 1	138.7	x	22, 47
F1SI16	Receptor protein serine/threonine kinase	115.0	x	23, 44
A0A287BIY4	Cadherin 8	88.2	x	44
A0A287AEM7	Cadherin EGF LAG seven-pass G-type receptor 2	315.2	x	45
A0A287BL69	Cadherin related family member 1	87.5	x	44
F1RSA2	Calcium-transporting ATPase	104.2	x	27
C3VPJ4	Claudin	22.3	x	44
A0A287ATF2	Desmoglein 2	102.9	x	34
A0A287AA14	Desmoplakin	228.9	x	49
E7FM66	Disintegrin and metalloprotease domain-containing protein 5 (Fragment)	45.2	x	47
K7GPY3	Ectodysplasin A	41.3	x	47
I3LEB9	EPH receptor B1	109.7	x	44
A0A287BQC4	FAT atypical cadherin 3	354.5	x	20
F1SFE3	Fermitin family member 2	80.7	x	46
A0A287BGJ4	FRAS1 related extracellular matrix 1	244.7	x	40
F1S794	Hepatic and glial cell adhesion molecule	51.6	x	26
F1RYP4	Integrin subunit alpha 4	107.4	x	50
K7GSU6	Integrin subunit alpha E	125.2	x	46
K7GT68	Integrin subunit alpha 6	121.4	x	19
F1SGE7	Integrin beta	87.4	x	44
A0A287BHP4	Integrin beta	85.0	x	32
A0A287BCR9	Junctional cadherin 5 associated	125.5	x	19
F1SGG1	Keratin 18	47.4	x	27
Q7YS22	Lymphatic endothelial hyaluronan receptor LYVE-1 (Fragment)	22.2	x	26
A0A287A7V5	Myelin-oligodendrocyte glycoprotein	23.7	x	34
F1SRM1	Myosin X	236.0	x	22
Q2EN76	Nucleoside diphosphate kinase B (NDK B)	17.2	x	19

F1RUR8	Par-3 family cell polarity regulator	129.2	x	49
I3LGN8	Plakophilin 1	80.6	x	49
F1SPK1	Plexin D1	213.9	x	24
A0A287ABC9	Protein tyrosine kinase 2	105.8	x	22
A0A287ARL0	Protein tyrosine kinase 2 beta	113.8	x	28
F1S1M6	Protocadherin 19	125.8	x	45
A0A287ARC5	Protocadherin gamma subfamily C, 4	100.9	x	21
F1S0W0	Rap guanine nucleotide exchange factor 1	119.8	x	38
F1RNT6	Repulsive guidance molecule family member b	43.0	x	34
F1SG15	Rho GTPase activating protein 6	77.4	x	30
I3L9Z3	Serine/threonine-protein kinase	98.0	x	21
I3L8F6	SH3 domain binding protein 1	61.6	x	49
A0A286ZNC2	SRC kinase signaling inhibitor 1	130.9	x	25
F1SI04	Sushi, nidogen and EGF like domains 1	147.4	x	25
A0A287BF71	Tight junction protein 1	199.0	x	49
F1SP25	Transmembrane protein 245	80.3	x	23
I3LFP3	Versican core protein precursor	261.8	x	33
F1SMF4	Integrin subunit alpha 2	129.3	x	45
F1S9C8	Cadherin 24	83.7	x	47
A0A286ZTM0	Integrin subunit alpha X	126.8	x	49
K9J6K2	Utrophin	393.8	x	47
Q29123	Vascular cell adhesion molecule	58.7	x	27
A0A2C9F393	Vinculin	121.7	x	49
F1RFK7	BAI1 associated protein 2 like 1	56.2	x	28
K7GT47	Linker for activation of T-cells	25.0	x	48
K9IVR7	WD repeat domain 1	66.1	x	23

4.4 Discussion

EMD is predominantly composed by amelogenin (>90%) along with other ECM proteins, such as enamelin and ameloblastin, that are secreted by ameloblasts during tooth development [37]. It has been shown that EMD influences a variety of cell such as osteoblasts, endothelial cells, epithelial cells, and fibroblasts [16, 38, 39]. Most of the work investigating the effect of EMD on fibroblast was done on periodontal fibroblasts (PDLF) demonstrating that EMD promote cell adhesion, migration, proliferation and differentiation [19-21]. On the other hand, biological effects on HGF has been restricted to proliferation and migration, but not on adhesion [23, 27]. Considered a complex proteins mixture, EMD have been explored through chromatography by various studies to identify bioactive components that promote hard and soft tissue regeneration [28-30]. In this work, SEC was used in a FPLC system to fractionate EMD in an attempt to identify proteins through mass spectrometry that could promote adhesion of HGF, which is highly required for dental implants treatment to prevent epithelial down growth and bacterial colonization at the implant abutment. Different from previous studies that used SEC [28, 30], EMD proteins were eluted through the column at a slower flow-rate (0.1 mL/min) to increase resolution and maximize protein separation [40], resulting in a total of 32 fractions collected. Instead of choosing specific fractions with higher protein amount as shown elsewhere [28], we considered analyzing all fractions aiming to cover the whole EMD content, including fractions with low protein amount that were collected repeatedly until reaching minimum amount necessary for further analysis.

The proteome analysis of EMD fractions identified 44 ECM proteins that are distributed across all fractions, including the recognized EMD constituents amelogenins, enamelin [4], ameloblastin [5], and the recently detected alpha-2-HS-glycoprotein [41]. Other ECM proteins were also identified, such as AnxA1, AnxA2, pigment epithelium-derived factor, and lumican precursor (Table 4.1). Interestingly, DSSP, the most abundant non-collagenous ECM protein during dentinogenesis, was detected in most fractions [42]. These findings suggest that dentine-matrix proteins are also present in EMD, which could explain the potential of EMD to repair dentin and to promote pulpal mineralization in reactive dentine indicated by few studies [43, 44]. Moreover, 89 proteins involved in biological adhesion were detected throughout the majority of EMD fractions, many of which are ECM proteins, such as collagen, and laminin (Table 4.1, Figure 4.2). The fractions with the higher number of proteins associated with ECM and biological adhesion were found in the high-molecular range, particularly fractions F19, F22, F23, F24, and F26, as well as the low-molecular weight fraction F49 that includes peptides originated from proteins that undergo proteolytic degradation that occur within the enamel matrix [45]. The importance of ECM and adhesive proteins such as collagen and fibronectin is that these proteins are essential for fibroblast interaction to the ECM for promoting cell adhesion, which is the crucial event that regulates further cellular responses such as spreading, cell migration, cell differentiation, and cell survival that result in cell proliferation and tissue development [46].

The results of the adhesion assay indicated that neither EMD nor its derived-fractions were capable of promoting early adhesion of HGF at the degree showed by fibronectin (Figure 4.3). However, we observed that EMD fraction F23 and F24 showed a significantly higher response than the whole EMD and other fractions. The limited adhesion of HGF on EMD-coated surface was confirmed through phase-contrast microscopy that revealed rounded cells without showing any spreading morphology (Figure 4.4B). Conversely, HGF exposed to fibronectin-coated surface displayed a star-shape morphology that is consistent to initial phase of integrin-mediated adhesion (Figure 4.4A) [47]. These findings corroborate previous studies that indicated lack of attachment and spreading ability of HGF when exposed to the whole EMD either on culture plates [23, 48] or titanium-coated surfaces [49], which was also demonstrated for HPLD [20]. In their work, Van der Pauw and collaborators showed that HGF only started to attach and spread after 48 hours post-seeding [23]. Contrasting results were found in another study in which zirconium surface coated with EMD showed increasing in HGF attachment in comparison to non-coated surfaces [24]. However, the authors measured the adhesion after 4 hours using HGF immortalized cell line. Differently, we used primary fibroblasts that were exposed to EMD samples for 40 min, which is a time frame suitable to evaluated early cell adhesion since HGFs are recognized to show specific adhesion to fibronectin on coated-surfaces within few minutes of exposure rather than hours as also confirmed in our study [50]. Hence, the distinct results between these studies

are likely related to differences in methodologies applied, specifically regarding incubation time for cell adhesion.

The present study showed that the whole EMD along with the majority of EMD fractions did not promote attachment of HGF, while the fractions F23 and F24 delivered a significant superior adhesion than EMD (Figure 4.3). In particular, these high-molecular weight fractions comprised proteins associated with the ECM that are known to promote adhesion of fibroblasts (Figure 4.2), such as collagen type I (F23) and laminin (F23, F24) [50, 51]. The contribution of collagen type I on HGF adhesion would be more significant than laminin since it has been demonstrated that HGF adhered considerably more to collagen type I than to laminin, which preferably promotes attachment of HPDL and gingival epithelial cell [13, 52, 53]. Another protein identified in F24 was the 312-kDa fibrillin-1 that was only found in two other fractions (F19, and F26). Fibrillin-1 contains one RGD motif in its sequence that is known to mediates cell adhesion through transmembrane integrins αvβ3 and α5β1 on both cell-substratum and cell-cell interactions [54]. These integrins are expressed in both HGF and HPDL, having an essential role in attachment and spreading of HGF [13].

Interestingly, another protein involved in adhesion that was only found in F24 was tenascin C. Tenascin C is a large ECM glycoprotein that interacts with various ECM molecules and cell surface receptors including integrins expressed on fibroblasts [55]. Tenascin C is also recognized to regulate cell adhesion on fibroblasts by inhibiting cell spreading on fibronectin [56] while modulating fibroblast recruitment and migration during wound healing [57]. Even identifying

in these fractions many proteins associated with cells adhesion, it was not possible to determine which proteins were responsible for the effects observed on the adhesion of HGF because many proteins are also present in other fractions such as collagen type I (7 fractions), and laminin (8 fractions). Likewise, the presence of amelogenins in fraction F23 and F24 cannot be associated with HGF adhesion since amelogenin and derived-peptides were identified in whole EMD and in all fractions, which also applies to ameloblastin, enamelin, and DSPP detected in fractions F23 and F24. Conversely, the presence of these proteins in the majority of fractions that showed lack of cell adhesion suggest that these proteins do not mediate adhesion of HGF, despite previous studies that demonstrated the influence of amelogenin on cell attachment [58].

In conclusion, we showed in this study that the fractionation of EMD in combination with mass spectrometry allowed the identification of various ECM proteins within the enamel matrix that are involved in biological adhesion processes, mostly the high-molecular weight fractions. In addition, our findings suggested that two high-molecular height fractions of EMD promoted adhesion of gingival fibroblasts in comparison to whole EMD and other EMD fractions that did not provide necessary cues to induce HGF attachment. Further investigation is needed to determine whether the proteins identified in these fractions may assist in the adhesion of gingival or periodontal fibroblasts to enhance the integration with dental materials in the oral cavity.

4.5 References

1. Cochran, D.L., et al., *Periodontal regeneration with a combination of enamel matrix proteins and autogenous bone grafting.* J Periodontol, 2003. **74**(9): p. 1269-81.

2. Mellonig, J.T., et al., *Clinical and histologic evaluation of non-surgical periodontal therapy with enamel matrix derivative: a report of four cases.* J Periodontol, 2009. **80**(9): p. 1534-40.

3. Brookes, S.J., et al., *Biochemistry and molecular biology of amelogenin proteins of developing dental enamel.* Arch Oral Biol, 1995. **40**(1): p. 1-14.

4. Uchida, T., et al., *Immunocytochemical and immunochemical detection of a 32 kDa nonamelogenin and related proteins in porcine tooth germs.* Arch Histol Cytol, 1991. **54**(5): p. 527-38.

5. Hu, C.C., et al., *Sheathlin: cloning, cDNA/polypeptide sequences, and immunolocalization of porcine enamel sheath proteins.* J Dent Res, 1997. **76**(2): p. 648-57.

6. Moffatt, P., et al., *Identification of secreted and membrane proteins in the rat incisor enamel organ using a signal-trap screening approach.* Eur J Oral Sci, 2006. **114 Suppl 1**: p. 139-46; discussion 164-5, 380-1.

7. Fukae, M. and T. Tanabe, *Degradation of enamel matrix proteins in porcine secretory enamel.* Connect Tissue Res, 1998. **39**(1-3): p. 123-9; discussion 141-9.

8. Hammarstrom, L., L. Heijl, and S. Gestrelius, *Periodontal regeneration in a buccal dehiscence model in monkeys after application of enamel matrix proteins.* J Clin Periodontol, 1997. **24**(9 Pt 2): p. 669-77.

9. Yoneda, S., et al., *The effects of enamel matrix derivative (EMD) on osteoblastic cells in culture and bone regeneration in a rat skull defect.* J Periodontal Res, 2003. **38**(3): p. 333-42.

10. Groeger, S., A. Windhorst, and J. Meyle, *Influence of Enamel Matrix Derivative on Human Epithelial Cells In Vitro.* J Periodontol, 2016. **87**(10): p. 1217-27.

11. Schlueter, S.R., D.L. Carnes, and D.L. Cochran, *In vitro effects of enamel matrix derivative on microvascular cells.* J Periodontol, 2007. **78**(1): p. 141-51.

12. Bertl, K., et al., *Effects of enamel matrix derivative on proliferation/viability, migration, and expression of angiogenic factor and adhesion molecules in endothelial cells in vitro.* J Periodontol, 2009. **80**(10): p. 1622-30.

13. Palaiologou, A.A., et al., *Gingival, dermal, and periodontal ligament fibroblasts express different extracellular matrix receptors.* J Periodontol, 2001. **72**(6): p. 798-807.

14. Miron, R.J., et al., *Osteogain improves osteoblast adhesion, proliferation and differentiation on a bovine-derived natural bone mineral.* Clin Oral Implants Res, 2017. **28**(3): p. 327-333.

15. Reseland, J.E., et al., *The effect of enamel matrix derivative on gene expression in osteoblasts.* Eur J Oral Sci, 2006. **114 Suppl 1**: p. 205-11; discussion 254-6, 381-2.

16. He, J., et al., *Emdogain promotes osteoblast proliferation and differentiation and stimulates osteoprotegerin expression.* Oral Surg Oral Med Oral Pathol Oral Radiol Endod, 2004. **97**(2): p. 239-45.

17. Jiang, J., et al., *Emdogain-gel stimulates proliferation of odontoblasts and osteoblasts.* Oral Surg Oral Med Oral Pathol Oral Radiol Endod, 2006. **102**(5): p. 698-702.

18. Cattaneo, V., et al., *Effect of enamel matrix derivative on human periodontal fibroblasts: proliferation, morphology and root surface colonization. An in vitro study.* J Periodontal Res, 2003. **38**(6): p. 568-74.

19. Rincon, J.C., H.R. Haase, and P.M. Bartold, *Effect of Emdogain on human periodontal fibroblasts in an in vitro wound-healing model.* J Periodontal Res, 2003. **38**(3): p. 290-5.

20. Rodrigues, T.L., et al., *Effects of enamel matrix derivative and transforming growth factor-beta1 on human periodontal ligament fibroblasts.* J Clin Periodontol, 2007. **34**(6): p. 514-22.

21. Hoang, A.M., T.W. Oates, and D.L. Cochran, *In vitro wound healing responses to enamel matrix derivative.* J Periodontol, 2000. **71**(8): p. 1270-7.

22. Davenport, D.R., et al., *Effects of enamel matrix protein application on the viability, proliferation, and attachment of human periodontal ligament fibroblasts to diseased root surfaces in vitro.* J Clin Periodontol, 2003. **30**(2): p. 125-31.

23. Van der Pauw, M.T., et al., *Enamel matrix-derived protein stimulates attachment of periodontal ligament fibroblasts and enhances alkaline phosphatase activity and transforming growth factor beta1 release of periodontal ligament and gingival fibroblasts.* J Periodontol, 2000. **71**(1): p. 31-43.

24. Kwon, Y.D., et al., *Cellular viability and genetic expression of human gingival fibroblasts to zirconia with enamel matrix derivative (Emdogain(R)).* J Adv Prosthodont, 2014. **6**(5): p. 406-14.

25. Suzuki, N., et al., *Attachment of human periodontal ligament cells to enamel matrix-derived protein is mediated via interaction between BSP-like molecules and integrin alpha(v)beta3.* J Periodontol, 2001. **72**(11): p. 1520-6.

26. Lyngstadaas, S.P., et al., *Autocrine growth factors in human periodontal ligament cells cultured on enamel matrix derivative.* J Clin Periodontol, 2001. **28**(2): p. 181-8.

27. Wyganowska-Swiatkowska, M., et al., *Human gingival fibroblast response to enamel matrix derivative, porcine recombinant 21.3-kDa amelogenin and 5.3-kDa tyrosine-rich amelogenin peptide.* Hum Cell, 2017. **30**(3): p. 181-191.

28. Johnson, D.L., et al., *Cellular effects of enamel matrix derivative are associated with different molecular weight fractions following separation by size-exclusion chromatography.* J Periodontol, 2009. **80**(4): p. 648-56.

29. Stout, B.M., et al., *Enamel matrix derivative: protein components and osteoinductive properties.* J Periodontol, 2014. **85**(2): p. e9-e17.

30. Villa, O., et al., *Subfractions of enamel matrix derivative differentially influence cytokine secretion from human oral fibroblasts.* J Tissue Eng, 2015. **6**: p. 2041731415575857.

31. Nanci, A. and D.D. Bosshardt, *Structure of periodontal tissues in health and disease.* Periodontol 2000, 2006. **40**: p. 11-28.

32. Miron, R.J., et al., *The effect of enamel matrix proteins on the spreading, proliferation and differentiation of osteoblasts cultured on titanium surfaces.* Biomaterials, 2010. **31**(3): p. 449-60.

33. Brunette, D.M., G.S. Kenner, and T.R. Gould, *Grooved titanium surfaces orient growth and migration of cells from human gingival explants.* J Dent Res, 1983. **62**(10): p. 1045-8.

34. Chen, Y., et al., *CCN2 (connective tissue growth factor) promotes fibroblast adhesion to fibronectin.* Mol Biol Cell, 2004. **15**(12): p. 5635-46.

35. Humphries, M.J., *Cell adhesion assays.* Methods Mol Biol, 2009. **522**: p. 203-10.

36. Xu, M., D.J. McCanna, and J.G. Sivak, *Use of the viability reagent PrestoBlue in comparison with alamarBlue and MTT to assess the viability of human corneal epithelial cells.* J Pharmacol Toxicol Methods, 2015. **71**: p. 1-7.

37. Lyngstadaas, S.P., et al., *Enamel matrix proteins; old molecules for new applications.* Orthod Craniofac Res, 2009. **12**(3): p. 243-53.

38. Wyganowska-Swiatkowska, M., et al., *Effects of enamel matrix proteins on adherence, proliferation and migration of epithelial cells: A real-time in vitro study.* Exp Ther Med, 2017. **13**(1): p. 160-168.

39. Andrukhov, O., et al., *Effect of different enamel matrix derivative proteins on behavior and differentiation of endothelial cells.* Dent Mater, 2015. **31**(7): p. 822-32.

40. Hong, P., S. Koza, and E.S. Bouvier, *Size-Exclusion Chromatography for the Analysis of Protein Biotherapeutics and their Aggregates.* J Liq Chromatogr Relat Technol, 2012. **35**(20): p. 2923-2950.

41. Zilm, P.S. and P.M. Bartold, *Proteomic identification of proteinase inhibitors in the porcine enamel matrix derivative, EMD((R)).* J Periodontal Res, 2011. **46**(1): p. 111-7.

42. MacDougall, M., et al., *Dentin phosphoprotein and dentin sialoprotein are cleavage products expressed from a single transcript coded by a gene on human chromosome 4. Dentin phosphoprotein DNA sequence determination.* J Biol Chem, 1997. **272**(2): p. 835-42.

43. Nakamura, Y., et al., *Immunohistochemical characterization of rapid dentin formation induced by enamel matrix derivative.* Calcif Tissue Int, 2004. **75**(3): p. 243-52.

44. Riksen, E.A., et al., *Enamel matrix derivative promote primary human pulp cell differentiation and mineralization.* Int J Mol Sci, 2014. **15**(5): p. 7731-49.

45. Bartlett, J.D., *Dental enamel development: proteinases and their enamel matrix substrates.* ISRN Dent, 2013. **2013**: p. 684607.

46. Khalili, A.A. and M.R. Ahmad, *A Review of Cell Adhesion Studies for Biomedical and Biological Applications.* Int J Mol Sci, 2015. **16**(8): p. 18149-84.

47. Hong, S., et al., *Real-time analysis of cell-surface adhesive interactions using thickness shear mode resonator.* Biomaterials, 2006. **27**(34): p. 5813-20.

48. van der Pauw, M.T., V. Everts, and W. Beertsen, *Expression of integrins by human periodontal ligament and gingival fibroblasts and their involvement in fibroblast adhesion to enamel matrix-derived proteins.* J Periodontal Res, 2002. **37**(5): p. 317-23.

49. Wang, Y., et al., *Enamel matrix derivative improves gingival fibroblast cell behavior cultured on titanium surfaces.* Clin Oral Investig, 2016. **20**(4): p. 685-95.

50. Guo, F., et al., *Gingival fibroblasts display reduced adhesion and spreading on extracellular matrix: a possible basis for scarless tissue repair?* PLoS One, 2011. **6**(11): p. e27097.

51. Zhang, Z.G., et al., *Interactions of primary fibroblasts and keratinocytes with extracellular matrix proteins: contribution of alpha2beta1 integrin.* J Cell Sci, 2006. **119**(Pt 9): p. 1886-95.

52. Kinumatsu, T., et al., *Involvement of laminin and integrins in adhesion and migration of junctional epithelium cells.* J Periodontal Res, 2009. **44**(1): p. 13-20.

53. Pakkala, T., et al., *Function of laminins and laminin-binding integrins in gingival epithelial cell adhesion.* J Periodontol, 2002. **73**(7): p. 709-19.

54. Bax, D.V., et al., *Cell adhesion to fibrillin-1 molecules and microfibrils is mediated by alpha 5 beta 1 and alpha v beta 3 integrins.* J Biol Chem, 2003. **278**(36): p. 34605-16.

55. Midwood, K.S. and G. Orend, *The role of tenascin-C in tissue injury and tumorigenesis.* J Cell Commun Signal, 2009. **3**(3-4): p. 287-310.

56. Chiquet-Ehrismann, R. and R.P. Tucker, *Tenascins and the importance of adhesion modulation.* Cold Spring Harb Perspect Biol, 2011. **3**(5).

57. Trebaul, A., E.K. Chan, and K.S. Midwood, *Regulation of fibroblast migration by tenascin-C.* Biochem Soc Trans, 2007. **35**(Pt 4): p. 695-7.

58. Hoang, A.M., et al., *Amelogenin is a cell adhesion protein.* J Dent Res, 2002. **81**(7): p. 497-500.

Chapter 5

Discussion

5.1 General discussion

In dental practice, dental implant treatment has become one of the standard treatments in oral rehabilitation to replace damage or lost tooth [1]. The most used material is titanium due to its resistance to corrosion, an excellent biocompatibility, and high resistance to wear, which are key features to an effective treatment [2]. To achieve a successful long-term survival, it is necessary that the implant integrate properly to the adjacent hard (bone) and soft tissues (mucosa connective tissue and epithelium). The biointegration is, therefore, dependent on the implant outermost surface that interact with the surrounding environment rich in molecules such as proteins that adsorb onto the surface that will influence tissue response. In particular, the integration with the soft tissue is of great importance since the implant is exposed to the oral cavity and prone to bacterial invasion and colonization that could lead to infection, inflammation, and implant loss [3]. Therefore, the adhesion of connective tissue to the implant transmucosal component is highly required to seal the communication to the oral cavity.

The ultimate objective of this thesis was to create a biomimetic surface utilizing certain EMD proteins as the bioactive components to promote biological adhesion to the titanium surface. EMD is a complex biological compound extract

from 6 months old piglets that is recognized to modulate activity of a variety of cells involved in soft tissue regeneration, including gingival fibroblasts [4, 5]. However, little is known about its composition and which constituents are responsible to its biological properties. The formation of a protein pellicle with EMD would, therefore, improve the integration of the implant transmucosal component with the surrounding connective tissue by stimulating the adhesion of gingival fibroblasts onto the surface to prevent further access of bacteria to the intraosseous interface.

To this end, we utilized in chapter 2 salivary proteins as a model to investigate protein binding specificity of three different titanium surfaces, PT, SLA, and SLActive, when exposed to a complex protein mixture. The hypothesis behind this approach was to explore the possibility of using titanium surfaces with different properties to influence the formation of a surface-specific protein layer with EMD to study their impact on adhesion of gingival fibroblasts. In this way, we would be able to identify through mass spectrometry, EMD proteins that could deliver an enhanced cell response to each bioactive surface.

5.2 Specificity of titanium surface for protein adsorption

Mass spectrometry is a very powerful tool in proteomics to study the composition of complex samples, and protein-surface interactions as showed in this thesis. Mass spectrometry-based proteomics was therefore applied to examine the interaction of salivary proteins to different titanium surfaces. Our attempt in applying a surface-affinity approach using salivary proteins as a model

indicated initially that the protein pellicles formed on the Ti surfaces had distinct compositions between surfaces modifications (PT, SLA and SLActive) with regards to independent experiments (Figure 2.2). The difference in protein adsorption could be explained by the variances in characteristics between surfaces that are recognized to influence protein binding on surfaces in a protein-rich aqueous environment [6]. However, after considering only proteins with affinity to a given surface, i.e., proteins identified in at least two experiments, we noticed different degrees of specificity for each surface that were evident by the overlaps between surfaces, particularly between all three surfaces (Figure 2.3). Since the majority of proteins adsorbed on a surface were common to others, we concluded that the Ti surfaces studied herein presented a low surface specificity for proteins binding despite the different characteristics between surfaces (Table 2.1). As surface characteristics work in concert to influence proteins binding, we recognize that it was not possible to determine which feature/features influenced protein-surface interactions that resulted in a low surface specificity particularly, when proteins mixtures are involved as they add more variables in the interaction equation such as sample complexity and competition for binding [7, 8].

Parallel to studying saliva-surface interaction, we further extended our investigation to explore the proteome of the salivary pellicle formed onto each surface since titanium implants are exposed to saliva during implant placement, which extends to the healing phase, and continue throughout the time it remains in the oral cavity. The characterization of the so-called salivary-titanium pellicle is important regarding the implant biointegration in the oral cavity because saliva

contain thousands of proteins, some of which are recognized to modulate adhesion of microorganisms on the enamel surface while others participate in wound healing, which are features that promote the maintenance of oral health [9-11]. Our study revealed that many salivary proteins that are involved in immune defense have affinity for all surfaces, such as cystatin B, protein S100-A8 and S100-A9, lactoperoxidase, BPI fold-containing family A member 2, and lysozyme C. Another example is lactotransferrin that not only inhibits biofilm formation of *Porphyromonas gingivalis* and *Prevotella intermedia*, species recognized to cause periodontal diseases [12, 13], but also is known to regulate osteoblast proliferation and differentiation [14, 15]. Is worth mentioning that other proteins involved in host defense are also associated with bone metabolism, such as cystatin B and C that are modulators of osteoclast activity [16-18], and S100A8 that are linked to maturation processes of osteoblast [19]. Finally, we also identified proteins that participate in cell adhesion such as zinc-alpha2-glycoprotein that carries RGD motif in its sequence, which mediates attachment of fibroblasts and osteoblastic cells via integrins [20, 21], and histatin-1 that is known to stimulate not only adhesion of epithelial cell but also endothelial cells to promote angiogenesis that may contribute to wound healing in the oral cavity [22, 23]. The evidence provided here can be used in further studies to explore the impact that salivary proteins have on titanium implant integration with the surrounding tissues, whether preventing bacterial colonization on dental implant's surface or assisting in tissue regeneration in the oral environment.

5.3 Proteome of enamel matrix derivative (EMD)

The high variability and lack of specificity for protein binding observed on different Ti surfaces demonstrated that the separation of EMD proteins based on the surface characteristics was not applicable. Due to EMD complexity and the need for a consistent protein separation, size-exclusion chromatography was selected as the fractionation method for its well-known high reproducibility. SEC was then utilized off-line in a MudPIT approach as the first dimension to fractionate EMD proteins, while a RP-LC in-line with the mass spectrometer was set as the second dimension in a bottom-up approach to maximize protein identification and characterization of EMD proteome (Chapter 3).

As part of our efforts to characterize and identify novel EMD constituents through MudPIT methodology, EMD were separated in 32 fractions from which 2000 proteins were identified. As expected, we detected proteins that were previously classified as EMD components, including amelogenins (more than >90%), enamelin, ameloblastin, and odontogenic ameloblast-associated protein, along with the enzymes kallikrein-4, and MMP-20 [24-29]. In addition to the classical EMD proteins, we identified many other proteins that have not been previously described as EMD constituent, such as annexin A1 (AnxA1), protein S100-A6, fibrillin-1, and dentin sialophosphoprotein (DSSP) to name just a few. Interestingly, DSPP is not an enamel protein but rather, is the most abundant non-collagenous extracellular matrix protein in dentin that is proteolytic cleavage during dentinogenesis in three proteins [30]. Although DSPP is secreted by odontoblasts during dentinogenesis, our results indicated that EMD also contains

dentin-matrix proteins as the DSPP, which could explain the regenerative affect in dentin-pulp when treated with EMD achieved in earlier studies [31-33]. Hence, future investigation will be required to understand the role of DSPP or its derived-proteins in EMD biological effect.

In the MS-based proteomics analysis, we detected a large number of proteins that are involved in a variety of biological processes, such as cell metabolism, development, biological regulation, cell cycle, transport, immune response, and protein with catalytic activity, among other (Figure 3.4). The identified proteins are mostly cellular components that are part of membranes, cytoskeleton, organelles, and also found in the nucleus, while 59 are found in the extracellular space, including 44 extracellular matrix proteins. We also found many proteins derived from blood, for instance, serotransferrin, serum albumin, and mainly hemoglobin, along with circulating proteins involved in immune response such as immunoglobulin G, hemoperix, and alpha-1 acid glycoprotein. Although EMD is mainly used in regeneration of periodontal tissues, studies have shown that it also has antimicrobial activity against biofilm formation [34] and the periodontal pathogen *Porphyromonas gingivalis* [35]. Another interesting result was the identification of more than 400 proteins that carry catalytic activity, which suggests a high enzymatic activity within the enamel matrix including the most abundant enzymes kallikrein-4 [29], and MMP-20 [36] that are known to play critical roles in dental enamel formation [37]. These results clearly indicate that EMD is a very complex proteins mixture that is constituted of diverse intracellular proteins originated from cells that surround the

enamel matrix and of proteins that are exported to the extracellular space by ameloblasts during enamel development [38].

The relevance of investigating the proteome of EMD was to identify proteins that may be associated with EMD biological activity in tissue regeneration. Hence, the further analysis focused towards EMD constituents that could be implicated in biological adhesion, biomineralization, and wound healing. Our results indicated that mostly of proteins in those categories were identified in the high molecular-weight fractions and fewer in the low molecular-weight range. Many studies that have fractionated EMD through SEC suggested that EMD biological effects were not related to one protein but associated with components found in fractions containing proteins with different molecular-weight [39, 40]. For example, two studies have shown that EMD proteins present in low molecular-weight fractions induced a significantly higher response of osteogenic and endothelial cells comparing to cells that were exposed to fraction containing high-molecular weight proteins [39, 41]. Results showed by Villa et al. indicated that EMD fraction in the low molecular-weight range stimulated the release of chemokines (interleukin-8 and monocyte chemoattractant protein-1) and promoted a higher proliferation rate in PDLF. However, when cells were treated with EMD proteins above 20 kDa, different cytokines (vascular endothelial growth factor-VEGF and interleukin-6) were released by the PDLF [42]. These studies, therefore, indicate that the mechanism of action of EMD is associated with different constituents in EMD.

Amelogenins and derived peptides are recognized as the most abundant ECM components in EMD, but they are not the solely responsible for EMD biological activity. Although 25 kDa amelogenins has been shown to promote osteoblastic differentiation and mineralization in bone marrow mesenchymal stem cells, but it did not affect proliferation or induced change in cell morphology [43]. The lack of activity of amelogenin was also observed in a wound healing model study that showed no effect on proliferation and migration of periodontal ligament fibroblasts (PDLF), whereas other proteins present in native EMD promoted increase in migration of PDLF even in lower amount [44]. Amelogenin-derived peptides known as TRAP and LRAP are also involved in EMD activity. The 5 kDa TRAP has been shown to positively regulate cell differentiation on endothelial cells by [45] but, apparently, TRAP does not have any significant influence on epithelial cells [46], while the 6.5 kDa LRAP demonstrated to upregulated osteogenic differentiation of bone precursor cells in vitro [47, 48]. Another traditional EMD protein, ameloblastin, have been recently implicated in osteogenesis and mineralization [48-50]. Other studies indicated that it is a potent regulator of gene expression in cementoblasts [51], while an inhibitor of epithelial cell proliferation [52], which shows the multi-action of ameloblastin.

Besides detecting the classical EMD proteins – amelogenin, ameloblastin, and enamelin – we identified other proteins that can be associated with EMD biological activity. We identified ECM proteins in high molecular-weight fraction that may play a direct role in osteogenesis and bone metabolism, such as alpha-2-HS-glycoprotein (AHSG), AnxA1 and AnxA2. AHSG is a calcium-binding

protein was initially through to be secreted solely by hepatocytes, but recent studies have found that it can also be produced in bone by osteocytes and in lower amount by osteoblasts [53]. Since AHSG has been found at high levels in mineralized bone, studies have indicated that it has an important role in mineralization by regulating endochondral ossification and calcified matrix metabolism [54]. Likewise, both member of the annexin family, AnxA1 and AnxA2 are also proteins with high affinity to Ca^{2+} ions that have been proposed to participate in bone metabolism and matrix mineralization [55-57]. Although AnxA2 was identified in EMD in a recent proteomics study, this is the first time that AnxA1 is detected. AnxA2 could be part of the enamel matrix composition for it has been found inside secretory vesicles of ameloblasts during tooth development [58, 59], but its role in EMD activity is yet to be determined. Differently, AnxA1 is considered a multi-function protein as it participate in innate immune response, inflammation, and wound repair [60], which are important features in wound healing of hard and soft tissues delivered by EMD. Lastly, it is worth mentioning the identification of fibrilin-1, which is another ECM protein that not only has a role in bone metabolism and bone remodeling [61], but also in cell adhesion along with other proteins that were found in fewer EMD fractions, including tenascin C [62], tenascin X [63], lumican precursor [64], fibromodulin [65], fibronectin 1 [66], and fibroblast growth factor (FGF) [67]. Therefore, the characterization of EMD proteome shed some light on its complex composition with the identification of novel proteins that might be associated with EMD biological activity in tissue regeneration in the oral cavity.

5.4 Contribution of EMD proteins to adhesion of human gingival fibroblast

As the ultimate objective of this thesis, we targeted proteins that contribute in biological adhesion that could promote attachment of human gingival fibroblasts (HGF) (Chapter 4). The MS analysis showed that all fractions contained a total of 89 proteins that are involved directly or indirectly with adhesion processes, but they were more concentrated in the high molecular-weight fractions, and at a lesser extent, in fraction at peptides range (Figure 4.2).

In examining the outcome from the *in-vitro* adhesion assay when HGF was exposed to EMD, we observed that both native EMD, and its derived-fractions were unable to enhance cellular attachment or stimulate early adhesion of HGF at the degree presented by the positive control fibronectin. Additional confirmation was obtained through microscopy that revealed lack of attachment of HGF on EMD-treated surface by showing rounded morphology and lack of cell spreading, which was seen in HGF seeded on fibronectin coated surface. Fibronectin is a ECM protein well-knwon to promote adhesion to diverse fibroblast types, including HGF by having in its amino acid sequence the RGD motif (arginine–glycine–aspartic acid), which is the most recognized peptide motif that specifically binds to transmembrane integrins αvβ3 and α5β1 that are expressed by HGF to mediate adhesion to the ECM [20]. These results are similar to previous studies that investigated the effects of EMD on HGF, although few reports showed distinct results [4, 68, 69]. In the study that evaluated how EMD influenced both PDLF and HGF, Van der Pauw et al. showed that EMD did

not promote attachment of HGF, whereas it increased adhesion of PDLF [4]. Similarly, adhesion of HGF was not improved when the cells were exposed to native EMD and two of its known components, a recombinant 21.3 kDa amelogenin and its derived peptide TRAP [68]. Contrarily, using as a coating on zirconia surface utilized in dental implants, EMD appeared to enhance HGF attachment comparing to zirconia surface alone [69].

In this thesis, although we showed that EMD did not effectively influence the adhesion of HGF, the EMD high-molecular weight fraction F23 and F24 showed a significantly higher response than other EMD fractions and native EMD (Figure 4.3). When the MS-based proteome analysis was carried out, it revealed that both fractions contained the ECM proteins collagen type I and laminin, which are known to promote adhesion of fibroblasts. Interestingly, fraction F24 also contained two other proteins involved in cell attachment that were detected for the first time in EMD; 312 kDa fibrillin-1 and tenascin C. Fibrillin-1 is a large glycoprotein component of microfibrils in ECM that contains one RGD motif known to mediate cell adhesion of HGF to the ECM through integrin [20, 70]. Likewise, tenascin C, which was only found in fraction F24, is a large ECM protein that also regulates cell adhesion of fibroblasts [62]. Although both fractions F23 and F24 contained proteins involved in cell adhesion, it is very challenging to determine which constituent had promoted or caused a major impact on the adhesion of HGF, since protein such as collagen I and laminin were also found in other fractions along with amelogenin, and ameloblastin. It is possible, however, that several proteins herein identified could have worked

cooperatively to enhance adhesion of HGF, but more studies are required to understand the role of these proteins in the biological effect that EMD stimulates on oral tissues.

5.5 Perspectives and conclusions

The investigation of titanium surface specificity for proteins binding provided some evidence that different surface characteristics such as chemistry, energy, and topography may work in concert to modulate the interaction between protein mixtures and Ti surfaces. The low surface specificity showed by the formation of similar protein pellicle on each surface highlight the need for more studies on surface-proteins interaction, particularly involving protein-rich body fluid as saliva and blood. Since the interaction between salivary proteins and titanium implants continuously occur in the mouth, is also necessary to investigate the biological impact that salivary proteins adsorbed onto titanium would have on cells that interact with the implant transmucosal component, for instance, the role that antimicrobial proteins would have on protecting the surface against bacterial colonization. From a clinical perspective, engineering customized bioactive surfaces by coating with specific proteins would be highly desirable. In this way, it would initiate a faster response from adjacent tissues to the implant to enhanced biointegration with hard and soft tissues. Therefore, as it has been shown in this thesis, EMD could be a potential candidate for developing a tissue-specific bioactive surface due to various novel proteins herein identified that are associated with EMD biological activity. Although our results suggest that whole EMD did not promote an enhanced attachment of

human gingival fibroblasts, we identified two EMD fractions that provided a superior response than the native EMD. These findings, therefore, can be used in further studies to investigate the applicability of those EMD fractions in other cells. Additional studies are necessary to determine whether a higher concentration of these proteins would be favorable to stimulate adhesion of gingival fibroblast.

5.6 References

1. Feine, J.S., et al., *The McGill consensus statement on overdentures. Mandibular two-implant overdentures as first choice standard of care for edentulous patients. Montreal, Quebec, May 24-25, 2002.* Int J Oral Maxillofac Implants, 2002. **17**(4): p. 601-2.

2. Guo, C.Y., J.P. Matinlinna, and A.T. Tang, *Effects of surface charges on dental implants: past, present, and future.* Int J Biomater, 2012. **2012**: p. 381535.

3. Tonetti, M.S., *Risk factors for osseodisintegration.* Periodontol 2000, 1998. **17**: p. 55-62.

4. Van der Pauw, M.T., et al., *Enamel matrix-derived protein stimulates attachment of periodontal ligament fibroblasts and enhances alkaline phosphatase activity and transforming growth factor beta1 release of periodontal ligament and gingival fibroblasts.* J Periodontol, 2000. **71**(1): p. 31-43.

5. Rincon, J.C., H.R. Haase, and P.M. Bartold, *Effect of Emdogain on human periodontal fibroblasts in an in vitro wound-healing model.* J Periodontal Res, 2003. **38**(3): p. 290-5.

6. Kilpadi, D.V. and J.E. Lemons, *Surface energy characterization of unalloyed titanium implants.* J Biomed Mater Res, 1994. **28**(12): p. 1419-25.

7. Rabe, M., D. Verdes, and S. Seeger, *Understanding protein adsorption phenomena at solid surfaces.* Adv Colloid Interface Sci, 2011. **162**(1-2): p. 87-106.

8. Wilson, C.J., et al., *Mediation of biomaterial-cell interactions by adsorbed proteins: a review.* Tissue Eng, 2005. **11**(1-2): p. 1-18.

9. Shimotoyodome, A., et al., *Saliva-promoted adhesion of Streptococcus mutans MT8148 associates with dental plaque and caries experience.* Caries Res, 2007. **41**(3): p. 212-8.

10. Whittaker, C.J., C.M. Klier, and P.E. Kolenbrander, *Mechanisms of adhesion by oral bacteria.* Annu Rev Microbiol, 1996. **50**: p. 513-52.

11. Scannapieco, F.A., *Saliva-bacterium interactions in oral microbial ecology.* Crit Rev Oral Biol Med, 1994. **5**(3-4): p. 203-48.

12. Dashper, S.G., et al., *Lactoferrin inhibits Porphyromonas gingivalis proteinases and has sustained biofilm inhibitory activity.* Antimicrob Agents Chemother, 2012. **56**(3): p. 1548-56.

13. Wakabayashi, H., et al., *Inhibitory effects of lactoferrin on growth and biofilm formation of Porphyromonas gingivalis and Prevotella intermedia.* Antimicrob Agents Chemother, 2009. **53**(8): p. 3308-16.

14. Hou, J.M., et al., *Lactoferrin Induces Osteoblast Growth through IGF-1R.* Int J Endocrinol, 2015. **2015**: p. 282806.

15. Cornish, J., *Lactoferrin promotes bone growth.* Biometals, 2004. **17**(3): p. 331-5.

16. Manninen, O., et al., *Impaired osteoclast homeostasis in the cystatin B-deficient mouse model of progressive myoclonus epilepsy.* Bone Rep, 2015. **3**: p. 76-82.

17. Laitala-Leinonen, T., et al., *Cystatin B as an intracellular modulator of bone resorption.* Matrix Biol, 2006. **25**(3): p. 149-57.

18. Brage, M., et al., *Different cysteine proteinases involved in bone resorption and osteoclast formation.* Calcif Tissue Int, 2005. **76**(6): p. 439-47.

19. Zreiqat, H., et al., *S100A8/S100A9 and their association with cartilage and bone.* J Mol Histol, 2007. **38**(5): p. 381-91.

20. Palaiologou, A.A., et al., *Gingival, dermal, and periodontal ligament fibroblasts express different extracellular matrix receptors.* J Periodontol, 2001. **72**(6): p. 798-807.

21. Ogikubo, O., et al., *Regulation of Zn-alpha2-glycoprotein-mediated cell adhesion by kininogens and their derivatives.* Biochem Biophys Res Commun, 1998. **252**(1): p. 257-62.

22. Torres, P., et al., *The salivary peptide histatin-1 promotes endothelial cell adhesion, migration, and angiogenesis.* FASEB J, 2017. **31**(11): p. 4946-4958.

23. van Dijk, I.A., et al., *Human salivary peptide histatin-1 stimulates epithelial and endothelial cell adhesion and barrier function.* FASEB J, 2017. **31**(9): p. 3922-3933.

24. Uchida, T., et al., *Immunocytochemical and immunochemical detection of a 32 kDa nonamelogenin and related proteins in porcine tooth germs.* Arch Histol Cytol, 1991. **54**(5): p. 527-38.

25. Brookes, S.J., et al., *Biochemistry and molecular biology of amelogenin proteins of developing dental enamel.* Arch Oral Biol, 1995. **40**(1): p. 1-14.

26. Lyngstadaas, S.P., et al., *Enamel matrix proteins; old molecules for new applications.* Orthod Craniofac Res, 2009. **12**(3): p. 243-53.

27. Hu, C.C., et al., *Sheathlin: cloning, cDNA/polypeptide sequences, and immunolocalization of porcine enamel sheath proteins.* J Dent Res, 1997. **76**(2): p. 648-57.

28. Fukae, M. and T. Tanabe, *Degradation of enamel matrix proteins in porcine secretory enamel.* Connect Tissue Res, 1998. **39**(1-3): p. 123-9; discussion 141-9.

29. Simmer, J.P., et al., *Purification, characterization, and cloning of enamel matrix serine proteinase 1.* J Dent Res, 1998. **77**(2): p. 377-86.

30. Prasad, M., W.T. Butler, and C. Qin, *Dentin sialophosphoprotein in biomineralization.* Connect Tissue Res, 2010. **51**(5): p. 404-17.

31. Darwish, S.S., et al., *Root maturation and dentin-pulp response to enamel matrix derivative in pulpotomized permanent teeth.* J Tissue Eng, 2014. **5**: p. 2041731414521707.

32. Igarashi, R., et al., *Porcine enamel matrix derivative enhances the formation of reparative dentine and dentine bridges during wound healing of amputated rat molars.* J Electron Microsc (Tokyo), 2003. **52**(2): p. 227-36.

33. Nakamura, Y., et al., *The induction of reparative dentine by enamel proteins.* Int Endod J, 2002. **35**(5): p. 407-17.

34. Arweiler, N.B., et al., *Antibacterial effect of an enamel matrix protein derivative on in vivo dental biofilm vitality.* Clin Oral Investig, 2002. **6**(4): p. 205-9.

35. Walter, C., et al., *Moderate effect of enamel matrix derivative (Emdogain Gel) on Porphyromonas gingivalis growth in vitro.* Arch Oral Biol, 2006. **51**(3): p. 171-6.

36. Bartlett, J.D., et al., *Enamelysin mRNA displays a developmentally defined pattern of expression and encodes a protein which degrades amelogenin.* Connect Tissue Res, 1998. **39**(1-3): p. 101-9; discussion 141-9.

37. Lu, Y., et al., *Functions of KLK4 and MMP-20 in dental enamel formation.* Biol Chem, 2008. **389**(6): p. 695-700.

38. Bartlett, J.D., *Dental enamel development: proteinases and their enamel matrix substrates.* ISRN Dent, 2013. **2013**: p. 684607.

39. Stout, B.M., et al., *Enamel matrix derivative: protein components and osteoinductive properties.* J Periodontol, 2014. **85**(2): p. e9-e17.

40. Johnson, D.L., et al., *Cellular effects of enamel matrix derivative are associated with different molecular weight fractions following separation by size-exclusion chromatography.* J Periodontol, 2009. **80**(4): p. 648-56.

41. Andrukhov, O., et al., *Effect of different enamel matrix derivative proteins on behavior and differentiation of endothelial cells.* Dent Mater, 2015. **31**(7): p. 822-32.

42. Villa, O., et al., *Subfractions of enamel matrix derivative differentially influence cytokine secretion from human oral fibroblasts.* J Tissue Eng, 2015. **6**: p. 2041731415575857.

43. Izumikawa, M., et al., *Effects of amelogenin on proliferation, differentiation, and mineralization of rat bone marrow mesenchymal stem cells in vitro.* ScientificWorldJournal, 2012. **2012**: p. 879731.

44. Chong, C.H., et al., *Human periodontal fibroblast response to enamel matrix derivative, amelogenin, and platelet-derived growth factor-BB.* J Periodontol, 2006. **77**(7): p. 1242-52.

45. Jonke, E., et al., *Effect of tyrosine-rich amelogenin peptide on behavior and differentiation of endothelial cells.* Clin Oral Investig, 2016. **20**(8): p. 2275-2284.

46. Wyganowska-Swiatkowska, M., et al., *Effects of enamel matrix proteins on adherence, proliferation and migration of epithelial cells: A real-time in vitro study.* Exp Ther Med, 2017. **13**(1): p. 160-168.

47. Amin, H.D., et al., *Differential effect of amelogenin peptides on osteogenic differentiation in vitro: identification of possible new drugs for bone repair and regeneration.* Tissue Eng Part A, 2012. **18**(11-12): p. 1193-202.

48. Grandin, H.M., A.C. Gemperli, and M. Dard, *Enamel matrix derivative: a review of cellular effects in vitro and a model of molecular arrangement and functioning.* Tissue Eng Part B Rev, 2012. **18**(3): p. 181-202.

49. Stakkestad, O., et al., *Ameloblastin Peptides Modulates the Osteogenic Capacity of Human Mesenchymal Stem Cells.* Front Physiol, 2017. **8**: p. 58.

50. Lu, X., et al., *Ameloblastin, an Extracellular Matrix Protein, Affects Long Bone Growth and Mineralization.* J Bone Miner Res, 2016. **31**(6): p. 1235-46.

51. Hakki, S.S., et al., *Recombinant amelogenin regulates the bioactivity of mouse cementoblasts in vitro.* Int J Oral Sci, 2018. **10**(2): p. 15.

52. Kuramitsu-Fujimoto, S., et al., *Novel biological activity of ameloblastin in enamel matrix derivative.* J Appl Oral Sci, 2015. **23**(1): p. 49-55.

53. Mattinzoli, D., et al., *FGF23-regulated production of Fetuin-A (AHSG) in osteocytes.* Bone, 2016. **83**: p. 35-47.

54. Jahnen-Dechent, W., et al., *Fetuin-A regulation of calcified matrix metabolism.* Circ Res, 2011. **108**(12): p. 1494-509.

55. Genetos, D.C., et al., *Impaired osteoblast differentiation in annexin A2- and -A5-deficient cells.* PLoS One, 2014. **9**(9): p. e107482.

56. Gillette, J.M. and S.M. Nielsen-Preiss, *The role of annexin 2 in osteoblastic mineralization.* J Cell Sci, 2004. **117**(Pt 3): p. 441-9.

57. Xiao, Z., et al., *Analysis of the extracellular matrix vesicle proteome in mineralizing osteoblasts.* J Cell Physiol, 2007. **210**(2): p. 325-35.

58. Goldberg, M., et al., *Annexins I-VI in secretory ameloblasts and odontoblasts of rat incisor.* J Biol Buccale, 1990. **18**(4): p. 289-98.

59. Bartlett, J.D., et al., *3. Protein-protein interactions of the developing enamel matrix.* Curr Top Dev Biol, 2006. **74**: p. 57-115.

60. Leoni, G. and A. Nusrat, *Annexin A1: shifting the balance towards resolution and repair.* Biol Chem, 2016. **397**(10): p. 971-9.

61. Smaldone, S. and F. Ramirez, *Fibrillin microfibrils in bone physiology.* Matrix Biol, 2016. **52-54**: p. 191-197.

62. Chiquet-Ehrismann, R. and R.P. Tucker, *Tenascins and the importance of adhesion modulation.* Cold Spring Harb Perspect Biol, 2011. **3**(5).

63. Egging, D., et al., *Wound healing in tenascin-X deficient mice suggests that tenascin-X is involved in matrix maturation rather than matrix deposition.* Connect Tissue Res, 2007. **48**(2): p. 93-8.

64. Karamanou, K., et al., *Lumican as a multivalent effector in wound healing.* Adv Drug Deliv Rev, 2018. **129**: p. 344-351.

65. Zheng, Z., et al., *Fibromodulin Is Essential for Fetal-Type Scarless Cutaneous Wound Healing.* Am J Pathol, 2016. **186**(11): p. 2824-2832.

66. Lenselink, E.A., *Role of fibronectin in normal wound healing.* Int Wound J, 2015. **12**(3): p. 313-6.

67. Matsumoto, S., et al., *The Effect of Control-released Basic Fibroblast Growth Factor in Wound Healing: Histological Analyses and Clinical Application.* Plast Reconstr Surg Glob Open, 2013. **1**(6): p. e44.

68. Wyganowska-Swiatkowska, M., et al., *Human gingival fibroblast response to enamel matrix derivative, porcine recombinant 21.3-kDa amelogenin and 5.3-kDa tyrosine-rich amelogenin peptide.* Hum Cell, 2017. **30**(3): p. 181-191.

69. Kwon, Y.D., et al., *Cellular viability and genetic expression of human gingival fibroblasts to zirconia with enamel matrix derivative (Emdogain(R)).* J Adv Prosthodont, 2014. **6**(5): p. 406-14.

70. Bax, D.V., et al., *Cell adhesion to fibrillin-1 molecules and microfibrils is mediated by alpha 5 beta 1 and alpha v beta 3 integrins.* J Biol Chem, 2003. **278**(36): p. 34605-16.

71. Buser, D., et al., *Enhanced bone apposition to a chemically modified SLA titanium surface.* J Dent Res, 2004. **83**(7): p. 529-33.

Appendix I

Supplementary material for Salivary Pellicle Proteome Formed onto Three Different Titanium Surfaces

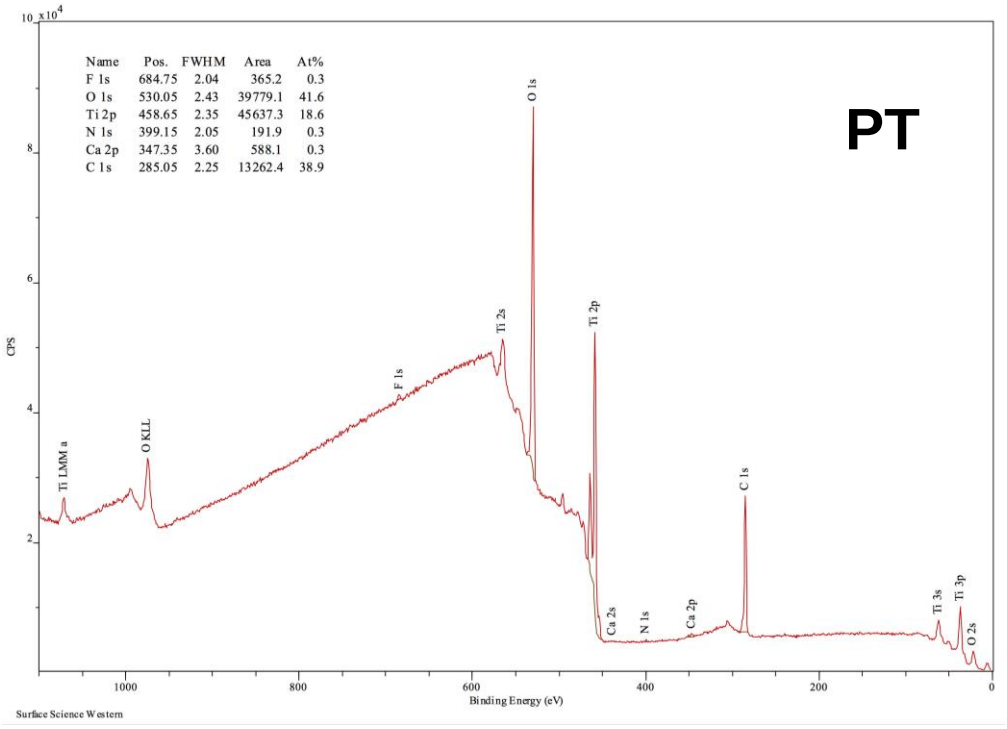

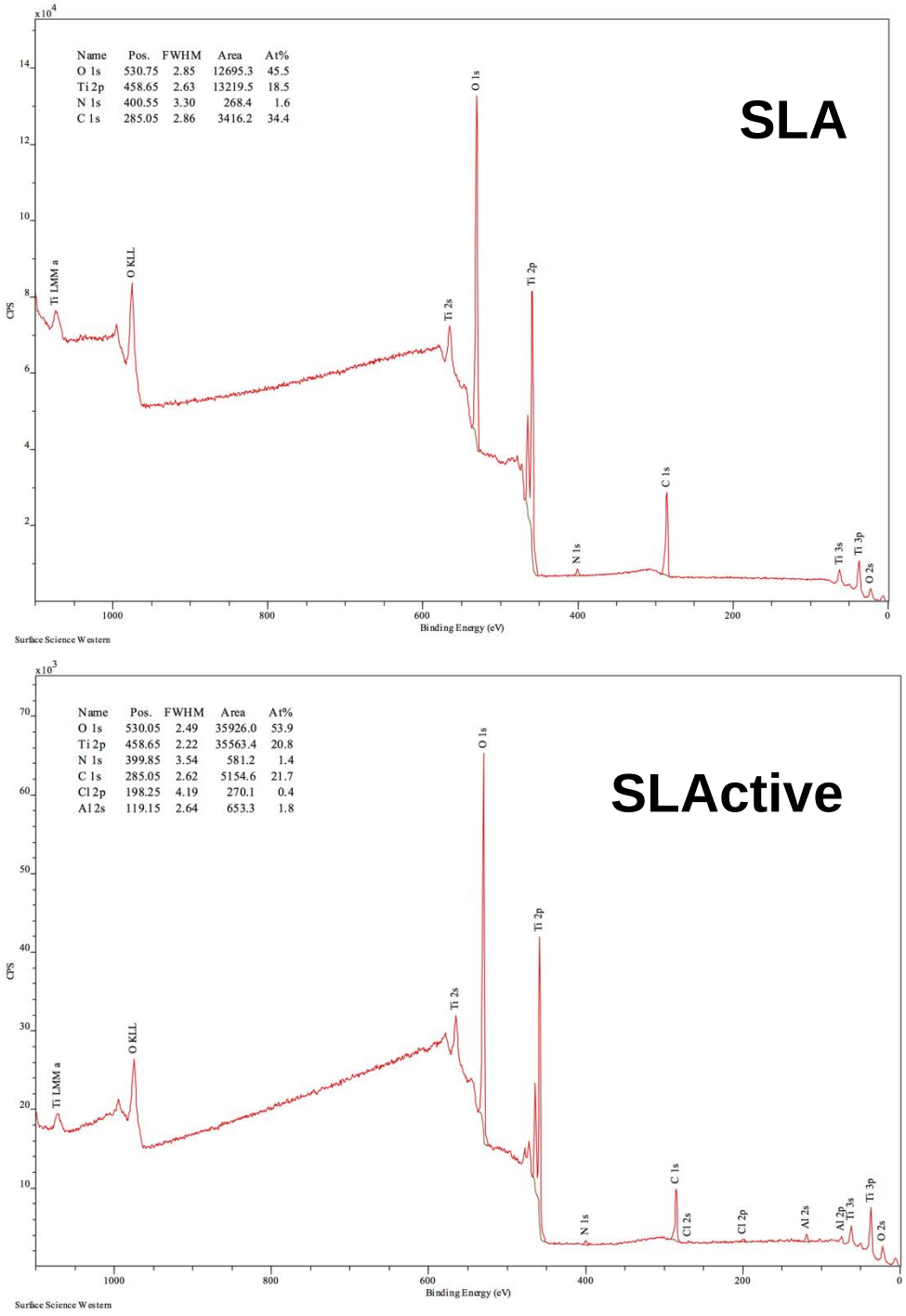

Supplementary Figure A2.1. XPS wide scan spectrum of titanium surfaces PT, SLA, and SLActive. CPS = counts per second

Supplementary Table A2.1. List of all salivary proteins adsorbed onto all Titanium surfaces separated by independent experiments

Accession Number	Protein name	Score	No. Peptides	MW (kDa)	Calc pI
	PT Surface				
	Experiment #1 (65 proteins)				
P04745	Alpha-amylase	709.12	23	57.76	6.93
P23280	Carbonic anhydrase 6	200.06	8	35.34	7.02
P02814	Submaxillary gland androgen-regulated protein 3B	142.10	2	8.18	9.57
P06702	Protein S100-A9	107.95	6	13.23	6.13
A0A075B6K9	Ig lambda-2 chain C regions (Fragment)	96.10	3	11.34	7.24
Q96DA0	Zymogen granule protein 16 homolog B	82.23	4	19.59	5.95
P02788	Lactotransferrin	78.64	10	77.92	8.12
Q8WVW5	Putative uncharacterized protein (Fragment)	72.85	9	40.48	6.14
P01036	Cystatin-S	69.72	3	16.20	5.02
Q96DR5	BPI fold-containing family A member 2	69.34	8	26.99	5.59
P04406	Glyceraldehyde-3-phosphate dehydrogenase	54.88	4	36.03	8.46
P61626	Lysozyme C	54.75	4	16.53	9.16
P22079	Lactoperoxidase	52.61	5	80.29	8.15
P25311	Zinc-alpha-2-glycoprotein	47.18	5	34.24	6.05
P12273	Prolactin-inducible protein	45.66	2	16.56	8.05
P07737	Profilin-1	45.54	4	15.04	8.27
P02647	Apolipoprotein A-I	33.71	3	30.76	5.76
P01876	Ig alpha-1 chain C region	33.50	2	37.63	6.51
P68871	Hemoglobin subunit beta	30.52	3	6.69	4.88
P01833	Polymeric immunoglobulin receptor	28.29	3	83.23	5.74
P01034	Cystatin-C	21.41	2	15.79	8.75
P14618	Pyruvate kinase	21.29	4	37.53	6.39
Q8TDL5	BPI fold-containing family B member 1	20.35	3	52.48	7.55
P05109	Protein S100-A8	18.95	2	10.83	7.03
P05164	Myeloperoxidase	17.89	5	83.81	8.97
S6AWD9	IgG H chain	15.14	2	33.28	7.85
P23284	Peptidyl-prolyl cis-trans isomerase	13.81	2	22.73	9.32
Q5QP82	DDB1- and CUL4-associated factor 10	13.12	3	43.17	7.46
Q8WZ42	Titin, isoform CRA_b	12.56	4	2991.19	6.74
Q8WXI7	Mucin-16	12.29	4	1518.24	5.26
Q7Z5P9	Mucin-19	12.07	4	804.77	5.01
Q8IVL1	cDNA FLJ59292, highly similar to neuron navigator 2	11.95	2	85.62	9.44
B7Z2W3	cDNA FLJ54432, highly similar to Alpha-actinin-1	11.73	2	67.10	6.24
P01009	Alpha-1-antitrypsin	11.12	2	46.68	5.59
O95996	Adenomatous polyposis coli protein 2	10.34	3	243.80	8.82
Q12955	Ankyrin-3	9.96	2	480.11	6.49
Q59H97	Zinc finger protein ZNF-U69274 variant (Fragment)	9.94	2	79.37	8.87
P02768	Serum albumin	9.82	2	66.49	6.04
Q8N4F0	BPI fold-containing family B member 2	9.66	2	49.14	8.72
P04080	Cystatin-B	9.46	2	11.13	7.56
P32926	Desmoglein-3	9.11	2	107.44	5.00
P31327	Carbamoylphosphate synthetase I	8.99	3	102.08	7.31
Q9HC84	Mucin-5B	7.94	3	595.96	6.64
P29401	Transketolase	7.43	2	36.43	7.77

Q9UPP5	Uncharacterized protein KIAA1107	7.35	2	155.59	6.19
P20930	Filaggrin	7.15	2	259.56	9.50
Q96HP0	Dedicator of cytokinesis protein 6	7.04	2	229.41	6.74
Q6ZUJ8	Phosphoinositide 3-kinase adapter protein 1	6.74	2	90.34	5.40
B4DIZ8	cDNA FLJ54084, moderately similar to Spliceosome RNA helicase Bat1	6.72	2	23.94	10.07
B3KSR1	cDNA FLJ36817 fis, clone ASTRO2004032	6.72	2	39.38	6.73
Q92610	Zinc finger protein 592	6.71	2	137.44	7.84
P30281	G1/S-specific cyclin-D3	6.69	2	26.22	6.96
P98088	Mucin-5AC	6.64	2	585.57	6.76
Q14679	Tubulin polyglutamylase TTLL4	6.61	2	125.58	8.44
O15014	Zinc finger protein 609	6.51	2	151.10	8.03
P01270	Parathyroid hormone	6.51	2	8.77	9.86
B7Z838	cDNA FLJ53253, highly similar to T-cell lymphoma invasion and metastasis 2	6.50	2	117.29	6.37
Q5CZC0	Fibrous sheath-interacting protein 2	6.49	2	780.12	6.71
Q6PJF5	Inactive rhomboid protein 2 (Fragment)	6.48	2	2.65	11.00
B4DZV8	cDNA FLJ52816, highly similar to MLN 64 protein	6.43	2	29.67	11.21
Q9UHB7	AF4/FMR2 family member 4	6.38	2	127.38	9.31
Q6ZS17	Rho family-interacting cell polarization regulator 1	5.93	2	98.38	5.52
O14827	Ras-specific guanine nucleotide-releasing factor 2	5.77	2	130.61	7.97
Q5TAX3	Terminal uridylyltransferase 4 (Fragment)	5.71	2	103.11	6.79
Q9P225	Dynein heavy chain 2, axonemal	5.61	2	507.37	6.37

Experiment #2 (78 proteins)

P04745	Alpha-amylase	498.62	20	57.76	6.93
P02808	Statherin	369.39	2	7.30	8.47
P02814	Submaxillary gland androgen-regulated protein 3B	176.54	2	8.18	9.57
P23280	Carbonic anhydrase 6	155.99	7	35.34	7.02
Q96DA0	Zymogen granule protein 16 homolog B	139.89	5	19.59	5.95
P06702	Protein S100-A9	101.67	6	13.23	6.13
Q96DR5	BPI fold-containing family A member 2	84.61	10	26.99	5.59
P01036	Cystatin-S	79.55	3	16.20	5.02
A0A075B6K9	Ig lambda-2 chain C regions (Fragment)	75.34	4	11.34	7.24
P22079	Lactoperoxidase	67.29	6	73.88	8.15
P01834	Ig kappa chain C region	53.54	3	11.60	5.87
P61626	Lysozyme C	51.31	3	16.53	9.16
Q8TDL5	BPI fold-containing family B member 1	44.80	5	52.48	7.55
P02647	Apolipoprotein A-I	44.70	5	30.76	5.76
P25311	Zinc-alpha-2-glycoprotein	41.04	4	34.24	6.05
P60709	Actin, cytoplasmic 1	38.69	3	38.61	5.35
B9A064	Immunoglobulin lambda-like polypeptide 5	37.19	4	24.88	6.73
Q6MZM9	Proline-rich protein 27	36.43	2	22.71	4.87
P12273	Prolactin-inducible protein	33.02	3	16.56	8.05
P98088	Mucin-5AC	32.56	5	585.57	6.76
P04406	Glyceraldehyde-3-phosphate dehydrogenase	31.39	3	36.03	8.46
P01876	Ig alpha-1 chain C region	31.35	2	37.63	6.51
Q8WZ42	Titin	24.10	8	3711.40	6.52
P07737	Profilin-1	21.99	3	15.04	8.27
P68871	Hemoglobin subunit beta	21.35	2	6.69	4.88
F4MH30	Ubiquitously transcribed tetratricopeptide repeat protein Y-linked transcript variant 63	21.24	4	147.59	7.91
P01034	Cystatin-C	19.60	2	15.79	8.75

Q96Q06	Perilipin-4	19.56	2	134.35	8.73
Q0PNF2	FEX1	16.91	2	275.27	6.49
Q7Z5P9	Mucin-19	16.77	5	804.77	5.01
P14618	Pyruvate kinase	16.18	3	37.53	6.39
P04080	Cystatin-B	13.51	2	11.13	7.56
Q7Z460	CLIP-associating protein 1	13.02	3	136.72	8.84
Q03164	Histone-lysine N-methyltransferase 2A	12.91	4	431.50	9.09
H0YNU5	Bloom syndrome protein	12.79	2	144.38	6.96
Q5SW79	Centrosomal protein 170kDa	12.43	3	161.34	7.01
Q92887	Canalicular multispecific organic anion transporter 1	11.41	4	174.10	8.32
P32926	Desmoglein-3	10.69	3	107.44	5.00
Q12955	Ankyrin-3	10.69	3	480.11	6.49
Q12888	Tumor suppressor p53-binding protein 1	10.62	2	189.80	4.69
E9PAV3	Nascent polypeptide-associated complex subunit alpha, muscle-specific form	10.18	2	205.29	9.58
Q8WXI7	Mucin-16	10.10	3	1518.24	5.26
Q9C0A6	SET domain-containing protein 5	9.86	3	99.76	7.88
Q9P281	BAH and coiled-coil domain-containing protein 1	9.77	3	276.73	8.81
P20929	Nebulin	9.72	3	990.22	9.01
A0A087WXZ5	Anthrax toxin receptor-like	9.71	2	28.37	6.40
Q461N2	Ciprofibrate bound protein p240 isoform PRIC320-2	9.55	2	222.80	7.09
Q5MJ70	Speedy protein A	8.52	2	36.44	8.85
P02768	Albumin	8.44	3	66.49	6.04
P80303	Nucleobindin-2	8.01	2	40.34	5.17
D3DPR0	Arginine decarboxylase, isoform CRA_e	6.77	2	39.67	5.49
A8K5H6	cDNA FLJ76659, highly similar to Homo sapiens exonuclease 1 (EXO1)	6.69	2	93.84	8.40
Q9NQC3	Reticulon-4	6.68	2	89.46	4.42
Q5VST9	Obscurin	6.61	2	175.02	6.20
Q9ULL5	Proline-rich protein 12	6.56	2	129.91	8.00
Q7Z6Z7	E3 ubiquitin-protein ligase HUWE1	6.54	2	373.96	5.10
J3QS80	Uncharacterized protein C19orf47 (Fragment)	6.53	2	17.66	9.88
E9PJN4	Short transient receptor potential channel 6	6.45	2	97.24	6.80
A0A024R914	Centrosomal protein 350kDa, isoform CRA_a	6.41	2	350.71	6.34
Q6ZV13	cDNA FLJ43127 fis, clone CTONG3004712	6.37	2	26.67	11.88
A0A024RD92	HCG39854, isoform CRA_a	6.36	2	75.39	9.48
P49842	Serine/threonine kinase 19	6.34	2	35.52	9.23
Q5W9G3	LAR splice variant 1 (Fragment)	6.31	2	166.53	6.20
P46013	Proliferation marker protein Ki-67	6.23	2	358.41	9.42
Q9HCK1	DBF4-type zinc finger-containing protein 2	6.22	2	264.89	6.11
Q6UXF1	Transmembrane protein 108	6.12	2	49.91	10.32
Q8N2H3	Pyridine nucleotide-disulfide oxidoreductase domain-containing protein 2	6.10	2	63.03	6.95
Q9BUN1	Protein MENT	6.03	2	36.75	8.59
Q02641	Voltage-dependent L-type calcium channel subunit beta-1	5.99	2	23.82	9.11
Q9C0G6	Dynein heavy chain 6, axonemal	5.95	2	475.68	6.00
Q96IC2	Putative RNA exonuclease NEF-sp	5.90	2	86.83	8.32
Q8NEY1	Neuron navigator 1	5.88	2	197.28	8.22
Q6IQ55	Tau-tubulin kinase 2	5.78	2	137.33	7.01
D7PBN3	ESRP1/RAF1 fusion protein	5.76	2	118.54	8.22
Q9UBC9	Small proline-rich protein 3 (Fragment)	5.70	2	16.95	8.09
Q13563	Polycystin-2	5.21	2	109.62	5.69
O15061	Synemin	4.94	2	172.66	5.16

B3KUL7	cDNA FLJ40192 fis, clone TESTI2019336	4.86	2	30.78	7.62
	Experiment #3 (81 proteins)				
P04745	Alpha-amylase	772.17	22	57.76	6.93
P02814	Submaxillary gland androgen-regulated protein 3B	214.48	2	8.18	9.57
P23280	Carbonic anhydrase 6	193.09	8	35.34	7.02
P61626	Lysozyme C	125.38	2	16.53	9.16
Q96DA0	Zymogen granule protein 16 homolog B	122.73	6	19.59	5.95
Q96DR5	BPI fold-containing family A member 2	121.68	10	26.99	5.59
P06702	Protein S100-A9	85.72	3	13.20	6.13
P02812	Basic salivary proline-rich protein 2	83.84	2	40.77	11.63
P02788	Lactotransferrin	78.56	11	77.92	8.12
P12273	Prolactin-inducible protein	67.17	4	16.56	8.05
P0DOX7	Immunoglobulin kappa light chain	65.93	3	24.01	8.06
A0A075B6K9	Ig lambda-2 chain C regions	63.27	4	11.34	7.24
P01036	Cystatin-S	59.39	2	16.20	5.02
P68871	Hemoglobin subunit beta	54.75	5	15.99	7.28
P60709	Actin, cytoplasmic 1	50.79	4	38.61	5.35
P15515	Histatin-1	50.08	2	6.96	9.13
P63267	Actin, gamma-enteric smooth muscle	41.75	5	41.85	5.48
P07737	Profilin-1	41.30	4	15.04	8.27
P25311	Zinc-alpha-2-glycoprotein	39.95	5	34.24	6.05
Q8TDL5	BPI fold-containing family B member 1	37.47	4	52.48	7.55
Q8NCL6	cDNA FLJ90170 fis highly similar to Ig alpha-1 chain C region	36.46	4	53.19	6.52
P02647	Apolipoprotein A-I	35.21	4	30.76	5.76
P01833	Polymeric immunoglobulin receptor	34.95	2	83.23	5.74
Q6ZVX0	cDNA FLJ41981 fis highly similar to Protein Tro alpha1 H,myeloma	31.84	4	52.84	5.92
P22079	Lactoperoxidase	31.19	4	80.29	8.15
P04406	Glyceraldehyde-3-phosphate dehydrogenase	30.87	2	24.60	8.51
F4MH35	Ubiquitously transcribed tetratricopeptide repeat protein Y-linked transcript variant 59	28.24	3	160.07	7.85
P05109	Protein S100-A8	25.64	2	10.83	7.03
P98088	Mucin-5AC	24.86	5	585.57	6.76
P14618	Pyruvate kinase	24.49	6	49.87	7.83
F4MHH5	Ubiquitously transcribed tetratricopeptide repeat protein Y-linked transcript variant 189	24.23	3	125.07	7.81
Q5T4S7	E3 ubiquitin-protein ligase UBR4	24.02	2	573.48	6.04
P05164	Myeloperoxidase	23.47	5	83.81	8.97
Q93074	Mediator of RNA polymerase II transcription subunit 12	23.28	2	222.29	6.95
Q8WXI7	Mucin-16	22.12	6	1518.24	5.26
P04080	Cystatin-B	20.24	2	11.13	7.56
Q8TAX7	Mucin-7	19.53	2	15.45	10.07
P02768	Serum albumin	18.29	3	66.49	6.04
P01034	Cystatin-C	17.78	2	15.79	8.75
E1B2D1	Hemoglobin alpha-1 globin chain variant (Fragment)	14.18	2	10.76	8.48
P42331	Rho GTPase-activating protein 25	13.09	2	38.13	5.97
H0YJS3	Fanconi anemia group M protein (Fragment)	12.14	2	178.03	5.73
Q9P243	ZFAT protein (Fragment)	10.81	2	133.16	7.87
Q08289	Voltage-dependent L-type calcium channel subunit beta-2	10.30	2	71.31	7.94
Q8IVL0	Neuron navigator 3	10.15	3	255.49	8.76

P25054	Adenomatous polyposis coli protein	9.84	3	311.45	7.80
Q59F18	Smoothelin isoform b variant (Fragment)	9.82	3	55.78	6.73
P29401	Transketolase	9.81	2	36.43	7.77
P08684	Cytochrome P450 3A4	9.61	2	37.06	6.93
Q76N74	Decay accelerating factor (Fragment)	9.61	2	5.94	10.56
B4DK23	cDNA FLJ61300	9.50	2	121.24	7.61
Q7Z5P9	Mucin-19	9.25	3	804.77	5.01
Q8N4F0	BPI fold-containing family B member 2	9.09	2	49.14	8.72
Q7Z460	CLIP-associating protein 1	8.93	3	162.66	8.72
Q7Z5N4	Protein sidekick-1	7.22	2	239.85	6.34
P49790	Nuclear pore complex protein Nup153	6.99	2	153.84	8.73
Q14669	E3 ubiquitin-protein ligase TRIP12	6.83	2	220.30	8.48
Q15772	Striated muscle preferentially expressed protein kinase	6.80	2	354.07	8.51
Q9HCK4	Roundabout homolog 2	6.76	2	157.26	6.30
A6NJZ7	RIMS-binding protein 3C	6.76	2	180.84	6.77
Q9BTX1	Nucleoporin NDC1	6.75	2	37.90	9.70
Q9UPN3	Microtubule-actin cross-linking factor 1, isoforms 1/2/3/5	6.70	2	22.03	11.21
Q6RW13	Type-1 angiotensin II receptor-associated protein	6.62	2	16.42	10.62
Q12955	Ankyrin-3	6.59	2	480.11	6.49
P01857	Immunoglobulin heavy constant gamma 1	6.58	2	36.08	8.19
Q9C0G6	Dynein heavy chain 6, axonemal	6.54	2	475.68	6.00
Q9ULT8	E3 ubiquitin-protein ligase HECTD1	6.43	2	289.20	5.35
Q7Z3B3	KAT8 regulatory NSL complex subunit 1	6.40	2	41.17	9.04
Q9BYE2	Transmembrane protease serine 13	6.34	2	61.04	8.69
Q2TBE0	CWF19-like protein 2	6.33	2	63.53	8.98
P52209	6-phosphogluconate dehydrogenase, decarboxylating	6.07	2	27.86	6.79
A8KAN9	cDNA FLJ78030	6.03	2	112.03	6.70
Q9Y2K9	Syntaxin-binding protein 5-like	5.99	2	111.67	7.37
Q5VVJ2	Histone H2A deubiquitinase MYSM1	5.83	2	94.97	5.53
Q9Y2V7	Conserved oligomeric Golgi complex subunit 6	5.81	2	73.23	5.76
B4DET2	cDNA FLJ53029, highly similar to solute carrier family 25 (mitochondrial carrier), member 18	5.75	2	18.60	9.64
Q15911	ZFHX3 protein	5.72	2	98.52	6.90
P55196	Afadin	5.70	2	189.04	6.49
Q8NDA2	Hemicentin-2	5.09	2	541.64	5.87
Q96T58	Msx2-interacting protein	4.98	2	402.00	7.64
P51532	Transcription activator BRG1	4.07	2	85.60	6.46

SLA Surface

Experiment #1 (126 proteins)

P04745	Alpha-amylase	1151.24	26	57.76	6.93
P23280	Carbonic anhydrase 6	331.16	9	35.34	7.02
P02788	Lactotransferrin	174.19	14	77.92	8.12
P02814	Submaxillary gland androgen-regulated protein 3B	157.54	2	8.18	9.57
Q96DA0	Zymogen granule protein 16 homolog B	137.13	5	19.59	5.95
P60709	Actin, cytoplasmic 1	135.94	9	38.61	5.35
Q99102	Mucin-4	134.20	2	231.37	6.27
P06702	Protein S100-A9	132.12	6	13.23	6.13
Q96DR5	BPI fold-containing family A member 2	125.10	10	26.99	5.59
A8K3K1	cDNA FLJ78096, highly similar to actin, alpha, cardiac muscle (ACTC)	119.03	8	42.02	5.39
A0A075B6K9	Ig lambda-2 chain C regions (Fragment)	103.61	4	11.34	7.24

P22079	Lactoperoxidase	83.94	7	80.29	8.15
P0DOX7	Immunoglobulin kappa light chain	69.04	2	24.01	8.06
P61626	Lysozyme C	67.51	3	16.53	9.16
P12273	Prolactin-inducible protein	67.12	4	16.56	8.05
P07737	Profilin-1	59.42	5	15.04	8.27
P01036	Cystatin-S	57.87	2	16.20	5.02
P25311	Zinc-alpha-2-glycoprotein	55.65	4	34.24	6.05
Q8TDL5	BPI fold-containing family B member 1	52.26	5	52.48	7.55
P05109	Protein S100-A8	47.43	3	10.83	7.03
P02647	Apolipoprotein A-I	41.35	6	30.76	5.76
P04406	Glyceraldehyde-3-phosphate dehydrogenase	38.12	3	36.03	8.46
P02812	Basic salivary proline-rich protein 2	35.20	2	40.77	11.63
P68871	Hemoglobin subunit beta	34.48	5	15.99	7.28
Q8WZ42	Titin	31.07	11	3711.40	6.52
Q12955	Ankyrin-3	28.73	8	480.11	6.49
F4MH51	Ubiquitously transcribed tetratricopeptide repeat protein Y-linked transcript variant 60	27.92	3	147.07	7.84
P01877	Ig alpha-2 chain C region	27.82	2	36.50	6.10
P14618	Pyruvate kinase	25.33	5	53.01	6.84
P01833	Polymeric immunoglobulin receptor	25.29	2	83.23	5.74
P05164	Myeloperoxidase	24.84	6	83.81	8.97
F4MH28	Ubiquitously transcribed tetratricopeptide repeat protein Y-linked transcript variant 35	23.44	3	133.40	8.09
B2R935	cDNA, FLJ94190, highly similar to CDC6 cell division cycle 6 homolog (S. cerevisiae)(CDC6)	22.75	2	62.73	9.58
P23528	Cofilin 1	20.21	3	16.80	8.35
Q8WXI7	Mucin-16	19.70	6	1518.24	5.26
Q9C0D9	Ethanolaminephosphotransferase 1	16.15	2	43.96	6.77
P01034	Cystatin-C	14.74	2	15.79	8.75
P52732	Kinesin-like protein KIF11	13.83	2	119.06	5.72
Q9Y4D8	Probable E3 ubiquitin-protein ligase HECTD4	13.16	3	439.07	6.19
Q9UGM3	Deleted in malignant brain tumors 1 protein	13.16	2	260.57	5.44
P04080	Cystatin-B	12.62	2	11.13	7.56
P01009	Alpha-1-antitrypsin	12.47	2	46.68	5.59
Q6N021	Methylcytosine dioxygenase TET2	12.38	3	223.67	7.99
Q8N4F0	BPI fold-containing family B member 2	12.26	2	49.14	8.72
P80303	Nucleobindin-2	11.99	2	40.34	5.17
Q6ZUJ8	Phosphoinositide 3-kinase adapter protein 1	11.82	2	90.34	5.40
Q13023	A-kinase anchor protein 6	11.72	4	229.32	5.10
Q6N095	Putative uncharacterized protein DKFZp686K03196	11.25	3	52.33	8.57
O15265	Ataxin-7	10.82	2	95.39	9.85
Q86UK7	Zinc finger protein 598	10.74	2	93.23	8.53
Q68DE3	Basic helix-loop-helix domain-containing protein KIAA2018	10.65	2	241.53	7.61
P98088	Mucin-5AC	10.49	2	585.57	6.76
Q9H165	B-cell lymphoma/leukemia 11A	10.46	2	84.45	6.28
Q8NFC6	Biorientation of chromosomes in cell division protein 1-like 1	10.30	3	330.27	5.08
P25440	Bromodomain-containing protein 2	10.30	3	83.10	9.07
Q5VVW2	GTPase-activating Rap/Ran-GAP domain-like protein 3	10.08	2	93.45	6.92
Q8N7Z5	Putative ankyrin repeat domain-containing protein 31	9.73	3	210.68	6.20
B4E0Y1	cDNA FLJ61599	9.71	2	91.35	9.16
Q99661	Kinesin-like protein KIFC2	9.69	2	90.09	9.48

Q7Z2D5	Lipid phosphate phosphatase-related protein type 4	9.62	3	66.16	8.56
Q9Y617	Phosphoserine aminotransferase	9.59	2	40.40	7.66
P46013	Proliferation marker protein Ki-67	9.54	3	358.41	9.42
Q96QS3	Homeobox protein ARX	9.50	2	58.12	5.24
Q9UQ35	Serine/arginine repetitive matrix protein 2	9.36	3	299.44	12.06
Q9Y485	DmX-like protein 1	9.31	3	318.44	6.34
H9A532	BCL6 corepressor-cyclin B3 fusion protein	9.22	3	337.51	6.28
Q86VM9	Zinc finger CCCH domain-containing protein 18	9.13	3	106.32	8.32
Q92954	Proteoglycan 4	9.01	3	150.98	9.50
Q15772	Striated muscle preferentially-expressed protein kinase	8.91	3	93.14	9.92
Q96T21	Selenocysteine insertion sequence-binding protein 2	8.75	2	87.95	8.63
Q6ZP01	RNA-binding protein 44	8.68	3	117.91	5.72
A0A024RA78	Phosphodiesterase 1C, calmodulin-dependent 70kDa, isoform CRA_a	8.38	2	67.43	9.10
P10909	Clusterin	8.28	2	52.46	6.27
Q5HYC2	Uncharacterized protein KIAA2026	7.62	2	227.95	9.04
Q7Z5J4	Retinoic acid-induced protein 1	7.54	2	203.23	8.79
Q9NQ75	Cas scaffolding protein family member 4	7.36	2	81.08	7.09
Q5VV67	Peroxisome proliferator-activated receptor gamma coactivator-related protein 1	7.34	2	69.06	10.04
Q8IUK8	Cerebellin-2	7.28	2	24.07	8.48
Q9C0I4	Thrombospondin type-1 domain-containing protein 7B	7.17	2	175.54	7.42
Q7Z407	CUB and sushi domain-containing protein 3	7.16	2	405.74	6.00
Q68DX3	FERM and PDZ domain-containing protein 2	7.13	2	144.19	6.74
Q70CQ4	Ubiquitin carboxyl-terminal hydrolase 31	7.08	2	146.56	9.22
P20930	Filaggrin	7.05	2	277.11	9.41
Q8N8K9	Uncharacterized protein KIAA1958	6.93	2	79.16	6.83
B3KNZ5	cDNA FLJ30812 fis, highly similar to Mus musculus pecanex-like 2 (Drosophila)	6.91	2	102.21	6.95
Q68DX6	Putative uncharacterized protein DKFZp686P0776	6.91	2	78.02	8.91
O75335	Liprin-alpha-4	6.84	2	42.55	8.50
Q8WXG9	G-protein coupled receptor 98	6.80	2	116.77	4.73
A0A024R8V1	SEC14-like 1 (S. cerevisiae), isoform CRA_a	6.77	2	81.19	6.43
P54578	Ubiquitin carboxyl-terminal hydrolase 14	6.73	2	42.69	7.53
A8K0Y1	cDNA FLJ75576, highly similar to brain-specific angiogenesis inhibitor 3 (BAI3)	6.71	2	171.37	7.05
Q57Z89	HCG1732469	6.70	2	24.38	7.44
A6NGG8	Uncharacterized protein C2orf71	6.67	2	139.57	8.07
Q53EV4	Leucine-rich repeat-containing protein 23	6.61	2	39.77	4.63
Q502W6	von Willebrand factor A domain-containing protein 3B	6.60	2	106.94	8.31
Q53HW5	Excision repair cross-complementing rodent repair deficiency, complementation group 3 variant (Fragment)	6.57	2	89.09	7.23
F5H858	Phosphatase and actin regulator (Fragment)	6.56	2	17.54	8.35
Q86YS7	C2 domain-containing protein 5	6.55	2	110.38	5.69
Q92766	Ras-responsive element-binding protein 1	6.54	2	181.31	6.98
B4DL85	6-phosphogluconate dehydrogenase, decarboxylating	6.54	2	47.44	6.47
Q5VST9	Obscurin	6.44	2	867.94	5.99
Q6ZRI6	Uncharacterized protein C15orf39	6.43	2	110.60	7.64
A8MUU9	Putative uncharacterized protein ENSP00000383309	6.39	2	55.27	13.30
Q14155	Rho guanine nucleotide exchange factor 7	6.38	2	89.96	7.09
B3KUF3	cDNA FLJ39738 fis, highly similar to chloride channel, calcium activated, family member 1 (CLCA1)	6.38	2	34.90	7.80
Q6DN90	IQ motif and SEC7 domain-containing protein 1	6.38	2	108.25	6.93

Q6ZNT7	CDNA FLJ27195 fis, clone SYN02786	6.35	2	20.27	5.67
Q12830	Nucleosome-remodeling factor subunit BPTF (Fragment)	6.26	2	271.36	6.13
Q7Z5P9	Mucin-19	6.09	2	804.77	5.01
M0QZD8	Protein LOC400499	6.08	2	354.00	7.88
Q9NZJ0	Denticleless protein homolog	6.07	2	74.96	8.98
Q5SW79	cDNA FLJ10802 fis highly similar to centrosomal protein 170 kDa (CEP170)	6.05	2	76.19	8.92
P06733	Alpha-enolase	6.00	2	21.01	8.88
Q5THJ4	Vacuolar protein sorting-associated protein 13D	5.92	2	356.81	6.80
D6RAW6	Cell cycle checkpoint protein RAD17 (Fragment)	5.89	2	19.09	6.55
Q6ZVA0	cDNA FLJ42842 fis, clone BRCOC2007034	5.86	2	18.83	7.61
O94916	Nuclear factor of activated T-cells 5, tonicity-responsive, isoform CRA_b	5.85	2	157.88	5.40
H3BV80	RNA-binding protein with serine-rich domain 1	5.76	2	24.55	11.90
P34932	Heat shock 70 kDa protein 4	5.69	2	63.79	4.84
Q14789	Golgin subfamily B member 1	5.69	2	375.79	5.00
O15021	Microtubule-associated serine/threonine-protein kinase 4	5.28	2	179.92	9.23
Q8N532	TUBA1C protein	5.05	2	36.62	7.96
Q5H9F3	BCL-6 corepressor-like protein 1 (Fragment)	4.85	2	150.51	8.56
P10071	Transcriptional activator GLI3	4.81	2	163.23	7.40
Q9Y6J0	Calcineurin-binding protein cabin-1	4.79	2	240.61	6.02
A0A087X0K8	Probable G-protein-coupled receptor 179	4.71	2	257.18	5.71

Experiment #2 (119 proteins)

P04745	Alpha-amylase	616.89	25	57.76	6.93
Q99102	Mucin-4	462.56	2	231.37	6.27
P23280	Carbonic anhydrase 6	259.80	8	35.34	7.02
P02814	Submaxillary gland androgen-regulated protein 3B	168.41	2	8.18	9.57
Q96DR5	BPI fold-containing family A member 2	160.71	11	26.99	5.59
Q96DA0	Zymogen granule protein 16 homolog B	145.76	6	19.59	5.95
A2NUT2	Lambda-chain (AA -20 to 215)	145.31	4	24.64	7.62
P22079	Lactoperoxidase	94.70	9	80.29	8.15
P06702	Protein S100-A9	86.27	6	13.23	6.13
P0DOX7	Immunoglobulin kappa light chain	72.92	4	24.01	8.06
P12273	Prolactin-inducible protein	71.91	5	16.56	8.05
P01036	Cystatin-S	71.38	3	16.20	5.02
P02647	Apolipoprotein A-I	58.09	9	30.76	5.76
P02788	Lactotransferrin	52.45	7	77.92	8.12
P60709	Actin, cytoplasmic 1	52.16	4	38.61	5.35
Q8TDL5	BPI fold-containing family B member 1	50.16	6	52.41	7.23
P02812	Basic salivary proline-rich protein 2	47.45	2	40.77	11.63
Q8WXI7	Mucin-16	43.42	11	1518.24	5.26
Q96K68	cDNA FLJ14473 fis highly similar to SNC73 protein (SNC73)	42.32	4	53.05	6.86
Q9H799	Protein JBTS17	42.18	3	361.52	6.99
Q6MZM9	Proline-rich protein 27	39.62	2	22.71	4.87
Q8WZ42	Titin	38.50	11	3711.40	6.52
P04406	Glyceraldehyde-3-phosphate dehydrogenase	37.70	4	36.03	8.46
P15515	Histatin-1	37.09	2	6.96	9.13
P07737	Profilin-1	35.64	4	15.04	8.27
P98088	Mucin 5AC	33.02	6	648.39	6.76

P04080	Cystatin-B	32.73	3	11.13	7.56
Q9H7U1	Serine-rich coiled-coil domain-containing protein 2	30.43	2	93.49	6.87
P25311	Zinc-alpha-2-glycoprotein	27.68	4	34.24	6.05
P01833	Polymeric immunoglobulin receptor	27.33	2	83.23	5.74
Q15751	Probable E3 ubiquitin-protein ligase HERC1	26.52	2	531.89	6.04
Q5SW79	Centrosomal protein 170kDa	26.23	2	161.34	7.01
P01034	Cystatin-C	25.84	3	15.79	8.75
Q8TAX7	Mucin-7	24.05	2	15.45	10.07
F4MHR8	Ubiquitously transcribed tetratricopeptide repeat protein Y-linked transcript variant 192	23.86	3	124.80	7.85
Q68DE3	Basic helix-loop-helix domain-containing protein KIAA2018	21.71	2	241.53	7.61
E9PAV3	Nascent polypeptide-associated complex subunit alpha, muscle-specific form	21.39	2	205.29	9.58
Q5VWP3	Muscular LMNA-interacting protein Isoform 4	21.28	4	77.19	8.72
P01009	Alpha-1-antitrypsin	19.60	3	46.68	5.59
P14618	Pyruvate kinase	19.49	5	37.53	6.39
A0A024RDF7	Uncharacterized protein	18.95	4	130.17	7.80
P68871	Hemoglobin subunit beta	17.90	2	6.69	4.88
P23528	Cofilin-1	17.12	2	9.08	8.38
Q2M1Z1	MutL homolog 3 (E. coli)	16.58	5	160.94	6.68
Q15648	Mediator of RNA polymerase II transcription subunit 1	16.26	3	140.08	8.90
Q13635	Protein patched homolog 1	14.77	2	160.44	6.89
Q8N4F0	BPI fold-containing family B member 2	14.19	3	49.14	8.72
O15018	PDZ domain-containing protein 2	13.78	3	301.46	7.43
Q7Z589	BRCA2-interacting transcriptional repressor EMSY	12.85	4	130.61	9.28
Q5VV67	Peroxisome proliferator-activated receptor gamma coactivator-related protein 1	11.99	4	69.06	10.04
P16444	Dipeptidase 1	11.52	2	45.64	6.15
Q63HN8	E3 ubiquitin-protein ligase RNF213	11.51	3	591.03	6.48
F8W9U4	Microtubule-associated protein	11.38	3	88.22	9.22
P80303	Nucleobindin-2	10.67	3	40.34	5.17
A0A024QZH6	Serine arginine-rich pre-mRNA splicing factor SR-A1, isoform CRA_a	10.60	3	139.18	9.25
S6AWD9	IgG H chain	10.36	2	33.28	7.85
Q9UBC9	Small proline-rich protein 3	10.18	2	16.95	8.09
Q13129	Zinc finger protein Rlf Homo sapiens	10.04	2	184.58	7.12
P35227	Polycomb group RING finger protein 2	9.90	2	6.97	10.15
Q9H7D0	Dedicator of cytokinesis protein 5	9.89	3	215.17	7.96
Q9UF83	Uncharacterized protein DKFZp434B061	9.83	3	59.38	13.07
Q9UIG0	Tyrosine-protein kinase BAZ1B	9.68	2	170.80	8.48
Q9ULT8	E3 ubiquitin-protein ligase HECTD1 (Fragment)	9.59	2	135.49	5.06
B3KMW2	cDNA FLJ12778 fis moderately similar to Ubiquitin carboxyl-terminal hydrolase 36	9.41	2	78.73	9.85
B3KX38	cDNA FLJ44659 fis highly similar to voltage gated channel like 1 (VGCNL1)	9.35	2	107.08	8.82
O15534	Period circadian protein homolog 1	9.19	3	133.57	6.14
O95425	Supervillin	7.86	2	247.59	6.98
A2KUC3	UGa8H (Fragment)	7.58	2	13.05	7.94
P08238	Heat shock protein HSP 90-beta	7.57	3	79.15	5.02
Q8WXG9	G-protein coupled receptor 98	7.50	3	692.64	4.64
Q93033	Immunoglobulin superfamily member 2	7.46	2	115.04	6.96
Q96CN9	GRIP and coiled-coil domain-containing protein 1	7.08	2	87.70	5.45
Q9Y4D8	Probable E3 ubiquitin-protein ligase HECTD4	6.91	2	468.36	6.14

B4DEW8	cDNA FLJ58144, weakly similar to Zinc finger protein 416	6.88	2	27.52	6.33
Q9NRA8	Eukaryotic translation initiation factor 4E transporter	6.87	2	68.89	9.54
Q9H728	CDNA: FLJ21463 fis, clone COL04765	6.86	2	18.42	8.56
P46100	Transcriptional regulator ATRX	6.85	2	19.66	8.87
Q14686	Nuclear receptor coactivator 6	6.82	2	219.01	9.36
Q8WXV2	SPPR-1	6.81	2	26.67	9.35
P43146	Netrin receptor DCC	6.78	2	117.85	7.61
Q8IWV2	Contactin-4	6.76	2	76.55	6.77
Q8N944	APC membrane recruitment protein 3	6.76	2	90.39	5.69
A0PJE4	JMJD1C protein (Fragment)	6.71	2	48.24	9.48
A0A024R856	HCG96198, isoform CRA_a	6.70	2	287.13	9.10
Q9ULK2	Ataxin-7-like protein 1	6.61	2	78.14	9.94
Q9Y222	Cyclin-D-binding Myb-like transcription factor 1	6.56	2	84.42	4.61
A6H8Y1	Transcription factor TFIIIB component B" homolog	6.49	2	95.54	8.15
O14974	Protein phosphatase 1 regulatory subunit 12A (Fragment)	6.49	2	40.59	9.47
Q86W92	PTPRF interacting protein, binding protein 1 (Liprin beta 1), isoform CRA_a	6.49	2	96.90	6.54
Q6GTX8	Leukocyte-associated immunoglobulin-like receptor 1	6.46	2	29.67	5.53
Q96RV3	Pecanex-like protein 1	6.44	2	258.51	7.21
Q86TC9	Myopalladin	6.44	2	112.65	7.12
Q9NSI6	Bromodomain and WD repeat-containing protein 1	6.40	2	262.77	8.46
Q9UIW0	Ventral anterior homeobox 2	6.38	2	30.86	9.47
Q6ZRS2	Helicase SRCAP	6.37	2	315.42	5.67
P55198	Protein AF-17	6.37	2	31.18	7.37
O43426	SYNJ1 protein	6.34	2	139.86	7.14
Q9UDT6	CAP-GLY domain containing linker protein 2	6.29	2	111.65	6.76
A1XP52	Catecholamine-regulated protein 40	6.27	2	38.06	5.39
Q5T5U3	Rho GTPase-activating protein 21	6.07	2	155.89	7.68
Q9Y566	SH3 and multiple ankyrin repeat domains protein 1	6.04	2	224.82	8.15
P21941	Cartilage matrix protein	6.01	2	53.61	7.50
Q9Y4A5	Transformation/transcription domain-associated protein variant (Fragment)	5.99	2	405.56	8.18
A5PLN4	Splicing factor 4	5.92	2	72.48	7.90
P08575	Receptor-type tyrosine-protein phosphatase C	5.89	2	147.16	6.15
Q59EF4	CDC14 homolog A isoform 1 variant (Fragment)	5.87	2	58.87	9.28
P11047	Laminin subunit gamma-1	5.82	2	177.49	5.12
Q5SY80	Uncharacterized protein C1orf101	5.79	2	109.59	7.27
J3KPH3	Protein FAM208B (Fragment)	5.78	2	26.87	7.27
D3DTC3	HCG1742968, isoform CRA_c	5.77	2	20.34	8.43
Q14207	Protein NPAT	5.77	2	52.57	9.66
Q7Z460	CLIP-associating protein 1	5.73	2	48.49	6.73
B3KS81	Serine/arginine repetitive matrix protein 5	5.71	2	80.31	12.06
Q9BTC0	Death-inducer obliterator 1	5.70	2	243.72	7.88
A0A0A0MTS5	HCG1811249, isoform CRA_f	5.68	2	183.91	8.15
P59044	NACHT, LRR and PYD domains-containing protein 6	4.81	2	98.71	8.07
Q14204	Cytoplasmic dynein 1 heavy chain 1	4.67	2	532.07	6.40
Q6UB98	Ankyrin repeat domain-containing protein 12	4.64	2	235.51	7.01
Q7Z5N4	Protein sidekick-1	4.17	2	239.85	6.34
	Experiment #3 (89 proteins)				
P04745	Alpha-amylase	828.54	21	57.76	6.93

P23280	Carbonic anhydrase 6	382.85	9	35.34	7.02
P02788	Lactotransferrin	247.39	17	77.92	8.12
P61626	Lysozyme C	231.69	3	16.53	9.16
P02814	Submaxillary gland androgen-regulated protein 3B	227.53	2	8.18	9.57
Q96DR5	BPI fold-containing family A member 2	203.92	11	26.99	5.59
Q96DA0	Zymogen granule protein 16 homolog B	171.45	5	19.59	5.95
P06702	Protein S100-A9	116.67	6	13.23	6.13
P60709	Actin, cytoplasmic 1	102.28	10	38.61	5.35
Q8TDL5	BPI fold-containing family B member 1	101.59	9	52.48	7.55
A0A075B6K9	Ig lambda-2 chain C regions (Fragment)	84.74	3	11.34	7.24
P22079	Lactoperoxidase	76.08	8	73.88	8.15
P68871	Hemoglobin subunit beta	66.21	4	9.46	6.79
P01037	Cystatin-SN	61.33	3	16.38	7.21
P01834	Ig kappa chain C region	56.78	2	11.60	5.87
P04406	Glyceraldehyde-3-phosphate dehydrogenase	52.77	4	36.03	8.46
P12273	Prolactin-inducible protein	49.72	3	16.56	8.05
P02647	Apolipoprotein A-I	43.94	5	30.76	5.76
Q8WZ42	Titin	37.58	11	3711.40	6.52
P05109	Protein S100-A8	33.16	3	10.83	7.03
Q8WXI7	Mucin-16	31.38	10	1518.24	5.26
P05164	Myeloperoxidase	31.24	6	83.81	8.97
P25311	Zinc-alpha-2-glycoprotein	29.97	4	34.24	6.05
P07737	Profilin-1	29.74	3	15.04	8.27
P98088	Mucin-5AC	28.92	6	585.57	6.76
P69905	Hemoglobin alpha-1 globin chain	28.62	3	10.78	8.48
Q9HBL0	Tensin-1	28.10	2	85.61	7.42
Q96K68	cDNA FLJ14473 fis highly similar to SNC73 protein (SNC73)	27.23	3	53.05	6.86
P14618	Pyruvate kinase	25.18	5	37.53	6.39
P01034	Cystatin-C	24.95	3	15.79	8.75
P04080	Cystatin-B	23.09	3	11.13	7.56
Q5T4S7	E3 ubiquitin-protein ligase UBR4	23.04	3	573.48	6.04
Q7Z5P9	Mucin-19	20.12	6	804.77	5.01
P23528	Cofilin 1	18.88	3	16.80	8.35
Q15772	Striated muscle preferentially expressed protein kinase	16.35	4	354.07	8.51
P51649	Succinate-semialdehyde dehydrogenase, mitochondrial	15.32	2	48.31	7.02
Q96Q15	Serine/threonine-protein kinase SMG1	14.06	3	398.59	6.33
Q5SW79	cDNA FLJ10802 fis highly similar to centrosomal protein 170 kDa (CEP170)	13.45	4	76.19	8.92
Q8TAX7	Mucin-7	13.05	2	15.45	10.07
Q8WXG9	G-protein coupled receptor 98	12.23	3	692.64	4.64
Q9H2X6	Homeodomain interacting protein kinase 2	12.15	3	88.59	8.47
Q03164	Histone-lysine N-methyltransferase 2A	11.80	3	155.36	10.36
Q9UBC9	Small proline-rich protein 3	11.04	2	16.95	8.09
Q12955	Ankyrin-3	10.65	3	480.11	6.49
Q5T5Y3	Calmodulin-regulated spectrin-associated protein 1	10.59	2	163.16	6.95
L8E8H6	Alternative protein MCRS1	10.01	3	8.49	7.30
Q6N096	Putative uncharacterized protein DKFZp686I15196	9.97	3	50.89	8.06
Q9Y485	DmX-like protein 1	9.49	2	318.44	6.34
A0A024RDF7	Uncharacterized protein	9.36	3	130.17	7.80
B4DHC2	cDNA FLJ56434, highly similar to p130Cas-associated protein	8.47	3	111.03	9.41
P01871	Immunoglobulin heavy constant mu	8.24	3	49.28	6.77

Q9Y3D8	Adenylate kinase isoenzyme 6	7.63	2	21.69	9.91
Q8TAX5	AFF4 protein	7.57	2	40.17	9.51
Q6P5S2	Protein LEG1 homolog	7.03	2	37.90	6.15
Q86SQ4	G-protein coupled receptor 126	6.97	2	136.61	7.87
P23284	Peptidyl-prolyl cis-trans isomerase	6.96	2	22.73	9.32
Q8TCH5	CDNA FLJ23893 fis, clone LNG14589	6.86	2	18.78	12.23
Q92954	Proteoglycan 4	6.78	2	150.98	9.50
Q9ULT8	E3 ubiquitin-protein ligase HECTD1	6.77	2	162.09	5.36
Q14005	Pro-interleukin-16	6.72	2	123.22	7.44
Q6DRA6	Putative histone H2B type 2-D	6.66	2	18.01	10.58
Q8N7U6	EF-hand domain-containing family member B	6.65	2	69.40	8.72
B4DJU9	cDNA FLJ55278, highly similar to AF4/FMR2 family member 1	6.55	2	91.55	9.42
Q8WX93	Palladin, cytoskeletal associated protein	6.53	2	121.97	6.92
Q8N5U1	Membrane-spanning 4-domains subfamily A member 15	6.53	2	19.85	8.53
Q6ZSZ6	Teashirt homolog 1	6.51	2	117.84	7.06
Q13023	A-kinase anchor protein 6	6.50	2	229.32	5.10
Q9UQ26	Regulating synaptic membrane exocytosis protein 2	6.49	2	160.30	9.07
Q6R327	Rapamycin-insensitive companion of mTOR	6.43	2	192.10	7.47
B7Z2I8	PDZ domain containing RING finger 3, isoform CRA_a	6.39	2	82.24	5.06
O15018	PDZ domain-containing protein 2	6.39	2	301.46	7.43
A4D1Z4	AP-5 complex subunit zeta-1	6.35	2	164.57	8.41
Q86XX4	Extracellular matrix protein FRAS1	6.33	2	442.93	5.57
P98160	Basement membrane-specific heparan sulfate proteoglycan core protein	6.32	2	463.72	6.51
A8K2W3	cDNA FLJ78516	6.30	2	47.07	5.25
Q9UKN8	General transcription factor 3C polypeptide 4	6.29	2	62.64	7.77
A0A024QZV4	HCG2044008, isoform CRA_a	6.23	2	7.78	8.88
Q9HCK4	Roundabout homolog 2	6.10	2	37.29	5.69
Q8N3P4	Vacuolar protein sorting-associated protein 8 homolog	6.02	2	18.21	4.45
Q5T481	RNA-binding protein 20	5.96	2	134.27	5.69
Q01538	MYT1 protein	5.82	2	64.55	6.84
H3BQ24	Fanconi-associated nuclease 1	5.82	2	47.99	6.57
Q8NFP9	Neurobeachin	5.81	2	327.34	6.16
P49759	Dual specificity protein kinase CLK1, Isoform 3	5.72	2	61.67	8.88
P30622	CAP-Gly domain-containing linker protein 1	5.66	2	71.69	7.56
Q92733	Proline-rich protein PRCC	5.13	2	52.39	5.10
Q9UDT6	CAP-GLY domain containing linker protein 2	4.92	2	111.65	6.76
Q8IX06	Putative exonuclease GOR	4.81	2	73.81	9.14
P08684	Cytochrome P450 3A4	4.27	2	37.06	6.93

SLActive Surface

Experiment #1 (158 proteins)

P04745	Alpha-amylase	708.27	26	57.76	6.93
P02808	Statherin	497.77	2	7.30	8.47
P06702	Protein S100-A9	209.80	8	13.23	6.13
P02814	Submaxillary gland androgen-regulated protein 3B	166.21	2	8.18	9.57
P23280	Carbonic anhydrase 6	142.90	7	35.34	7.02
P12273	Prolactin-inducible protein	120.67	8	16.56	8.05
A0A075B6K9	Ig lambda-2 chain C regions	108.18	3	11.34	7.24
P02788	Lactotransferrin	88.86	10	77.92	8.12
P60709	Actin, cytoplasmic 1	81.29	9	38.61	5.35

P15515	Histatin-1	75.64	2	6.96	9.13
P61626	Lysozyme C	74.90	3	16.53	9.16
Q96DA0	Zymogen granule protein 16 homolog B	73.75	4	19.59	5.95
P01036	Cystatin-S	65.53	3	16.20	5.02
P0DOX7	Immunoglobulin kappa light chain	64.35	3	24.01	8.06
P23284	Peptidyl-prolyl cis-trans isomerase	58.74	7	22.73	9.32
P05109	Protein S100-A8	58.34	5	10.83	7.03
P04406	Glyceraldehyde-3-phosphate dehydrogenase	56.55	5	36.03	8.46
P80303	Nucleobindin-2	51.99	5	40.34	5.17
P14618	Pyruvate kinase	51.29	7	49.87	7.83
P25311	Zinc-alpha-2-glycoprotein	48.29	5	34.24	6.05
Q8WXI7	Mucin-16	40.16	12	1518.24	5.26
P01876	Ig alpha-1 chain C region	36.83	2	37.63	6.51
Q8WZ42	Titin	33.83	11	3711.40	6.52
P22079	Lactoperoxidase	29.46	4	80.29	8.15
Q5VV67	Peroxisome proliferator-activated receptor gamma coactivator-related protein 1	25.91	5	69.06	10.04
P02768	Albumin	22.65	3	66.49	6.04
P68871	Beta globin chain	22.51	3	9.46	6.79
Q99102	Mucin-4	21.18	3	231.37	6.27
Q12955	Ankyrin-3	20.17	6	480.11	6.49
P07737	Profilin-1	18.02	4	15.04	8.27
Q92824	Proprotein convertase subtilisin/kexin type 5	16.92	3	206.80	6.10
P25054	Adenomatous polyposis coli protein	16.55	5	311.45	7.80
P23528	Cofilin-1	16.38	2	9.08	8.38
P30740	Leukocyte elastase inhibitor	15.79	4	38.66	6.67
Q7Z589	cDNA FLJ43124 fis, highly similar to Protein EMSY	15.57	4	130.70	9.31
Q9Y4D8	Probable E3 ubiquitin-protein ligase HECTD4	14.13	5	468.36	6.14
Q7Z351	Putative uncharacterized protein DKFZp686N02209	13.94	3	52.82	8.48
Q96NE9	FERM domain-containing protein 6	13.92	4	62.86	7.31
Q9Y6V0	Protein piccolo	13.80	4	410.91	5.40
Q5JRM2	Uncharacterized protein CXorf66	13.54	2	39.92	9.54
Q13535	Serine/threonine-protein kinase ATR	13.46	2	301.17	7.43
Q8IZF6	Probable G-protein coupled receptor 112	13.21	3	333.16	6.21
B8Y0L3	Aspartate beta-hydroxylase (Fragment)	13.20	4	47.98	4.69
Q9NQ36	Signal peptide, CUB and EGF-like domain-containing protein 2	13.11	2	106.69	6.81
Q9UF83	Uncharacterized protein DKFZp434B061	13.09	4	59.38	13.07
Q13023	A-kinase anchor protein 6	13.07	3	229.32	5.10
P98088	Mucin-5AC	12.94	3	585.57	6.76
P20930	Filaggrin	12.81	4	430.16	9.29
Q8TBN0	Guanine nucleotide exchange factor for Rab-3A	12.75	3	42.61	6.47
Q8TDL5	cDNA, FLJ93674	12.70	3	52.48	7.55
E7EVA0	Microtubule-associated protein	12.67	3	245.29	6.23
Q8IVL1	Neuron navigator 2	12.45	3	261.56	8.98
O43166	SIPA1L1 protein	12.28	4	199.84	8.19
B2RTY4	Unconventional myosin-IXa	11.87	3	275.83	8.73
P07900	HSP90AA1 protein (Fragment)	11.78	3	68.33	5.19
P06396	Gelsolin	11.24	2	52.34	5.34
Q02505	Mucin-3A	10.39	3	265.71	5.49
Q5VWN6	Protein FAM208B	10.37	3	268.68	5.90
Q6ZTR5	Cilia- and flagella-associated protein 47	10.29	2	58.02	6.90
E9PAV3	Nascent polypeptide-associated complex subunit alpha, muscle-specific form	10.24	3	205.29	9.58

O60494	Cubilin	10.15	2	146.01	5.95
Q4ZHG4	Fibronectin type III domain-containing protein 1	10.13	3	194.42	9.22
Q7Z5P9	Mucin-19	9.99	3	804.77	5.01
Q9Y485	DmX-like protein 1	9.95	3	318.44	6.34
P49792	E3 SUMO-protein ligase RanBP2	9.87	3	357.97	6.20
Q86V42	Protein FAM124A	9.85	3	60.07	6.60
Q12888	Tumor suppressor p53-binding protein 1	9.85	2	189.80	4.69
B7Z7S7	cDNA FLJ60964, weakly similar to dentin sialophosphoprotein (DSPP)	9.85	3	37.67	8.15
Q92833	Protein Jumonji	9.83	2	138.65	9.38
A0A024RDD6	Uncharacterized protein	9.75	2	82.36	7.56
Q6P0Q8	Microtubule-associated serine/threonine-protein kinase 2	9.72	3	196.31	8.16
Q9P2D3	HEAT repeat containing 5B	9.70	3	224.13	7.18
Q8WXG9	G-protein coupled receptor 98	9.56	3	692.64	4.64
Q12860	Contactin-1	9.47	3	113.25	5.90
A0A0A0MT16	ATP-binding cassette sub-family A member 13	9.43	3	575.79	6.43
A7E2V7	TUBGCP6 protein	9.41	2	163.78	6.87
Q9UKA4	A-kinase anchor protein 11	9.41	3	210.38	5.39
Q7Z6Z7	HECT, UBA and WWE domain containing 1	9.33	3	479.85	5.21
Q5QP82	DDB1- and CUL4-associated factor 10	9.28	3	60.54	7.50
Q5SW79	Centrosomal protein of 170 kDa	9.28	3	29.03	9.92
P02647	Apolipoprotein A-I	9.15	3	30.76	5.76
Q9BXW9	Fanconi anemia group D2 protein	9.01	3	164.02	5.88
Q5VYJ5	MAM and LDL-receptor class A domain-containing protein 1 (Fragment)	9.01	3	165.33	5.92
Q09666	Neuroblast differentiation-associated protein AHNAK	8.85	3	628.70	6.15
O14513	Nck-associated protein 5	8.49	3	208.35	8.06
P0DMV8	Heat shock 70kDa protein 1A variant (Fragment)	8.47	2	77.45	6.30
O95263	High affinity cAMP-specific and IBMX-insensitive 3',5'-cyclic phosphodiesterase 8B	8.43	3	98.92	6.83
Q9P243	ZFAT protein (Fragment)	8.32	2	133.16	7.87
Q96JH7	Deubiquitinating protein VCIP135	8.17	2	134.24	7.20
Q8TAX7	Mucin-7	7.82	2	15.45	10.07
B4DNY3	Adenylyl cyclase-associated protein	7.33	2	43.68	8.54
Q9C0G6	Dynein heavy chain 6, axonemal	7.21	3	475.68	6.00
Q8IUG5	Unconventional myosin-XVIIIb	7.19	2	85.50	7.47
Q5SZK8	FRAS1-related extracellular matrix protein 2	7.18	2	350.94	5.03
A2VDJ0	Transmembrane protein 131-like	7.03	2	179.22	6.86
B4DFV7	cDNA FLJ60481	7.02	2	67.21	5.49
Q9H694	Protein bicaudal C homolog 1	6.97	2	53.24	8.57
Q5U623	Activating transcription factor 7-interacting protein 2	6.94	2	75.72	7.75
Q99661	Kinesin-like protein KIF2C	6.92	2	52.30	7.12
Q8TEG5	FLJ00232 protein (Fragment)	6.92	2	35.74	9.23
Q9NXR1	Nuclear distribution protein nudE homolog 1 (Fragment)	6.88	2	21.27	9.14
P09848	Lactase-phlorizin hydrolase	6.86	2	218.45	6.34
Q6R2W3	SCAN domain-containing protein 3	6.82	2	151.57	6.73
Q14571	Inositol 1,4,5-trisphosphate receptor type 2	6.82	2	307.87	6.43
Q9C0C7	Activating molecule in BECN1-regulated autophagy protein 1	6.82	2	129.52	6.98
B4E033	Oxysterol-binding protein	6.81	2	69.18	8.24
P30622	CAP-Gly domain-containing linker protein 1	6.81	2	36.94	9.63
Q96DR5	BPI fold-containing family A member 2	6.78	3	26.99	5.59

O00555	Voltage-dependent P/Q-type calcium channel subunit alpha	6.74	2	256.98	8.43
Q5VUA4	Zinc finger protein 318	6.74	2	250.96	7.20
D6W633	Protein tyrosine phosphatase, receptor type, S, isoform CRA_a	6.73	2	143.34	6.24
Q8IVF2	Protein AHNAK2	6.72	2	616.24	5.36
Q07065	Cytoskeleton-associated protein 4	6.71	2	65.98	5.92
Q9NRE2	Teashirt homolog 2	6.67	2	114.93	7.83
A7MAP6	MHC class I antigen (Fragment)	6.67	2	40.91	6.47
P21439	Multidrug resistance protein 3	6.65	2	141.43	8.48
B4DHX2	cDNA FLJ58181, highly similar to ATP/GTP binding protein 1 (AGTPBP1)	6.64	2	72.56	5.54
Q16643	Drebrin	6.64	2	40.34	4.03
Q9NZL4	Hsp70-binding protein 1	6.62	2	14.29	4.45
Q96IQ7	V-set and immunoglobulin domain-containing protein 2	6.61	2	34.33	7.55
E7EX40	Rab11 family-interacting protein 1	6.55	2	54.80	9.01
Q9BZE9	Tether-containing UBX domain for GLUT4	6.51	2	32.74	6.04
Q68DQ2	Very large A-kinase anchor protein	6.45	2	330.43	5.20
Q9NWC0	cDNA FLJ10141 fis, clone HEMBA1003199	6.43	2	17.43	11.63
Q9HCH5	Synaptotagmin-like protein 2	6.42	2	104.87	8.00
Q9H2P0	Activity-dependent neuroprotector homeobox protein	6.41	2	123.54	7.42
Q9H5Y7	SLIT and NTRK-like protein 6	6.40	2	95.05	6.52
B7ZKN7	BLM protein	6.40	2	116.99	8.63
P25440	Bromodomain-containing protein 2	6.39	2	83.10	9.07
P46013	Proliferation marker protein Ki-67	6.37	2	358.41	9.42
Q9UDT6	CAP-GLY domain containing linker protein 2	6.33	2	111.65	6.76
O60292	Signal-induced proliferation-associated 1 like 3	6.31	2	194.50	8.32
Q8N3X1	Formin-binding protein 4	6.30	2	14.85	7.78
B7Z2I8	PDZ domain containing RING finger 3, isoform CRA_a	6.26	2	82.24	5.06
P27448	MAP/microtubule affinity-regulating kinase 3	6.25	2	24.27	9.52
Q92954	Proteoglycan 4	6.22	2	89.50	8.91
P54108	Cysteine-rich secretory protein 3	6.21	2	27.61	7.80
Q96D09	G-protein coupled receptor-associated sorting protein 2	6.10	2	93.74	5.05
Q9UGJ0	5'-AMP-activated protein kinase subunit gamma-2	5.93	2	24.62	10.77
F8W9U4	Microtubule-associated protein	5.89	2	88.22	9.22
Q5TBA9	Protein furry homolog	5.84	2	193.57	5.40
Q08AL8	ADAM metallopeptidase domain 22	5.82	2	96.63	7.20
Q9ULI3	Protein HEG homolog 1	5.80	2	147.37	6.18
P0CW27	Coiled-coil domain-containing protein 166	5.78	2	48.68	10.59
Q5QGS0	Protein KIAA2022	5.78	2	167.45	6.40
D6RIA3	Protein LOC285556	5.78	2	189.96	8.98
Q9UBW7	Zinc finger MYM-type protein 2	5.77	2	139.64	6.71
Q2Z1P3	Putative uncharacterized protein GAF1 (Fragment)	5.76	2	55.91	9.35
P23588	EIF4B protein	5.73	2	39.19	7.43
P0CAP1	Myocardial zonula adherens protein	5.68	2	54.17	6.18
O14511	Pro-neuregulin-2, membrane-bound isoform	5.67	2	84.25	9.44
B4DHW5	cDNA FLJ53328, highly similar to Methylcrotonoyl-CoA carboxylase subunit alpha, mitochondrial	5.65	2	52.62	8.59
Q5TAX3	Terminal uridylyltransferase 4 (Fragment)	5.64	2	103.11	6.79
Q6ZR29	cDNA FLJ46702 fis, clone TRACH3014183	5.56	2	160.05	5.62
O15050	TPR and ankyrin repeat-containing protein 1	5.27	2	336.01	6.76
Q9NSD9	Phenylalanine--tRNA ligase beta subunit	5.23	2	54.78	7.50
Q6NT04	Tigger transposable element-derived protein 7	5.16	2	63.20	8.75

B4DVL0	cDNA FLJ61174, highly similar to WWC family member 3	5.12	2	21.93	5.57
	Experiment #2 (126 proteins)				
P04745	Alpha-amylase	564.99	21	57.76	6.93
P02814	Submaxillary gland androgen-regulated protein 3B	205.01	2	8.18	9.57
P06702	Protein S100-A9	177.61	8	13.23	6.13
P12273	Prolactin-inducible protein	121.86	7	16.56	8.05
A0A075B6K9	Ig lambda-2 chain C regions (Fragment)	103.28	3	11.34	7.24
P23280	Carbonic anhydrase 6	100.12	6	35.34	7.02
Q96DA0	Zymogen granule protein 16 homolog B	94.16	6	19.59	5.95
P0DOX7	Immunoglobulin kappa light chain	69.04	4	24.01	8.06
P01036	Cystatin-S	68.73	3	16.20	5.02
P80303	Nucleobindin-2	64.22	5	40.34	5.17
P23284	Peptidyl-prolyl cis-trans isomerase	56.48	6	22.73	9.32
P04406	Glyceraldehyde-3-phosphate dehydrogenase	44.67	4	36.03	8.46
P05109	Protein S100-A8	41.48	4	10.83	7.03
Q01546	Keratin, type II cytoskeletal 2 oral	37.13	3	65.80	8.12
P01876	Ig alpha-1 chain C region	36.10	4	37.63	6.51
P25311	Zinc-alpha-2-glycoprotein	34.02	5	34.24	6.05
Q8WXI7	Mucin-16	33.03	9	1518.24	5.26
Q13707	ACTA2 protein (Fragment)	31.35	5	36.78	5.35
Q8WZ42	Titin	30.48	9	3711.40	6.52
P01871	Immunoglobulin heavy constant mu	29.59	5	49.28	6.77
P04080	Cystatin-B	27.27	3	11.13	7.56
Q7Z5P9	Mucin-19	23.46	7	804.77	5.01
Q4G0X9	Coiled-coil domain-containing protein 40	22.63	2	130.03	5.29
Q5SW79	Centrosomal protein 170kDa	21.99	5	161.34	7.01
P22079	Lactoperoxidase	20.63	3	73.88	8.15
P98088	Mucin-5AC	19.72	5	585.57	6.76
P02647	Apolipoprotein A-I	19.29	4	30.76	5.76
Q8IVL0	Neuron navigator 3	19.22	4	255.49	8.76
P02788	Lactotransferrin	18.57	3	77.92	8.12
Q8TDL5	BPI fold-containing family B member 1	18.34	3	52.41	7.23
Q08188	Protein-glutamine gamma-glutamyltransferase E	18.13	4	76.58	5.86
A0A087X010	Ig gamma-1 chain C region	15.78	3	50.79	8.18
P08238	Heat shock protein HSP 90-beta	15.13	3	79.15	5.02
P02768	Serum albumin	13.94	2	66.49	6.04
Q1RMC9	ERBB2IP protein	13.65	3	153.42	5.47
Q9UGM3	Deleted in malignant brain tumors 1 protein	13.57	2	260.57	5.44
B4DNY3	Adenylyl cyclase-associated protein	12.84	2	43.68	8.54
P01009	Alpha-1-antitrypsin	12.51	2	46.68	5.59
P14618	Pyruvate kinase	12.43	4	37.53	6.39
Q96DR5	BPI fold-containing family A member 2	12.19	4	26.99	5.59
P46013	Proliferation marker protein Ki-67	11.57	3	358.41	9.42
O60673	DNA polymerase zeta catalytic subunit	11.50	4	352.55	8.47
Q8N4F0	BPI fold-containing family B member 2	11.32	3	49.14	8.72
E2QRD4	Protein MMS22-like	10.68	2	137.42	7.33
O75129	Astrotactin 2	10.63	3	99.83	5.33
Q9UPN3	Microtubule-actin cross-linking factor 1, isoforms 1/2/3/5	10.61	3	837.79	5.39
Q12955	Ankyrin-3	10.36	3	480.11	6.49
Q5M9Q1	NKAP-like protein	10.24	3	46.28	9.72

Q6ZS81	WD repeat- and FYVE domain-containing protein 4	10.17	2	142.99	6.87
Q9Y6V0	Protein piccolo	10.15	3	552.94	6.51
P06733	Alpha-enolase	10.13	3	47.14	7.39
L8E7G9	Alternative protein ZNF74	10.13	3	32.45	12.07
Q7Z589	BRCA2-interacting transcriptional repressor EMSY	10.07	3	60.47	6.10
Q461N2	Ciprofibrate bound protein p240 isoform PRIC320-2	10.06	2	222.80	7.09
Q6H8Q1	Actin-binding LIM protein 2	10.05	3	43.14	7.71
Q96AX9	E3 ubiquitin-protein ligase MIB2	9.80	2	11.56	11.37
P20930	Truncated profilaggrin	9.77	3	259.56	9.50
Q5H9P1	Putative uncharacterized protein DKFZp686F1345 (Fragment)	9.66	3	192.26	4.58
B7ZKN7	BLM protein	9.63	2	116.99	8.63
Q96RU2	Ubiquitin carboxyl-terminal hydrolase 28	9.55	2	21.15	5.01
P68871	Hemoglobin subunit beta	9.55	2	15.99	8.06
Q14781	Chromobox protein homolog 2	9.55	3	56.05	10.01
Q9UPU5	Ubiquitin carboxyl-terminal hydrolase 24	9.46	3	294.18	6.14
O15018	PDZ domain-containing protein 2	9.25	3	301.46	7.43
Q9UF83	Uncharacterized protein DKFZp434B061	9.17	3	59.38	13.07
Q8NAN2	Protein FAM73A	9.00	3	70.96	5.63
Q5VV67	Peroxisome proliferator-activated receptor gamma coactivator-related protein 1	8.96	3	69.06	10.04
P31025	Lipocalin-1	8.94	2	19.24	5.58
Q8NFC6	Biorientation of chromosomes in cell division protein 1-like 1	8.88	3	330.27	5.08
Q9UBC9	Small proline-rich protein 3	8.72	3	16.95	8.09
B3KX05	Protein KIBRA	8.33	3	79.49	7.43
Q7Z2Z1	Treslin	8.13	3	210.73	8.78
Q68DA7	Formin-1	8.04	2	146.41	8.70
Q68DE3	Basic helix-loop-helix domain-containing protein KIAA2018	8.04	2	241.53	7.61
Q99665	Interleukin-12 receptor subunit beta-2	7.49	2	97.07	7.75
Q3MIW9	Diffuse panbronchiolitis critical region protein 1	7.22	2	151.08	5.17
Q6P0Q8	Microtubule-associated serine/threonine-protein kinase 2	7.18	2	196.31	8.16
Q6EMB2	TTLL5 protein	7.17	2	80.00	9.16
Q5VW22	Arf-GAP with GTPase, ANK repeat and PH domain-containing protein 6	7.14	2	61.21	7.81
O75037	Kinesin-like protein KIF21B	6.98	2	182.55	7.08
Q15772	Striated muscle preferentially expressed protein kinase	6.97	2	354.07	8.51
Q8NDA2	Hemicentin-2	6.97	2	541.64	5.87
Q9ULK2	Ataxin-7-like protein 1	6.92	2	78.14	9.94
Q9NUQ6	SPATS2-like protein	6.91	2	52.39	9.66
Q8NG31	Kinetochore scaffold 1	6.86	2	154.98	5.24
Q8N7X4	Melanoma-associated antigen B6	6.80	2	43.96	5.55
A0A075B7B8	Protein IGHV3OR16-12 (Fragment)	6.78	2	12.87	6.51
Q6PCT2	F-box/LRR-repeat protein 19	6.78	2	75.67	9.17
A4D299	TAF6 RNA polymerase II, TATA box binding protein (TBP)-associated factor	6.78	2	71.44	8.51
Q6ZSE3	cDNA FLJ45597 fis, weakly similar to Mus musculus synaptotagmin-like 4 (Sytl4)	6.72	2	95.18	4.92
Q86YX3	Metallothionein	6.69	2	6.16	7.88
Q9H7H0	Methyltransferase-like protein 17, mitochondrial	6.63	2	50.70	9.33
P07237	Protein disulfide-isomerase	6.61	2	23.01	5.06
Q6PGN9	Proline/serine-rich coiled-coil protein 1	6.61	2	22.32	8.92

O43324	Eukaryotic translation elongation factor 1 epsilon-1	6.61	2	10.42	8.75
O15075	Serine/threonine-protein kinase DCLK1	6.58	2	82.17	8.66
Q685J3	Mucin-17	6.57	2	425.29	4.03
Q5VUA4	Zinc finger protein 318	6.57	2	250.96	7.20
Q99700	Ataxin-2	6.56	2	31.86	10.02
Q9BTC0	Death-inducer obliterator 1	6.55	2	243.72	7.88
Q8NA90	cDNA FLJ35733 fis, weakly similar to ANTER-SPECIFIC PROLINE-RICH PROTEIN APG	6.54	2	29.45	10.23
Q9NY74	Ewing's tumor-associated antigen 1	6.51	2	103.38	7.62
Q8N2S1	Latent-transforming growth factor beta-binding protein 4	6.50	2	169.34	5.29
O75445	Usherin	6.50	2	575.23	6.83
Q9UKN1	Mucin-12	6.50	2	557.83	5.55
B2R9R2	cDNA, FLJ94517, highly similar to baculoviral IAP repeat-containing 4 (BIRC4)	6.49	2	56.59	6.65
P13611	Versican core protein	6.46	2	372.59	4.51
Q8TCH5	CDNA FLJ23893 fis, clone LNG14589	6.44	2	18.78	12.23
Q8TEM4	FLJ00169 protein (Fragment)	6.43	2	46.49	11.55
P04114	Apolipoprotein B-100	6.41	2	489.53	7.15
Q8NEZ4	Histone-lysine N-methyltransferase 2C	6.39	2	541.03	6.49
B4DNP9	cDNA FLJ59939, highly similar to Protein disulfide-isomerase	6.37	2	24.52	9.57
Q7Z5Q5	DNA polymerase nu	6.36	2	100.24	8.29
Q75T13	GPI inositol-deacylase	6.29	2	105.32	9.01
O43166	SIPA1L1 protein	6.27	2	199.84	8.19
P02545	Prelamin-A/C	6.22	2	74.09	7.02
Q15287	RNA-binding protein with serine-rich domain 1	6.14	2	14.63	11.75
P32926	Desmoglein-3	6.00	2	107.44	5.00
O60488	Long-chain-fatty-acid--CoA ligase 4	5.99	2	72.10	8.22
A0A090N7X3	Uncharacterized protein	5.97	2	29.02	8.66
Q7Z460	cDNA FLJ61355, highly similar to CLIP-associating protein 1	5.95	2	135.70	8.85
H3BUA3	Carboxylic ester hydrolase	5.82	2	40.11	6.23
Q8N3C7	CAP-Gly domain-containing linker protein 4	5.77	2	61.45	9.36
P07332	Tyrosine-protein kinase Fes/Fps	5.75	2	76.75	6.71
P42166	Lamina-associated polypeptide 2, isoform alpha	5.72	2	75.45	7.66
Q86Z02	Homeodomain interacting protein kinase 1	4.23	2	89.42	8.25
	Experiment #3 (143 proteins)				
P04745	Alpha-amylase	665.05	20	57.76	6.93
P02808	Statherin	479.58	2	7.30	8.47
P06702	Protein S100-A9	227.82	7	13.23	6.13
P02814	Submaxillary gland androgen-regulated protein 3B	179.00	2	8.18	9.57
P61626	Lysozyme C	147.07	2	16.53	9.16
P12273	Prolactin-inducible protein	140.55	7	16.56	8.05
P23280	Carbonic anhydrase 6	137.30	6	35.34	7.02
P02788	Lactotransferrin	119.42	12	77.92	8.12
P15515	Histatin-1	96.68	2	6.96	9.13
P04406	Glyceraldehyde-3-phosphate dehydrogenase	77.67	5	36.03	8.46
Q96DA0	Zymogen granule protein 16 homolog B	71.45	4	19.59	5.95
P01834	Ig kappa chain C region	67.84	2	11.60	5.87
P01036	Cystatin-S	62.84	3	16.20	5.02
P23284	Peptidyl-prolyl cis-trans isomerase	60.19	7	22.73	9.32

P05109	Protein S100-A8	59.64	4	10.83	7.03
A0A075B6K9	Ig lambda-2 chain C regions (Fragment)	57.25	2	11.34	7.24
P14618	Pyruvate kinase	52.17	8	49.87	7.83
Q13707	ACTA2 protein (Fragment)	47.23	5	36.78	5.35
P25311	Zinc-alpha-2-glycoprotein	39.98	4	34.24	6.05
Q8WXI7	Mucin-16	38.51	12	1518.24	5.26
P68871	Beta globin chain	38.13	4	9.46	6.79
Q7Z5P9	Mucin-19	26.58	8	804.77	5.01
P0DOX5	Immunoglobulin gamma-1 heavy chain	25.25	4	56.39	6.93
Q99102	Mucin-4	24.14	3	231.37	6.27
P80303	Nucleobindin-2	22.64	3	40.34	5.17
P98088	Mucin-5AC	19.74	3	585.57	6.76
Q9Y6V0	Protein piccolo	19.38	6	552.94	6.51
P30740	Leukocyte elastase inhibitor	18.34	4	38.66	6.67
Q5TAX3	Terminal uridylyltransferase 4	17.66	3	103.11	6.79
P05164	Myeloperoxidase	17.38	4	83.81	8.97
Q9H2X6	Homeodomain-interacting protein kinase 2	17.22	3	130.88	8.43
A0A087WU78	Nance-Horan syndrome protein	17.17	5	157.67	7.02
P46013	Proliferation marker protein Ki-67	16.85	4	358.41	9.42
P22079	Lactoperoxidase	16.65	3	73.88	8.15
P08235	Mineralocorticoid receptor	16.03	3	67.76	7.06
Q7Z460	CLIP-associating protein 1	14.63	4	162.66	8.72
Q9HC84	Mucin-5B	13.66	4	595.96	6.64
Q8TDL5	cDNA, FLJ93674	13.62	3	52.48	7.55
P02768	Serum albumin	13.10	2	66.49	6.04
Q99683	Mitogen-activated protein kinase kinase kinase 5	13.08	2	127.03	6.28
Q8NDH2	Coiled-coil domain-containing protein 168	13.07	4	277.78	9.31
P30414	NK-tumor recognition protein	12.86	4	165.58	9.99
Q6ZR21	Peptidylprolyl isomerase	12.05	2	50.93	6.16
Q96DR5	BPI fold-containing family A member 2	11.42	4	26.99	5.59
F4MH42	Ubiquitously transcribed tetratricopeptide repeat protein Y-linked transcript variant 38	10.58	2	140.12	7.90
P04080	Cystatin-B	10.54	3	11.13	7.56
Q13635	Protein patched homolog 1	10.49	2	37.20	6.84
Q96CN9	GRIP and coiled-coil domain-containing protein 1	10.35	3	87.70	5.45
Q9BX84	Transient receptor potential cation channel subfamily M member 6	10.19	2	231.56	7.77
A8K1Z3	cDNA FLJ75002, highly similar to neural cell expressed,developmentally down-regulated gene 1	10.17	3	71.88	7.83
P01857	Immunoglobulin heavy constant gamma 1	10.12	3	52.01	8.06
Q9BQF6	Sentrin-specific protease 7	10.11	2	112.41	6.71
Q9NSI6	Bromodomain and WD repeat-containing protein 1	10.10	3	262.77	8.46
Q5VV67	Peroxisome proliferator-activated receptor gamma coactivator-related protein 1	10.07	2	69.06	10.04
O43707	Alpha-actinin-4	10.04	3	59.53	4.94
Q5VT52	Regulation of nuclear pre-mRNA domain-containing protein 2	9.91	3	155.92	7.42
Q8N2C7	Protein unc-80 homolog	9.81	2	363.16	6.86
Q9Y2H9	Microtubule-associated serine/threonine-protein kinase 1	9.81	3	170.57	8.44
Q9UBF2	Coatomer subunit gamma-2	9.76	2	89.33	5.68
B4DM60	cDNA FLJ51499, highly similar to BR serine/threonine-protein kinase 2	9.75	3	40.61	9.66
Q8TAX7	Mucin-7	9.74	2	15.45	10.07

P51610	Host cell factor 1	9.73	3	208.60	7.46
O60664	Perilipin-3	9.72	3	47.05	5.44
Q8WZ42	Titin	9.66	3	2991.19	6.74
Q92503	SEC14-like protein 1	9.62	2	51.34	7.25
H3BTF6	Uncharacterized protein C16orf59 (Fragment)	9.52	3	30.42	9.88
P69905	Hemoglobin alpha-1 globin chain	9.46	3	10.78	8.48
P23528	Cofilin 1	9.43	2	16.80	8.35
Q92824	Proprotein convertase subtilisin/kexin type 5	9.08	2	206.80	6.10
Q96PY0	Putative uncharacterized protein PSMG3-AS1	8.57	2	28.23	11.15
Q9UKN1	Mucin-12	8.18	3	557.83	5.55
Q6MZL5	Putative uncharacterized protein DKFZp686C06243 (Fragment)	8.13	2	195.52	5.22
Q8IVF2	Protein AHNAK2	7.81	3	616.24	5.36
Q7Z494	Nephrocystin-3	7.18	2	150.77	6.76
Q14005	Pro-interleukin-16	7.16	2	76.77	8.06
Q8N2Y8	Iporin	7.15	2	161.13	6.62
Q08AD1	Calmodulin-regulated spectrin-associated protein 2	7.09	2	167.98	6.80
A0A024RAC8	Chromosome 1 open reading frame 201, isoform CRA_b	7.05	2	36.75	9.76
Q7Z6Z7	E3 ubiquitin-protein ligase HUWE1	6.99	2	373.96	5.10
Q59H97	Zinc finger protein ZNF-U69274 variant (Fragment)	6.97	2	79.37	8.87
Q9UPZ6	Thrombospondin type-1 domain-containing protein 7A	6.94	2	185.32	7.43
Q9P278	Folliculin-interacting protein 2	6.93	2	74.67	7.91
Q6LCG8	Catenin-4 (Fragment)	6.89	2	67.96	9.29
Q19VH1	Actin-binding LIM protein 2 splice variant 1	6.88	2	71.73	8.06
O75900	Matrix metalloproteinase-23	6.85	2	27.34	11.85
Q9NQS7	Inner centromere protein	6.84	2	105.36	9.44
B4DYH3	cDNA FLJ54441, highly similar to ankyrin repeat domain 36 (ANKRD36)	6.80	2	59.98	5.69
Q9UPN3	Microtubule-actin cross-linking factor 1, isoforms 1/2/3/5	6.80	2	856.35	5.39
B4DTD3	cDNA FLJ50209, highly similar to DNA-repair protein XRCC1	6.79	2	65.97	5.85
Q9NR09	Baculoviral IAP repeat-containing protein 6	6.74	2	529.92	6.05
Q9HCE3	Zinc finger protein 532	6.69	2	141.62	8.65
O43157	Plexin-B1	6.68	2	232.15	5.49
Q86TH5	ARFGEF2 protein (Fragment)	6.64	2	92.94	6.02
O15164	Transcription intermediary factor 1-alpha	6.62	2	107.64	7.17
F8VWH5	Amiloride-sensitive sodium channel subunit delta	6.60	2	35.05	11.18
O75376	Nuclear receptor corepressor 1	6.59	2	258.83	6.95
Q9H1Y3	Opsin-3	6.58	2	44.84	9.14
Q13011	Delta(3,5)-Delta(2,4)-dienoyl-CoA isomerase, mitochondrial	6.57	2	29.23	8.00
L8E8C0	Alternative protein MLH1	6.57	2	7.16	9.04
G3XAL8	HCG21296, isoform CRA_a	6.55	2	104.93	5.06
Q5T5Y3	Calmodulin-regulated spectrin-associated protein 1	6.55	2	163.16	6.95
Q12797	Aspartyl/asparaginyl beta-hydroxylase	6.54	2	11.78	6.79
Q8WX93	Palladin, cytoskeletal associated protein	6.53	2	121.97	6.92
Q9H400	Lck-interacting transmembrane adapter 1	6.52	2	31.27	9.58
Q5T376	FERM domain containing 4A, isoform CRA_c (Fragment)	6.51	2	60.16	8.82
Q9Y2F5	Little elongation complex subunit 1	6.49	2	247.74	5.48
Q8N122	Regulatory-associated protein of mTOR	6.49	2	148.94	6.89
Q712L1	AF-4 protein (Fragment)	6.49	2	45.82	8.35

O14594	Neurocan core protein	6.47	2	83.14	5.27
Q70CQ4	Ubiquitin carboxyl-terminal hydrolase 31	6.46	2	146.56	9.22
Q8IZC6	Collagen alpha-1(XXVII) chain	6.46	2	186.78	9.82
Q86UU1	Pleckstrin homology-like domain family B member 1	6.43	2	19.13	9.77
Q9NVP4	Double zinc ribbon and ankyrin repeat-containing protein 1	6.42	2	60.82	7.77
Q01484	Ankyrin-2	6.41	2	114.63	4.42
A0A0C4DG26	Carbohydrate-responsive element-binding protein	6.39	2	78.18	8.43
Q5VVU5	Transmembrane protein 39B (Fragment)	6.39	2	21.51	9.95
Q9Y653	Adhesion G-protein coupled receptor G1	6.37	2	57.44	8.48
Q96T21	Selenocysteine insertion sequence-binding protein 2	6.36	2	87.95	8.63
Q02505	Mucin-3A	6.34	2	265.71	5.49
Q5TCY1	Tau-tubulin kinase 1	6.33	2	142.65	5.60
Q5VTM2	Arf-GAP with GTPase, ANK repeat and PH domain-containing protein 9	6.33	2	77.92	7.90
Q9UHC1	DNA mismatch repair protein Mlh3	6.32	2	143.40	6.89
Q9BZI7	Regulator of nonsense transcripts 3B	6.29	2	25.22	8.57
Q96KW2	POM121-like protein 2	6.27	2	109.84	9.89
K9J9K9	GRM5 variant 9	6.22	2	125.23	7.85
A0A087WV64	Putative uncharacterized protein C3orf49	6.21	2	33.47	10.17
Q6ZUX3	TOG array regulator of axonemal microtubules protein 2	6.17	2	111.08	9.42
P25685	DnaJ homolog subfamily B member 1	6.16	2	38.02	8.63
O95684	FGFR1 oncogene partner	6.04	2	38.08	4.72
O43597	Protein sprouty homolog 2	6.02	2	34.67	8.35
Q14865	AT-rich interactive domain-containing protein 5B	6.02	2	132.29	8.72
O15075	Serine/threonine-protein kinase DCLK1	5.99	2	40.43	9.67
Q8N3C7	CAP-Gly domain-containing linker protein 4	5.95	2	61.45	9.36
Q15345	Leucine-rich repeat-containing protein 41	5.94	2	56.36	8.73
G9G6D7	KIAA0101 (Fragment)	5.94	2	4.41	11.85
Q86WI1	Fibrocystin-L	5.92	2	153.61	8.27
Q6P5Q4	Leiomodin-2	5.88	2	56.85	9.33
O94901	SUN domain-containing protein 1	5.83	2	90.06	7.05
Q96Q06	Perilipin-4	5.80	2	134.35	8.73
Q13516	Oligodendrocyte transcription factor 2	5.79	2	32.36	9.13
O75592	E3 ubiquitin-protein ligase MYCBP2	5.78	2	117.83	6.83
B4DN12	cDNA FLJ57750	5.69	2	21.33	8.65
O94915	Protein furry homolog-like	5.21	2	162.41	4.93

Supplementary Table A2.3 – Proteins that adsorbed onto titanium surfaces that have been also detected in plasma after matching to plasma protein database (PPD).

Proteins identified in Plasma (56 proteins)		
Accession Number	**PPD ID Number**	**Protein name**
Q13023	HPRD_05257	A kinase (PRKA) anchor protein 6
P60709	HPRD_00032	actin, beta
P02768	HPRD_00062	albumin
P25311	HPRD_01910	alpha-2-glycoprotein 1, zinc-binding
Q12955	HPRD_02715	ankyrin 3, node of Ranvier (ankyrin G)
P46013	HPRD_08902	antigen identified by monoclonal antibody Ki-67
P02647	HPRD_02517	apolipoprotein A-I
Q96DR5	HPRD_12781	BPI fold containing family A, member 2
Q8TDL5	HPRD_12740	BPI fold containing family B, member 1
Q8N4F0	HPRD_10690	BPI fold containing family B, member 2
Q9UDT6	HPRD_09140	CAP-GLY domain containing linker protein 2
Q8N3C7	HPRD_08634	CAP-GLY domain containing linker protein family, member 4
P23280	HPRD_00264	carbonic anhydrase VI
Q7Z589	HPRD_10544	chromosome 11 open reading frame 30
P23528	HPRD_03261	cofilin 1 (non-muscle)
P04080	HPRD_03091	cystatin B (stefin B)
P01034	HPRD_05056	cystatin C
P01036	HPRD_00462	cystatin S
P32926	HPRD_01355	desmoglein 3
O15075	HPRD_09202	doublecortin-like kinase 1
Q9C0G6	HPRD_19502	dynein, axonemal, heavy chain 6
P20930	HPRD_15920	filaggrin
Q8WXG9	HPRD_09111	G protein-coupled receptor 98
P04406	HPRD_00713	glyceraldehyde-3-phosphate dehydrogenase
Q9ULT8	HPRD_17098	HECT domain containing E3 ubiquitin protein ligase 1
Q7Z6Z7	HPRD_06608	HECT, UBA and WWE domain containing 1, E3 ubiquitin protein ligase
P68871	HPRD_00786	hemoglobin, beta
P22079	HPRD_11825	lactoperoxidase
P02788	HPRD_01028	lactotransferrin
P61626	HPRD_01085	lysozyme
Q6P0Q8	HPRD_11294	microtubule associated serine/threonine kinase 2

Q8WXI7	HPRD_07548	mucin 16, cell surface associated
Q8TAX7	HPRD_11759	mucin 7, secreted
P05164	HPRD_06102	myeloperoxidase
P80303	HPRD_09726	nucleobindin 2
O15018	HPRD_10142	PDZ domain containing 2
P23284	HPRD_00458	peptidylprolyl isomerase B (cyclophilin B)
Q9Y6V0	HPRD_16078	piccolo presynaptic cytomatrix protein
P01833	HPRD_01436	polymeric immunoglobulin receptor
P07737	HPRD_01452	profilin 1
P12273	HPRD_07179	prolactin-induced protein
Q92824	HPRD_08985	proprotein convertase subtilisin/kexin type 5
Q92954	HPRD_05047	proteoglycan 4
P14618	HPRD_01529	pyruvate kinase, muscle
P05109	HPRD_00471	S100 calcium binding protein A8
P06702	HPRD_00472	S100 calcium binding protein A9
P01009	HPRD_02463	serpin peptidase inhibitor, clade A (alpha-1 antiproteinase, antitrypsin), member 1
P30740	HPRD_00555	serpin peptidase inhibitor, clade B (ovalbumin), member 1
O43166	HPRD_11559	signal-induced proliferation-associated 1 like 1
Q9UBC9	HPRD_01652	small proline-rich protein 3
Q15772	HPRD_10653	SPEG complex locus
P02808	HPRD_01696	statherin
P02814	HPRD_18078	submaxillary gland androgen regulated protein 3B
P29401	HPRD_06001	transketolase
Q5TAX3	HPRD_15700	zinc finger, CCHC domain containing 11
Q96DA0	HPRD_14024	zymogen granule protein 16B

Appendix II

Supplementary material for New insights on the proteome of enamel matrix derivative (EMD)

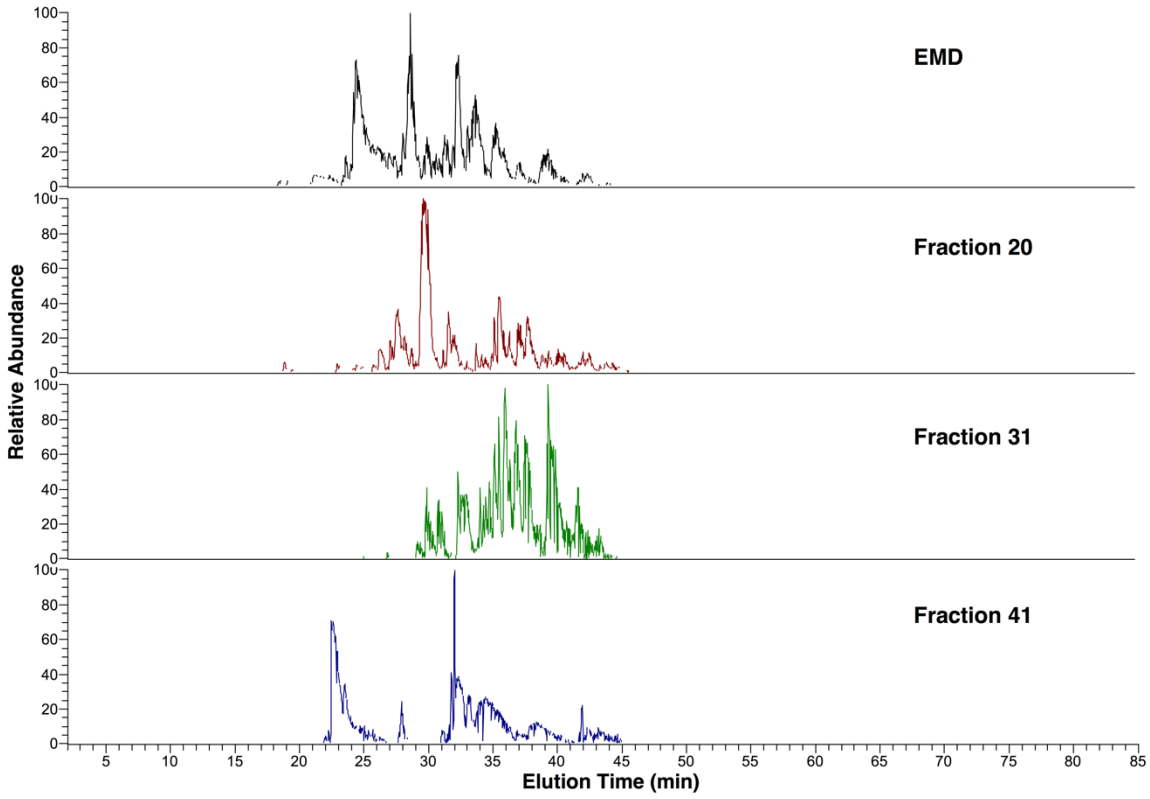

Supplementary Figure A3.1- Example of base-peak chromatograms of whole EMD, EMD fractions F20, F31, and F41. Peptide separation was achieved using a nano-flow reverse-phase HPLC column, with gradient elution ranging from 5 to 55% solvent B in 85 min.

A

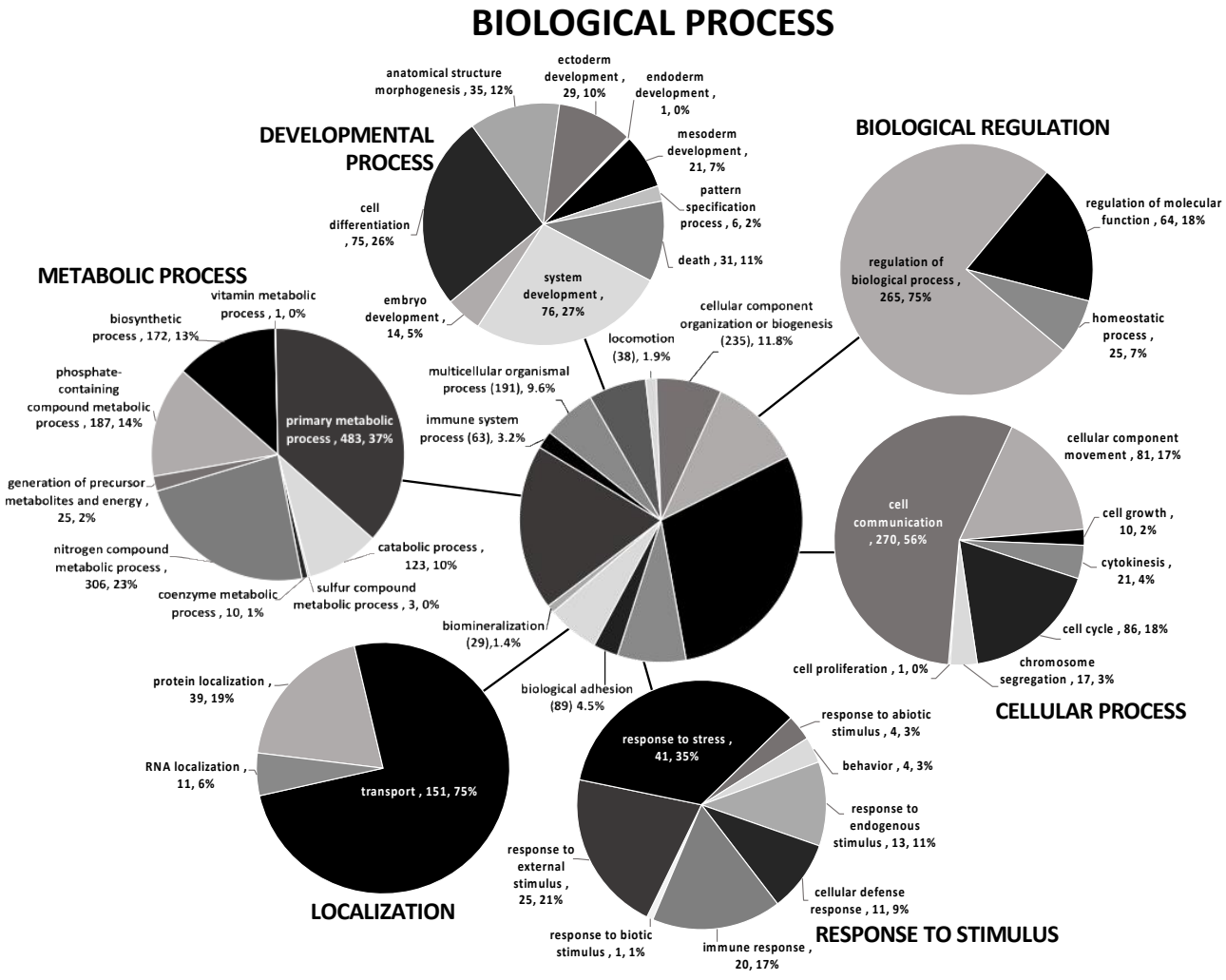
BIOLOGICAL PROCESS
DEVELOPMENTAL PROCESS
anatomical structure morphogenesis , 35, 12%
ectoderm development , 29, 10%
endoderm development , 1, 0%
mesoderm development , 21, 7%
pattern specification process , 6, 2%
death , 31, 11%
system development , 76, 27%
embryo development , 14, 5%
cell differentiation , 75, 26%
BIOLOGICAL REGULATION
regulation of molecular function , 64, 18%
homeostatic process , 25, 7%
regulation of biological process , 265, 75%
METABOLIC PROCESS
vitamin metabolic process , 1, 0%
biosynthetic process , 172, 13%
phosphate-containing compound metabolic process , 187, 14%
primary metabolic process , 483, 37%
generation of precursor metabolites and energy , 25, 2%
nitrogen compound metabolic process , 306, 23%
coenzyme metabolic process , 10, 1%
sulfur compound metabolic process , 3, 0%
catabolic process , 123, 10%
cellular component organization or biogenesis (235), 11.8%
locomotion (38), 1.9%
multicellular organismal process (191), 9.6%
immune system process (63), 3.2%
biomineralization (29),1.4%
biological adhesion (89) 4.5%
CELLULAR PROCESS
cellular component movement , 81, 17%
cell growth , 10, 2%
cytokinesis , 21, 4%
cell cycle , 86, 18%
chromosome segregation , 17, 3%
cell proliferation , 1, 0%
cell communication , 270, 56%
LOCALIZATION
protein localization , 39, 19%
RNA localization , 11, 6%
transport , 151, 75%
RESPONSE TO STIMULUS
response to stress , 41, 35%
response to abiotic stimulus , 4, 3%
behavior , 4, 3%
response to endogenous stimulus , 13, 11%
cellular defense response , 11, 9%
immune response , 20, 17%
response to biotic stimulus , 1, 1%
response to external stimulus , 25, 21%

B

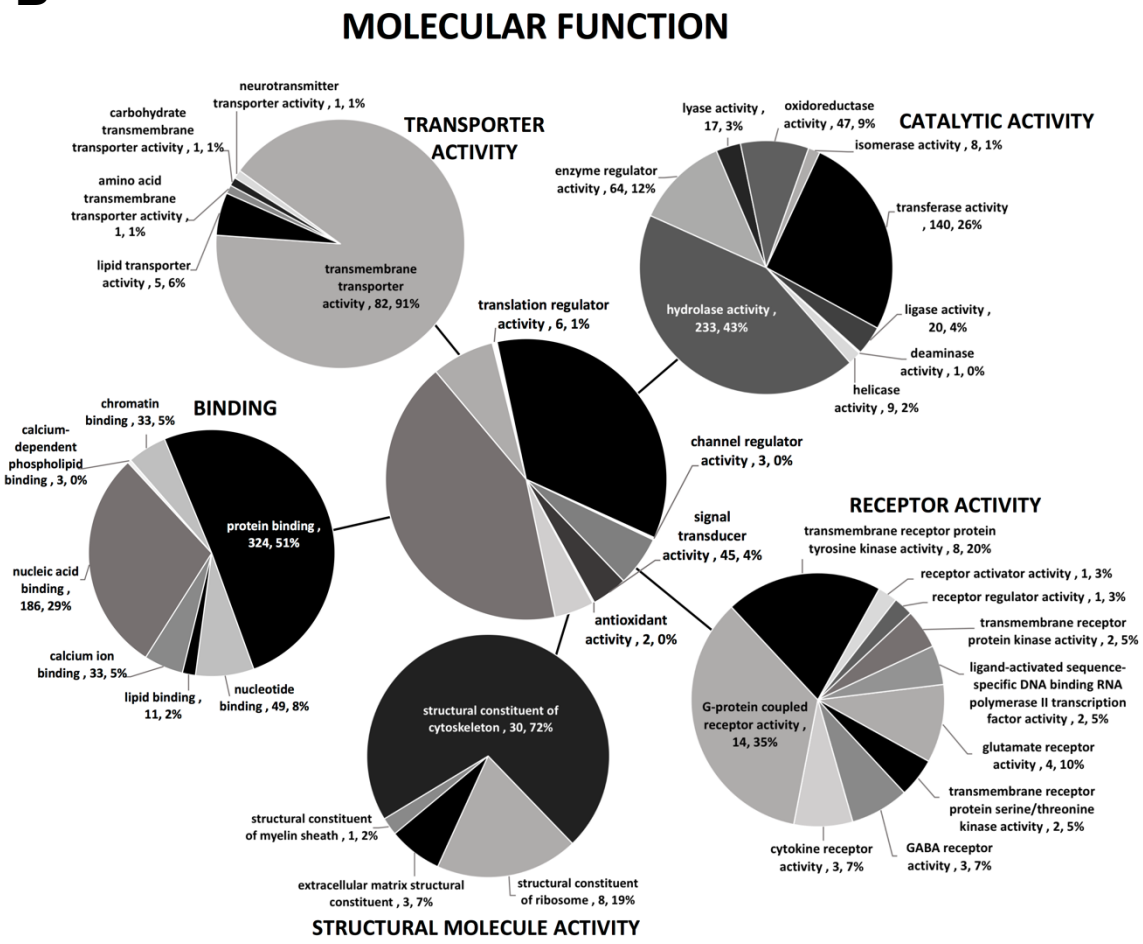
MOLECULAR FUNCTION
TRANSPORTER ACTIVITY
neurotransmitter transporter activity , 1, 1%
carbohydrate transmembrane transporter activity , 1, 1%
amino acid transmembrane transporter activity , 1, 1%
lipid transporter activity , 5, 6%
transmembrane transporter activity , 82, 91%
CATALYTIC ACTIVITY
lyase activity , 17, 3%
oxidoreductase activity , 47, 9%
isomerase activity , 8, 1%
enzyme regulator activity , 64, 12%
transferase activity , 140, 26%
hydrolase activity , 233, 43%
ligase activity , 20, 4%
deaminase activity , 1, 0%
helicase activity , 9, 2%
translation regulator activity , 6, 1%
channel regulator activity , 3, 0%
signal transducer activity , 45, 4%
antioxidant activity , 2, 0%
BINDING
chromatin binding , 33, 5%
calcium-dependent phospholipid binding , 3, 0%
protein binding , 324, 51%
nucleic acid binding , 186, 29%
calcium ion binding , 33, 5%
lipid binding , 11, 2%
nucleotide binding , 49, 8%
RECEPTOR ACTIVITY
transmembrane receptor protein tyrosine kinase activity , 8, 20%
receptor activator activity , 1, 3%
receptor regulator activity , 1, 3%
transmembrane receptor protein kinase activity , 2, 5%
ligand-activated sequence-specific DNA binding RNA polymerase II transcription factor activity , 2, 5%
glutamate receptor activity , 4, 10%
transmembrane receptor protein serine/threonine kinase activity , 2, 5%
GABA receptor activity , 3, 7%
cytokine receptor activity , 3, 7%
G-protein coupled receptor activity , 14, 35%
STRUCTURAL MOLECULE ACTIVITY
structural constituent of cytoskeleton , 30, 72%
structural constituent of myelin sheath , 1, 2%
extracellular matrix structural constituent , 3, 7%
structural constituent of ribosome , 8, 19%

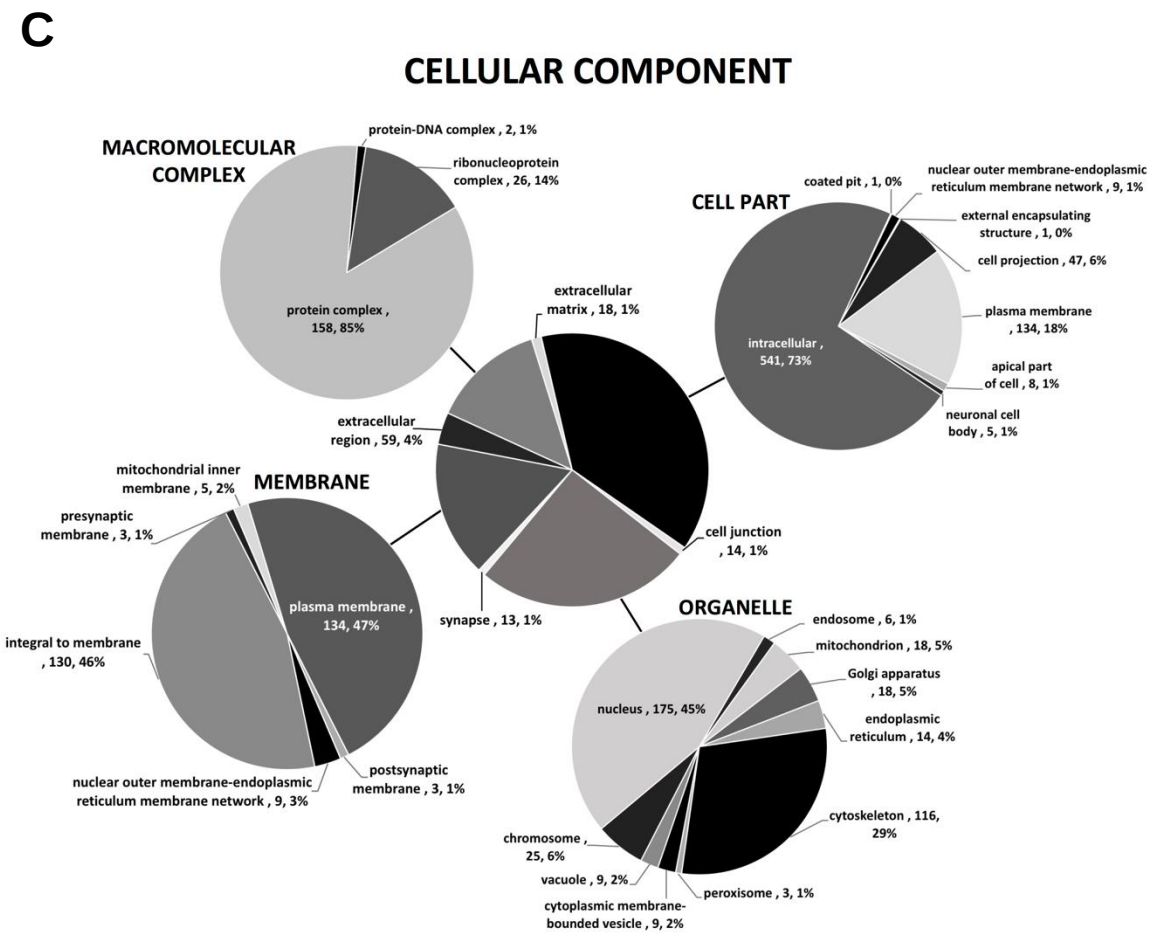

Supplementary Figure A3.2 – Proteomic analysis of identified proteins from fractionated EMD regarding biological processes (A) molecular functions (B) and cellular components (C). Information on biological functions was obtained from PANTHER classification system and GO annotation terms (GO). Proteins involved in more than one category were counted multiple times.

Supplementary Table A3.1- List of all 2000 proteins identified in EMD fractions, gene associated, molecular weight (MW), isoelectric point at physiological pH (pI), and number of fractions detected.

Accession	Protein Name	Gene	MW (kDa)	calc. pI	No. of Fractions
Q9TQY2	23 kDa amelogenin		18.32	7.24	32
F1RUQ1	Enamelin	ENAM	128.28	6.18	31
Q28989	Ameloblastin	AMBN	44.90	5.69	27
F1RII7	Hemoglobin subunit beta	HBB	16.16	7.25	27
P01965	Hemoglobin subunit alpha	HBA	15.03	8.70	25
P79287	Matrix metalloproteinase-20	MMP20	54.05	8.87	24
C9W8E7	Dentin sialophosphoprotein (Fragment)	DSPP	57.37	3.71	21
A0A287BHY5	Keratin, type II cytoskeletal 2 epidermal	KRT2	65.62	7.52	18
P00761	Trypsin		24.39	7.18	16
F1RT10	CDKN2A interacting protein	CDKN2AIP	61.47	8.97	15
F1SGG3	Keratin 1	KRT1	64.83	8.15	14
D4PEB7	Adenomatous polyposis coli (Fragment)	APC	258.94	8.34	13
L8B0V6	IgG heavy chain	IGHG	52.26	6.79	13
F1RP76	Sciellin	SCEL	67.02	9.39	13
P09571	Serotransferrin	TF	76.92	7.14	13
A0A287B7U5	CAP-Gly domain containing linker protein 1	CLIP1	130.43	5.44	12
K7GMX1	Neuron navigator 1	NAV1	199.79	8.28	12
P29700	Alpha-2-HS-glycoprotein (Fragment)	AHSG	38.40	5.85	11
P00346	Malate dehydrogenase, mitochondrial	MDH2	35.57	8.68	11
F1SLI3	Microtubule-associated protein	MAP4	116.91	5.11	11
A0A287AH52	Mucin 5B, oligomeric mucus/gel-forming	MUC5B	473.47	5.94	11
K7GLD0	Uncharacterized protein		21.41	9.06	11
F1RFJ6	ADP-ribosylation factor-like protein 6-interacting protein 4 isoform a	ARL6IP4	26.48	11.03	10
I3LVK9	ALMS1, centrosome and basal body associated protein	ALMS1	381.93	6.60	10
A0A287B3M7	Histone-lysine N-methyltransferase	KMT2A	402.25	8.84	10
I3LCF3	Papilin, proteoglycan like sulfated glycoprotein	PAPLN	95.01	7.99	10
A0A287AE24	Uncharacterized protein		23.50	8.31	10
A0A286ZVI2	Thyroid hormone receptor interactor 12	TRIP12	222.02	8.43	10
A0A286ZRV2	Triosephosphate isomerase	TPI1	34.33	6.99	10
A0A287AAR4	Actin, cytoplasmic 1	ACTB	39.99	5.48	9
I3L5I7	ASH1 like histone lysine methyltransferase	ASH1L	324.76	9.38	9
F1RZU8	Dystonin	DST	853.89	5.27	9
A0A286ZIC1	Gelsolin	GSN	80.73	5.85	9
A0A287BBI5	Glyceraldehyde-3-phosphate dehydrogenase	GAPDH	35.03	8.13	9

F1RMN7	Hemopexin	HPX	51.19	6.96	9
P01846	Ig lambda chain C region		11.00	7.08	9
A0A286ZYH7	Mediator of RNA polymerase II transcription subunit 1	MED1	148.94	8.84	9
I3LGB9	Neuron navigator 2	NAV2	221.66	8.78	9
I3LRV9	Neuron navigator 3	NAV3	226.02	8.79	9
A0A287AV63	Perilipin 4	PLIN4	149.25	9.20	9
Q0PM28	Pigment epithelium-derived factor	SERPINF1	45.60	6.81	9
I3L7Z6	Protein S100	S100A6	10.08	5.17	9
F1RFA3	RNA binding protein with serine rich domain 1	RNPS1	34.20	11.84	9
P50390	Transthyretin	TTR	16.07	6.77	9
I3LHG4	Ubiquitin specific peptidase 31	USP31	141.23	9.29	9
F1SCD0	Uncharacterized protein	LOC396685	46.61	6.21	9
A0A287BKM2	Xin actin binding repeat containing 2	XIRP2	370.79	6.19	9
K7GKJ8	Phosphoglycerate kinase	PGK1	42.53	7.65	9
Q9TQY1	18 kDa amelogenin	AMELX AMELY	15.02	8.70	8
F1S518	Additional sex combs like 1, transcriptional regulator	ASXL1	164.00	6.55	8
A0A287AAD5	Alpha-1B-glycoprotein	A1BG	53.23	6.42	8
P19619	Annexin A1	ANXA1	38.73	6.89	8
A0A287BI04	Annexin A2	ANXA2	38.55	7.31	8
F1SB35	Ataxin 7 like 1	ATXN7L1	79.78	10.04	8
A0A2C9F3A3	ATP synthase subunit O, mitochondrial	ATP5O	23.37	9.96	8
F1SPS8	Bassoon presynaptic cytomatrix protein	BSN	388.90	7.02	8
Q07717	Beta-2-microglobulin	B2M	13.35	7.50	8
A0A287B8P2	Bromodomain PHD finger transcription factor	BPTF	268.79	7.85	8
A0A287BS87	Carbonic anhydrase 1	CA1	26.68	6.71	8
A0A287B6M0	Carbonic anhydrase 2	CA2	24.60	6.52	8
F1S5P1	Collagen type XVII alpha 1 chain	COL17A1	144.72	8.70	8
I3L7I3	Filaggrin family member 2	FLG2	270.67	8.27	8
A0A286ZYX8	Fructose-bisphosphate aldolase	ALDOA	39.40	8.25	8
I3L770	HECT, UBA and WWE domain containing 1, E3 ubiquitin protein ligase	HUWE1	482.29	5.25	8
I3LDS3	Keratin 10	KRT10	58.94	4.96	8
F1SBB3	Laminin subunit alpha 3	LAMA3	367.76	6.96	8
I3LDI0	Muscular LMNA interacting protein	MLIP	76.89	9.45	8
A0A287APK8	Nipped-B protein	NIPBL	257.21	8.28	8
A0A286ZU95	NOP2 nucleolar protein	NOP2	75.44	8.70	8
F1SHL9	Pyruvate kinase	PKM	57.84	7.85	8

A0A287ACR9	Uncharacterized protein		13.29	7.83	8
A0A287BBS4	ATP synthase subunit alpha	ATP5A1	59.32	9.36	7
A0A286ZYL7	ATP synthase subunit delta, mitochondrial	ATP5D	17.46	5.25	7
A0A287BD83	ATP synthase, H+ transporting, mitochondrial F1 complex, gamma polypeptide 1	ATP5C1	30.54	9.29	7
F1RMZ8	ATPase H+ transporting V1 subunit B2	ATP6V1B2	56.58	5.81	7
F1RKN9	Centrosomal protein 120	CEP120	112.88	6.51	7
A0A287BLD2	Collagen type I alpha 1 chain	COL1A1	137.97	5.78	7
F1SI77	Creatine kinase U-type, mitochondrial	CKMT1A	46.91	8.34	7
I3LK59	Enolase 1	ENO1	47.26	6.87	7
F1RYK8	Fibrous sheath interacting protein 2	FSIP2	760.61	6.71	7
P08059	Glucose-6-phosphate isomerase	GPI	63.09	7.99	7
I3LRA3	HECT and RLD domain containing E3 ubiquitin protein ligase family member 1	HERC1	523.33	6.10	7
A0A287AS35	Immunoglobulin superfamily member 10	IGSF10	283.31	9.31	7
A0A287AD16	L-lactate dehydrogenase	LDHA	30.92	8.76	7
A0A075B7I5	Uncharacterized protein		11.86	8.51	7
Q0Z8U2	40S ribosomal protein S3	RPS3	26.67	9.66	6
Q29014	Alpha-1 acid glycoprotein (Fragment)		20.89	6.21	6
F1S146	Ankyrin 2	ANK2	421.87	5.02	6
A0A287AI01	Aspartate beta-hydroxylase	ASPH	85.07	5.07	6
Q0QEM6	ATP synthase subunit beta (Fragment)	ATP5B	47.06	5.11	6
F1S5F9	Biorientation of chromosomes in cell division 1 like 1	BOD1L1	315.24	5.06	6
I3LMI5	Bromodomain and PHD finger containing 1	BRPF1	127.83	7.09	6
B3F0B7	Cellular retinoic acid-binding protein 1	CRABP1	15.56	5.38	6
A0A287BDE0	Centrosomal protein 295	CEP295	237.99	6.14	6
F1S697	Centrosomal protein 350	CEP350	350.46	6.57	6
Q9GLP1	Coagulation factor V	F5	255.92	6.38	6
A0A287A9C3	Coilin	COIL	45.28	9.57	6
I3LUY9	Crystallin beta-gamma domain containing 3	CRYBG3	328.20	5.11	6
A0A286ZP90	Cytoplasmic linker associated protein 1	CLASP1	160.08	8.60	6
Q9TT01	Doublesex- and mab-3-related transcription factor 1	DMRT1	39.32	8.09	6
F1SGT7	DS cell adhesion molecule	DSCAM	208.94	8.07	6
A0A287AG62	EMSY, BRCA2 interacting transcriptional repressor	EMSY	139.76	9.42	6
F1SFI6	Fetuin B	FETUB	41.20	7.52	6
A0A287BAX3	FRY like transcription coactivator	FRYL	292.32	6.21	6
P80031	Glutathione S-transferase P	GSTP1	23.48	7.80	6
F1S700	Human immunodeficiency virus type I	HIVEP2	267.38	7.08	6

	enhancer binding protein 2				
A0A287BQK2	Inter-alpha-trypsin inhibitor heavy chain 3	ITIH3	96.90	6.21	6
A5A759	Keratin 2A	KRT2A	65.83	7.52	6
F1S8K8	KIAA0232	KIAA0232	150.73	4.75	6
A0A286ZPV5	KIAA1109	KIAA1109	471.01	6.51	6
I3LF70	Marker of proliferation Ki-67	MKI67	345.16	9.95	6
A0A287BQL9	Microtubule associated serine/threonine kinase 3	MAST3	137.30	7.44	6
F1SKS0	Microtubule associated serine/threonine kinase family member 4	MAST4	260.01	8.65	6
A0A287BKZ5	PNN interacting serine and arginine rich protein	PNISR	79.81	10.15	6
A0A287ALC2	RAN binding protein 2	RANBP2	348.03	6.34	6
A0A287BG41	Serine/arginine repetitive matrix 2	SRRM2	269.07	12.07	6
F1RKH3	Serine/arginine repetitive matrix 4	SRRM4	68.50	11.81	6
A0A287ADP6	StAR related lipid transfer domain containing 9	STARD9	277.05	6.25	6
F1RG65	Tetratricopeptide repeat domain 28	TTC28	230.24	7.02	6
A8U4R4	Transketolase	TKT	67.79	7.49	6
F1SKM0	Ubiquinol-cytochrome c reductase core protein I	UQCRC1	50.58	6.29	6
A0A287BLW8	Uncharacterized protein		54.78	8.41	6
F1SIL5	Uncharacterized protein		291.70	6.44	6
I3L936	Uncharacterized protein	CIR1	50.52	9.92	6
F1RMW4	X-ray repair cross complementing 1	XRCC1	59.23	8.65	6
F1RWK5	Zinc finger homeobox 4	ZFHX4	397.05	6.27	6
A0A286ZY93	Zinc finger protein 106	ZNF106	174.26	6.74	6
F1RRM3	Zinc finger protein 318	ZNF318	250.65	7.40	6
A0A287BER6	Zinc finger protein 827	ZNF827	87.07	7.87	6
F1SC67	Phosphoinositide phospholipase C	PLCE1	256.38	6.34	5
F2X0U7	Adenomatous polyposis coli 2	APC2	240.72	8.69	5
A0A286ZR09	Anillin actin binding protein	ANLN	114.86	6.90	5
A0A287BC65	Ankyrin repeat domain 12	ANKRD12	224.71	7.12	5
P12021	Apomucin (Fragment)		109.55	5.30	5
A0A287B053	BCL6 corepressor like 1	BCORL1	165.16	8.43	5
I3LFN0	BRCA2, DNA repair associated	BRCA2	360.51	6.51	5
A0A287B091	Capping actin protein, gelsolin like	CAPG	33.69	5.85	5
F1S2Y5	Centromere protein F	CENPF	348.59	5.08	5
A0A286ZRH1	Chromosome 6 open reading frame 132	C6orf132	137.03	9.73	5
Q29549	Clusterin	CLU	51.74	5.88	5
I3LPB5	Creatine kinase B-type	CKB	42.66	5.78	5

F1RWC3	Cubilin	CUBN	397.11	5.54	5
A0A286ZIT1	Cyclin B3	CCNB3	128.24	8.81	5
Q9XSN6	Enamel matrix serine proteinase 1	KLK4	27.22	5.00	5
I3LBX4	Family with sequence similarity 160 member A1	FAM160A1	112.51	4.81	5
F1SHF6	HECT domain E3 ubiquitin protein ligase 1	HECTD1	235.99	5.48	5
P00348	Hydroxyacyl-coenzyme A dehydrogenase, mitochondrial	HADH	34.14	9.00	5
A0A287AJG8	Jumonji domain containing 1C	JMJD1C	283.35	8.10	5
A0A287BP20	Kinesin family member 26A	KIF26A	191.50	8.95	5
P11708	Malate dehydrogenase, cytoplasmic	MDH1	36.43	6.58	5
Q767L8	Mediator of DNA damage checkpoint protein 1	MDC1	217.78	5.48	5
P02189	Myoglobin	MB	17.07	7.31	5
A0A287AW64	Natural killer cell triggering receptor	NKTR	137.76	10.15	5
I3LP18	Nuclear receptor interacting protein 1	NRIP1	126.40	8.15	5
I3LKK9	Olfactory receptor		34.58	8.53	5
A0A287BCP3	Plexin A2	PLXNA2	209.26	7.11	5
F1RFY1	Profilin	PFN1	15.03	8.28	5
A0A287AZ18	Rho GTPase activating protein 21	ARHGAP21	115.40	7.59	5
A0A286ZT13	Serum albumin	ALB	68.13	6.38	5
A0A287BKZ7	Sp4 transcription factor	SP4	57.53	4.44	5
I3LM69	Spindle and centriole associated protein 1	SPICE1	96.05	6.86	5
F1S1U4	Tousled like kinase 1	TLK1	85.77	8.66	5
F1RPD2	Ubiquinol-cytochrome c reductase core protein II	UQCRC2	48.18	8.88	5
A0A286ZK47	Uncharacterized protein	LOC100626097	763.61	6.61	5
A0A286ZRU9	Uncharacterized protein	SERPINH1	46.50	8.97	5
A0A286ZX08	Uncharacterized protein	CLIP2	111.77	7.11	5
F1SCC9	Uncharacterized protein	LOC106504545	46.36	6.55	5
F1SP92	Upstream transcription factor family member 3	USF3	241.45	7.50	5
F1SP93	V-type proton ATPase catalytic subunit A	ATP6V1A	68.40	5.52	5
A0A287A1B9	Zinc finger MYM-type containing 1	ZMYM1	122.11	7.87	5
A0A287AJP3	Zinc finger protein 292	ZNF292	275.35	7.99	5
A0A287AVJ8	Trinucleotide repeat containing 6A	TNRC6A	171.08	6.90	5
B5KJG2	Phosphoglycerate mutase	PGAM2	28.66	8.72	4
F1RTR5	Ubiquitinyl hydrolase 1	USP51	80.18	8.22	4
F1RGG1	40S ribosomal protein S19	RPS19	16.05	10.32	4
A0A286ZQT4	ADAMTS like 1	ADAMTSL1	192.17	7.83	4

D0G0C3	Adenosylhomocysteinase	AHCY	47.69	6.29	4
I3L7N2	AF4/FMR2 family member 4	AFF4	124.06	9.33	4
Q8HYZ6	Alkaline phosphatase (Fragment)	ALPL	18.67	9.26	4
A0A287AKS4	Alpha kinase 3	ALPK3	130.50	8.50	4
F1SKF2	ArfGAP with GTPase domain, ankyrin repeat and PH domain 2	AGAP2	87.95	9.28	4
A0A287BJ46	ATP binding cassette subfamily A member 13	ABCA13	505.86	6.96	4
A5A788	ATPase, Cu(2+)-transporting, alpha polypeptide (Fragment)	ATP7A	140.52	6.51	4
A0A287B2Z9	CDC42 binding protein kinase alpha	CDC42BPA	190.22	6.42	4
F1SFM2	Cell adhesion molecule L1 like	CHL1	130.72	5.94	4
F1RJU0	Cell division cycle associated 2	CDCA2	108.71	8.65	4
K9J4Q9	Centrosome-associated protein 350	CEP350	351.00	6.51	4
I3VKE6	Ceruloplasmin	CP	125.47	6.07	4
F1RZQ5	Cilia and flagella associated protein 97	CFAP97	56.57	7.83	4
A0A287BCU6	Coiled-coil domain containing 88A	CCDC88A	201.71	6.21	4
K7GPT4	Cullin 4B	CUL4B	98.77	7.50	4
A0A286ZPL6	D-2-hydroxyglutarate dehydrogenase	D2HGDH	50.41	6.98	4
A0A287A2N5	Dedicator of cytokinesis 1	DOCK1	214.75	7.64	4
I3LFL8	Dedicator of cytokinesis 4	DOCK4	220.45	7.59	4
A0A286ZXW8	DNA polymerase theta	POLQ	266.23	7.17	4
F1SHF0	Family with sequence similarity 117 member B	FAM117B	62.17	9.77	4
F1RXK4	FERM and PDZ domain containing 3	FRMPD3	178.11	8.47	4
F1RS31	FRAS1 related extracellular matrix protein 2	FREM2	351.11	5.10	4
F1SRH1	Growth arrest specific 2 like 3	GAS2L3	60.65	9.88	4
F1SPG1	H1 histone family member X	H1FX	22.51	10.71	4
A0A287B726	Insulin receptor substrate 2	IRS2	129.61	8.73	4
F1SH92	Inter-alpha-trypsin inhibitor heavy chain H4	ITIH4	100.30	6.71	4
A0A287APM4	Keratin 75	KRT75	57.39	8.25	4
A0A287BDG5	Kinesin family member 20B	KIF20B	203.01	5.41	4
A0A286ZP53	Kinesin family member 26B	KIF26B	191.45	8.65	4
A0A287BAD8	LIM domain 7	LMO7	147.45	6.60	4
F1SQ09	Lumican precursor	LUM	38.75	6.24	4
F1SSW5	MGA, MAX dimerization protein	MGA	283.45	7.84	4
F1SV22	Microtubule-actin crosslinking factor 1	MACF1	499.11	5.21	4
A0A287A6Y7	Microtubule-associated protein	MAP2	182.94	4.89	4
I3LQZ3	Mucin 6, oligomeric mucus/gel-forming	MUC6	200.09	6.34	4
F1RP77	MYC binding protein 2, E3 ubiquitin protein ligase	MYCBP2	504.03	6.80	4

A0A287BEF6	Neurofascin	NFASC	140.22	6.95	4
F1S8T1	Nucleolar and coiled-body phosphoprotein 1	NOLC1	73.99	9.47	4
F1RVB3	Odontogenic ameloblast-associated protein	ODAM	30.58	5.10	4
A0A287A5X4	PKHD1, fibrocystin/polyductin	PKHD1	433.76	6.57	4
I3LQP2	Pleckstrin homology like domain family B member 2	PHLDB2	139.97	8.00	4
F1SG35	Protein O-fucosyltransferase 2	POFUT2	39.83	6.64	4
A0A287ATW2	Protein phosphatase 1 regulatory subunit 12A	PPP1R12A	80.83	5.49	4
A0A287B2L1	PTPRF interacting protein alpha 1	PPFIA1	132.45	6.19	4
F1RTX9	Rap guanine nucleotide exchange factor 2	RAPGEF2	173.30	6.49	4
A0A287B013	Ras-related protein Rab-1B	RAB1B	20.53	5.43	4
F1S0P1	Regulator of G protein signaling 22	RGS22	146.08	8.19	4
F1SHX3	Replication timing regulatory factor 1	RIF1	271.55	5.34	4
A0A286ZLC4	Serine/arginine repetitive matrix 3	SRRM3	64.86	11.66	4
A0A287AR67	Sorcin	SRI	20.33	5.34	4
F1RLT5	Synaptotagmin 17	SYT17	51.17	7.77	4
I3LDQ1	Talin 2	TLN2	267.28	5.60	4
A0A287B4C3	Tetratricopeptide repeat, ankyrin repeat and coiled-coil containing 1	TANC1	197.44	8.25	4
F1RFK3	Transformation/transcription domain associated protein	TRRAP	399.74	8.25	4
K7GT58	Transforming acidic coiled-coil-containing protein 2	TACC2	108.97	5.08	4
F1RJ93	Transgelin	TAGLN2	22.36	8.25	4
F1SUQ5	Ubiquitin protein ligase E3 component n-recognin 4	UBR4	572.42	6.05	4
K7GNT3	Ubiquitin protein ligase E3 component n-recognin 5	UBR5	279.45	5.87	4
I3LDL4	Unc-80 homolog, NALCN channel complex subunit	UNC80	368.20	7.06	4
A0A287AE45	Uncharacterized protein	AHNAK2	382.07	5.26	4
A0A287AM15	Uncharacterized protein	SYTL2	203.00	6.28	4
F1RXQ4	Uncharacterized protein	BCOR	191.98	6.30	4
F1SCD1	Uncharacterized protein	SERPINA3-2	46.79	6.09	4
F1SRM6	Uncharacterized protein		96.97	10.45	4
A0A287BFT9	Vacuolar protein sorting 13 homolog D	VPS13D	472.58	6.43	4
I3LEU1	Zinc finger protein 280D	ZNF280D	107.67	7.50	4
A0A287A7V0	Zinc finger protein 469	ZNF469	395.44	8.51	4
F1SM53	Zinc finger protein 532	ZNF532	136.85	8.68	4
A0A286ZKD0	Zinc finger SWIM-type containing 8	ZSWIM8	180.96	7.05	4
A0A287AWR3	Phosphodiesterase	PDE3A	91.37	5.49	3

A0A287AJQ2	Phosphoglycerate mutase	PGAM1	28.79	7.18	3
I3LDB1	Poly [ADP-ribose] polymerase	PARP4	204.38	7.02	3
F1SB86	Tyrosine-protein phosphatase	PTPN12	81.75	6.54	3
I3LNV8	Phosphatase and actin regulator	PHACTR2	70.55	8.24	3
F1SFS3	ADAM metallopeptidase with thrombospondin type 1 motif 9	ADAMTS9	204.47	7.56	3
F1SAK2	Additional sex combs like 3, transcriptional regulator	ASXL3	240.15	6.04	3
F1RK47	Adenylate cyclase 9	ADCY9	130.64	6.87	3
K7GSM4	ADP ribosylation factor guanine nucleotide exchange factor 1	ARFGEF1	186.52	5.52	3
K7GQ48	Alpha-2-macroglobulin	A2M	163.89	6.11	3
I3LVP6	Ankyrin repeat and LEM domain containing 2	ANKLE2	105.96	6.87	3
A0A287AJ68	Ankyrin repeat and sterile alpha motif domain containing 1A	ANKS1A	122.85	6.49	3
A0A286ZRF8	Ankyrin repeat domain 11	ANKRD11	284.43	7.01	3
F1SMK1	AT-hook transcription factor	AKNA	153.63	6.18	3
A0A287BPR5	Ataxin 7	ATXN7	78.80	10.13	3
F1SC09	ATP binding cassette subfamily B member 5	ABCB5	138.47	7.53	3
F1SLA0	ATP synthase subunit beta	ATP5B	48.63	5.14	3
I3LME9	ATRX, chromatin remodeler	ATRX	274.50	6.64	3
A0A287APN3	B double prime 1, subunit of RNA polymerase III transcription initiation factor IIIB	BDP1	232.87	5.06	3
A0A287B926	Bromodomain and WD repeat domain containing 1	BRWD1	246.24	8.50	3
A0A287A7A8	Bromodomain containing 1	BRD1	114.61	8.97	3
A0A287BCB4	Calcineurin binding protein 1	CABIN1	214.01	5.92	3
F1S018	Calmodulin regulated spectrin associated protein 1	CAMSAP1	172.40	6.98	3
A0A287B6U2	Centrosomal protein 290	CEP290	262.12	6.04	3
F1S8J5	Chromodomain-helicase-DNA-binding protein 8	CHD8	290.57	6.47	3
A0A287AGB2	Coiled-coil domain containing 88C	CCDC88C	55.29	9.04	3
F1RQI0	Collagen type XII alpha 1 chain	COL12A1	332.58	5.49	3
F1RHF2	COMM domain-containing protein 6	TBC1D4	113.76	6.95	3
A0A287AA72	Dedicator of cytokinesis 6	DOCK6	229.18	6.77	3
A0A286ZZP0	Dedicator of cytokinesis 7	DOCK7	221.92	7.59	3
F1RRB8	Deleted in lung and esophageal cancer 1	DLEC1	192.10	6.48	3
D0G6S3	Dihydrolipoamide dehydrogenase (Fragment)	DLD	33.24	8.95	3
A0A287AQ05	Dmx like 2	DMXL2	328.14	6.23	3
A0A287AF97	Dynein axonemal heavy chain 10	DNAH10	521.50	5.72	3
A0A287AHU7	E1A binding protein p400	EP400	351.52	9.50	3

A0A287BJG5	Elongation factor 1-alpha	EEF1A1	46.56	8.16	3
Q4QZ00	Elongation factor 1-alpha 1 (Fragment)	EF1A1	33.57	6.80	3
P37176	Endoglin	ENG	70.24	5.85	3
I3LNF1	Family with sequence similarity 208 member B	FAM208B	244.48	6.43	3
F1ST70	FERM and PDZ domain containing 1	FRMPD1	171.47	5.22	3
F1SN67	Fibrillin-1	FBN1	312.21	4.93	3
F1S6B5	Fibromodulin	FMOD	43.17	6.14	3
F1RSU5	Fms related tyrosine kinase 1	FLT1	149.70	8.73	3
A0A287A0I4	Folliculin interacting protein 2	FNIP2	101.47	6.30	3
F1RJ25	Fructose-bisphosphate aldolase	ALDOC	39.35	6.65	3
I3LCR7	Glutamate metabotropic receptor 5	GRM5	128.57	7.59	3
F1SQ16	Golgin B1	GOLGB1	375.44	5.03	3
F1S9P9	GRAM domain containing 1B	GRAMD1B	87.69	5.99	3
A0A287APE3	Gse1 coiled-coil protein	GSE1	127.13	7.47	3
A0A287B8Q2	Guanylate cyclase		104.99	6.86	3
A0A287BQW3	H1 histone family member 0	H1F0	20.88	10.90	3
A0A287AQV2	Helicase with zinc finger	HELZ	169.54	7.42	3
F1SM16	Holliday junction recognition protein	HJURP	79.62	9.45	3
I3LN45	Homeodomain interacting protein kinase 2	HIPK2	130.03	8.43	3
F1RV84	Human immunodeficiency virus type I enhancer binding protein 1	HIVEP1	286.95	8.16	3
C3S7K3	Insulin receptor substrate-1 (Fragment)		125.25	8.59	3
A0A287AT14	Inter-alpha-trypsin inhibitor heavy chain family member 6	ITIH6	123.10	8.69	3
A0A287B7K6	Keratin 78	KRT78	62.57	8.78	3
I3LLY8	Keratin 79	KRT79	57.87	6.90	3
A0A287B3B0	KIAA1211	KIAA1211	124.50	6.28	3
A0A287BGU3	KIAA1217	KIAA1217	142.35	6.21	3
F1SRA8	Kinesin family member 15	KIF15	135.67	6.09	3
A0A287BLS1	Kinesin family member 21B	KIF21B	153.86	7.18	3
A0A287AUN7	Kinesin-like protein	KIFC2	89.66	9.09	3
F1SR93	Leucine rich repeat kinase 1	LRRK1	225.48	6.79	3
F1SHN7	Leucine-rich repeat serine/threonine-protein kinase 2	LRRK2	285.04	6.73	3
A0A286ZYC5	MAP kinase activating death domain	MADD	135.65	5.59	3
B9DR52	MATER protein	NALP5	130.30	9.57	3
A0A287A6R1	MDM2 binding protein	MTBP	95.29	7.93	3
I3LNV7	Meiosis regulator and mRNA stability factor 1	MARF1	188.20	8.18	3
A0A287BD85	MICAL C-terminal like	MICALCL	78.57	8.78	3

A0A287AZL4	MLLT6, PHD finger containing	MLLT6	93.50	8.70	3
A0A286ZY54	Myelin transcription factor 1	MYT1	118.84	5.30	3
A0A287BJU4	Myelin transcription factor 1 like	MYT1L	120.58	6.15	3
A0A287BPU2	Nebulin		651.06	9.14	3
A0A287AKL8	NOVA alternative splicing regulator 1	NOVA1	38.70	8.78	3
F1SDA5	NRDE-2, necessary for RNA interference, domain containing	NRDE2	133.08	8.02	3
F1S6F0	Nuclear factor related to kappaB binding protein	NFRKB	138.17	9.31	3
A0A287B9T7	Nuclear protein, coactivator of histone transcription	NPAT	148.35	5.67	3
A0A286ZML8	Nuclear receptor coactivator 3	NCOA3	143.74	7.25	3
A0A286ZMG5	Oligodendrocyte transcription factor 2	OLIG2	32.30	9.13	3
A0A287AN95	PDZ and LIM domain 5	PDLIM5	63.44	8.37	3
I3LRP4	PDZ domain containing 2	PDZD2	257.77	8.41	3
A0A287BLZ0	Pecanex homolog 1	PCNX1	239.91	6.86	3
P62936	Peptidyl-prolyl cis-trans isomerase A	PPIA	17.86	8.16	3
A0A287A9A2	Peroxisomal biogenesis factor 1	PEX1	141.27	6.09	3
F1S8T2	Peroxisome proliferator-activated receptor gamma, coactivator-related 1	PPRC1	173.31	6.18	3
A0A287A428	Plakophilin 4	PKP4	115.59	9.28	3
F1RQK4	Pleckstrin homology domain interacting protein	PHIP	206.74	8.88	3
I3LFD9	Pleckstrin homology, MyTH4 and FERM domain containing H2	PLEKHH2	160.71	7.55	3
A0A287AES8	Plexin A4	PLXNA4	148.35	6.90	3
F1RL90	PPARG coactivator 1 beta	PPARGC1B	111.08	5.17	3
A0A286ZLW5	Proline rich 14 like	PRR14L	203.25	5.55	3
F1RGH4	Proline rich basic protein 1	PROB1	107.19	9.74	3
F1S2Y2	Prospero homeobox 1	PROX1	83.15	7.18	3
F1SCG2	Protein phosphatase 4 regulatory subunit 4	PPP4R4	86.89	8.25	3
A0A287AUM0	Protein tyrosine phosphatase, non-receptor type 13	PTPN13	265.04	6.65	3
F1SGH5	Pyruvate dehydrogenase E1 component subunit beta, mitochondrial	PDHB	39.25	6.65	3
I3LEQ6	Ral GTPase activating protein catalytic alpha subunit 2	RALGAPA2	204.24	6.30	3
A0A287A2F1	Regulating synaptic membrane exocytosis 1	RIMS1	170.98	9.51	3
I3LSK9	Retrotransposon Gag like 9	RTL9	144.23	6.34	3
F1SUP8	Ring finger protein 169	RNF169	76.81	9.32	3
F1RZA6	Ring finger protein 213	RNF213	555.23	7.02	3
F1SK64	Roundabout guidance receptor 1	ROBO1	161.21	6.23	3
F1SN75	RPTOR independent companion of MTOR complex 2	RICTOR	188.37	8.07	3

A0A287A818	Sacsin molecular chaperone	SACS	517.87	7.03	3
A0A287AP36	SCO-spondin	SSPO	538.28	5.97	3
A0A287AC84	Senataxin	SETX	289.70	7.88	3
F1RHR8	Serine/threonine-protein kinase mTOR	MTOR	263.57	7.24	3
Q6R2V0	Serine/threonine-protein kinase WNK1	WNK1	248.82	6.32	3
A0A287BPS0	SET domain containing 2	SETD2	240.56	6.28	3
A0A287A8X0	SH3 and PX domains 2A	SH3PXD2A	105.58	8.88	3
A0A287BI87	Signal induced proliferation associated 1 like 3	SIPA1L3	190.40	8.40	3
F1SEA2	SLAIN motif family member 2	SLAIN2	62.84	9.45	3
A0A287B556	SMG1, nonsense mediated mRNA decay associated PI3K related kinase	SMG1	408.75	6.43	3
I3L8Z2	Solute carrier family 22 member 13	SLC22A13	56.13	7.90	3
A0A287A506	Spectrin repeat containing nuclear envelope protein 2	SYNE2	751.78	5.22	3
I3LM75	SPG7, paraplegin matrix AAA peptidase subunit	SPG7	86.30	9.19	3
B0FRD5	Steroid receptor coactivator 1 isoform 2	SRC1	152.60	6.14	3
F1RNM6	Stromal antigen 3	STAG3	135.33	6.58	3
I3L6A2	Teashirt zinc finger homeobox 3	TSHZ3	110.42	7.43	3
A5A8W4	Tenascin XB	TNXB	446.81	5.08	3
F1RXE4	Tensin 4	TNS4	75.96	7.37	3
F1RX69	Testis expressed 15, meiosis and synapsis associated	TEX15	311.51	7.06	3
F1S300	Translocated promoter region, nuclear basket protein	TPR	274.55	5.05	3
F1RL66	Treacle ribosome biogenesis factor 1	TCOF1	138.22	9.39	3
A0A286ZN11	Trinucleotide repeat containing 6B	TNRC6B	183.24	6.65	3
F1S6A1	Tudor domain containing 5	TDRD5	97.35	7.71	3
A0A287B6J2	Tumor protein p53 binding protein 1	TP53BP1	205.75	4.65	3
A0A287AIY3	Ubiquitin carboxyl-terminal hydrolase 37	USP37	94.68	5.66	3
F1SQM5	Ubiquitin specific peptidase 34	USP34	353.46	5.94	3
A0A287ABM5	Ubiquitin specific peptidase 54	USP54	180.58	7.52	3
A0A075B7J0	Uncharacterized protein		10.24	6.40	3
A0A286ZIF5	Uncharacterized protein		161.47	5.21	3
A0A287A1P9	Uncharacterized protein	LOC102162205	174.93	8.72	3
A0A287ACE7	Uncharacterized protein		112.40	11.00	3
A0A287ALS7	Uncharacterized protein		12.46	5.11	3
A0A287BM14	Uncharacterized protein		29.23	6.34	3
F1RM66	Uncharacterized protein		206.38	8.54	3
F1RX33	Uncharacterized protein		120.72	10.14	3

F1SDV2	Uncharacterized protein		135.31	4.98	3
F1SLF0	Uncharacterized protein	SPR	28.55	8.66	3
I3L728	Uncharacterized protein		15.05	6.01	3
F1SUK5	Unconventional myosin-VIIa	MYO7A	250.41	8.68	3
F1S2F6	Voltage-dependent anion-selective channel protein 2	VDAC2	31.58	7.55	3
F1SMK0	Whirlin	WHRN	93.86	8.66	3
F1RUG5	WNK lysine deficient protein kinase 3	WNK3	191.42	5.47	3
F1SGA4	YEATS domain containing 2	YEATS2	145.39	8.87	3
M3UZ00	Zinc finger CCCH-type containing 18	ZC3H18	103.08	9.09	3
A0A286ZTL1	Zinc finger MYM-type containing 4	ZMYM4	168.29	6.76	3
F1SRY7	Zinc finger protein 142	ZNF142	182.91	7.99	3
F1S0A9	Zinc finger protein 609	ZNF609	131.54	7.42	3
I3L5T4	Zinc finger protein 638	ZNF638	225.44	6.35	3
A5A776	Lysosomal trafficking regulator (Fragment)	LYST	427.15	6.43	3
Q9XSW7	Phosphodiesterase		108.77	6.27	2
A0A287ANB2	Sodium channel protein	SCN3A	209.87	5.86	2
F1SNS2	Phospholipid-transporting ATPase	ATP10A	163.49	6.99	2
F1RFX4	Sodium/hydrogen exchanger	SLC9A5	99.16	7.55	2
A0A287A985	Abnormal spindle microtubule assembly	ASPM	364.47	10.71	2
F1SRC5	Aconitate hydratase, mitochondrial	ACO2	85.40	7.71	2
F1S7Y2	Actin binding LIM protein family member 2	ABLIM2	73.23	8.72	2
A0A287BAR4	Actin binding LIM protein family member 3	ABLIM3	60.27	8.47	2
A0A287ALZ4	Actin-related protein 2/3 complex subunit 3	ARPC3	17.80	8.51	2
A0A286ZVT8	Alpha kinase 2	ALPK2	200.81	4.96	2
Q9GMA6	Alpha-1-antichymotrypsin 2	SERPINA3-2	46.62	6.76	2
F1RUN7	Anion exchange protein	SLC4A4	121.39	6.87	2
I3LL82	Ankyrin repeat and sterile alpha motif domain containing 6	ANKS6	79.77	6.90	2
E7EI19	Ankyrin repeat domain 17	ANKRD17	247.34	6.70	2
F1SCV9	Apolipoprotein B	APOB	476.02	7.61	2
I3LLV2	ARFGEF family member 3	ARFGEF3	235.89	5.73	2
F1S702	Astrotactin 1	ASTN1	140.73	5.17	2
A0A287A3H9	AT-hook containing transcription factor 1	AHCTF1	244.93	6.34	2
F1SB28	AT-rich interaction domain 1B	ARID1B	172.08	6.40	2
F1SLN0	ATP-dependent RNA helicase DHX29	DHX29	131.35	8.47	2
F1S402	Baculoviral IAP repeat containing 6	BIRC6	528.72	6.15	2
I3LQH7	Biliverdin reductase B	BLVRB	22.20	6.86	2

I3LSV8	BOC cell adhesion associated, oncogene regulated	BOC	120.12	7.20	2
A0A287AXR1	BR serine/threonine kinase 1	BRSK1	85.07	9.32	2
A0A287BKD3	Bromodomain adjacent to zinc finger domain 2B	BAZ2B	224.89	6.15	2
F1SJY4	BTB domain containing 18	BTBD18	68.23	4.79	2
F1SKK7	Cadherin EGF LAG seven-pass G-type receptor 3	CELSR3	357.80	6.35	2
F1RGR0	Calcium-transporting ATPase	ATP2A3	95.39	7.24	2
O46391	Calmodulin (Fragment)	CALM1	9.74	4.34	2
A0A287BHV7	Calpain 8	CAPN8	78.71	5.55	2
P43368	Calpain-3	CAPN3	94.49	6.01	2
A0A287BLC8	Capping protein regulator and myosin 1 linker 3	CARMIL3	129.53	8.46	2
B6VNT8	Cardiac muscle alpha actin 1	ACTC1	41.99	5.39	2
I3L9T1	Cardiomyopathy associated 5	CMYA5	366.86	4.69	2
K7GLC3	CD101 molecule	CD101	113.96	7.34	2
A0A286ZZ83	CD84 molecule	CD84	35.13	8.31	2
A0A287AFV9	Cell adhesion associated, oncogene regulated	CDON	130.07	6.62	2
A0A287AIB3	Centromere protein C	CENPC	99.36	8.68	2
A0A287AL60	Centromere protein E	CENPE	313.15	5.40	2
A0A287BL41	Chromobox protein homolog 8	CBX8	34.40	9.98	2
F1SEF3	Chromosome 2 open reading frame 16	C2orf16	221.07	9.86	2
I3LKT9	Chromosome 2 open reading frame 71	C2orf71	138.37	7.91	2
F1SIH9	Chromosome 9 open reading frame 131	C9orf131	118.47	7.33	2
A0A287BR23	Chromosome 9 open reading frame 50	C9orf50	42.38	11.55	2
A0A287AK64	Cilia and flagella associated protein 54	CFAP54	349.03	8.13	2
F1SRW7	Cilia and flagella associated protein 65	CFAP65	198.03	6.00	2
K7GK75	Cofilin-1	CFL1	16.82	8.27	2
A0A287AMK3	Coiled-coil domain containing 187	CCDC187	136.43	10.18	2
F1SGC2	Coiled-coil domain containing 39	CCDC39	110.04	7.46	2
F1SKM1	Collagen type VII alpha 1 chain	COL7A1	294.90	6.32	2
F1S284	Collagen type XIV alpha 1 chain	COL14A1	43.05	8.47	2
A0A287AWP8	Complement C5a anaphylatoxin	C5	180.27	6.76	2
A5A8W8	Complement component 4A	C4A	192.27	7.15	2
K7GLI4	Connector enhancer of kinase suppressor of Ras 2	CNKSR2	101.96	6.95	2
A0A286ZNY6	CST complex subunit STN1	STN1	45.01	6.37	2
A0A287A6D7	Cystic fibrosis transmembrane conductance regulator	CFTR	148.95	8.91	2
F1RMD2	Cytoskeleton associated protein 2	CKAP2	68.04	8.87	2

A0A287AIF6	Death inducer-obliterator 1	DIDO1	234.03	8.12	2
F1SNP7	Dedicator of cytokinesis 10	DOCK10	220.58	7.12	2
I3LG79	Desmocollin 3	DSC3	99.82	5.69	2
A0A286ZMN5	Diphosphoinositol pentakisphosphate kinase 2	PPIP5K2	134.11	7.99	2
I3LJR4	DNA-directed RNA polymerase subunit	POLR2A	215.73	7.49	2
F1RS88	Doublecortin like kinase 2	DCLK2	77.81	8.60	2
I3LPH8	Dystrophin	DMD	63.84	7.39	2
I3LGA5	Echinoderm microtubule associated protein like 6	EML6	211.11	7.58	2
A0A287A6C0	Endothelin converting enzyme 2	ECE2	98.59	5.81	2
A0A287A6K2	Epiplakin 1	EPPK1	483.87	5.62	2
A0A286ZJB3	Epithelial cell transforming 2	ECT2	105.98	7.24	2
A0A286ZYU9	Erbb2 interacting protein	ERBIN	145.76	5.36	2
A0A287B3N0	Eukaryotic translation initiation factor 4B	EIF4B	67.12	6.99	2
F1SV17	Exophilin 5	EXPH5	214.09	6.92	2
F1SFR3	Extra spindle pole bodies like 1, separase	ESPL1	229.58	7.08	2
F1RTD5	Family with sequence similarity 122B	FAM122B	25.87	6.37	2
F1SI11	Fanconi anemia complementation group M	FANCM	226.65	6.19	2
A0A286ZXU9	FAT atypical cadherin 4	FAT4	529.88	4.98	2
A0A287AXD5	FERM domain containing 4A	FRMD4A	112.36	9.31	2
F1SFF5	FERM domain containing 6	FRMD6	70.66	7.58	2
A0A287B7X6	FGFR1 oncogene partner	FGFR1OP	34.77	5.60	2
F1RSS5	FRY microtubule binding protein	FRY	335.48	6.06	2
A3EX84	Galectin	LGALS3	27.20	8.68	2
Q6J267	Galectin (Fragment)		14.59	5.24	2
A0A286ZYU3	GATA zinc finger domain containing 2A	GATAD2A	65.82	9.86	2
F1RJK5	GCN1, eIF2 alpha kinase activator homolog	GCN1	271.25	6.81	2
A0A287A3Z9	GIT ArfGAP 2	GIT2	78.97	7.37	2
F1SGR1	Glutamine and serine rich 1	QSER1	185.91	7.31	2
F1S7K5	HDGF like 2	HDGFL2	73.80	7.84	2
A0A287AQQ1	HDGF like 3	HDGFL3	22.61	7.99	2
F1SQ60	Heart development protein with EGF like domains 1	HEG1	138.68	6.25	2
F1RHL7	HEAT repeat containing 1	HEATR1	207.69	7.42	2
A0A287B1U2	HECT and RLD domain containing E3 ubiquitin protein ligase 2	HERC2	526.71	6.27	2
I3LKD5	HECT domain E3 ubiquitin protein ligase 4	HECTD4	477.46	6.13	2
F1RMM8	Helicase with zinc finger 2	HELZ2	321.57	7.97	2
A0A287BSS3	Hemicentin 1	HMCN1	597.52	6.44	2

A0A287BBY1	Hepatitis A virus cellular receptor 1 precursor	HAVCR1	37.06	8.16	2
A5A774	Hermansky-Pudlak syndrome 5 protein	HPS5	127.31	5.44	2
I3LSH6	HERV-H LTR-associating 1	HHLA1	55.19	8.63	2
F1SE29	Histone acetyltransferase	KAT6A	218.25	5.80	2
Q53DY5	Histone H1.3-like protein		22.14	10.96	2
A5D9N2	HLA-B associated transcript 2	BAT2	228.94	9.47	2
A5D9M2	HLA-B associated transcript 3 (Fragment)	BAT3	27.85	5.20	2
K7GSX0	Host cell factor C1	HCFC1	199.10	7.02	2
A0A287A7G3	Human immunodeficiency virus type I enhancer binding protein 3	HIVEP3	247.95	8.15	2
A0A286ZP34	HYDIN, axonemal central pair apparatus protein	HYDIN	564.86	6.55	2
F1SIC3	Hyperpolarization activated cyclic nucleotide gated potassium channel 4	HCN4	128.70	8.97	2
K7GMQ2	Immediate early response 3	IER3	14.26	10.35	2
K7GS48	Inhibitor of nuclear factor kappa B kinase subunit epsilon	IKBKE	77.67	7.75	2
F1RPW7	Inner centromere protein	INCENP	95.65	9.60	2
A0A287AEE9	Inositol polyphosphate-5-phosphatase E	INPP5E	71.91	9.17	2
F1RIV4	Integrator complex subunit 1	INTS1	243.28	6.39	2
A0A287B2D4	Integrator complex subunit 11	INTS11	78.13	8.60	2
A0A287BM82	Keratin 14	KRT14	54.16	5.33	2
F1SGG7	Keratin 71	KRT71	56.47	8.00	2
A0A287BRS0	KIAA0368	KIAA0368	200.74	7.12	2
A0A287BQ24	KIAA1210	KIAA1210	179.70	7.83	2
A0A287BIC6	KIAA1522	KIAA1522	103.20	9.88	2
A0A287AFN1	KIAA2026	KIAA2026	220.42	9.16	2
F1RJP9	Kinesin family member 13B	KIF13B	194.86	5.77	2
I3LEH8	Kinesin family member 19	KIF19	111.99	9.13	2
A0A287AW85	Kinesin-like protein	KIF3C	79.12	8.51	2
A0A287AQS1	L-lactate dehydrogenase B chain	LDHB	35.02	7.23	2
F1RKM0	Lamin B1	LMNB1	66.45	5.14	2
I3LKQ7	Lamin tail domain containing 2	LMNTD2	69.42	7.75	2
A0A287AG36	Laminin subunit alpha 1	LAMA1	333.56	6.13	2
A0A287AEH1	Laminin subunit alpha 5	LAMA5	395.41	6.74	2
F1SF45	Laminin subunit beta 3	LAMB3	128.66	7.12	2
A0A287B2N7	LDL receptor related protein 12	LRP12	85.95	6.01	2
F1S2I9	Leucine rich repeat containing 36	LRRC36	84.40	7.25	2
A0A287AQY5	Leucine rich repeats and calponin homology domain containing 4	LRCH4	76.63	8.27	2
F1SFR8	Leucine rich repeats and immunoglobulin like	LRIG1	119.90	6.92	2

	domains 1				
F1SPX1	Leucine rich repeats and IQ motif containing 1	LRRIQ1	196.07	6.35	2
F1S629	Ligand dependent nuclear receptor interacting factor 1	LRIF1	83.24	9.60	2
A0A286ZJT9	LIM domain binding 2	LDB2	37.99	9.00	2
C0HL13	Low-density lipoprotein receptor-related protein 2	LRP2	520.96	5.21	2
I3LL74	Lysine demethylase 2B	KDM2B	126.04	8.54	2
A0A286ZNY8	Lysine methyltransferase 2E	KMT2E	169.67	7.69	2
Q95LC9	Mannose-6-phosphate/insulin-like growth factor II receptor (Fragment)	m6p/igf2r	252.39	6.14	2
F1RQW0	MAP7 domain containing 3	MAP7D3	84.84	4.74	2
A0A287AG74	Membrane associated guanylate kinase, WW and PDZ domain containing 2	MAGI2	139.49	6.05	2
F1RRU8	Membrane associated ring-CH-type finger 10	MARCH10	84.86	7.02	2
K7GQR3	Membrane bound transcription factor peptidase, site 2	MBTPS2	57.68	7.49	2
I3L5P6	Microtubule affinity regulating kinase 4	MARK4	75.28	9.79	2
F1SHR1	Microtubule associated monooxygenase, calponin and LIM domain containing 3	MICAL3	213.58	5.62	2
F1SK12	Microtubule associated protein 1B	MAP1B	245.82	4.77	2
I3LU86	Microtubule associated scaffold protein 2	MTUS2	138.92	6.98	2
F1S3V0	Microtubule associated serine/threonine kinase 2	MAST2	177.62	7.55	2
F1RY22	Midasin	MDN1	629.65	5.72	2
I3LCF4	Minichromosome maintenance complex component 3 associated protein	MCM3AP	217.55	6.90	2
A0A287AQX8	Mitochondrial ribosomal protein S31	MRPS31	40.47	8.02	2
A0A287ABQ5	Mitogen-activated protein kinase kinase kinase 1	MAP3K1	148.41	7.75	2
K7GPY0	Mitogen-activated protein kinase kinase kinase 3	MAP3K3	70.84	9.01	2
A0A287BF57	MTSS1, I-BAR domain containing	MTSS1	75.29	7.31	2
A0A287B5M2	Mucin-4 precursor	MUC4	131.94	7.36	2
A0A287AMS2	Murine retrovirus integration site 1 homolog	MRVI1	98.41	5.96	2
F1RND9	Myeloid cell nuclear differentiation antigen	MNDA	45.27	9.54	2
A0A287BQ73	Myotubularin related protein 4	MTMR4	132.27	6.05	2
O99997	NADH-ubiquinone oxidoreductase chain 5	NADH5	68.55	9.00	2
F1S4H4	NEDD4 binding protein 2	N4BP2	192.61	5.10	2
I3LS05	Neuregulin 2	NRG2	77.65	9.11	2
A0A287B170	Neuronal tyrosine phosphorylated phosphoinositide-3-kinase adaptor 1	NYAP1	83.46	9.67	2
A0A287AQH6	NHS like 1	NHSL1	136.23	7.61	2
A0A287BT13	Non-specific serine/threonine protein kinase	MARK3	81.33	9.50	2

A0A287ACY0	Nuclear factor 1	NFIC	49.49	7.77	2
F1S3C1	Nuclear receptor binding SET domain protein 1	NSD1	267.71	8.53	2
F1SDC8	Nuclear receptor corepressor 1	NCOR1	260.64	7.47	2
F1RJ55	Oligodendrocyte myelin glycoprotein	OMG	49.82	8.16	2
A0A287BMV3	PAN2-PAN3 deadenylation complex catalytic subunit PAN2	PAN2	127.30	5.86	2
F1SAB7	Partner and localizer of BRCA2	PALB2	109.30	7.06	2
A0A287AVB6	PEAK1 related kinase activating pseudokinase 1	PRAG1	123.99	6.87	2
A0A287AIJ2	Pecanex homolog 2	PCNX2	234.43	6.61	2
F1RRK1	Pecanex homolog 3	PCNX3	220.85	6.67	2
A0A287BSX1	Peptidylprolyl isomerase G	PPIG	88.50	10.29	2
F1SUD5	PHD finger protein 2	PHF2	108.41	9.31	2
A0A287A3L4	PHD finger protein 3	PHF3	217.51	7.43	2
A0A287AQP4	Phosphatidylinositol 4-kinase alpha	PI4KA	194.99	6.83	2
F1SSZ9	Phosphatidylinositol 4-kinase beta	PI4KB	93.60	6.38	2
A0A286ZU42	Phosphatidylinositol binding clathrin assembly protein	PICALM	65.75	9.00	2
I3LLX2	Phosphatidylinositol-4-phosphate 3-kinase catalytic subunit type 2 alpha	PIK3C2A	190.57	7.69	2
A0A286ZQ01	Phosphofurin acidic cluster sorting protein 2	PACS2	92.15	6.47	2
A0A287B7V0	Phosphoinositide kinase, FYVE-type zinc finger containing	PIKFYVE	230.92	6.64	2
F1STJ5	Piwil4 protein	PIWIL4	95.70	8.84	2
A0A287BSV6	Pleckstrin homology domain containing A7	PLEKHA7	114.42	9.61	2
A0A287BBZ9	Pleckstrin homology like domain family B member 1	PHLDB1	150.16	9.31	2
A0A287B5Z2	Poly(A) RNA polymerase D5, non-canonical	PAPD5	68.38	8.78	2
A0A286ZXC2	Polycomb group ring finger 2	PCGF2	31.51	7.75	2
A0A286ZKR8	Polycystin 1, transient receptor potential channel interacting	PKD1	457.45	6.79	2
A0A287A6W8	Polycystin family receptor for egg jelly	PKDREJ	234.11	8.62	2
F1SA91	Potassium channel tetramerization domain containing 3	KCTD3	88.91	7.14	2
D2SQP2	Proliferator-activated receptor gamma coactivator-related 1 (Fragment)	PPRC1	45.85	10.14	2
A0A287BL34	Protein phosphatase 1 regulatory subunit 21	PPP1R21	82.72	6.62	2
F1SH38	Protein tyrosine phosphatase, receptor type B	PTPRB	224.16	8.13	2
A0A287ASE8	Protein tyrosine phosphatase, receptor type Q	PTPRQ	255.55	5.76	2
I3LUE2	Protein tyrosine phosphatase, receptor type S	PTPRS	211.09	7.01	2
P45845	Protein-lysine 6-oxidase	LOX	29.05	6.44	2
A0A287BIK6	Pseudopodium enriched atypical kinase 1	PEAK1	167.71	7.24	2
A0A287B7E9	PTPRF interacting protein alpha 3	PPFIA3	132.10	5.74	2

I3LJE6	PWWP domain containing 2B	PWWP2B	59.90	8.98	2
A0A286ZLJ5	Ral GTPase-activating protein subunit alpha-1	RALGAPA1	280.27	6.38	2
F1S6Y8	RAS protein activator like 2	RASAL2	128.44	8.16	2
F1SI16	Receptor protein serine/threonine kinase	BMPR2	114.96	6.20	2
K7GLX7	Retinitis pigmentosa GTPase regulator	RPGR	78.65	5.63	2
F1S8J2	Retinitis pigmentosa GTPase regulator interacting protein 1	RPGRIP1	134.89	5.38	2
I3L6U8	REV3 like, DNA directed polymerase zeta catalytic subunit	REV3L	343.92	8.44	2
A0A287AV22	Rho GTPase activating protein 12	ARHGAP12	99.72	7.74	2
F1S291	Rho GTPase activating protein 4	ARHGAP4	88.03	6.51	2
A0A286ZZ99	Rho guanine nucleotide exchange factor 10 like	ARHGEF10L	116.18	7.34	2
F1SUT6	Rho guanine nucleotide exchange factor 17	ARHGEF17	219.08	6.55	2
A0A288CFX3	Rho related BTB domain containing 2	RHOBTB2	82.42	6.84	2
A0A287BMD1	Ring finger and CCCH-type domains 2	RC3H2	131.59	6.77	2
A0A286ZPL0	RUN domain containing 3A	RUNDC3A	49.41	5.43	2
F1SNX8	Sad1 and UNC84 domain containing 2	SUN2	81.54	7.23	2
A0A287BCA4	Scavenger receptor cysteine rich family member with 5 domains	SSC5D	136.43	6.27	2
A0A287A778	Serine and arginine repetitive matrix 1	SRRM1	92.62	11.96	2
K9IVJ5	Serine dehydrates	SDS	34.21	7.71	2
A0A287BG48	Serine/arginine repetitive matrix 5	SRRM5	74.63	11.97	2
A0A287B026	Serine/threonine-protein phosphatase	PPP3CC	51.32	6.09	2
Q95MZ3	Serine/threonine-protein phosphatase	PPP3CA	57.60	6.27	2
A0A287AG90	Signal induced proliferation associated 1 like 1	SIPA1L1	193.42	8.51	2
F1RGU5	Signal induced proliferation associated 1 like 2	SIPA1L2	182.97	7.11	2
A0A286ZIX9	SMG6, nonsense mediated mRNA decay factor	SMG6	149.83	7.33	2
A0A287BFW1	Sodium/glucose cotransporter 5	SLC5A10	37.94	7.06	2
F1SJK4	Solute carrier family 24 member 1	SLC24A1	118.33	4.97	2
A0A286ZN88	Sorbin and SH3 domain-containing protein 2	SORBS2	128.97	8.19	2
A0A286ZJD3	Spen family transcriptional repressor	SPEN	345.61	7.87	2
A0A287BLM0	Sprouty related EVH1 domain containing 1	SPRED1	50.53	6.71	2
F1SFX2	SPT2 chromatin protein domain containing 1	SPTY2D1	65.61	9.72	2
A0A287BMR4	SRP receptor alpha subunit	SRPRA	69.57	8.94	2
Q0QF01	Succinate dehydrogenase [ubiquinone] flavoprotein subunit, mitochondrial	SDHA	72.79	7.50	2
F1S682	Sulfhydryl oxidase	QSOX1	81.43	8.41	2
Q95ME5	Superoxide dismutase 1 (Fragment)	SOD1	15.24	6.52	2

A0A287B4D0	Supervillin	SVIL	199.00	6.89	2
F1RGC1	Suppression of tumorigenicity 5	ST5	124.68	9.51	2
F1RJ15	Synaptonemal complex protein 2	SYCP2	169.39	8.88	2
A0A287B600	Synemin	SYNM	162.76	5.21	2
A0A287A5A6	Syntaxin binding protein 5 like	STXBP5L	134.35	7.09	2
I3LFX3	T-cell lymphoma invasion and metastasis 2	TIAM2	186.56	7.24	2
A0A287BLY8	Talin 1	TLN1	239.18	5.97	2
F1SFP6	TATA element modulatory factor 1	TMF1	119.24	4.93	2
F1RU60	Teneurin transmembrane protein 1	TENM1	285.35	6.54	2
A0A287AMI1	Teneurin transmembrane protein 3	TENM3	260.05	6.29	2
I3LT49	Testis and ovary specific PAZ domain containing 1	TOPAZ1	177.83	8.27	2
F1S116	Tet methylcytosine dioxygenase 2	TET2	225.57	8.07	2
F1S5I2	THADA, armadillo repeat containing	THADA	216.69	6.30	2
A0A287ALN4	THO complex 5	THOC5	70.88	7.06	2
F1SK20	TOPBP1 interacting checkpoint and replication regulator	TICRR	209.11	9.01	2
A0A287BBZ3	Transducin like enhancer of split 4	TLE4	81.10	7.50	2
A0A287AUN9	Transient receptor potential cation channel subfamily M member 4	TRPM4	121.76	8.19	2
F1RIH6	Transmembrane protein 201	TMEM201	71.56	9.16	2
F1SRN4	Trio Rho guanine nucleotide exchange factor	TRIO	348.37	6.40	2
A0A286ZWL0	Tubulin gamma complex associated protein 6	TUBGCP6	176.30	6.77	2
F1SRW9	Tubulin tyrosine ligase like 4	TTLL4	127.83	9.31	2
A0A287AXR8	Ubinuclein 2	UBN2	120.01	9.54	2
I3LGC6	Ubiquitin specific peptidase 24	USP24	293.66	6.19	2
A0A287B0S8	Ubiquitously transcribed tetratricopeptide repeat containing, Y-linked	UTY	85.37	7.80	2
A0A286ZME3	Uncharacterized protein		87.61	8.44	2
A0A286ZNZ5	Uncharacterized protein		109.21	6.33	2
A0A286ZQD6	Uncharacterized protein		29.82	8.35	2
A0A286ZVE3	Uncharacterized protein	PNN	68.43	6.14	2
A0A286ZZI0	Uncharacterized protein		43.56	6.90	2
A0A286ZZT2	Uncharacterized protein	USP32	179.84	6.58	2
A0A287A2Z3	Uncharacterized protein	AMMECR1	31.17	8.29	2
A0A287AHI6	Uncharacterized protein	TRAPPC10	139.97	6.29	2
A0A287AHM5	Uncharacterized protein	LOC100737030	49.99	5.16	2
A0A287AJE3	Uncharacterized protein	LOC106504547	43.55	7.96	2
A0A287AJT1	Uncharacterized protein		110.92	10.99	2

A0A287ARQ1	Uncharacterized protein	LOC110258677	113.48	11.03	2
A0A287AUW4	Uncharacterized protein	LOC100512195	14.39	9.60	2
A0A287AY66	Uncharacterized protein		55.44	8.88	2
A0A287B324	Uncharacterized protein		365.70	7.11	2
A0A287B7B5	Uncharacterized protein	LOC100518417	86.39	7.37	2
A0A287B879	Uncharacterized protein	LOC100524773	232.64	5.34	2
A0A287B8V1	Uncharacterized protein	RAPGEF6	162.66	6.37	2
A0A287BAM3	Uncharacterized protein	ECSCR	25.34	7.84	2
A0A287BE84	Uncharacterized protein		115.85	10.64	2
A0A287BLI2	Uncharacterized protein	EPB41L1	101.84	5.58	2
A0A287BM11	Uncharacterized protein	LOC396684	45.37	6.47	2
A0A287BSG3	Uncharacterized protein		109.72	10.89	2
F1RJX0	Uncharacterized protein		107.42	5.41	2
F1RLM0	Uncharacterized protein	GON4L	240.26	4.92	2
F1RLS1	Uncharacterized protein	SPECC1L	121.27	5.62	2
F1RPD7	Uncharacterized protein	SMTN	98.70	9.03	2
F1RQ17	Uncharacterized protein		75.20	8.53	2
F1RTL7	Uncharacterized protein		127.03	9.19	2
F1S0D2	Uncharacterized protein	CCNT2	68.67	9.16	2
F1S144	Uncharacterized protein		86.28	7.40	2
F1SB95	Uncharacterized protein		15.20	11.00	2
F1SCU0	Uncharacterized protein	LOC100516797	64.91	8.90	2
F1SER9	Uncharacterized protein	FAT1	505.93	5.01	2
F1SRH9	Uncharacterized protein	OFD1	115.27	5.96	2
F6Q8N2	Uncharacterized protein	MUC20	49.94	5.87	2
I3LC88	Uncharacterized protein		233.87	6.05	2
I3LNS2	Uncharacterized protein		332.93	5.26	2
I3LP90	Uncharacterized protein		365.35	6.11	2
I3LTW9	Uncharacterized protein		505.57	5.36	2
F1RFL9	V-type proton ATPase subunit a	ATP6V0A2	97.93	6.77	2
A0A287BLY6	Vaccinia related kinase 3	VRK3	44.43	9.17	2
A0A286ZMH4	WNK lysine deficient protein kinase 2	WNK2	218.64	6.02	2
A0A287AU21	Zinc finger C3H1-type containing	ZFC3H1	202.62	7.77	2
I3LAN0	Zinc finger E-box binding homeobox 2	ZEB2	123.90	6.70	2
F1S5D4	Zinc finger protein 281	ZNF281	93.04	8.47	2
A0A286ZRJ6	Zinc finger protein 445	ZNF445	99.84	9.10	2

A0A287AJ56	Phosphodiesterase	PDE4A	94.71	5.15	1
I3LEE8	Phosphodiesterase	PDE1A	56.80	6.46	1
A0A286ZLW9	Phosphoinositide phospholipase C	PLCL2	125.57	6.86	1
I3LFF0	Phosphoinositide phospholipase C	PLCH1	182.60	7.59	1
F1SMF8	Poly [ADP-ribose] polymerase	PARP8	95.78	8.28	1
F1SQ35	Poly [ADP-ribose] polymerase	PARP15	65.39	8.53	1
I3L916	Protein tyrosine phosphatase, non-receptor type 11	PTPN11	58.87	7.12	1
A0A287BC16	Sodium channel protein	SCN5A	207.01	5.58	1
F1S1Z0	Sodium channel protein	SCN2A	199.21	5.53	1
I3LPL6	Sodium channel protein	SCN11A	200.43	7.84	1
A0A287BD80	Tyrosine-protein phosphatase	PTPN22	90.22	7.02	1
A0A287BDT6	Ubiquitinyl hydrolase 1	USP13	90.36	5.39	1
I3LRQ5	Phosphatase and actin regulator	PHACTR4	76.93	6.60	1
A0A287B7D1	Phospholipid-transporting ATPase	ATP11A	114.51	6.30	1
A0A287BQK1	Phospholipid-transporting ATPase	ATP10D	141.99	6.04	1
F1STQ3	Sodium/hydrogen exchanger	SLC9A1	90.98	7.02	1
A0A287BDY7	Serine/threonine-protein kinase	PRKD1	101.54	6.55	1
I3L9Z3	Serine/threonine-protein kinase	PRKD2	97.96	7.01	1
A0A287ASK6	Tyrosine-protein kinase receptor	ROS1	222.84	5.54	1
K7GQT6	Tyrosine-protein kinase receptor	ALK	145.22	6.96	1
Q6XGY2	2,4-dienoyl-CoA reductase (Fragment)	DECR	31.84	8.13	1
I2E6E0	4-1BB variant 2 (TNF receptor superfamily member 9)	TNFRSF9	26.40	5.95	1
A0A287B2M3	40S ribosomal protein SA	RPSA	30.69	5.38	1
A0A286ZL81	5-aminolevulinate synthase	ALAS1	70.35	7.99	1
F1SKV3	5-hydroxytryptamine receptor 1A	HTR1A	46.34	9.16	1
A0A287A3W2	6-phosphofructo-2-kinase/fructose-2,6-biphosphatase 3	PFKFB3	55.08	7.42	1
F1SMZ7	60 kDa heat shock protein, mitochondrial	HSPD1	60.87	5.87	1
A0A286ZLX0	60S ribosomal protein L18	RPL18	19.33	11.52	1
A0A287AKM5	A-kinase anchor protein 10, mitochondrial	AKAP10	61.19	6.00	1
A0A287AUQ9	A-kinase anchoring protein 12	AKAP12	176.98	4.45	1
A0A286ZWG3	A-kinase anchoring protein 6	AKAP6	232.48	5.01	1
A0A287A579	A-kinase anchoring protein 9	AKAP9	445.31	5.01	1
A0A0A0R2Y4	Abca1 protein	abca1	254.04	7.30	1
I3LHA4	Abl interactor 1	ABI1	42.64	6.04	1
A0A286ZJZ4	Abraxas 1, BRCA1 A complex subunit	ABRAXAS1	40.84	8.50	1
A0A286ZXW1	Acetyl-CoA acetyltransferase 1	ACAT1	40.07	9.20	1

F1RGB5	Acetyl-CoA carboxylase 2 precursor	ACACB	275.65	6.48	1
A0A287AT81	Activated leukocyte cell adhesion molecule	ALCAM	58.09	8.13	1
A0A287A8T8	Activating transcription factor 7 interacting protein	ATF7IP	121.37	4.60	1
A5GHK7	Activity-dependent neuroprotector	ADNP	123.68	7.14	1
F1RPB1	Acyl-CoA synthetase medium chain family member 3	ACSM3	65.73	9.00	1
B8XY19	Acyl-CoA synthetase short-chain family member 2	ACSS2	78.70	6.67	1
A0A287BJR8	Acyl-CoA-binding protein	DBI	7.96	8.88	1
F1SGH9	Acyl-coenzyme A oxidase	ACOX2	76.74	7.44	1
A0A287BFS0	ADAM metallopeptidase domain 22	ADAM22	101.16	7.25	1
F1SP19	ADAM metallopeptidase with thrombospondin type 1 motif 12	ADAMTS12	91.63	7.65	1
I3LKV5	ADAM metallopeptidase with thrombospondin type 1 motif 13	ADAMTS13	112.13	6.90	1
F1S046	ADAM metallopeptidase with thrombospondin type 1 motif 16	ADAMTS16	133.58	8.98	1
F1S1A7	ADAM metallopeptidase with thrombospondin type 1 motif 4	ADAMTS4	93.67	8.31	1
A5HJZ3	ADAM3b	ADAM3b	83.53	7.87	1
F1RIC0	ADAMTS like 3	ADAMTSL3	176.40	7.99	1
A0A287ANN1	ADAMTS like 4	ADAMTSL4	98.77	7.91	1
F1SDL7	Additional sex combs like 2, transcriptional regulator	ASXL2	165.00	8.94	1
E7EI18	Adenosylhomocysteinase	AHCYL1	58.91	6.89	1
A0A287BPU6	Adenylate cyclase 3	ADCY3	148.15	7.59	1
A0A287AJJ9	Adenylate kinase 5	AK5	57.28	6.10	1
F1RX85	Adhesion G protein-coupled receptor A2	ADGRA2	141.73	8.72	1
A0A287BET6	Adhesion G protein-coupled receptor B1	ADGRB1	170.81	7.66	1
A0A286ZP81	Adhesion G protein-coupled receptor B2	ADGRB2	155.46	7.06	1
F1RTT7	Adhesion G protein-coupled receptor B3	ADGRB3	138.53	6.90	1
A0A287A168	Adhesion G protein-coupled receptor E1	ADGRE1	102.63	7.40	1
A0A287B387	Adhesion G protein-coupled receptor G6	ADGRG6	122.68	7.24	1
A0A287AE93	Adhesion G protein-coupled receptor L2	ADGRL2	165.46	6.40	1
A0A287AQV7	Adhesion G protein-coupled receptor V1	ADGRV1	653.20	4.67	1
A0A287AQ96	ADP ribosylation factor GTPase activating protein 1	ARFGAP1	44.91	5.67	1
I3LU23	ADP ribosylation factor like GTPase 13B	ARL13B	49.04	6.33	1
F1RQT7	Alanyl-tRNA synthetase 2, mitochondrial	AARS2	101.53	6.21	1
F1S3H1	Aldehyde dehydrogenase 6 family member A1	ALDH6A1	57.67	8.24	1
A0A287AS89	Alpha-1,3-mannosyl-glycoprotein 4-beta-N-acetylglucosaminyltransferase C	MGAT4C	56.18	8.66	1

Q9TSW7	Alpha-1A adrenergic receptor	alpha-1A	51.64	8.95	1
A0A287A5D8	Alpha-2,8-sialyltransferase 8B precursor	ST8SIA2	40.24	9.04	1
A0A287A0Z8	Amine oxidase	AOC1	89.41	8.34	1
I3L8L2	Aminopeptidase	ERAP2	109.30	6.40	1
I3L664	Amyloid beta precursor protein binding family A member 1	APBA1	91.47	4.83	1
A0A287BSR1	Anaphase promoting complex subunit 16	ANAPC16	11.69	4.97	1
A0A287B7V1	Anaphase promoting complex subunit 2	ANAPC2	93.32	5.39	1
F1RG45	Angiotensinogen	AGT	51.05	6.39	1
I3L7Z1	Anion exchange protein	SLC4A5	109.39	8.21	1
F1SP04	Ankycorbin	RAI14	107.78	6.23	1
F1SFC9	Ankyrin repeat and IBR domain containing 1	ANKIB1	122.25	5.08	1
A0A287AX90	Ankyrin repeat and sterile alpha motif domain containing 3	ANKS3	63.87	6.11	1
A0A287AZX6	Ankyrin repeat domain 24	ANKRD24	102.00	4.94	1
A0A287ADT3	AP complex subunit beta	AP4B1	72.19	5.92	1
F1SPM8	AP2-associated protein kinase 1	AAK1	104.25	6.90	1
Q29433	Apolipoprotein B (Fragment)	apoB	174.55	7.33	1
A0A140TAK8	Apolipoprotein H	APOH	31.93	8.07	1
F1SSY8	Arachidonate 12-lipoxygenase, 12R type	ALOX12B	79.61	7.24	1
I3L621	ArfGAP with GTPase domain, ankyrin repeat and PH domain 3	AGAP3	106.60	9.51	1
A0A287AKZ3	ArfGAP with RhoGAP domain, ankyrin repeat and PH domain 2	ARAP2	165.37	5.85	1
A0A287BGR6	Armadillo repeat containing, X-linked 5	ARMCX5	56.28	9.04	1
V5PZZ6	Arrestin domain-containing 5	ARRDC5	37.56	7.24	1
K9J4M4	Aryl hydrocarbon receptor nuclear translocator isoform 3	ARNT	84.96	6.80	1
F1S978	Aryl hydrocarbon receptor nuclear translocator like	ARNTL	66.14	6.67	1
A0A286ZT02	Asparaginase like 1	ASRGL1	30.13	6.73	1
P00506	Aspartate aminotransferase, mitochondrial	GOT2	47.41	9.01	1
F1SMI1	Astrotactin 2	ASTN2	142.48	5.83	1
A0A287BN71	AT-rich interaction domain 4B	ARID4B	136.55	5.43	1
F1RFC2	AT-rich interaction domain 5B	ARID5B	110.04	9.13	1
I3LGU8	Ataxin 2	ATXN2	113.14	8.65	1
A0A287BEI0	ATP binding cassette subfamily A member 10	ABCA10	119.45	6.07	1
A0A287BNF0	ATP binding cassette subfamily A member 12	ABCA12	261.51	7.93	1
F1S539	ATP binding cassette subfamily A member 4	ABCA4	259.53	6.60	1
A0A286ZJ46	ATP binding cassette subfamily B member 4	ABCB4	136.68	8.66	1
A0A287BB75	ATP binding cassette subfamily G member 1	ABCG1	74.08	7.09	1

A0A286ZZU0	ATP/GTP binding protein 1	AGTPBP1	133.20	6.44	1
A0A287AE67	ATP/GTP binding protein like 1	AGBL1	97.59	6.58	1
F1RR16	ATPase family, AAA domain containing 2	ATAD2	123.83	6.18	1
A0A287BJ84	ATPase family, AAA domain containing 5	ATAD5	201.95	9.17	1
A0A286ZTP1	Autophagy and beclin 1 regulator 1	AMBRA1	138.78	7.17	1
F2Z5U2	B-cell CLL/lymphoma 11A	BCL11A	83.78	6.28	1
F1SFH8	B-cell CLL/lymphoma 6	BCL6	78.60	7.94	1
F1RZB0	BAI1 associated protein 2	BAIAP2	57.18	8.88	1
F1RFK7	BAI1 associated protein 2 like 1	BAIAP2L1	56.20	8.37	1
I3LT30	Bardet-Biedl syndrome 2 protein homolog	BBS2	80.69	6.01	1
A0A287AJ07	BARX homeobox 2	BARX2	30.72	9.22	1
I3LIF5	Basic leucine zipper nuclear factor 1	BLZF1	44.67	7.78	1
A0A287BRB7	BBX, HMG-box containing	BBX	97.88	8.62	1
A0A286ZNT2	BCAS3, microtubule associated cell migration factor	BCAS3	77.79	7.17	1
A0A286ZZW0	BCR, RhoGEF and GTPase activating protein	BCR	140.20	8.00	1
A0A286ZQY8	Beta-1,3-N-acetylglucosaminyltransferase	RFNG	36.72	8.48	1
A7YB43	Beta-globin (Fragment)		13.95	6.52	1
F1RG08	BicC family RNA binding protein 1	BICC1	95.95	9.06	1
A0A287AKX6	Bloom syndrome RecQ like helicase	BLM	153.11	7.96	1
F1SA93	BMP/retinoic acid inducible neural specific 3	BRINP3	88.36	7.81	1
I3LTP1	BPI fold containing family B member 6	BPIFB6	50.81	7.39	1
A0A287BGU1	BR serine/threonine kinase 2	BRSK2	76.79	8.88	1
F1S219	BRCA1 interacting protein C-terminal helicase 1	BRIP1	81.91	5.41	1
I3LLE2	BRD4 interacting chromatin remodeling complex associated protein	BICRA	147.03	6.62	1
A0A287AR43	Breast cancer type 1 susceptibility protein homolog	BRCA1	184.39	5.78	1
A0A287BD36	Bromodomain adjacent to zinc finger domain 2A	BAZ2A	182.73	6.76	1
A0A287AQH7	Bromodomain containing 2	BRD2	84.53	9.17	1
F1RY18	BTB domain and CNC homolog 2	BACH2	92.19	5.14	1
A0A287ADJ5	BTB domain containing 3	BTBD3	58.84	7.65	1
F1SD53	BTB domain containing 7	BTBD7	125.63	6.87	1
K9J6J5	C-type lectin domain family 4 member A isoform 1	CLEC4A_tv 1	27.57	7.68	1
F1RJF6	C1q and TNF related 12	C1QTNF12	33.11	10.24	1
F1SUR6	C2 calcium dependent domain containing 3	C2CD3	252.20	7.06	1
A0A287BPK3	C2 calcium dependent domain containing 4C	C2CD4C	44.57	9.72	1
A0A286ZQJ3	C2CD2 like	C2CD2L	71.68	8.32	1

A0A287ARR7	C3 and PZP like, alpha-2-macroglobulin domain containing 8		115.94	7.53	1
F1SNS3	Cache domain containing 1	CACHD1	135.09	6.68	1
A0A287BJU2	Cactin, spliceosome C complex subunit	CACTIN	88.64	9.25	1
F1S9C8	Cadherin 24	CDH24	83.74	4.77	1
A0A287BIY4	Cadherin 8	CDH8	88.22	4.73	1
A0A287AEM7	Cadherin EGF LAG seven-pass G-type receptor 2	CELSR2	315.17	5.44	1
A0A287BL69	Cadherin related family member 1	CDHR1	87.55	6.01	1
F1S9W3	Calcium homeostasis endoplasmic reticulum protein	CHERP	103.77	9.10	1
F1SJ19	Calcium voltage-gated channel auxiliary subunit alpha2delta 2	CACNA2D2	122.00	5.38	1
A0A287B9W6	Calcium voltage-gated channel auxiliary subunit beta 3	CACNB3	53.11	6.74	1
F1RNJ2	Calcium voltage-gated channel auxiliary subunit gamma 8	CACNG8	43.10	9.20	1
A0A286ZUU7	Calcium voltage-gated channel subunit alpha1 G	CACNA1G	249.20	7.21	1
A0A287B1I7	Calcium voltage-gated channel subunit alpha1 H	CACNA1H	255.56	7.47	1
A0A287BKH5	Calcium-transporting ATPase	ATP2B3	130.86	5.83	1
F1RSA2	Calcium-transporting ATPase	ATP2C1	104.24	6.90	1
F1SF44	Calcium/calmodulin dependent protein kinase IG	CAMK1G	52.88	8.37	1
F1SSH3	Calcium/calmodulin dependent protein kinase II beta	CAMK2B	70.84	7.78	1
A0A287BFW8	Calmodulin binding transcription activator 1	CAMTA1	78.79	9.33	1
F1SCH4	Calmodulin regulated spectrin associated protein family member 3	CAMSAP3	119.35	8.78	1
A0A287ASZ8	Calpain 10	CAPN10	79.69	8.47	1
F6PU32	Calpastatin	CAST	89.73	5.85	1
F1RTQ8	Capping protein regulator and myosin 1 linker 1	CARMIL1	147.61	7.87	1
F1SSS0	Carbamoyl-phosphate synthase 1	CPS1	153.91	6.68	1
B8LFE3	Cardiomyopathy associated 1	CMYA1	198.68	5.97	1
I3LPD6	Cardiomyopathy associated 5	CMYA5	436.95	4.68	1
O19112	Cartilage intermediate layer protein 1 (Fragment)	CILP	67.39	7.02	1
C1PIJ2	Caspase 10	CASP10	59.01	6.46	1
F1RY23	Caspase 8 associated protein 2	CASP8AP2	205.08	6.28	1
F1RHS4	Castor zinc finger 1	CASZ1	175.31	8.51	1
A0A287BL30	Cation channel sperm associated 2	CATSPER2	55.17	9.19	1
F1S4Q6	CCAAT/enhancer binding protein zeta	CEBPZ	120.75	5.59	1
A0A287A280	CCM2 scaffolding protein	CCM2	45.44	5.10	1

A0A287AK97	CCR4-NOT transcription complex subunit 1	CNOT1	240.70	6.96	1
F1RQH9	CD109 molecule	CD109	154.93	5.45	1
I3LVM3	CD300 molecule like family member g	CD300LG	40.11	7.78	1
A0A286ZXA8	CDK5 regulatory subunit associated protein 1 like 1	CDKAL1	67.79	8.38	1
F1RXE3	Cell division control protein	CDC6	62.32	9.50	1
A0A287B1H7	Cell division cycle 27	CDC27	89.06	7.11	1
F1RQS5	Cell division cycle 5 like	CDC5L	92.16	8.18	1
I3LD81	Cell division cycle 7	CDC7	61.44	8.59	1
F1SNE3	Centlein	CNTLN	154.25	8.54	1
A0A286ZY18	Centromere protein B	CENPB	66.19	4.50	1
I3LA62	Centrosomal protein 112	CEP112	100.56	6.80	1
A0A287AKX3	Centrosomal protein 126	CEP126	108.15	9.07	1
A0A287AVF1	Centrosomal protein 152	CEP152	173.58	5.63	1
F1SB97	Centrosomal protein 164	CEP164	152.71	5.44	1
A0A287ANL3	Centrosomal protein 170	CEP170	140.48	7.91	1
A0A287AKA8	Centrosomal protein 170B	CEP170B	166.48	7.44	1
F1SMB8	Centrosomal protein 192		305.17	6.19	1
F1RJ04	Centrosomal protein 44	CEP44	40.59	5.57	1
F1SF36	Centrosomal protein 85 like	CEP85L	91.11	6.10	1
I3LC74	Chloride channel protein	CLCN7	101.42	9.09	1
A0A286ZW38	Chondroitin sulfate proteoglycan 5	CSPG5	62.72	4.75	1
F1S7L7	Chromatin assembly factor 1 subunit A	CHAF1A	105.30	5.73	1
A0A287BS23	Chromatin licensing and DNA replication factor 1	CDT1	54.79	10.43	1
I3L6N4	Chromodomain helicase DNA binding protein 1	CHD1	166.75	6.54	1
A0A286ZUW6	Chromodomain helicase DNA binding protein 3	CHD3	193.62	6.74	1
A0A287AIJ1	Chromodomain helicase DNA binding protein 6	CHD6	298.55	6.33	1
F1RPY8	Chromosome 11 open reading frame 84	C11orf84	41.26	4.78	1
F1SSL7	Chromosome 14 open reading frame 37	C14orf37	81.99	4.31	1
F1SSR1	Chromosome 15 open reading frame 52	C15orf52	48.61	10.08	1
F1RK67	Chromosome 16 open reading frame 96	C16orf96	83.14	6.06	1
F1RQY0	Chromosome 17 open reading frame 53	C17orf53	60.75	7.90	1
A0A287B8C7	Chromosome 18 open reading frame 54	C18orf54	57.14	7.72	1
A0A287AEB0	Chromosome 19 open reading frame 57	C19orf57	62.16	4.79	1
A0A287A943	Chromosome 2 open reading frame 42	C2orf42	56.06	9.04	1
A0A287B136	Chromosome 4 open reading frame 36	C4orf36	12.40	7.90	1
A0A287B7K2	Chromosome 5 open reading frame 15	C5orf15	29.44	5.02	1

I3LQ30	Chromosome 5 open reading frame 30	C5orf30	23.09	9.45	1
A0A287B2F6	Chromosome 5 open reading frame 42	C5orf42	226.10	6.79	1
A0A287BI14	Chromosome 7 open reading frame 31	C7orf31	67.40	7.68	1
A0A287AS77	Chromosome 9 open reading frame 3	C9orf3	92.15	6.58	1
K7GPI5	Chromosome X open reading frame 36	CXorf36	48.01	7.97	1
A0A286ZLQ5	Chromosome X open reading frame 67	CXorf67	52.15	11.97	1
F1SCV6	Cilia and flagella associated protein 46	CFAP46	248.27	7.34	1
A0A287A1C8	Cingulin like 1	CGNL1	141.24	5.68	1
A0A287AYK7	Class II major histocompatibility complex transactivator	CIITA	108.48	7.06	1
C3VPJ4	Claudin	CLDN7	22.30	8.22	1
A7UGA9	Coagulation factor II receptor (Fragment)	F2R	12.68	6.44	1
K7GQL2	Coagulation factor XIII A chain	F13A1	83.29	6.40	1
F1RJX8	Coatomer subunit alpha	COPA	138.35	7.66	1
A0A286ZXP6	Coatomer subunit gamma	COPG2	85.18	6.67	1
F1SPF9	Coatomer subunit gamma	COPG1	96.33	5.38	1
A0A287BDQ0	Coiled-coil domain containing 110	CCDC110	81.92	7.05	1
I3L859	Coiled-coil domain containing 114	CCDC114	67.62	6.87	1
F1SIK0	Coiled-coil domain containing 129	CCDC129	111.72	5.41	1
F1SMN4	Coiled-coil domain containing 136	CCDC136	133.43	5.12	1
A0A287B8B9	Coiled-coil domain containing 14	CCDC14	105.57	8.12	1
K7GLA1	Coiled-coil domain containing 160	CCDC160	37.69	9.04	1
F1SMR4	Coiled-coil domain containing 171	CCDC171	145.51	6.98	1
I3L6V1	Coiled-coil domain containing 181	CCDC181	53.96	5.11	1
F1RZ80	Coiled-coil domain containing 40	CCDC40	110.55	6.11	1
F1RG04	Coiled-coil domain containing 6	CCDC6	53.30	7.34	1
A0A287B162	Coiled-coil domain containing 61	CCDC61	58.18	10.39	1
I3LMB6	Coiled-coil domain containing 62	CCDC62	69.36	6.60	1
A0A287BC76	Coiled-coil domain containing 82	CCDC82	59.98	5.12	1
F1S6Y0	Coiled-coil domain-containing protein 28A	CCDC28A	20.40	8.13	1
A0A287BG56	Coiled-coil serine rich protein 1	CCSER1	80.53	8.29	1
F1SEP6	Coiled-coil serine rich protein 2	CCSER2	77.41	6.16	1
I3LUR7	Collagen type VI alpha 3 chain	COL6A3	317.61	6.30	1
A0A287A0A6	Collagen type VI alpha 6 chain	COL6A6	228.44	7.47	1
I3LDG8	Collagen type XXVII alpha 1 chain	COL27A1	183.37	9.77	1
I3LQQ8	Colony stimulating factor 3 receptor	CSF3R	94.18	6.23	1
F1SMJ1	Complement component C7	C7	92.79	6.79	1
I3LF91	Conserved oligomeric Golgi complex subunit 4	COG4	89.39	5.19	1

A0A287BPJ9	Contactin 1	CNTN1	70.65	6.29	1
F1RX25	Copine 4	CPNE4	64.35	6.64	1
F1RVT1	Copine 5	CPNE5	58.62	5.21	1
A0A287AKM8	Corneodesmosin	CDSN	49.07	8.72	1
A0A287ARJ6	Cramped chromatin regulator homolog 1	CRAMP1	105.18	7.30	1
K7GR17	Crystallin beta-gamma domain containing 1	CRYBG1	187.18	5.59	1
F1SQS3	CTP synthase	CTPS2	65.51	6.60	1
F1SBP5	CTTNBP2 N-terminal like	CTTNBP2NL	70.18	8.25	1
F1SV79	CUB and Sushi multiple domains 2	CSMD2	372.78	6.28	1
A0A287ALI0	CUB and Sushi multiple domains 3	CSMD3	380.83	5.91	1
A5GFR6	Cullin 7 (Fragment)	CUL7	130.97	6.70	1
F1RYI3	Cullin associated and neddylation dissociated 1	CAND1	119.51	5.92	1
F1S849	Cyclin and CBS domain divalent metal cation transport mediator 2	CNNM2	94.19	6.14	1
F1SSC2	Cyclin dependent kinase 13	CDK13	134.73	9.98	1
K7GRV3	Cyclin dependent kinase 16	CDK16	47.15	7.85	1
K7GL55	Cyclin dependent kinase like 5	CDKL5	105.84	9.58	1
F1SJR3	Cysteine and serine rich nuclear protein 1	CSRNP1	63.13	4.82	1
A0A287AWX7	Cysteine and serine rich nuclear protein 3	CSRNP3	66.62	4.75	1
Q68VB2	Cytochrome p450 2E1 (Fragment)	CYP2E1	7.00	9.01	1
A0A0H4IV24	Cytochrome P450 3A22	CYP3A22	57.28	9.11	1
A0A287BHW9	Cytochrome P450 family 2 subfamily W member 1	CYP2W1	49.91	9.41	1
A0A287AC13	Cytoplasmic linker associated protein 2	CLASP2	138.82	8.27	1
A0A287BLA0	DAZ interacting zinc finger protein 3	DZIP3	138.62	7.21	1
A0A287B5A7	DCC netrin 1 receptor	DCC	156.11	6.83	1
F1RT14	dCMP deaminase	DCTD	19.96	6.52	1
F1SJ00	DDB1 and CUL4 associated factor 1	DCAF1	149.53	5.05	1
A0A287BI06	DDB1 and CUL4 associated factor 5	DCAF5	94.87	5.33	1
A0A287BLY2	DDB1- and CUL4-associated factor 8	DCAF8	46.14	5.26	1
F1SLL4	DEAD (Asp-Glu-Ala-Asp) box polypeptide 4	DDX4	79.73	6.16	1
I3LU03	DEAD-box helicase 51	DDX51	75.12	8.53	1
I3LJ49	Decaprenyl diphosphate synthase subunit 1	PDSS1	41.99	7.93	1
F1SJ02	Dedicator of cytokinesis 3	DOCK3	216.26	6.92	1
A0A287BJH0	Dedicator of cytokinesis 8	DOCK8	236.51	6.89	1
A0A287AVY9	Dedicator of cytokinesis 9	DOCK9	258.27	8.57	1
Q4A3R3	Deleted in malignant brain tumors 1 protein	DMBT1	132.14	5.86	1
A0A287AF58	Delta-like protein	JAG1	127.69	5.91	1

A0A287BKW3	Dematin actin binding protein	DMTN	39.18	8.41	1
A0A287A999	DENN domain containing 1B	DENND1B	76.60	7.27	1
K7GN95	DENN domain containing 3	DENND3	128.75	7.09	1
I3L8H8	DENN domain containing 5B	DENND5B	127.87	6.98	1
A0A287BN08	DEP domain containing 5	DEPDC5	171.41	6.73	1
A0A287AQA5	Dermatan sulfate epimerase-like	DSEL	138.71	8.53	1
A0A287ATF2	Desmoglein 2	DSG2	102.90	5.10	1
A0A287AA14	Desmoplakin	DSP	228.93	6.68	1
F1RLY9	DExH-box helicase 34	DHX34	111.04	8.72	1
F1SF62	Diacylglycerol kinase	DGKB	87.39	8.24	1
F1RJ64	Diaphanous related formin 3	DIAPH3	134.53	7.11	1
A0A287A263	Dicer 1, ribonuclease III	DICER1	211.34	5.94	1
A0A287BQR7	Dihydropyrimidinase like 2	DPYSL2	59.73	6.67	1
K7GMK0	Dipeptidyl peptidase 4	DPP4	83.05	5.88	1
I3L8J8	Disco interacting protein 2 homolog B	DIP2B	169.82	8.44	1
F1STU6	Discs large MAGUK scaffold protein 2	DLG2	92.61	6.77	1
A0A287BN19	Dishevelled associated activator of morphogenesis 1	DAAM1	122.15	7.34	1
F1RJE5	Dishevelled segment polarity protein 1	DVL1	75.41	7.61	1
E7FM66	Disintegrin and metalloprotease domain-containing protein 5 (Fragment)	ADAM5	45.17	7.93	1
F1SM80	DLG associated protein 1	DLGAP1	75.52	5.91	1
A0A287AJA2	DLG associated protein 3	DLGAP3	106.78	8.70	1
A0A286ZIC4	DLG associated protein 4	DLGAP4	105.73	7.17	1
F1SSN9	DLG associated protein 5	DLGAP5	96.19	8.98	1
I3LDN4	Dmx like 1	DMXL1	342.10	6.42	1
F1S5H8	DNA cross-link repair 1A	DCLRE1A	119.14	8.18	1
A0A287AFT6	DNA polymerase alpha 2, accessory subunit	POLA2	54.08	5.14	1
A0A287A3Z7	DNA polymerase iota	POLI	65.04	7.43	1
B0M1M8	DNA repair protein RAD54	pigRAD54	84.27	8.79	1
O46374	DNA topoisomerase 2-alpha	TOP2A	174.20	8.69	1
F1RWU2	Doublecortin	DCX	39.98	9.39	1
A0A286ZWQ7	Doublecortin like kinase 1	DCLK1	82.21	8.66	1
F1S252	Dual specificity phosphatase 27 (putative)	DUSP27	129.30	5.16	1
A0A286ZRC7	Dynactin subunit 1	DCTN1	138.39	5.44	1
F1S8V8	Dynamin binding protein	DNMBP	177.35	5.55	1
I3LNF2	Dynein axonemal heavy chain 1	DNAH1	497.36	6.14	1
F1SC07	Dynein axonemal heavy chain 11	DNAH11	518.31	6.34	1
F1ST22	Dynein axonemal heavy chain 2	DNAH2	499.57	6.48	1

A0A286ZQY1	Dynein axonemal heavy chain 5	DNAH5	527.61	6.06	1
A0A287AHL5	Dynein axonemal heavy chain 7	DNAH7	460.26	6.09	1
A0A286ZSC6	Dynein axonemal heavy chain 8	DNAH8	508.78	6.27	1
F1SS52	Dynein axonemal heavy chain 9	DNAH9	509.28	5.91	1
A0A287B9W3	Dynein cytoplasmic 1 heavy chain 1	DYNC1H1	428.13	6.34	1
A0A286ZWC7	Dynein cytoplasmic 1 intermediate chain 1	DYNC1I1	70.72	5.22	1
F1RRE0	Dynein cytoplasmic 1 light intermediate chain 1	DYNC1LI1	52.73	6.24	1
K9IVT3	E3 ubiquitin-protein ligase RBBP6	RBBP6	200.98	9.61	1
K9J4S2	E3 ubiquitin-protein ligase TRIM11	TRIM11	53.00	5.54	1
K9J6M4	E3 ubiquitin-protein ligase UBR4	UBR4	572.61	6.04	1
I3LDY1	Echinoderm microtubule associated protein like 1	EML1	92.03	7.80	1
K7GPY3	Ectodysplasin A	EDA	41.34	9.03	1
A0A287B922	EH domain binding protein 1	EHBP1	120.40	5.24	1
A0A0U2ETC2	Emerin	EMD	29.19	5.52	1
F1SMM0	Endoplasmic reticulum metallopeptidase 1	ERMP1	111.00	8.48	1
F1S2J4	Enhancer of mRNA decapping 4	EDC4	151.56	5.90	1
F1S0I9	Enhancer of polycomb homolog	EPC2	75.57	8.88	1
A0A287ACP9	Enoyl-CoA hydratase and 3-hydroxyacyl CoA dehydrogenase	EHHADH	79.63	8.75	1
F1RW07	Envoplakin	EVPL	214.34	7.55	1
A0A286ZX47	Eomesodermin	EOMES	74.73	7.36	1
I3LEB9	EPH receptor B1	EPHB1	109.74	6.35	1
B5M6R3	Ephrin receptor A4	EphA4	109.87	6.81	1
F1RLP4	Ephrin-B2	EFNB2	33.72	8.97	1
A0A287AWG7	Epidermal growth factor receptor pathway substrate 15 like 1	EPS15L1	94.08	5.12	1
F1RLA2	Epididymal sperm-binding protein 1	ELSPBP1	26.21	7.39	1
A0A287BSL2	ERCC excision repair 2, TFIIH core complex helicase subunit	ERCC2	81.11	6.67	1
F1RLR4	ERCC excision repair 4, endonuclease catalytic subunit	ERCC4	102.16	6.79	1
I3LFY4	ERCC excision repair 6 like, spindle assembly checkpoint helicase	ERCC6L	140.40	5.14	1
K9J6J2	Erythrocyte band 7 integral membrane protein isoform a	STOM_tv1	31.17	7.75	1
A0A287A1W8	Erythrocyte membrane protein band 4.1	EPB41	83.57	5.34	1
I3LUL5	Erythrocyte membrane protein band 4.1 like 2	EPB41L2	110.34	5.17	1
A0A287A7J6	Erythroid differentiation regulatory factor 1	EDRF1	132.99	6.02	1
F1SJI0	Espin like	ESPNL	105.25	6.65	1
A0A287ACC5	Eukaryotic elongation factor, selenocysteine-tRNA specific	EEFSEC	39.58	8.85	1

F1S1J9	Eukaryotic translation initiation factor 3 subunit H	EIF3H	37.12	6.96	1
A0A287BKE1	Eukaryotic translation initiation factor 4 gamma 2	EIF4G2	102.85	7.56	1
A0A287B8Y7	Eukaryotic translation initiation factor 4 gamma 3	EIF4G3	176.02	5.29	1
F1RLV6	Eukaryotic translation initiation factor 4E nuclear import factor 1	EIF4ENIF1	108.19	8.48	1
A0A287APJ8	Exonuclease 3'-5' domain containing 1	EXD1	53.71	6.48	1
A0A286ZTA7	Exportin 6	XPO6	128.17	6.46	1
F1RMC3	Exportin 7	XPO7	123.85	6.32	1
A0A287AH93	Extended synaptotagmin 1	ESYT1	115.10	6.34	1
O62714	Extracellular calcium-sensing receptor	CASR	120.28	5.86	1
I3LGM0	F-box and WD repeat domain containing 11	FBXW11	60.98	7.27	1
F1S8T9	F-box and WD repeat domain containing 4	FBXW4	45.74	7.99	1
I3LJX1	Family with sequence similarity 126 member A	FAM126A	57.43	8.16	1
K7GR11	Family with sequence similarity 133 member A	FAM133A	28.71	10.01	1
F1RRW0	Family with sequence similarity 135 member B	FAM135B	154.40	5.63	1
A0A286ZQL4	Family with sequence similarity 169 member A	FAM169A	63.91	4.50	1
A0A287AE59	Family with sequence similarity 185 member A	FAM185A	37.97	6.98	1
F1SHB0	Family with sequence similarity 186 member B	FAM186B	91.83	9.19	1
I3L912	Family with sequence similarity 205 member A	FAM205A	152.72	7.93	1
A0A287AVE7	Family with sequence similarity 214 member A	FAM214A	112.14	7.68	1
F1RQD7	Family with sequence similarity 71 member B	FAM71B	61.35	9.74	1
F1RZW2	Family with sequence similarity 83 member B	FAM83B	114.41	9.01	1
A0A286ZLX4	Family with sequence similarity 83 member E	FAM83E	46.30	5.25	1
A0A286ZMB6	Family with sequence similarity 91 member A1	FAM91A1	84.53	5.85	1
A0A287AKI1	Fanconi anemia complementation group D2	FANCD2	154.23	6.01	1
F1ST47	FAST kinase domain-containing protein 4	TBRG4	58.76	9.13	1
A0A287BQC4	FAT atypical cadherin 3	FAT3	354.54	4.91	1
A0SXU8	Fatty acid binding protein 4 (Fragment)	FABP4	12.67	4.81	1
Q58GK8	Fatty acid synthase (Fragment)	FASN	250.98	6.60	1
K7GP71	Fc fragment of IgA and IgM receptor	FCAMR	50.78	8.54	1
F1RJ82	Fc receptor like 6	FCRL6	52.76	8.84	1
A0A286ZT03	FCH domain only 2	FCHO2	82.67	6.51	1
B7TJ17	Feline leukemia virus subgroup C cellular receptor family member 2		59.42	7.11	1

A0A286ZIC2	FERM domain containing 4B	FRMD4B	89.32	9.00	1
F1SN02	FERM domain containing 5	FRMD5	28.51	7.24	1
F1SFE3	Fermitin family member 2	FERMT2	80.74	6.92	1
F1RSA9	FH2 domain containing 1	FHDC1	102.16	9.16	1
F1SA65	Fibrillin 3	FBN3	297.82	5.08	1
A0A287B086	Fibroblast growth factor (FGF)	FGF8	24.91	10.33	1
F1SS24	Fibronectin 1	FN1	270.43	5.60	1
F1SUA0	Fibulin 7	FBLN7	60.67	8.43	1
A0A287A305	Filamin A	FLNA	244.39	6.16	1
A0A286ZRX8	Filamin C	FLNC	286.40	5.96	1
F1RKS3	Flap endonuclease 1	FEN1	42.38	8.62	1
A0A286ZX52	Flavin-containing monooxygenase	LOC100151788	59.64	8.82	1
A0A287B3W9	FMR1 autosomal homolog 2	FXR2	63.56	8.03	1
A0A287AVP3	Focadhesin	FOCAD	196.51	6.35	1
F1RR95	Forkhead box I1	FOXI1	40.22	6.68	1
F1SDA9	Forkhead box protein N3	FOXN3	50.99	7.33	1
A0A286ZUP3	Formin 1	FMN1	93.51	7.40	1
A0A287A2S9	Formin binding protein 1	FNBP1	67.02	6.02	1
A0A287B9J8	Formin homology 2 domain containing 3	FHOD3	156.55	5.97	1
A0A287BKE6	Forty-two-three domain containing 1	FYTTD1	30.56	11.74	1
A0A287BGJ4	FRAS1 related extracellular matrix 1	FREM1	244.74	6.07	1
A0A287BDX3	Furin, paired basic amino acid cleaving enzyme	FURIN	78.36	6.70	1
A0A287AC26	FYVE, RhoGEF and PH domain containing 4	FGD4	76.91	5.69	1
F1SPI5	FYVE, RhoGEF and PH domain containing 5	FGD5	163.50	5.00	1
K7GPE3	G protein nucleolar 3 like	GNL3L	76.73	9.19	1
F1S3A2	G protein regulated inducer of neurite outgrowth 1	GPRIN1	101.97	7.56	1
I3LGL5	G protein signaling modulator 2	GPSM2	73.45	6.62	1
I3L9D3	G protein-coupled receptor 149	GPR149	72.76	6.67	1
F1SQJ6	G protein-coupled receptor 75	GPR75	58.53	9.13	1
M9NIX2	G protein-coupled receptor 84	GPR84	43.65	9.50	1
A0A287ANR1	G protein-coupled receptor 88	GPR88	40.05	9.67	1
F2YHM2	G protein-regulated inducer of neurite outgrowth 2	GPRIN2	47.28	6.35	1
A0A287BKS3	Gametogenetin binding protein 2	GGNBP2	72.99	6.24	1
A0A287A779	Gamma-aminobutyric acid type A receptor alpha2 subunit	GABRA2	56.07	9.41	1
I3LIV9	Gamma-aminobutyric acid type A receptor alpha4 subunit	GABRA4	61.16	9.26	1

A0A287A460	Gamma-aminobutyric acid type A receptor gamma3 subunit	GABRG3	35.52	8.00	1
I3L6R6	Gamma-aminobutyric acid type B receptor subunit 2	GABBR2	105.74	8.66	1
F1SM11	Gastrulation brain homeobox 2	GBX2	37.29	8.38	1
I3LQJ4	GDNF family receptor alpha 2	GFRA2	36.58	8.16	1
I3LFM4	GDNF family receptor alpha 4	GFRA4	30.04	9.17	1
A0A287AU82	Gem nuclear organelle associated protein 5	GEMIN5	140.10	6.60	1
A0A287BA83	General transcription factor IIH subunit 1	GTF2H1	51.04	7.85	1
I3LSG1	General transcription factor IIi	GTF2I	108.13	7.94	1
A0A287BNN6	Gephyrin	GPHN	37.47	5.15	1
A0A287AUV0	GIT ArfGAP 1	GIT1	77.43	6.51	1
M4QCJ2	Glucocorticoid receptor variant P	NR3C1	73.67	6.71	1
F1S070	Glucosaminyl (N-acetyl) transferase 3, mucin type	GCNT3	51.20	8.50	1
A0A287B6T4	Glutamate ionotropic receptor AMPA type subunit 4	GRIA4	95.63	7.75	1
A0A068F143	Glutathione peroxidase		22.65	6.55	1
A0A287A6H1	Glutathione S-transferase alpha M14	GSTA1	20.29	9.11	1
F1SMN8	Glycine cleavage system P protein	GLDC	113.09	7.09	1
A0A287A756	Glycogenin 2	GYG2	51.39	5.05	1
F1SII4	Glycyl-tRNA synthetase	GARS	83.21	7.37	1
F1ST73	Glyoxylate and hydroxypyruvate reductase	GRHPR	35.80	7.94	1
A0A287A4T8	Glyoxylate reductase 1 homolog	GLYR1	60.52	9.17	1
A5GFU3	GNAS complex locus (Fragment)	GNAS	44.54	9.01	1
A0A287BTI4	Golgin A3	GOLGA3	158.17	5.31	1
F1RRC2	Golgin A4	GOLGA4	253.80	5.22	1
A0A287AE97	GPI-anchor transamidase	PIGK	45.16	6.47	1
F1STW0	Grainyhead like transcription factor 3	GRHL3	62.16	6.84	1
A0A287AFV0	GRAM domain containing 1C	GRAMD1C	52.56	8.07	1
A0A286ZI87	Granzyme B precursor	GZMB	27.38	9.47	1
F1SAL5	GRB2 associated regulator of MAPK1 subtype 1	GAREM1	96.23	6.67	1
F1S4G0	Growth factor independent 1 transcriptional repressor	GFI1	44.49	9.11	1
F1RPN5	Growth factor receptor bound protein 14	GRB14	51.91	8.60	1
F1SBC3	Growth regulation by estrogen in breast cancer 1 like	GREB1L	211.46	6.68	1
I3LIY1	GTPase activating Rap/RanGAP domain like 3	GARNL3	119.58	7.81	1
A0A286ZY37	Guanine monophosphate synthase	GMPS	76.68	6.87	1
A0A287BAY2	Guanine nucleotide-binding protein subunit gamma		11.43	8.63	1

A0A287A0M1	Heat shock protein beta-7	HSPB7	18.47	6.13	1
A0A286ZJM5	HECT, C2 and WW domain containing E3 ubiquitin protein ligase 2	HECW2	160.97	5.44	1
A0A287AP70	Helicase like transcription factor	HLTF	107.81	8.78	1
F1S0Y1	Hemicentin 2	HMCN2	539.63	6.01	1
A0A286ZHV7	Heparan sulfate proteoglycan 2	HSPG2	450.80	6.52	1
F1S794	Hepatic and glial cell adhesion molecule	HEPACAM	51.62	8.91	1
K7GPY4	Hepatocyte growth factor receptor	MET	147.45	7.14	1
A0A287A5A9	Hephaestin	HEPH	116.08	6.33	1
F1RWM2	Hes related family bHLH transcription factor with YRPW motif 1	HEY1	32.53	8.95	1
Q06A94	Heterogeneous nuclear ribonucleoprotein A1	HNRNPA1L2	34.18	9.23	1
A0A287AEJ3	Heterogeneous nuclear ribonucleoprotein A2/B1	HNRNPA2B1	31.14	9.14	1
A0A287BMJ1	HFM1, ATP dependent DNA helicase homolog	HFM1	154.17	7.87	1
A0A286ZYE1	HID1 domain containing	HID1	81.84	5.90	1
A0A286ZIF3	High density lipoprotein binding protein	HDLBP	131.32	7.12	1
A0A2C9F359	Hippocalcin-like protein 1	HPCAL1	23.35	5.94	1
A0A287A876	Histidyl-tRNA synthetase 2, mitochondrial	HARS2	51.24	8.27	1
A0A287AZX7	Histone acetyltransferase	KAT6B	210.26	5.48	1
A0A287BQF9	Histone deacetylase	HDAC4	118.35	6.92	1
K7GKQ3	Histone deacetylase 9	HDAC9	71.91	8.68	1
B1PEY3	Histone H2A	H2A.Z	13.54	10.58	1
A0A287BKD2	Histone-lysine N-methyltransferase	SETDB1	126.13	7.74	1
A0A287BNJ8	Histone-lysine N-methyltransferase	KMT5B	98.16	8.97	1
F1S1G9	Histone-lysine N-methyltransferase EZH1	EZH1	85.65	7.31	1
F1S8I5	Histone-lysine N-methyltransferase, H3 lysine-79 specific	DOT1L	136.73	9.82	1
I3LHP9	HMG-box containing 3	HMGXB3	127.33	6.80	1
A0A287ALW7	Homeobox protein cut-like	CUX2	153.59	5.50	1
A0A287AUN5	Homeobox protein engrailed-like	EN2	34.96	9.52	1
A0A286ZNT4	Homeodomain interacting protein kinase 3	HIPK3	129.22	7.28	1
A0A287AYK4	HPS4, biogenesis of lysosomal organelles complex 3 subunit 2	HPS4	66.31	5.17	1
A0A286ZRA0	Huntingtin	HTT	286.61	6.35	1
F1REX8	Huntingtin interacting protein 1 related	HIP1R	119.68	6.61	1
I3LBK1	HUS1 checkpoint clamp component	HUS1	29.65	7.66	1
K7GSC4	Hyaluronan mediated motility receptor	HMMR	82.31	5.83	1
B2ZF49	Hydroxyacyl-coenzyme A dehydrogenase/3-ketoacyl-coenzyme A thiolase/enoyl-coenzyme A hydratase alpha subunit	HADHA	83.20	9.20	1

Q8MKG1	Hydroxysteroid 11-beta dehydrogenase 2	HSD11B2	43.55	8.73	1
A0A287A3B5	Hydroxysteroid 17-beta dehydrogenase 4	HSD17B4	77.92	8.18	1
A0A287ARN0	Hyperpolarization activated cyclic nucleotide gated potassium and sodium channel 2	HCN2	82.05	9.28	1
K7ZRJ8	IgD heavy chain constant region (Fragment)	IGHD	42.59	8.65	1
A0A287A8D0	IGF like family receptor 1	IGFLR1	32.44	8.05	1
I3LDI3	Immunity related GTPase Q	IRGQ	56.21	4.91	1
F1SAX8	Immunoglobulin superfamily member 3	IGSF3	133.63	6.20	1
F1S6C8	Immunoglobulin superfamily member 9B	IGSF9B	135.22	7.80	1
A0A286ZZ03	Immunoglobulin-like and fibronectin type III domain containing 1	IGFN1	268.38	6.34	1
F1RGZ3	Inactive rhomboid protein	RHBDF1	93.80	8.63	1
F1RQL8	Inhibitor of Bruton tyrosine kinase	IBTK	149.37	7.90	1
F1SML7	Inosine-5'-monophosphate dehydrogenase	IMPDH1	61.28	6.77	1
F1RZR0	Inositol 1,4,5-trisphosphate receptor type 3	ITPR3	303.55	6.54	1
F1RRG5	Inositol polyphosphate-4-phosphatase type II B	INPP4B	104.95	6.40	1
B2CS61	Inositol polyphosphate-5-phosphatase F (Fragment)	INPP5F	28.93	5.59	1
C8ZKV5	Insulin receptor substrate 4	IRS4	133.37	8.56	1
Q8MJI5	Insulin-like-growth factor 2 preproprotein (Fragment)	IGF2	13.87	8.31	1
A0A286ZN02	Integrator complex subunit 12	INTS12	43.26	9.52	1
F1S2U7	Integrator complex subunit 7	INTS7	92.43	7.61	1
A0A287BHP4	Integrin beta	ITGB5	85.02	6.67	1
F1SGE7	Integrin beta	ITGB7	87.42	6.19	1
F1SMF4	Integrin subunit alpha 2	ITGA2	129.26	5.31	1
F1RYP4	Integrin subunit alpha 4	ITGA4	107.36	6.77	1
K7GT68	Integrin subunit alpha 6	ITGA6	121.37	7.25	1
K7GSU6	Integrin subunit alpha E	ITGAE	125.22	6.28	1
A0A286ZTM0	Integrin subunit alpha X	ITGAM	126.76	7.11	1
A0A287B963	Interferon gamma receptor 2 precursor	IFNGR2	41.36	7.40	1
F1RSZ7	Interferon regulatory factor	IRF2	39.28	7.15	1
F1SGL1	Interleukin 17 receptor D	IL17RD	81.89	7.36	1
K7GM13	Interleukin-27 receptor subunit alpha precursor	IL27RA	71.89	5.24	1
F1RQJ9	Interphotoreceptor matrix proteoglycan 1	IMPG1	79.61	5.57	1
A0A287B997	Intersectin 2		125.27	8.59	1
F1RUI3	IQ motif and Sec7 domain 2	IQSEC2	162.62	8.56	1
I3LV91	IQ motif containing GTPase activating protein 2	IQGAP2	171.65	6.04	1
F1S043	Iroquois homeobox 4	IRX4	53.89	6.47	1

I3LA26	Islet cell autoantigen 1	ICA1	57.37	5.80	1
A0A286ZQY6	Isocitrate dehydrogenase [NAD] subunit, mitochondrial	IDH3A	39.63	7.39	1
K7GRA9	Jade family PHD finger 3	JADE3	93.31	7.03	1
A0A287BJZ7	Jrk helix-turn-helix protein	JRK	56.62	8.98	1
A0A286ZMK7	Jumonji and AT-rich interaction domain containing 2	JARID2	133.56	9.25	1
A0A287BCR9	Junctional cadherin 5 associated	JCAD	125.53	6.92	1
A0A286ZVV5	KAT8 regulatory NSL complex subunit 3	KANSL3	89.39	9.36	1
A0A287BIU1	Kelch like family member 34	KLHL34	71.10	5.83	1
F1SUM8	Kelch like family member 35	KLHL35	62.20	6.86	1
F1SGG1	Keratin 18	KRT18	47.39	5.38	1
A0A287AZL3	Keratin 5	KRT5	60.42	8.27	1
A0A287ASI0	Keratin 7	KRT7	50.76	5.57	1
A0A286ZJM8	Keratin 77	KRT77	63.26	8.35	1
F1STQ5	Keratinocyte differentiation factor 1	KDF1	43.25	6.54	1
I3L5J8	Keratinocyte proline rich protein	KPRP	59.06	8.21	1
I3LM92	KIAA0586	KIAA0586	93.64	9.63	1
A0A286ZYH1	KIAA0895	KIAA0895	54.56	9.55	1
A0A287BGE3	KIAA1024	KIAA1024	87.48	7.12	1
F1SR15	KIAA1549	KIAA1549	198.92	6.00	1
F1SGR4	KIAA1549 like	KIAA1549L	153.47	9.55	1
A0A287BMQ9	KIAA1551	KIAA1551	185.10	8.05	1
F1S679	KIAA1614	KIAA1614	123.71	9.52	1
F1SNA7	KIAA1958	KIAA1958	79.13	6.83	1
F1SQ43	Killer cell lectin-like receptor subfamily A, member 1	LY49	30.74	8.15	1
F1SPR3	Kinase	IP6K1	50.05	7.24	1
F1SSV7	Kinase	ITPKA	46.93	7.91	1
F1S9L5	Kinase D interacting substrate 220	KIDINS220	168.59	6.81	1
I3L676	Kinesin family member 13A	KIF13A	197.40	5.57	1
A0A287B858	Kinesin family member 14	KIF14	174.19	7.52	1
I3LEQ5	Kinesin family member 16B	KIF16B	145.65	6.21	1
F1RIF9	Kinesin family member 1B	KIF1B	180.94	5.92	1
F1SEB0	Kinesin family member 24	KIF24	134.11	7.78	1
A0A286ZJV7	Kinesin-like protein	KIF12	58.83	9.01	1
A0A287A466	Kinesin-like protein	KIFC3	104.34	7.55	1
A0A287A7U4	Kinesin-like protein	KIF3A	78.28	6.34	1
A0A287AHP4	Kinesin-like protein	KIF18A	88.48	9.07	1

F1RH90	Kinesin-like protein	KIF20A	100.20	6.68	1
A0A287BG55	KN motif and ankyrin repeat domains 1	KANK1	127.31	5.03	1
C7EMF4	Kruppel-like factor 16	KLF16	25.67	10.13	1
D4N875	L-lactate dehydrogenase (Fragment)		17.07	9.52	1
A0A287AKJ3	La ribonucleoprotein domain family member 1	LARP1	102.74	8.44	1
F1S150	La-related protein 7	LARP7	66.65	9.55	1
A0A287BIL2	Lamin tail domain containing 1	LMNTD1	52.83	9.11	1
A0A287ACS7	Laminin subunit beta 4	LAMB4	186.34	6.60	1
F1S662	Laminin subunit gamma 2	LAMC2	130.80	6.64	1
F1S0W7	Laminin subunit gamma 3	LAMC3	169.90	6.86	1
A0A2C9F3H8	Large proline-rich protein BAG6	BAG6	118.47	5.66	1
A0A286ZJW0	Late cornified envelope 3B	LCE3B	9.58	8.29	1
I3LGU6	LCA5L, lebercilin like	LCA5L	74.57	9.45	1
A0A287A9G6	LDL receptor related protein 10	LRP10	61.53	5.10	1
A0A286ZWL1	Leiomodin 1	LMOD1	65.69	9.45	1
A0A287AYA3	Leucine rich adaptor protein 1 like	LURAP1L	24.94	5.34	1
I3LEH7	Leucine rich repeat and fibronectin type III domain containing 5	LRFN5	79.09	7.91	1
F1RWI9	Leucine rich repeat containing 46	LRRC46	35.60	5.49	1
I3LK56	Leucine rich repeat LGI family member 2	LGI2	62.29	6.80	1
A0A287BHH5	Leucine rich repeat LGI family member 3	LGI3	73.06	9.11	1
A0A287AQJ2	Leucine rich repeats and calponin homology domain containing 3	LRCH3	79.71	6.73	1
F1RKA3	Leucine zipper like transcription regulator 1	LZTR1	84.92	6.25	1
I3LI93	Leucyl-tRNA synthetase 2, mitochondrial	LARS2	98.24	7.96	1
A0A287AJF9	LIF receptor alpha	LIFR	118.65	5.58	1
A0A287BMW8	Ligand dependent nuclear receptor corepressor	LCOR	154.61	7.40	1
I3LDR7	Ligand of numb-protein X 1	LNX1	69.42	7.55	1
A0A287A5K6	LIM and calponin homology domains 1		101.54	5.66	1
A0A287BRA7	LIM domain-binding protein 1	LDB1	42.56	6.54	1
I3LB53	Lin-54 DREAM MuvB core complex component	LIN54	79.13	8.97	1
K7GT47	Linker for activation of T-cells	LAT	25.03	4.21	1
C5GZQ1	Lipin 1		98.77	6.60	1
K7GRR0	Low-density lipoprotein receptor	LDLR	87.34	4.93	1
F1RS89	LPS responsive beige-like anchor protein	LRBA	273.19	5.41	1
F1RMV7	LY6/PLAUR domain containing 3	LYPD3	35.97	7.59	1
Q7YS22	Lymphatic endothelial hyaluronan receptor LYVE-1 (Fragment)		22.21	8.63	1
A0A287AF50	Lysine demethylase 1B		108.47	8.48	1

I3LLP0	Lysine demethylase 2A	KDM2A	130.52	7.59	1
F1SVC8	Lysine demethylase 3A	KDM3A	141.24	7.74	1
F1RH75	Lysine demethylase 3B	KDM3B	189.09	7.20	1
I3LG07	Lysine demethylase 6B	KDM6B	154.71	8.48	1
I3L5A1	Lysine methyltransferase 2C	KMT2C	453.02	5.88	1
A0A287A2S7	Lysyl oxidase like 1	LOXL1	59.31	7.12	1
F2Z593	Mab-21 like 1	MAB21L1	42.45	8.85	1
Q2TLZ2	Macoilin	MACO1	76.10	9.07	1
I3LR56	MAM domain-containing protein 2	MAMDC2	61.94	5.16	1
K7GKU8	Mannan binding lectin serine peptidase 2	MASP2	90.86	6.57	1
I3W8V5	Mast/stem cell growth factor receptor	KIT	109.06	6.51	1
F1S0M0	Matrilin 2	MATN2	100.42	6.68	1
F1SV70	Matrix metalloproteinase	MMP27	58.87	8.31	1
A0A287AN90	Matrix metalloproteinase-9 precursor	MMP9	74.59	5.91	1
F1RZ06	Matrix remodeling associated 5	MXRA5	304.15	8.34	1
A0A287BLQ2	MCF.2 cell line derived transforming sequence like	MCF2L	114.06	6.52	1
A0A287AWR6	Mediator of RNA polymerase II transcription subunit 13	MED13L	227.45	6.05	1
F1SFN4	Melanogenesis associated transcription factor	MITF	54.58	6.71	1
F1SA51	Membrane associated ring-CH-type finger 2	MARCH2	27.06	7.68	1
I3LD34	Membrane spanning 4-domains A14	MS4A14	96.49	5.60	1
F1RYM0	Methyltransferase like 25	METTL25	53.24	7.40	1
L7WLW9	MHC class I antigen	SLA-1	40.13	5.72	1
Q0MRZ9	MHC class I antigen	SLA	40.04	5.49	1
Q8MHT8	MHC class I antigen	SLA-3	40.16	5.62	1
Q6PU47	Microphthalmia-associated transcription factor (Fragment)	Mitf	10.51	4.88	1
A0A287A4B3	Microtubule affinity regulating kinase 2	MARK2	71.38	9.89	1
A0A286ZMY1	Microtubule associated scaffold protein 1	MTUS1	136.58	6.40	1
F1SDY2	Microtubule associated serine/threonine kinase 1	MAST1	170.80	8.35	1
A0A287BS27	Microtubule associated serine/threonine kinase like	MASTL	91.82	5.82	1
I3LA85	Microtubule crosslinking factor 1	MTCL1	172.53	5.34	1
A0A287AAQ4	Microtubule-associated protein	MAPT	52.66	8.97	1
F1S6Q6	Midnolin	MIDN	48.41	9.54	1
F1SII8	MINDY lysine 48 deubiquitinase 4	MINDY4	82.00	6.18	1
A0A287AAJ6	Misshapen like kinase 1	MINK1	145.68	7.46	1
F1S8C6	Mitochondrial antiviral signaling protein	MAVS	55.06	5.66	1
F1RWE3	Mitochondrial poly(A) polymerase	MTPAP	66.90	9.07	1

E7BXW8	Mitochondrial poly(A) RNA polymerase		64.92	8.82	1
A0A287A9T5	Mitochondrial transcription termination factor 1	MTERF1	47.94	9.63	1
A0A287BGQ1	Mitofusin 2	MFN2	80.91	6.67	1
F1SSW0	Mitogen-activated protein kinase binding protein 1	MAPKBP1	157.84	6.98	1
A0A287B2Q3	Mitogen-activated protein kinase kinase kinase 11	MAP3K11	93.76	8.53	1
F1S066	Mitogen-activated protein kinase kinase kinase 20	MAP3K20	91.53	8.12	1
F1S495	Mitogen-activated protein kinase kinase kinase 9	MAP3K9	100.89	8.22	1
A0A287AAW0	Mitoguardin 1	MIGA1	65.79	6.67	1
A0A287AG21	MLLT10, histone lysine methyltransferase DOT1L cofactor	MLLT10	100.53	8.32	1
F1SNG3	MLLT3, super elongation complex subunit	MLLT3	63.21	8.57	1
A0A286ZYY9	MLX interacting protein like	MLXIPL	92.43	8.38	1
A0A287BQM3	MON2 homolog, regulator of endosome-to-Golgi trafficking	MON2	160.97	6.32	1
F1RPD9	MORC family CW-type zinc finger 2	MORC2	109.10	8.85	1
I3LA16	mRNA cap guanine-N7 methyltransferase	RNMT	53.55	6.29	1
A0A287BCF4	Msh homeobox 2	MSX2	28.95	9.67	1
A0A287B2N6	MTSS1L, I-BAR domain containing	MTSS1L	76.04	8.07	1
A0A287ANG4	Mucin 5AC, oligomeric mucus/gel-forming	MUC5AC	439.56	6.39	1
F1RW71	Multimerin 1	MMRN1	137.73	8.29	1
A0A286ZQ26	Multiple PDZ domain crumbs cell polarity complex component	MPDZ	212.10	5.15	1
A0A287ANI0	Muscarinic acetylcholine receptor	CHRM3	66.00	9.32	1
A0A287BAI1	Muscarinic acetylcholine receptor	CHRM2	51.67	8.85	1
F1RLH9	Mutated in colorectal cancers	MCC	92.85	5.52	1
F1RKR3	Myelin regulatory factor	MYRF	109.19	8.70	1
A0A287A7V5	Myelin-oligodendrocyte glycoprotein	MOG	23.67	7.81	1
A2TF48	Myeloid differentiation primary response protein MyD88	MYD88	33.23	6.55	1
A0A287B2V4	Myocardin	MYOCD	100.44	6.61	1
F1SM75	Myomesin 1	MYOM1	174.89	6.29	1
A0A286ZT24	Myosin IIIB	MYO3B	135.01	8.22	1
A0A287A896	Myosin IXA	MYO9A	295.99	9.01	1
A0A287BJA3	Myosin IXB	MYO9B	222.47	9.03	1
A0A287A9P3	Myosin light chain kinase, smooth muscle	MYLK	194.64	5.95	1
P60662	Myosin light polypeptide 6	MYL6	16.92	4.65	1
A0A287AQW0	Myosin phosphatase Rho interacting protein	MPRIP	110.16	6.47	1
F1RQH5	Myosin VIIB	MYO7B	244.32	8.78	1

F1SRM1	Myosin X	MYO10	236.05	6.38	1
F1RG85	Myosin XVIIIB	MYO18B	269.31	6.80	1
F1SKI0	Myosin-11	MYH11	197.17	5.81	1
F1RRV6	N-myc downstream regulated 1	NDRG1	40.39	5.95	1
A0A287B6Y5	N(alpha)-acetyltransferase 16, NatA auxiliary subunit	NAA16	63.17	8.07	1
A0A287AAH4	Na(+)/H(+) exchange regulatory cofactor NHE-RF	SLC9A3R1	36.26	6.05	1
A5GFM6	NACHT, leucine rich repeat and PYD containing 7 (Fragment)	NALP7	104.01	6.86	1
C3W331	NAD-dependent protein deacetylase	SIRT2	39.39	7.25	1
F1SHA6	NCK associated protein 5 like	NCKAP5L	138.79	8.05	1
I3LGV4	NDC1 transmembrane nucleoporin	NDC1	87.29	8.94	1
F1SBC5	NDC80, kinetochore complex component	NDC80	73.86	5.73	1
A2TEQ2	Nectin cell adhesion molecule 2	prr2	51.49	5.57	1
A0A287A7Y7	NEDD4 binding protein 1	N4BP1	95.58	5.59	1
F1S279	Nephroblastoma overexpressed	NOV	39.20	8.00	1
A0A287AE01	Neuregulin 1	NRG1	70.06	8.60	1
F1SCR9	Neuroblastoma amplified sequence	NBAS	263.16	5.94	1
F1SBI5	Neuroendocrine convertase 2	PCSK2	64.16	6.62	1
F1RJ58	Neurofibromin 1	NF1	319.26	7.39	1
F1SHH0	Neuronal PAS domain protein 3	NPAS3	72.22	6.80	1
A0A287A653	Neuronal tyrosine-phosphorylated phosphoinositide-3-kinase adaptor 2	NYAP2	70.12	8.94	1
F1SK07	Neuronal vesicle trafficking associated 2	NSG2	35.38	9.88	1
Q99331	Neutrophil protein (Fragment)		31.04	10.78	1
F1RUA7	NFKB activating protein	NKAP	47.18	10.07	1
I3L8Y5	NHS like 2	NHSL2	100.48	7.81	1
F1RS42	NIMA related kinase 10	NEK10	126.65	6.95	1
F1S2Q4	NIMA related kinase 9	NEK9	118.70	6.92	1
A0A287ACX2	Ninein	NIN	241.44	5.12	1
A0A287AUH8	Nitric oxide synthase	NOS2	131.23	7.66	1
F1SM91	NKAP domain containing 1	C11orf57	34.15	9.70	1
A0A287BNW3	NLR family CARD domain containing 5	NLRC5	184.72	6.74	1
F1RML0	NLR family pyrin domain containing 11	NLRP11	118.18	8.25	1
I3L713	NOP2/Sun RNA methyltransferase family member 7	NSUN7	81.98	8.53	1
A0A287B1L8	Notch 1	NOTCH1	271.65	5.10	1
B6ICX7	Novel protein similar to tripartite motif-containing protein 26 (Fragment)	SBAB-207G8.3	32.11	8.03	1
I3LP42	NPHS1, nephrin	NPHS1	134.85	6.32	1

A0A287AAR1	Nth like DNA glycosylase 1	NTHL1	33.20	9.83	1
F1S861	Nuclear factor kappa B subunit 2	NFKB2	86.52	6.51	1
A0A286ZN81	Nuclear mitotic apparatus protein 1	NUMA1	206.42	5.26	1
A0A287B4M5	Nuclear receptor binding SET domain protein 3	NSD3	72.66	9.07	1
F1S2V5	Nuclear receptor coactivator 7	NCOA7	106.61	5.36	1
F1RFN3	Nuclear receptor corepressor 2	NCOR2	269.18	7.64	1
A0A287B7Z3	Nucleolar and spindle associated protein 1	NUSAP1	49.69	9.92	1
F1SC66	Nucleolar complex protein 3 homolog	NOC3L	81.58	8.24	1
A0A287A1B0	Nucleolar protein 4	NOL4	63.27	5.10	1
F1SHV6	Nucleolar protein with MIF4G domain 1	NOM1	96.61	7.97	1
A0A287BF68	Nucleoporin 153	NUP153	152.44	8.70	1
F1RR49	Nucleoporin 188	NUP188	188.47	6.93	1
K7GLU3	Nucleoporin 214	NUP214	193.78	8.12	1
Q2EN76	Nucleoside diphosphate kinase B	NME2	17.16	7.97	1
K7GR29	OCRL, inositol polyphosphate-5-phosphatase	OCRL	95.71	6.92	1
F1S6H7	Origin recognition complex subunit 1	ORC1	81.07	9.32	1
A5GFR7	Orthologue of H. sapiens chromosome 20 open reading frame 174 (C20orf174)	C17H20orf174	170.46	8.47	1
A0A287AUV7	Otoferlin	OTOF	224.70	5.71	1
I3LK73	Otogelin	OTOG	307.81	5.64	1
F1SNR5	OTU deubiquitinase 7A	OTUD7A	101.71	8.19	1
F1SGB1	Ovochymase 1	OVCH1	132.39	7.03	1
A0A286ZHZ8	Oxysterol-binding protein	OSBPL6	98.53	6.68	1
F1RWJ1	Oxysterol-binding protein	OSBPL7	94.08	8.13	1
K7GSP8	PAK1 interacting protein 1	PAK1IP1	40.96	8.32	1
A0A287A370	Palmdelphin	PALMD	58.31	5.66	1
F1S703	Pappalysin 2	PAPPA2	197.26	5.88	1
F1RUR8	Par-3 family cell polarity regulator	PARD3	129.16	6.67	1
F1SHE2	Par-3 family cell polarity regulator beta	PARD3B	113.27	9.20	1
F1SAE7	Patatin like phospholipase domain containing 8	PNPLA8	88.78	9.17	1
I3LVF2	Patched 1	PTCH1	160.66	6.89	1
A0A287AK91	PDS5 cohesin associated factor B	PDS5B	160.80	8.31	1
F1SC59	PDX1 C-terminal inhibiting factor 1	PCIF1	80.44	7.42	1
K7GRK2	PDZ domain containing 4	PDZD4	86.46	5.86	1
A0A286ZXA7	PDZ domain containing ring finger 3	PDZRN3	87.07	5.16	1
F1SIY2	Pellino E3 ubiquitin protein ligase 1	PELI1	38.72	8.62	1
A0A287AZT1	Peptidyl arginine deiminase 2	PADI2	71.43	6.11	1

I3LVI2	Peptidylprolyl isomerase	FKBP15	112.62	6.65	1
A0A287A254	Period circadian clock 1	PER1	120.25	6.62	1
A0A287AWT9	PGAM family member 5, mitochondrial serine/threonine protein phosphatase	PGAM5	21.40	9.89	1
F1RRU2	PHD finger protein 20 like 1	PHF20L1	106.34	7.01	1
A0A287ASV5	PHD finger protein 21A	PHF21A	70.10	9.50	1
F1RUG9	PHD finger protein 8	PHF8	113.57	8.31	1
A0A287BIB2	Phosphatase domain containing, paladin 1	PALD1	95.27	6.84	1
F1SE25	Phosphate transporter	SLC20A2	71.23	6.42	1
I3LJB7	Phosphatidylinositol 4,5-bisphosphate 3-kinase catalytic subunit gamma isoform	PIK3CG	126.44	7.33	1
A0A287A0N3	Phosphatidylinositol glycan anchor biosynthesis class N	PIGN	93.84	7.78	1
A0A286ZXL2	Phosphatidylinositol transfer protein membrane associated 1	PITPNM1	132.38	5.91	1
F1RFJ7	Phosphatidylinositol transfer protein membrane associated 2	PITPNM2	141.80	7.15	1
F1RU39	Phosphofurin acidic cluster sorting protein 1	PACS1	100.52	8.12	1
F1S814	Phosphoglucomutase 1	PGM1	61.50	6.81	1
F1SS92	Phosphoinositide 3-kinase regulatory subunit 5	PIK3R5	94.53	7.44	1
A0A286ZM79	Phospholipase A(2)	PLA2G2F	22.51	7.84	1
F1RPR9	Phospholipase A2 receptor 1	PLA2R1	165.61	6.37	1
D0G7E0	Phosphomevalonate kinase	PMVK	21.92	5.63	1
A0A287AC69	Phosphoprotein enriched in astrocytes 15	PEA15	15.03	5.02	1
D9YJ48	Piwi-like 1		98.41	9.42	1
I3LGN8	Plakophilin 1	PKP1	80.64	8.97	1
I3LAZ5	Pleckstrin and Sec7 domain containing 2	PSD2	84.77	5.06	1
A0A287ACI0	Pleckstrin homology and RUN domain containing M2	PLEKHM2	91.36	5.03	1
F1RL82	Pleckstrin homology domain containing A4	PLEKHA4	76.05	10.73	1
A0A287AEM1	Pleckstrin homology domain containing A5	PLEKHA5	116.06	6.93	1
A0A287ABD3	Pleckstrin homology domain containing A6	PLEKHA6	112.37	9.00	1
F1SSU4	Pleckstrin homology domain containing M3	PLEKHM3	82.75	7.71	1
F1SA37	Pleckstrin homology, MyTH4 and FERM domain containing H1	PLEKHH1	148.64	7.84	1
A0A287B9H1	Plectin	PLEC	607.45	5.68	1
F1SPK1	Plexin D1	PLXND1	213.93	7.28	1
A0A287B8U7	Plexin domain containing 2	PLXDC2	59.10	6.49	1
F1S0S9	Poly(A) RNA polymerase D7, non-canonical	PAPD7	84.53	9.48	1
F1SQ36	Poly(ADP-ribose) polymerase family member 14	PARP14	178.20	6.98	1
F1S3A9	Polyamine modulated factor 1 binding protein 1	PMFBP1	118.87	6.18	1

I3LJU0	Polyhomeotic homolog 3	PHC3	98.82	6.49	1
Q762C2	Polypeptide chain elongation factor 1alpha (Fragment)	ef1alpha	11.97	6.54	1
A0A287AU26	Polypyrimidine tract-binding protein 1	PTBP1	57.23	9.17	1
F1RLF9	Potassium calcium-activated channel subfamily N member 2	KCNN2	91.62	9.17	1
F1RZZ8	Potassium sodium-activated channel subfamily T member 1	KCNT1	137.25	7.52	1
A0A287BG68	Potassium voltage-gated channel modifier subfamily S member 2	KCNS2	54.14	5.83	1
F1SBE6	Potassium voltage-gated channel subfamily B member 1	KCNB1	96.03	7.99	1
A0A286ZSX2	Potassium voltage-gated channel subfamily D member 3	KCND3	54.21	6.99	1
Q1AP78	Potassium voltage-gated channel, shaker-related subfamily, member 2	Kcna2	56.64	4.86	1
A5GFZ3	Potassium voltage-gated channel, subfamily G, member 1	KCNG1	58.07	5.83	1
A0A287AMW2	POU domain protein	POU6F2	27.98	8.98	1
F1RPB9	POZ/BTB and AT hook containing zinc finger 1	PATZ1	58.25	8.57	1
A0A287A6S6	PPARGC1 and ESRR induced regulator, muscle 1	PERM1	89.41	5.47	1
I3L9C5	PR/SET domain 16	PRDM16	124.75	6.60	1
A0A287AGK1	PR/SET domain 2		121.08	9.25	1
F1SHB1	Pre-mRNA processing factor 40 homolog B	PRPF40B	98.75	7.31	1
I3L5S2	Pre-mRNA-splicing factor CWC25 homolog	CWC25	45.51	10.18	1
F1RLQ2	Prelamin-A/C	LMNA	74.19	7.18	1
A0A287BRZ6	Presenilin	PSEN2	46.65	4.67	1
Q76KI7	Pro-interleukin-16	IL16	67.13	5.94	1
I3L7S0	Progesterone immunomodulatory binding factor 1	PIBF1	80.78	6.14	1
A0A287BD50	Proline and serine rich coiled-coil 1	PSRC1	34.53	11.12	1
F1SA83	Proline rich 36	PRR36	103.42	10.80	1
A0A287B509	Proline rich coiled-coil 2B	PRRC2B	240.02	8.29	1
F1S7T1	Proline rich coiled-coil 2C	PRRC2C	278.04	9.20	1
A0A286ZUW5	Prolyl 4-hydroxylase subunit alpha 1	P4HA1	60.81	6.01	1
A0A287B1A8	Prominin 1	PROM1	93.93	6.73	1
A0A287B4J7	Prominin 2	PROM2	88.87	6.89	1
A0A287BLN7	Proprotein convertase subtilisin/kexin type 5	PCSK5	209.40	6.16	1
A0A287AAR7	Proprotein convertase subtilisin/kexin type 6	PCSK6	105.13	7.43	1
A0A287B301	Proprotein convertase subtilisin/kexin type 7	PCSK7	85.78	6.19	1
O62636	Protease (Fragment)		10.22	9.70	1
I3LTE3	Protease, serine 54	PRSS54	43.91	6.52	1

F1RSM2	Proteasome 26S subunit, non-ATPase 12	PSMD12	52.99	7.36	1
A0A287A388	Protein HIRA	HIRA	96.27	8.25	1
F1SSN2	Protein kinase AMP-activated non-catalytic subunit gamma 2	PRKAG2	57.94	8.85	1
I3L5U4	Protein kinase N3	PKN3	97.11	8.37	1
A0A287AS98	Protein kinase, DNA-activated, catalytic polypeptide	PRKDC	459.51	7.09	1
A0A287B1L3	Protein phosphatase 1 regulatory subunit 13 like	PPP1R13L	87.00	6.51	1
A0A287A2R0	Protein phosphatase 4 regulatory subunit 2	PPP4R2	42.45	4.73	1
I3L778	Protein phosphatase, Mg2+/Mn2+ dependent 1H	PPM1H	52.48	6.54	1
A0A287ABC9	Protein tyrosine kinase 2	PTK2	105.81	6.27	1
A0A287ARL0	Protein tyrosine kinase 2 beta	PTK2B	113.82	6.67	1
A0A287BL66	Protein tyrosine phosphatase, receptor type G	PTPRG	144.89	6.30	1
A0A287A219	Protein tyrosine phosphatase, receptor type J	PTPRJ	144.81	6.76	1
A0A286ZUS2	Protein tyrosine phosphatase, receptor type K	PTPRK	168.34	5.96	1
F1SLX4	Protein tyrosine phosphatase, receptor type Z1	PTPRZ1	238.42	4.74	1
D3JCV7	Protein Wnt	wnt4	45.30	9.20	1
I3LBV3	Protein Wnt	WNT3A	39.45	7.99	1
F1S1M6	Protocadherin 19	PCDH19	125.81	5.39	1
A0A287ARC5	Protocadherin gamma subfamily C, 4	PCDHGC4	100.87	5.57	1
Q767N0	Putative a-helix coiled-coil rod homologue (Fragment)	HCR	39.07	6.15	1
F1SBQ8	Putative homeodomain transcription factor 1	PHTF1	80.77	9.52	1
A0A287BD49	R3H domain containing 2	R3HDM2	104.54	8.62	1
I3LK86	RAB33B, member RAS oncogene family	RAB33B	25.76	6.93	1
A0A287AC37	RAB3A interacting protein	RAB3IP	43.85	5.30	1
A0A287AVI7	Rabenosyn, RAB effector	RBSN	85.97	5.77	1
F1SH88	Rac GTPase activating protein 1	RACGAP1	59.66	8.91	1
B7TJ08	RAD18-like protein	RAD18	56.69	7.97	1
A0A287ASL1	RAD51 associated protein 2	RAD51AP2	124.57	7.53	1
F1RRH7	Radial spoke head 9 homolog	RSPH9	31.24	5.54	1
A0A287BAV9	Ral GEF with PH domain and SH3 binding motif 1	RALGPS1	54.38	9.45	1
F1SDX3	Ral GTPase activating protein non-catalytic beta subunit	RALGAPB	166.27	6.67	1
A0A286ZJ27	Ral guanine nucleotide dissociation stimulator	RALGDS	83.24	6.07	1
A0A287ASL3	Ral guanine nucleotide dissociation stimulator-like 2	RGL2	70.12	8.37	1
A0A287BEZ2	RAN binding protein 17	RANBP17	120.11	6.20	1
A0A287AKI6	Rap associating with DIL domain	RADIL	50.95	9.92	1

F1S0W0	Rap guanine nucleotide exchange factor 1	RAPGEF1	119.81	6.15	1
F1SBZ4	Rap guanine nucleotide exchange factor 5	RAPGEF5	84.53	5.90	1
F1RHG0	RAP1 GTPase activating protein 2	RAP1GAP2	87.88	7.27	1
F1S749	Ras-related protein Rab-32	RAB32	174.18	7.80	1
A0A287BJS3	RB transcriptional corepressor like 2	RBL2	103.48	8.22	1
A0A287BHU6	Receptor protein serine/threonine kinase	ACVR1	80.60	9.06	1
E9M2M3	Receptor protein serine/threonine kinase	BMPR1A	60.09	7.44	1
B4YYD7	Receptor protein-tyrosine kinase (Fragment)		72.18	5.27	1
A0A287B2J6	Regulating synaptic membrane exocytosis 3	RIMS3	32.75	9.38	1
F2Z5H3	Regulation of nuclear pre-mRNA domain containing 1B	RPRD1B	36.88	5.97	1
I3LG94	Regulation of nuclear pre-mRNA domain containing 2	RPRD2	152.60	6.98	1
A0A287AGV2	Regulator of chromosome condensation 2	RCC2	46.65	9.13	1
F1S3D6	Regulator of G protein signaling 14	RGS14	53.18	7.87	1
A0A287AL00	Regulator of G protein signaling 9	RGS9	76.32	9.26	1
A0A287BPB9	Regulatory associated protein of MTOR complex 1	RPTOR	127.90	6.95	1
A0A287AMD8	Regulatory factor X7	RFX7	147.02	6.55	1
A0A287BT28	Replication factor C subunit 1	RFC1	120.77	9.26	1
F1RHH4	Replication protein A subunit	RPA1	65.11	7.47	1
F1RNT6	Repulsive guidance molecule family member b	RGMB	42.95	6.23	1
A0A287B5H2	Retinoic acid induced 1	RAI1	199.32	8.78	1
F1SJU6	Retrotransposon Gag like 6	RTL6	26.03	11.06	1
A0A287ABS3	REV1, DNA directed polymerase	REV1	120.21	8.27	1
F1SRZ4	Rho GTPase activating protein 11A	ARHGAP11A	112.53	9.13	1
F1S0H3	Rho GTPase activating protein 15	ARHGAP15	51.87	9.50	1
A0A287BHC4	Rho GTPase activating protein 18	ARHGAP18	60.05	5.80	1
A0A287AJ81	Rho GTPase activating protein 24	ARHGAP24	66.16	6.62	1
F1RR27	Rho GTPase activating protein 27	ARHGAP27	96.15	5.95	1
A0A286ZRR8	Rho GTPase activating protein 32	ARHGAP32	189.24	6.99	1
I3LCC0	Rho GTPase activating protein 45	ARHGAP45	117.95	5.72	1
F1SG15	Rho GTPase activating protein 6	ARHGAP6	77.38	5.81	1
F1RHK9	Rho guanine nucleotide exchange factor 11	ARHGEF11	171.14	5.68	1
A0A286ZJ26	Rho guanine nucleotide exchange factor 2	ARHGEF2	119.45	7.18	1
I3LQ81	Rho guanine nucleotide exchange factor 5	ARHGEF5	173.44	5.52	1
Q06AT7	RHOF	RHOF	23.56	8.65	1
A0A287AK78	Ribosomal protein L19		19.11	10.58	1
A0A287BP56	Ribosomal protein S6 kinase	RPS6KA5	81.38	7.24	1

I3LGC2	Ribosome binding protein 1	RRBP1	160.66	9.04	1
F1S2J6	Ribosome-releasing factor 2, mitochondrial	GFM2	82.94	8.05	1
A0A287ATR3	RIC1 homolog, RAB6A GEF complex partner 1	RIC1	139.43	6.01	1
A0A286ZXW2	RIMS binding protein 2	RIMBP2	122.94	5.58	1
A0A287AU34	Ring finger and WD repeat domain 2	RFWD2	77.39	6.68	1
F1RJI6	Ring finger protein 10	RNF10	89.74	6.68	1
A0A287B6M6	Ring finger protein 223	RNF223	26.45	9.39	1
F1RG77	Ring finger protein 40	RNF40	113.63	6.48	1
A0A287B5R3	Ring finger protein 43	RNF43	72.94	8.63	1
A0A287AI72	Ring finger protein 6	RNF6	69.47	11.17	1
F1SFN1	RING1 and YY1 binding protein	RYBP	24.81	9.63	1
F1SBD9	RIPOR family member 3	RIPOR3	105.50	7.44	1
A0A287AVH9	RNA binding motif protein 15	RBM15	99.85	9.92	1
I3LPP8	RNA binding motif protein 23	RBM23	49.32	10.04	1
F1ST74	RNA polymerase I subunit E	POLR1E	47.10	8.92	1
F1S796	Roundabout guidance receptor 3	ROBO3	133.71	6.99	1
A0A287A454	RUN and SH3 domain containing 2	RUSC2	132.49	7.15	1
P16960	Ryanodine receptor 1	RYR1	564.97	5.29	1
I3LFY0	S100P binding protein	S100PBP	46.90	6.43	1
A0A287AL99	Sad1 and UNC84 domain containing 1	SUN1	74.84	7.21	1
I3L780	SAP30 binding protein	SAP30BP	32.00	5.07	1
A0A287AZE3	Scavenger receptor cysteine-rich type 1 protein M130	CD163	93.97	6.05	1
A0A287BR14	SCY1 like pseudokinase 2	SCYL2	94.55	7.74	1
A0A287A2X8	SECIS binding protein 2 like	SECISBP2L	110.18	5.81	1
A0A287A3E9	Semaphorin 3F	SEMA3F	84.96	7.96	1
B7U6F4	Serine/threonine protein kinase MST4	STK26	46.53	5.29	1
O19004	Serine/threonine-protein kinase A-Raf	ARAF	67.50	9.13	1
A0A287A9Z8	Serine/threonine-protein phosphatase 2A 56 kDa regulatory subunit	PPP2R5D	63.47	8.84	1
F1S8N4	Serologically defined colon cancer antigen 8	SDCCAG8	74.03	6.00	1
I3LJB0	Serpin family B member 11	SERPINB11	44.18	7.53	1
F1SMW3	Serpin family B member 5	SERPINB5	42.10	6.32	1
Q9BDK4	Serum-inducible kinase (Fragment)		35.31	7.05	1
F1RXT5	SET binding factor 1	SBF1	208.61	7.28	1
F1RQG5	SET binding protein 1	SETBP1	175.54	9.74	1
A0A287BC37	SET domain containing 1A		110.22	5.77	1
F1RNR2	SET domain containing 1B	SETD1B	174.86	6.51	1

A0A286ZSE7	SET domain containing 5	SETD5	127.79	8.79	1
A0A287AU02	Sex comb on midleg homolog 1 (Drosophila)	SCMH1	62.69	9.72	1
F1SQP2	Sex comb on midleg like 2 (Drosophila)	SCML2	73.75	8.56	1
A0A286ZR47	SGK2, serine/threonine kinase 2	SGK2	56.86	8.29	1
A0A287BQ68	SH2 domain containing 3C	SH2D3C	75.68	7.84	1
A0A287ASF0	SH3 and multiple ankyrin repeat domains 3	SHANK3	185.36	8.28	1
I3L8F6	SH3 domain binding protein 1	SH3BP1	61.55	5.39	1
A0A287AT29	SH3 domain binding protein 4	SH3BP4	100.43	8.21	1
F1RM16	SH3 domain containing ring finger 2	SH3RF2	75.95	9.63	1
A0A287BHM0	SH3 domain GRB2 like endophilin interacting protein 1	SGIP1	65.63	8.70	1
A0A287ATI2	Shroom family member 3	SHROOM3	197.44	7.39	1
A0A068F110	Sialic acid binding Ig-like lectin 10		76.97	6.71	1
A0A286ZYH0	Sialoadhesin	SIGLEC1	162.76	6.96	1
M3UZ58	Sialophorin	SPN	42.59	5.21	1
F1RI55	Sidekick cell adhesion molecule 1	SDK1	214.50	6.24	1
B3CL07	Signal recognition particle receptor B subunit (Fragment)	SRPRB	22.24	9.66	1
A0A287ARF9	Signal transducer and activator of transcription	STAT4	82.24	6.30	1
A0A287B2E6	Ski2 like RNA helicase	SKIV2L	143.09	7.12	1
Q6S7D8	SLA-1 (Fragment)		11.45	6.54	1
A0A287BBN7	Slingshot protein phosphatase 1	SSH1	97.31	5.68	1
F1S5C4	Slit guidance ligand 2	SLIT2	157.96	6.96	1
F1RR92	Slit guidance ligand 3	SLIT3	144.90	7.39	1
A0A287B8H5	SLIT-ROBO Rho GTPase activating protein 3	SRGAP3	122.42	6.67	1
F1RK43	SLX4 structure-specific endonuclease subunit	SLX4	189.98	6.04	1
A0A287BFZ4	SMC5-SMC6 complex localization factor 2	SLF2	133.94	9.11	1
A0A287B3B8	SMG7, nonsense mediated mRNA decay factor	SMG7	121.78	8.46	1
F1RGN8	Smoothelin like 2	SMTNL2	49.04	8.57	1
A0A286ZPE1	Sodium channel epithelial 1 alpha subunit	SCNN1A	59.88	8.53	1
A0A287A300	Sodium leak channel, non-selective	NALCN	197.28	8.76	1
A0A287AUP8	Sodium voltage-gated channel alpha subunit 1	SCN1A	157.58	5.82	1
D2WKD7	Sodium/potassium-transporting ATPase subunit alpha	ATP1A3	111.68	5.41	1
F1SKP1	Solute carrier family 16 member 8	SLC16A8	49.90	5.62	1
A0A287ADV5	Solute carrier family 2 member 10	SLC2A10	31.93	9.74	1
F1S0V7	Solute carrier family 36 member 2	SLC36A2	53.03	8.48	1
K7GM61	Solute carrier family 44 member 1	SLC44A1	69.67	8.82	1

A0A287BLA3	Solute carrier family 9 member C1	SLC9C1	130.41	6.95	1
Q866U3	Somatostatin receptor subtype 1	SSTR1	42.65	8.28	1
A0A287B6S0	Sorbin and SH3 domain containing 1	SORBS1	159.05	9.14	1
K7GNC0	Sortilin related VPS10 domain containing receptor 1	SORCS1	113.78	6.54	1
Q38Q18	Sox-2 (Fragment)		27.04	9.41	1
A0A286ZTZ1	Sp9 transcription factor	SP9	48.97	8.76	1
A0A286ZKN0	Spalt like transcription factor 3	SALL3	134.48	6.89	1
A0A286ZR85	Spectrin alpha, non-erythrocytic 1	SPTAN1	267.42	5.27	1
A0A287A113	Spectrin beta chain	SPTB	269.73	5.39	1
A0A287AQA6	SPEM family member 3		125.34	8.50	1
F1SNC1	Sperm flagellar protein 2	SPEF2	208.56	5.63	1
A0A287APE8	Sperm specific antigen 2	SSFA2	84.41	5.48	1
F1SKU5	Spermatid perinuclear RNA binding protein	STRBP	62.45	8.41	1
A0A287ANT4	Spermatogenesis associated serine rich 2 like	SPATS2L	54.08	9.63	1
F1RSY4	Sphingomyelin phosphodiesterase 2	SMPD2	47.54	6.98	1
A0A286ZLB6	Spindlin-1	SPIN1	27.07	6.24	1
A0A287AGN9	Spondin 1	SPON1	84.62	5.95	1
A0A287AVM4	Sprouty related EVH1 domain containing 3	SPRED3	42.48	8.27	1
F1RRA2	Sprouty RTK signaling antagonist 1	SPRY1	34.88	8.10	1
F1RS39	SPT20 homolog, SAGA complex component	SUPT20H	84.59	8.65	1
A0A287A268	SR-related CTD associated factor 1	SCAF1	133.59	9.13	1
A0A287A3Z8	SR-related CTD associated factor 11	SCAF11	144.30	8.79	1
A0A287BAS4	SR-related CTD associated factor 8	SCAF8	116.93	7.06	1
A0A286ZNC2	SRC kinase signaling inhibitor 1	SRCIN1	130.90	9.35	1
B8Y466	SRSF protein kinase 3	SRPK3	61.87	7.24	1
F1RQF2	SRY-box 30	SOX30	83.20	8.29	1
A0A287B8U4	STE20-related kinase adaptor alpha	STRADA	41.54	7.05	1
K7GSH0	Sterile alpha motif domain containing 14	SAMD14	44.62	9.80	1
A0A287AGC9	Sterile alpha motif domain containing 9	SAMD9	181.11	7.91	1
A0A287B7I0	Sterol regulatory element-binding protein cleavage-activating protein	SCAP	125.68	6.79	1
A0A286ZTH4	STIL, centriolar assembly protein	STIL	137.48	6.39	1
A0A286ZR30	Stonin 2	STON2	106.00	5.39	1
A0A287ALH0	Strawberry notch homolog 1	SBNO1	150.49	8.31	1
K7GQ86	Stromal antigen 2	STAG2	133.97	5.34	1
A0A287BFX9	Structural maintenance of chromosomes 5	SMC5	127.75	8.47	1
I3LPR6	Structural maintenance of chromosomes flexible hinge domain containing 1	SMCHD1	191.00	8.24	1

Q007T0	Succinate dehydrogenase [ubiquinone] iron-sulfur subunit, mitochondrial	SDHB	31.56	8.38	1
F1SH47	Sucrase-isomaltase, intestinal	SI	210.26	5.26	1
A0A287B4X5	SUMO1/sentrin specific peptidase 6	SENP6	113.08	6.35	1
A0A287AP17	Suppressor of glucose, autophagy associated 1	SOGA1	173.62	6.60	1
F1SI04	Sushi, nidogen and EGF like domains 1	SNED1	147.42	7.46	1
F1SLI6	SWI/SNF related, matrix associated, actin dependent regulator of chromatin subfamily c member 1	SMARCC1	121.68	6.20	1
I3L8U4	Synaptojanin 2	SYNJ2	154.10	7.93	1
A0A286ZLL9	Synaptopodin	SYNPO	117.27	10.10	1
F1SBR7	Synaptotagmin 6	SYT6	58.98	7.78	1
A0A287B286	Syndecan	SDC3	44.29	4.51	1
F1S1I1	Syntabulin	SYBU	70.51	6.46	1
F1SB58	T-cell activation RhoGTPase activating protein	TAGAP	91.52	7.97	1
I3LKZ0	T-cell lymphoma invasion and metastasis 1	TIAM1	153.93	7.27	1
A0A287AIV0	T-complex-associated-testis-expressed 1	TCTE1	52.25	7.20	1
A0A287B693	TATA-box binding protein associated factor 2	TAF2	119.01	7.90	1
F1SBA4	TATA-box binding protein associated factor 4b	TAF4B	90.82	9.52	1
I3LFP6	TATA-box binding protein associated factor 9b	TAF9B	27.54	9.67	1
F1SC65	TBC1 domain family member 12	TBC1D12	75.43	5.95	1
A0A287A9E6	TBC1 domain family member 23	TBC1D23	76.49	5.36	1
A0A287B6V7	TBC1 domain family member 31	TBC1D31	107.36	7.91	1
F1SF42	TBC1 domain family member 32	TBC1D32	149.31	6.61	1
F1STG0	TBC1 domain family member 8	TBC1D8	126.92	5.49	1
A5GFT6	Teashirt homolog 2	TSHZ2	114.53	7.58	1
F1SNN4	Teashirt zinc finger homeobox 1	TSHZ1	117.29	7.21	1
F1RNM5	Tectonic family member 1	TCTN1	59.17	8.07	1
F1SA08	Tectonin beta-propeller repeat containing 2	TECPR2	146.99	6.27	1
I3LHG2	Tectorin alpha	TECTA	230.26	5.27	1
F1S8G0	Telomerase associated protein 1	TEP1	290.38	7.62	1
A0A287BPQ0	Telomere repeat binding bouquet formation protein 1	TERB1	81.37	8.32	1
I3LJU9	Tenascin	TNC	205.28	5.43	1
A0A287BQG7	Tensin 3	TNS3	150.91	6.74	1
F1S264	Testis expressed 14, intercellular bridge forming factor	TEX14	98.96	5.15	1
F1SG05	Testis-specific kinase 1	TESK1	67.79	8.29	1
M9T0L3	Tet methylcytosine dioxygenase 3		178.84	7.59	1

A0A287AVL3	Tetratricopeptide repeat domain 14	TTC14	88.25	8.91	1
F1RS12	Tetratricopeptide repeat domain 16	TTC16	94.50	8.34	1
A0A287A9C5	TGFB induced factor homeobox 2	TGIF2	25.80	8.40	1
F1RL25	Thioredoxin domain containing 11	TXNDC11	106.69	7.20	1
A0A286ZIV5	THO complex 1	THOC1	76.09	4.89	1
F1RU72	THO complex 2	THOC2	155.60	8.87	1
A0A286ZT45	Thrombospondin type 1 domain containing 7A	THSD7A	173.45	7.42	1
F1SD86	Thyroid hormone receptor interactor 11	TRIP11	216.28	5.31	1
F1SV47	Thyroid hormone receptor-associated protein 3	THRAP3	108.96	10.15	1
A0A287BF71	Tight junction protein 1	TJP1	199.01	7.43	1
A0A286ZUC9	Tonsoku like, DNA repair protein	TONSL	137.00	6.32	1
A0A287AMD1	TOP1 binding arginine/serine rich protein	TOPORS	119.61	9.64	1
A0A286ZQT3	Tousled like kinase 2	TLK2	79.32	8.53	1
I3L726	TOX high mobility group box family member 2	TOX2	53.99	9.04	1
I3LA58	TRAF2 and NCK interacting kinase	TNIK	141.34	7.40	1
A0A287A0U8	Trafficking kinesin protein 1	TRAK1	73.88	5.08	1
F1RSJ3	Trafficking protein particle complex 9	TRAPPC9	103.99	7.77	1
A0A286ZX83	Transcription factor 12	TCF12	69.84	7.34	1
A0A286ZTB1	Transcription factor 20	TCF20	208.33	9.10	1
A0A287AH71	Transcription factor AP-4	TFAP4	38.63	6.42	1
F1SIJ5	Transducin like enhancer of split 1	TLE1	75.50	7.20	1
A0A287BLG6	Transglutaminase 6	TGM6	79.16	7.52	1
F1SJA5	Transient receptor potential cation channel subfamily M member 6	TRPM6	193.99	8.76	1
C0JJ16	Transient receptor potential channel subfamily C member 4	TRPC4	112.11	7.55	1
F1RX23	Transmembrane 131 like	TMEM131L	157.11	7.94	1
A0A287BCS7	Transmembrane and coiled-coil domain family 2	TMCC2	65.55	6.68	1
A0A287BEC5	Transmembrane protease, serine 11A	TMPRSS11A	36.17	9.31	1
A0A286ZRW8	Transmembrane protein 121B	TMEM121B	52.01	8.70	1
A0A287AEG9	Transmembrane protein 131	TMEM131	185.31	8.38	1
A0A287AP14	Transmembrane protein 135	TMEM135	48.86	9.55	1
F1SMR8	Transmembrane protein 209	TMEM209	62.69	8.73	1
F1SP25	Transmembrane protein 245	TMEM245	80.29	6.98	1
A0A287A4M2	Transmembrane protein 266	TMEM266	22.73	4.83	1
A0A287BSJ2	Transmembrane protein 94	TMEM94	121.87	6.20	1
K9J4W3	Transporter	SLC6A6	69.73	7.08	1
A6P353	TRDV5 protein (Fragment)	TRDV5	13.05	7.91	1

F1SMI2	Tripartite motif containing 32	TRIM32	71.79	6.93	1
F1SFF7	Tripartite motif containing 9	TRIM9	79.23	6.90	1
A0A287ASX0	Trophinin	TRO	129.64	8.27	1
Q1ELV1	Truncated MC1R melanocortin 1 receptor	MC1R	5.72	12.00	1
K7GRE1	TSPO associated protein 1	TSPOAP1	197.56	5.19	1
A0A286ZJB5	Tuberous sclerosis 2	TSC2	190.82	6.98	1
I3LKM6	Tudor domain containing 1	TDRD1	129.77	6.96	1
I3L8U6	Tudor domain containing 6	TDRD6	236.88	5.35	1
F1S2V2	Tumor protein D52 like 1	TPD52L1	22.60	5.47	1
A0A286ZMW9	Tumor protein D52 like 2	TPD52L2	23.30	6.10	1
F1SEI1	Twist family bHLH transcription factor 1	TWIST1	21.00	9.44	1
B8R0Y5	Type I inositol-3,4-bisphosphate 4-phosphatase	INPP4A	105.09	7.42	1
Q6WP71	Type XVII collagen (Fragment)	COL17A1	21.38	8.32	1
A0A287A6G1	Tyrosine kinase non receptor 2	TNK2	114.23	7.56	1
I3LSM3	Ubiquilin 1	UBQLN1	59.16	5.10	1
A0A287AAE6	Ubiquitin associated protein 2	UBAP2	97.85	7.02	1
F1S1V0	Ubiquitin protein ligase E3 component n-recognin 3 (putative)	UBR3	198.63	6.27	1
F1RTE2	Ubiquitin specific peptidase 26	USP26	102.65	8.46	1
A0A287BBW6	Ubiquitin specific peptidase 29	USP29	97.87	5.20	1
A0A287BLR3	Ubiquitin specific peptidase 53	USP53	111.57	7.94	1
F1RP50	UDP-glucose glycoprotein glucosyltransferase 2	UGGT2	185.42	6.44	1
A0A287AYR3	UHRF1 binding protein 1 like	UHRF1BP1L	135.79	6.48	1
F1SIH2	Unc-13 homolog B	UNC13B	174.60	5.97	1
A0A287BKT0	Unc-13 homolog C	UNC13C	247.85	6.00	1
A0A287A5I7	Unc-45 myosin chaperone A	UNC45A	87.20	6.46	1
A0A286ZI86	Uncharacterized protein		9.68	8.19	1
A0A286ZI90	Uncharacterized protein		67.05	5.48	1
A0A286ZIE2	Uncharacterized protein		47.85	5.82	1
A0A286ZIX6	Uncharacterized protein		64.42	12.44	1
A0A286ZJX1	Uncharacterized protein		83.08	9.52	1
A0A286ZK70	Uncharacterized protein		44.02	8.75	1
A0A286ZLI5	Uncharacterized protein		39.38	7.36	1
A0A286ZM55	Uncharacterized protein		115.49	8.48	1
A0A286ZMM7	Uncharacterized protein		15.29	11.77	1
A0A286ZNR8	Uncharacterized protein		78.68	9.63	1
A0A286ZP23	Uncharacterized protein		71.11	9.32	1

A0A286ZPF7	Uncharacterized protein		48.97	8.65	1
A0A286ZQ68	Uncharacterized protein		50.43	5.14	1
A0A286ZRJ7	Uncharacterized protein	CNTRL	265.29	5.58	1
A0A286ZWF5	Uncharacterized protein		12.85	8.48	1
A0A286ZWV3	Uncharacterized protein		13.15	9.76	1
A0A286ZYJ9	Uncharacterized protein		42.85	9.09	1
A0A286ZYR6	Uncharacterized protein	LOC110257970	188.21	7.37	1
A0A286ZZR8	Uncharacterized protein		24.26	9.55	1
A0A287A0P9	Uncharacterized protein		31.00	11.60	1
A0A287A0S2	Uncharacterized protein	ATF7	46.41	8.05	1
A0A287A0X8	Uncharacterized protein		26.26	8.34	1
A0A287A347	Uncharacterized protein		19.50	8.90	1
A0A287A3S2	Uncharacterized protein	LOC100523440	69.55	8.18	1
A0A287A3T5	Uncharacterized protein	LOC110257910	118.10	5.74	1
A0A287A5L2	Uncharacterized protein		10.13	11.84	1
A0A287A7M6	Uncharacterized protein	LOC100156694	57.98	8.75	1
A0A287A825	Uncharacterized protein		36.46	8.53	1
A0A287A8K2	Uncharacterized protein	SLFN11	102.48	7.62	1
A0A287A8K7	Uncharacterized protein	TYW1	89.36	8.24	1
A0A287A8U7	Uncharacterized protein		23.13	5.05	1
A0A287A994	Uncharacterized protein	TRAPPC13	39.11	5.55	1
A0A287A9K2	Uncharacterized protein	LOC100523736	23.22	9.80	1
A0A287A9Y8	Uncharacterized protein		268.25	5.88	1
A0A287AA28	Uncharacterized protein	SHROOM2	93.38	8.41	1
A0A287ABS1	Uncharacterized protein		45.93	6.60	1
A0A287AC61	Uncharacterized protein	LOC100523123	52.73	6.06	1
A0A287ACB2	Uncharacterized protein	LOC106510156	9.44	8.65	1
A0A287AFB0	Uncharacterized protein		35.10	9.41	1
A0A287AGW8	Uncharacterized protein	LOC110262260	35.76	8.78	1
A0A287AGY2	Uncharacterized protein	CLCA4	95.38	5.34	1
A0A287AH84	Uncharacterized protein	LOC100516390	160.18	5.26	1
A0A287AJI0	Uncharacterized protein		111.50	9.44	1
A0A287AK03	Uncharacterized protein	LOC100737912	163.18	9.09	1
A0A287AKA6	Uncharacterized protein		21.57	9.72	1

A0A287AM98	Uncharacterized protein		38.22	9.29	1
A0A287ANE7	Uncharacterized protein	KIAA0825	142.58	6.05	1
A0A287ANK8	Uncharacterized protein	NLRP12L	106.95	5.91	1
A0A287ANN8	Uncharacterized protein		48.39	8.48	1
A0A287AP95	Uncharacterized protein		11.75	8.18	1
A0A287APG4	Uncharacterized protein		12.97	8.69	1
A0A287AQ27	Uncharacterized protein	LOC100739163	21.74	7.11	1
A0A287ARA0	Uncharacterized protein		12.31	10.48	1
A0A287ARI8	Uncharacterized protein		55.18	9.41	1
A0A287ASJ0	Uncharacterized protein		13.29	9.83	1
A0A287ATG9	Uncharacterized protein	MYBL2	74.44	7.12	1
A0A287AUH2	Uncharacterized protein	PAK6	60.38	8.87	1
A0A287AUL4	Uncharacterized protein	SPATS2	59.22	9.06	1
A0A287AVL0	Uncharacterized protein		15.88	5.06	1
A0A287AW33	Uncharacterized protein		61.51	5.31	1
A0A287AWJ6	Uncharacterized protein	SMU1	51.46	7.31	1
A0A287AX82	Uncharacterized protein		15.70	9.11	1
A0A287AZX0	Uncharacterized protein	TBC1D10B	74.42	9.16	1
A0A287AZY4	Uncharacterized protein		79.55	9.58	1
A0A287B1I8	Uncharacterized protein	SMIM13	22.06	8.90	1
A0A287B1V2	Uncharacterized protein		32.47	7.43	1
A0A287B3T1	Uncharacterized protein	LOC100155249	61.58	6.68	1
A0A287B3W7	Uncharacterized protein		10.74	7.28	1
A0A287B423	Uncharacterized protein	SPESP1	39.84	5.50	1
A0A287B4H8	Uncharacterized protein	LOC100152428	135.08	8.85	1
A0A287B4T6	Uncharacterized protein	LOC102166104	21.90	5.59	1
A0A287B537	Uncharacterized protein		30.01	8.19	1
A0A287B620	Uncharacterized protein		32.04	8.76	1
A0A287B669	Uncharacterized protein	MYO5B	200.81	7.47	1
A0A287B6B5	Uncharacterized protein	LOC100517477	28.79	8.76	1
A0A287B7R2	Uncharacterized protein		96.41	10.17	1
A0A287B838	Uncharacterized protein	LOC100624559	265.02	5.48	1
A0A287BBY0	Uncharacterized protein		48.67	8.40	1
A0A287BCX2	Uncharacterized protein		29.86	9.55	1
A0A287BDU3	Uncharacterized protein		5.46	8.22	1

A0A287BE38	Uncharacterized protein	SRCAP	336.46	5.78	1
A0A287BI30	Uncharacterized protein		25.88	9.72	1
A0A287BK75	Uncharacterized protein	MAP2K1	43.41	6.62	1
A0A287BMH3	Uncharacterized protein		5.67	10.02	1
A0A287BNS4	Uncharacterized protein		80.36	7.58	1
A0A287BPZ5	Uncharacterized protein		70.25	10.35	1
A0A287BQ40	Uncharacterized protein		76.67	5.38	1
A0A287BRV7	Uncharacterized protein		17.51	7.61	1
A0A288CFW7	Uncharacterized protein	ZBP1	46.47	5.82	1
F1RF53	Uncharacterized protein	LOC100737926	56.43	6.34	1
F1RFH0	Uncharacterized protein	GAS2L1	72.21	10.29	1
F1RFN1	Uncharacterized protein		95.57	7.85	1
F1RG90	Uncharacterized protein		129.20	9.51	1
F1RGE8	Uncharacterized protein	ANKHD1	269.02	5.76	1
F1RID0	Uncharacterized protein	PPAG3	43.42	9.25	1
F1RKY6	Uncharacterized protein		158.39	5.85	1
F1RL14	Uncharacterized protein		355.54	7.75	1
F1RLQ7	Uncharacterized protein		200.32	9.31	1
F1RMT5	Uncharacterized protein		88.01	5.14	1
F1RN57	Uncharacterized protein		114.29	6.87	1
F1RNJ7	Uncharacterized protein		43.46	7.05	1
F1RP96	Uncharacterized protein	LOC100515551	59.43	8.19	1
F1RQ04	Uncharacterized protein		30.27	10.04	1
F1RVP4	Uncharacterized protein	MOCS1	60.75	8.70	1
F1RX38	Uncharacterized protein	PLRG1	56.40	9.17	1
F1RZ07	Uncharacterized protein	LOC110257935	198.69	9.32	1
F1RZP6	Uncharacterized protein	C1H6orf183	247.05	7.12	1
F1S1H9	Uncharacterized protein	PKHD1L1	460.24	6.43	1
F1S2W6	Uncharacterized protein	HINT3	20.52	6.51	1
F1S3L1	Uncharacterized protein	DCAF4	55.21	9.09	1
F1S418	Uncharacterized protein	PRDX3	28.45	7.62	1
F1S4L1	Uncharacterized protein	ERCC6L2	170.69	8.41	1
F1S4M8	Uncharacterized protein		54.61	8.78	1
F1S663	Uncharacterized protein	LAMC1	162.74	5.12	1
F1S6Q8	Uncharacterized protein		57.44	6.77	1
F1S8R7	Uncharacterized protein	HAUS3	69.34	5.47	1

F1S9P6	Uncharacterized protein		82.70	5.43	1
F1SAN0	Uncharacterized protein	WIZ	102.86	9.03	1
F1SAQ5	Uncharacterized protein	BCL11B	94.85	6.60	1
F1SAR7	Uncharacterized protein	CLMN	111.03	4.89	1
F1SBF4	Uncharacterized protein		71.57	5.63	1
F1SC62	Uncharacterized protein	CYP2C34	55.51	7.68	1
F1SER7	Uncharacterized protein		82.14	9.17	1
F1SER8	Uncharacterized protein		156.69	6.47	1
F1SF59	Uncharacterized protein		53.97	5.19	1
F1SFA7	Uncharacterized protein	COL1A2	104.38	9.67	1
F1SHQ0	Uncharacterized protein		40.71	7.30	1
F1SN86	Uncharacterized protein		67.01	7.97	1
F1SSR8	Uncharacterized protein	KNL1	171.50	5.62	1
F1SUW7	Uncharacterized protein	INPPL1	138.45	6.71	1
I3L6F0	Uncharacterized protein	PAPOLA	80.21	8.10	1
I3L7L0	Uncharacterized protein	GON4L	246.96	4.94	1
I3L986	Uncharacterized protein		124.91	5.53	1
I3LD49	Uncharacterized protein	LOC100522787	77.73	7.61	1
I3LDY2	Uncharacterized protein	LOC100625049	32.56	7.94	1
I3LE83	Uncharacterized protein		27.13	8.81	1
I3LEK0	Uncharacterized protein		160.34	5.43	1
I3LFP3	Uncharacterized protein	VCAN	261.76	4.51	1
I3LGA3	Uncharacterized protein		13.41	8.13	1
I3LJF8	Uncharacterized protein		69.90	8.56	1
I3LNV5	Uncharacterized protein	LGR6	182.68	6.76	1
I3LPG1	Uncharacterized protein		53.06	9.44	1
I3LPY1	Uncharacterized protein		143.15	8.31	1
I3LSP4	Uncharacterized protein	GOLGA2	112.85	5.02	1
I3LSS6	Uncharacterized protein	ZNF33B	89.10	8.32	1
K7GKS3	Uncharacterized protein	GP91-PHOX	53.66	8.31	1
K7GQZ0	Uncharacterized protein	SHROOM2	167.00	7.30	1
K7GS34	Uncharacterized protein	LOC100516420	68.31	7.08	1
F1RPJ7	Uracil phosphoribosyltransferase homolog	UPRT	33.48	6.16	1
I3LRA0	Uridine phosphorylase	UPP2	38.45	6.77	1
F1SRI4	UTP20, small subunit processome component	UTP20	317.84	7.52	1
K9J6K2	Utrophin	UTRN	393.79	5.29	1

A0A286ZMD0	UV radiation resistance associated	UVRAG	83.46	8.60	1
F1S3E8	Vac14-like protein	VAC14	87.98	6.35	1
F1S0N9	Vacuolar protein sorting 13 homolog B	VPS13B	442.84	6.57	1
Q767M3	Valine--tRNA ligase, mitochondrial	VARS2	118.21	7.68	1
Q29123	Vascular cell adhesion molecule	VCAM	58.68	5.10	1
Q27HS3	Vascular smooth muscle alpha-actin (Fragment)		7.90	8.19	1
A0A288CFZ7	Vasoactive intestinal polypeptide receptor 1	VIPR1	44.31	8.38	1
F1SX59	Versican	VCAN	369.23	4.53	1
E7CXS1	Very low density lipoprotein receptor	VLDLR	93.25	4.83	1
A5GFS8	Vesicle-associated membrane protein-associated protein B	VAPB	27.04	7.30	1
A0A2C9F3D9	Vimentin	VIM	49.19	5.16	1
A0A2C9F393	Vinculin	VCL	121.70	5.62	1
A0A287AVV2	Voltage-dependent anion-selective channel protein 1	VDAC1	32.05	8.73	1
A0A287AHZ5	Voltage-dependent L-type calcium channel subunit beta-4	CACNB4	56.51	9.06	1
A0A286ZJF1	Voltage-dependent N-type calcium channel subunit alpha	CACNA1B	259.24	8.56	1
A0A287BBV8	Voltage-dependent R-type calcium channel subunit alpha	CACNA1E	271.29	8.13	1
A0A287BMF4	von Willebrand factor A domain containing 3B	VWA3B	145.45	7.77	1
I3LR65	von Willebrand factor D and EGF domains	VWDE	151.59	5.14	1
I3LA14	VPS50, EARP/GARPII complex subunit	VPS50	89.67	5.80	1
F1SEP0	WAPL cohesin release factor	WAPL	124.44	5.47	1
I3L5A6	WAS/WASL interacting protein family member 1	WIPF1	51.37	11.47	1
F1RW14	WD repeat and FYVE domain containing 3	WDFY3	320.69	6.70	1
K9IVR7	WD repeat domain 1	WDR1	66.15	6.70	1
F1S3Z9	WD repeat domain 11	WDR11	133.53	7.47	1
A0A287AH47	WD repeat domain 49	WDR49	67.49	8.51	1
I3LJA5	WD repeat domain 72	WDR72	105.97	6.29	1
A0A287A9V3	WD repeat domain 81	WDR81	208.08	5.53	1
F2Z5U3	WD repeat domain 82	WDR82	35.06	7.69	1
A0A287AF85	WW and C2 domain containing 1	WWC1	123.60	6.57	1
I3L9Q5	X-ray radiation resistance associated 1	XRRA1	89.88	9.61	1
A0A287ABD7	XPC complex subunit, DNA damage recognition and repair factor	XPC	112.19	9.20	1
A0A287ADA2	YY1 associated factor 2	YAF2	19.87	9.72	1
D3K5L1	Zinc finger and BTB domain containing 38	ZBTB38	134.34	8.16	1
F1S6D5	Zinc finger and BTB domain containing 44	ZBTB44	50.31	6.29	1

A0A287BR05	Zinc finger BED-type containing 4	ZBED4	108.52	9.33	1
A0A287BSF1	Zinc finger BED-type containing 5	ZBED5	79.09	8.05	1
F1RWM0	Zinc finger C2HC-type containing 1A	ZC2HC1A	35.06	9.85	1
F1RK00	Zinc finger CCCH-type containing 13	ZC3H13	192.94	9.44	1
A0A287B8R9	Zinc finger CCCH-type containing 14	ZC3H14	65.27	8.02	1
M3VH53	Zinc finger CCCH-type containing 3 (Fragment)	ZC3H3	89.85	11.09	1
F1RM04	Zinc finger CCCH-type containing 4	ZC3H4	126.00	7.72	1
I1E439	Zinc finger CCCH-type containing protein 12C (Fragment)	ZC3H12C	29.52	7.14	1
A0A287B525	Zinc finger CCCH-type containing, antiviral 1	ZC3HAV1	86.26	8.79	1
A0A286ZPD4	Zinc finger CCHC-type containing 11	ZCCHC11	179.81	7.91	1
A0A287BAA9	Zinc finger CCHC-type containing 14	ZCCHC14	109.20	8.09	1
F1SHD3	Zinc finger DBF-type containing 2	ZDBF2	284.69	5.15	1
I3L587	Zinc finger FYVE-type containing 16	ZFYVE16	149.80	4.81	1
F1SA22	Zinc finger FYVE-type containing 26	ZFYVE26	283.17	6.49	1
F1S8Q5	Zinc finger FYVE-type containing 28	ZFYVE28	89.00	5.20	1
F1S397	Zinc finger homeobox 3	ZFHX3	405.76	6.20	1
A0A286ZRW4	Zinc finger MYM-type containing 2	ZMYM2	131.14	7.55	1
A0A287AKC8	Zinc finger protein 182	ZNF182	70.88	8.66	1
A0A286ZPY7	Zinc finger protein 205	ZNF205	59.50	8.79	1
A0A287A4E2	Zinc finger protein 226	ZNF226	78.34	8.75	1
A0A287AI91	Zinc finger protein 280A	ZNF280A	61.43	8.66	1
F1RTH2	Zinc finger protein 280C	ZNF280C	69.44	9.32	1
A0A287AUK4	Zinc finger protein 3	ZNF3	41.40	7.64	1
I3LPH9	Zinc finger protein 385B	ZNF385B	46.39	10.02	1
A0A287AUE1	Zinc finger protein 407	ZNF407	242.36	6.33	1
F1RWD8	Zinc finger protein 438	ZNF438	88.66	9.86	1
A0A287ADG0	Zinc finger protein 451	ZNF451	103.30	7.58	1
F1SC29	Zinc finger protein 518A	ZNF518A	167.63	9.20	1
F1RKM6	Zinc finger protein 608	ZNF608	152.19	8.91	1
F1SN72	Zinc finger protein 618	ZNF618	101.05	6.80	1
F1S4E8	Zinc finger protein 644	ZNF644	148.77	8.19	1
F1RIR3	Zinc finger protein 668	ZNF668	67.83	8.90	1
F1SCQ9	Zinc finger protein 684	ZNF684	45.15	8.85	1
F1RYL0	Zinc finger protein 804A	ZNF804A	121.68	7.65	1
F1S338	Zinc finger protein 804B	ZNF804B	133.28	8.54	1
F1S9Z3	Zinc finger protein 839	ZNF839	81.79	6.01	1
A0A287BD41	Zinc finger protein 862	ZNF862	123.34	8.57	1

F1SKG0	Zinc finger protein GLI1	GLI1	117.67	7.27	1
A0A287ATX5	Zinc finger protein ZFPM2	ZFPM2	121.56	7.39	1
A0A286ZWX1	Zinc finger protein, FOG family member 1	ZFPM1	98.10	8.38	1
F1RYJ1	Zinc finger SWIM-type containing 2	ZSWIM2	72.23	8.75	1
A0A287B0L4	Zinc finger ZZ-type and EF-hand domain containing 1	ZZEF1	320.35	5.94	1

Appendix III

Copyright Permission

SPRINGER NATURE

Title: Proteomics in heart failure: top-down or bottom-up?

Author: Zachery R. Gregorich, Ying-Hua Chang, Ying Ge

Publication: Pflügers Archiv European Journal of Physiology

Publisher: Springer Nature

Date: Jan 1, 2014

Logged in as:
David Zuanazzi Machado, Jr
LOGOUT

Order Completed

Thank you for your order.

This Agreement between David Zuanazzi Machado ("You") and Springer Nature ("Springer Nature") consists of your license details and the terms and conditions provided by Springer Nature and Copyright Clearance Center.

Your confirmation email will contain your order number for future reference.

printable details

License Number	4400410820661
License date	Aug 01, 2018
Licensed Content Publisher	Springer Nature
Licensed Content Publication	Pflügers Archiv European Journal of Physiology
Licensed Content Title	Proteomics in heart failure: top-down or bottom-up?
Licensed Content Author	Zachery R. Gregorich, Ying-Hua Chang, Ying Ge
Licensed Content Date	Jan 1, 2014
Licensed Content Volume	466
Licensed Content Issue	6
Type of Use	Thesis/Dissertation
Requestor type	academic/university or research institute
Format	print and electronic
Portion	figures/tables/illustrations
Number of figures/tables/illustrations	1
Will you be translating?	no
Circulation/distribution	<501
Author of this Springer Nature content	no
Title	Student
Instructor name	Walter Siqueira
Institution name	Western University
Expected presentation date	Oct 2018
Portions	Figure 1

Order Completed

Thank you for your order.

This Agreement between David Zuanazzi Machado ("You") and Springer Nature ("Springer Nature") consists of your license details and the terms and conditions provided by Springer Nature and Copyright Clearance Center.

Your confirmation email will contain your order number for future reference.

printable details

License Number	4400440564578
License date	Aug 01, 2018
Licensed Content Publisher	Springer Nature
Licensed Content Publication	Springer eBook
Licensed Content Title	Restoring the Dental Implant: The Biological Determinants
Licensed Content Author	Chandur P. K. Wadhwani
Licensed Content Date	Jan 1, 2015
Type of Use	Thesis/Dissertation
Requestor type	academic/university or research institute
Format	print and electronic
Portion	figures/tables/illustrations
Number of figures/tables/illustrations	2
Will you be translating?	no
Circulation/distribution	<501
Author of this Springer Nature content	no
Title	Student
Instructor name	Walter Siqueira
Institution name	Western University
Expected presentation date	Oct 2018
Portions	Fig 1.1 on page 2 Fig 1.2 on page 3

Curriculum Vitae
David Zuanazzi

Education

Sept. 2013-Dec 2018
University of Western Ontario, Canada
PhD Biochemistry
Supervisor: Dr. Walter L. Siqueira

March 2006-Feb 2009
Federal University of Rio de Janeiro, Brazil
MSc., Department of Clinical Dentistry - Periodontics
Thesis: Detections of Respiratory Pathogens in Dental Biofilm and Saliva of Hospitalized Individuals

Aug 1997- Jan 2002
Federal University of Rio de Janeiro, Brazil
Doctor of Dental Surgery

Awards/ Scholarships

CADR-NCOHR Student Research Award Competition 2016- Second place in senior category.

2016 Schulich Dentistry Annual Research Day – Second place in senior category

Foundation for Research Financial Support in the State of Rio de Janeiro (FAPERJ), Brazil. – Research Scholarship 2009-2012.

Federal University of Rio de Janeiro – First place in admission exam. Master's Scholarship 2006-2009

Work Experience

July 2009-June 2013
Research Assistant. Department of Virology, Institute of Microbiology
Federal University of Rio de Janeiro, Brazil.

2010-2011
Assistant Professor in Periodontology, Dentistry.

Faculdades São José, Rio de Janeiro – Brazil.

2006-2009
Master's Student.
Federal University of Rio de Janeiro, Brazil.

Publications

Crosara KTB, **Zuanazzi D**, Moffa EB, Xiao Y, Machado MA de AM, Siqueira WL. Revealing the Amylase Interactome in Whole Saliva Using Proteomic Approaches. BioMed Res Int. 2018 Jan 31;2018:6346954.

Zuanazzi D, Arts EJ, Jorge PK, Mulyar Y, Gibson R, Xiao Y, et al. Postnatal Identification of Zika Virus Peptides from Saliva. J Dent Res. 2017 Sep 1;96(10):1078–84.

Abdallah M-N, Tran SD, Abughanam G, Laurenti M, **Zuanazzi D**, Mezour MA, et al. Biomaterial surface proteomic signature determines interaction with epithelial cells. Acta Biomater. 2017 May 1;54:150–63.

Stevens RH, de Moura Martins Lobo Dos Santos C, **Zuanazzi D**, de Accioly Mattos MB, Ferreira DF, Kachlany SC, Tinoco EM. Prophage induction in lysogenic Aggregatibacter actinomycetemcomitans cells co-cultured with human gingival fibroblasts, and its effect on leukotoxin release. Microbial Pathogenesis 2013, Jan; v.54:54-9.

Zuanazzi D, Souto R, Mattos MBA, Zuanazzi MR, Tura BR, Sansone C, Colombo APV. Oral colonization by potential bacterial respiratory pathogens in hospitalized individuals. Archives of Oral Biology 2009, v.55, p.21-28, 2010.

Selected Presentations

D. Zuanazzi, P. K. Jorge, R. Gibson, Y. Mulyar, Y. Xiao, M. Bringel, E. J. Arts, M. A. Machado, W. L. Siqueira. Detection of Zika Virus in Saliva by Mass Spectrometry-Based Proteomic/Peptidomic. AADR 95th Annual Meeting, 2017, San Francisco, United States of America. Journal of Dental Research, 2017. v. 96A.

D. Zuanazzi, T. Basiri, M. A. Machado, E. B. Moffa, S. Hatibovic-Kofman, Y. Mulyar, E. J. Helmerhorst, F. Oppenheim, W. L. Siqueira. 2016. Duplication and Hybridization of Peptide Functional Domains for Oral Homeostasis. Poster. In: AADR 45th Annual Meeting, 2016, Los Angeles, United States of America. Journal of Dental Research, 2016. v. 95A.

D. Zuanazzi, X. Yizhi, D. W. Hamilton, W. L. Siqueira. Salivary proteome of the most used titanium surfaces in dental implants. Poster. London Health Research Day, 2016, London, Ontario, Canada.

Zuanazzi D, Mattos MBA, Souto R, Zuanazzi MR, Tura BR, Sansone C, Colombo APV. 2009. Respiratory pathogens in the oral cavity of hospitalized patients. Poster. IADR 87th General Session & Exhibition, 2009, Miami, United States of America. Journal of Dental Research, 2009. v. 88A.

Souto R, **Zuanazzi D**, Silva-Boghossian C, Zuanazzi MR, Colombo, APV. Prevalence of *Staphylococcus* spp carrying *mec*A gene in periodontitis subjects. Poster. IADR 86th General Session & Exhibition, 2008, Toronto, Canada. Journal of Dental Research, 2008. v. 87B.